Phenotypic and Genotypic Characterisation of Biofilm Formation in *Staphylococcus capitis*

A thesis is presented for the degree of Doctor of Philosophy

Bintao Cui
B.Sc, M.Sc

School of Applied Sciences
Science, Engineering and Technology Portfolio
RMIT University
August 2012

Declaration

This thesis is presented as part of the requirement for a doctorate of philosophy in biotechnology in RMIT University. The work described in this thesis is my own work unless otherwise stated, and has not been previously submitted for a degree at any tertiaty educational institute. The work was carried out under the supervision of Professor Margaret Deighton.

Bintao Cui

Acknowledgements

I wish to thank for the government of Australia for giving me the opportunity to pursue my PhD at RMIT University, Melbourne.

This dissertation wouldn't have been possible without the guidance and help of several individuals who in one way or another contributed the valuable assistance in completion of this study.

I am heartly thankful to my supervisor Margaret Deighton, whose encouragement, kindness from initial to the final enable me to develop an understanding of the subject. My research wouldn't go this far without her support.

I would like to show my gratitude to Dr Duncan Rouch for his friendship, guidance, constructive comments and input. He was made available his support in a number of ways.

I am grateful to Vennessa Fleming and Nerida Thurbon, for their kindness, patience and helps whenever in need. They always make me feel the lab like a family.

I would like to thank everyone in the laboratory for their friendship, accompany me through the most unforgettable moments in my life.

And most of all, thanks to my parents and sister for their love, care and encouragement.

Table of Contents

List of Figures

Figures in Chapter 1

Figures in Chapter 3

Figures in Chapter 4

Figures in Chapter 6

List of Tables

Tables in Chapter 5

Tables in Chapter 6

List of Abbreviations and Symbols

bp	Base pair
BSA	Bovine serum albumin
DIG probe	Digoxigenin labelled probe
DNA	Deoxyribonucleic acid
cDNA	Complementary DNA
DNase	Deoxyribonuclease
dNTP	Deoxyribonucleotide tiphoosphate
kb	Kilo base pairs
kV	Kilo volts
mg	Miligram
ml	Mililiter
mM	Millimole
M	Molarity
NaCl	Sodium chloride
ng	Nanogram
OD	Optical density
PCR	Polymerase chain reaction
RNA	Ribonucleic acid
RNase	Ribonuclease
TAE	Tris acetic acid and EDTA buffer
Tris	Tris(hydrochloride) amino methane
Tris-HCl	Tris hydrochloride
U	Unit
µg	Microgram
µL	Microliter
µm	Micrometre
UV	Ultraviolet
Ω	Ohms
λ	Lambda
δ	Sigma

Abstract

Biofilm formation is a major concern in nosocomial infection caused by staphylococci. *Staphylococcus epidermidis* and *S. aureus* are the most recognized species. The *ica* operon has been identified encoding an extracellular polysaccharide, which mediates bacterial cell-cell adhesion, is required for biofilm formation and regulated by numerous environmental factors.

The pathogenesis of *S. capitis* is of increasing concern due to its major clinical impact, especially in neonates, and its multi-resistance including hetero-resistance to vancomycin.

Little is known about the molecular basis of biofilm formation in this species, and the relations to its two subspecies. To address this question, the phenotypic and genotypic biofilm formation, antibiotic resistance, molecular epidemiology and the functional role and regulation of the *ica* operon in clinical *S. capitis* isolates from neonates in Royal Woman's Hospital in Melbourne were investigated.

Of 60 *S. capitis* isolates, biochemical tests showed that 52 belonged to the subspecies *urealyticus* and the remaining eight to the subsp. *capitis*. The two subspecies were separated into distinctive clusters by pulsed-field gel electrophoresis. This approach revealed that five clusters and unclustered isolates occurred in the unit between 2000 and 2005. The most prevalent cluster persisted for a prolonged 6-year period, and belonged to subsp. *urealyticus*. Biofilm formation and antibiotic resistance were also mainly displayed by subsp. *urealyticus*.

Sequence analysis showed that the *ica* operon in *S. capitis* was 4160 bp in length. PCR demonstrated its presence in all the isolates. The *ica* operon harboured in *S. capitis* is closely related to those of *S. epidermidis*, *S. aureus* and *S. caprae*. It contains four structural genes *icaA*, *icaD*, *icaB* and *icaC*, which are co-transcribed from the *icaA* promoter. A negative regulator *icaR* gene is located upstream of *icaA* and transcribed in an opposite orientation. The ICA proteins exhibited from 66% to 94% identity to those of the same three species. Further analysis in five isolates (two biofilm-positive subsp. *urealyticus,* one biofilm-negative subsp. *urealyticus* and two biofilm-negative subsp. *capitis*) revealed that the *ica* oprerons were identical in biofilm-positive subsp. *urealyticus* isolates, however, the biofilm-negative isolates showed variations; these point mutations, STOP codon or the modification of membrane protein topology could explain the inability to produce biofilm in these isolates.

In sillico analysis of *ica* operon demonstrated the putative function and mechanisms of ICA proteins in polysaccharide biosynthesis and the origin on *ica* genes present in *S. capitis* genomes.

In vitro biofilm formation and the expression of biofilm-related genes induced by sub-inhibitory concentrations of erythromycin were explored in the two subspecies. Results revealed different responses. The expression of *icaA* and *sarA* genes were up-regulated, and *icaR* was down-expressed in the subsp. *urealyticus* isolate biofilm producer, as occurs in *S. epidermidis*. In contrast, a reverse expression was displayed by the biofilm-negative subsp*. capitis* isolate. This suggests biofilm formation in *S. capitis* is regulated by *icaR* and *sarA*, and the two subspecies may adopt different regulatory pathways in the

two subspecies. Also, the erythromycin induced biofilm formation may have clinical implications according to the doses of erythromycin used clinically.

In addition, transformation protocols for *S. capitis* were developed and optimised and will be used as a platform for future work.

This study revealed distinctive phenotypic and genotypic characteristics of the two subspecies of *S. capitis* which was relate to their epidemiology under the clinical setting of neonate intensive care. Isolates of the predominant subsp. *urealyticus* clones were characterised by their higher antibiotic resistance and biofilm formation ability, and distinct gene expression profiles. Differentiating the subspecies *S. capitis* revealed be valuable in order to understand their role in bloodstream infections of newborns in hospitals.

CHAPTER 1

Introduction and Literature Review

1.0 Introduction

Coagulase-negative staphylococci (CoNS) are the most documented pathogens involved in catheter-related infections in modern hospitals (Venkatesh *et al.*, 2006b). The ability to form biofilm on medical devices has been recognized as the main mechanism of pathogenesis. Bacteria in the biofilm are protected from host defences and antibiotic therapies, although they may appear susceptible to antibiotics, infections are difficult to clear, causing an increased morbidity and mortality. Also, the densely compacted bacteria in a biofilm matrix facilitate spreading antibiotic resistance by horizontal gene transfer (Otto, 2009).

Staphylococcus epidermidis biofilm infections associated with indwelling medical devices are the most studied among CoNS biofilm-related infections. The best studied biofilm component, polysaccharide intercellular adhesin (PIA) has been shown to be an essential virulence factor of *S. epidermidis* (Fitzpatrick *et al*., 2005). The *ica* operon, which encodes the enzymes for PIA synthesis, has been identified in some other staphylococcal species, suggesting a more common pathogenic role in biofilm infections (Cramton *et al*., 2001, Fredheim *et al.*, 2009). Additionally, various surface proteins have been found to mediate the initial attachment in the process of biofilm formation, suggesting alternative mechanisms of biofilm formation (Otto, 2004). Biofilm bacteria are subject to a series of gene regulations, leading to the resistant phenotype revealed by transcriptional profiling data (Lazazzera, 2005, Kong *et al*., 2006b). Also, studies by using animal models provide more realistic information on biofilm formation *in vivo* (Rupp *et al.*, 1999a, Rupp *et al.*, 1999b). All these constitute the fundamental knowledge of the study of staphylococcal biofilms.

Recently, *S. capitis* has become endemic in Royal Women's Hospital, Melbourne, Australia. In contrast to *S. epidermidis*, much less is known about biofilm formation of *S. capitis* and of the two subspecies. A study on mechanisms underlying biofilm formation will facilitate the understanding of the particular role of the subspecies in infections in hospitals, and also may help to develop novel, efficient therapeutics for this species in the clinical setting.

1.1 What is biofilm?

A biofilm is a compacted assemblage of microorganisms enclosed in a matrix primarily composed of polysaccharide, and attached on a surface. Biofilms have been found on a variety of surfaces such as indwelling medical devices, industrial water system pipes or aquatic systems in the natural environment. The microbial organisms growing in a biofilm are physiologically distinct from their planktonic counterparts (Hall-Stoodley *et al.*, 2004).

Biofilm formation has been recognized as a protective mode of cell growth which allows for survival in hostile environments, and also under certain circumstances, such as nutrient deprivation. Biofilm dispersal in the form of clumps plays an important role in helping the cells to colonize new niches (Abee *et al.*, 2011).

At present, the general resistance of biofilms has been explained by several possible mechanisms. First, the biofilm matrix might react with superoxides, neutralized charged metals or dilute antimicrobial agents to generate sub-lethal concentrations. Moreover, resistant phenotypes referred to as "persisters", which have been found in a biofilm, contribute to the resistance. Whether these are indeed a unique resistant phenotype or are simply the most resistant cells remains unclear (Hall-Stoodley *et al*., 2004).

1.2 Biofilm formation and dispersal

1.2.1 Diversity in biofilms

Biofilm displays a variety of phenotypes depending on the specific system studied. The extracellular polymeric substance (EPS) matrix of biofilm plays a role in numerous processes including attachment, cell-to-cell interconnection, interactions between subpopulations, tolerance, and exchange of genetic material (Molin and Tolker-Nielsen, 2003, Friedman and Kolter, 2004, Jackson *et al*., 2004, Ma *et al*., 2009, Yang *et al.*, 2009). The composition of biofilm matrix is determined by surrounding environmental conditions, biofilm age, and even the particular strain that forms the biofilm (Hall-Stoodley and Stoodley, 2002).

Ventre *et al.* (2006) identified several signal sensor kinases (RetS, LadS, and GacS) responsible for the induction of biofilm components of *Pseudomonas aeruginosa* under certain environmental conditions. *Listeria monocytogenes* biofilms are grown as two types under static and flowing conditions, respectively (Rieu *et al.*, 2008). The SOS responsor, YneA, which is essential in cell elongation, mediates biofilm formation under flowing cultural conditions (van der Veen and Abee, 2010). Habimana *et al*. (2009) observed that densely layered cells were embedded in the EPS matrix of static and flowing cultural biofilms of *Lactobacillus plantarum* and *Lactococcus lactis*. Branda *et al.* (2001) demonstrated that two types of *Bacillus* spp. biofilms are usually developed under laboratory conditions; one is formed at the air-liquid interface where it develops pellicle structures floating on the liquid media, and the other forms colony complexes on solid agar surfaces, and then develops sites for sporulation. Moreover, *Bacillus* spp. were found to be capable of forming submersed biofilms under both static and continuous flow conditions (Wijman *et al.*, 2007).

1.2.2 Biofilm development

1.2.2.1 The process of biofilm formation

Recent advances have been made to show that biofilm development experiences a multiple-stage and differentiated process rather than a simple, uniform step. Five sequential regulated stages have been proposed for biofilm formation. During the first two stages, the cells are loosely adhered to surfaces. Further, the attached cells aggregate together and form micro-colonies; subsequently mature biofilm develops on surfaces in stages three and four. Then, under certain circumstances, the biofilm cells are shed off, return to the mobile mode characterized in stage five. The cells eventually attach to a surface when conditions are appropriate, start a new cycle of biofilm formation. Figure 1.1 shows the bacterial biofilm formation and detachment (Hall-Stoodley and Stoodley, 2002).

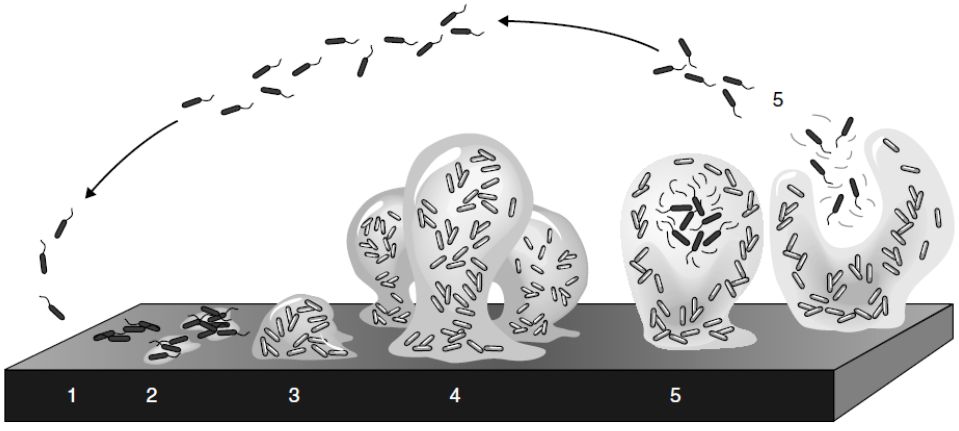

Figure 1.1. Bacterial biofilm formation and dispersal. 1. The bacterial cells attach loosely to the surface. 2. The cell attachment is mediated mainly by EPS, this is reversible. 3. Development of the early biofilm structure. 4. The fully mature biofilm complexes are formed. 5 cells are shed off (dark cells on the figure) from the mature biofilm microcolonies. Adapted from (Stoodley *et al*., 2002).

1.2.2.2 Biofilm determinants

There are intensive studies on the initial stages of biofilm formation. Considering the diversity in biofilms, the determinants of biofilm structure is a long-term debate in terms of the contributions of genetics and environmental conditions (Kjelleberg and Molin, 2002).

Numerous molecular strategies, such as gene knock-out, transposon mutagenesis, have been employed to identify the gene function in biofilm formation. In these studies, by comparison of biofilm forming ability of a mutant strain and that of its isogeneic wild-type, a particular role of a gene is defined. Also, arrays of gene loci and signals have been identified to be essential or required for biofilm formation by comparing the synthesis of biofilm components under different environmental conditions (Caiazza and O'Toole, 2003, Cucarella et al., 2001, Sarah E. Cramton, 1999 , Hamon and Lazazzera, 2001, Froeliger and Fives-Taylor, 2001, Gavín et al., 2002, Whitchurch et al., 2002, Valle et al., 2003). In addition, Davies *et al.* (1998) found that cell signalling, controlled by the quorum sensing system, plays an essential role in biofilm differentiation. In sum, both the environmental conditions and genetics show significant influence on the biofilm formation based on a series of laboratory experiments and naturally formed biofilm.

1.2.3 Biofilm dispersal

Biofilm bacteria can detach from food and water production facilities (Zottola and Sasahara, 1994, Piriou *et al.*, 1997), or medical and dental devices (Hall-Stoodley and Stoodley, 2005). Bacterial dispersal from mature biofilms allows for the colonization of new niches, and presumably, contributes to biological dispersal, bacterial survival. Disease transmission is believed to be an active process and an essential step for the biofilm life (Sauer *et al.*, 2002).

Research on biofilm dispersal is in its very early stages. Like other stages of biofilm development, dispersal can be regulated by numerous environmental signals, signal transduction pathways, and effectors. No single mechanism of biofilm dispersal is applied by all bacteria. In general, mechanisms of biofilm detachment can be divided into two broad categories: active and passive. Active detachment refers to mechanisms that are initiated by the bacteria themselves, such as endogenous enzymatic degradation (Kaplan, 2010). A number of degradative enzymes specific for biofilm components have been found to be produced by some species. For example, DspB (dispersin β-hexosaminidase), secreted by *E. coli* and several other bacteria, specifically hydrolyses the glycosidic linkages of exropolysaccharide of the biofilm matrix, therefore inhibits the biofilm formation of the host bacteria (Boles and Horswill, 2008, Nijland *et al.*, 2010) Also, Boles *et al*. (2005) showed that *Pseudomonas aeruginosa* biofilm dispersal was caused by rhamnolipids, surfactants produced by this organism. Another possible mechanism of biofilm dispersal involves cell detachment due to cell division at the outer surface of the biofilm colony (Costerton *et al*., 1999). Passive dispersal refers to biofilm cell detachment that is mediated by external forces such as fluid shear, abrasion (collision of solid particles with the biofilm), predator grazing, and human intervention (Ymele-Leki and Ross, 2007).

Many studies on the regulation of biofilm dispersal have focused on the identification of environmental conditions that trigger the dispersal process (Karatan and Watnick, 2009). In addition to environmentally induced biofilm dispersal, it is likely that mechanisms of genetically programmed biofilm dispersal also exist. In *Aggregatibacter actinomycetemcomitans,* biofilms undergo a reproducible, periodic detachment of biofilm biomass, even under conditions where nutrients are not limited (Kaplan, 2010).

In sum, biofilm formation is the primary mode of growth for bacteria in most natural and clinical environments. Biofilm dispersal acts as an essential role in the transmission of bacteria from the environment to humans, from human to human, and also the spread within a single host. A better conception of the process and mechanisms underlying biofilm formation and dispersal will facilitate development novel strategies in prevention of bacterial biofilm infections.

1.3 Clinical impact of bacterial biofilm

The study of bacteria residing in biofilms as an interactive community has recently gained a great deal of interest, in part, because a number of human diseases are involved in biofilms. Several mechanisms have been proposed to explain why pathogens in biofilms are more virulent than their planktonic counterparts. First, pathogens in biofilms can initiate an infection through the seeding or dispersal of biofilm clumps which contain large numbers of cells. Second, among the phenotypically heterogeneous pathogens within a biofilm, certain virulent phenotypes might survive and spread within biofilm matrix. Finally, the closely related cells within biofilms might initiate quorum sensing networks which regulate virulence gene expressions (Xu *et al.*, 2006b). Taken together, the dense aggregated virulent organisms within the context of biofilms might be a major contributor to the pathogenesis of bacterial biofilm related infections.

1.3.1 Biofilm infections

Many pathogenic microorganisms have been found capable of forming biofilm on the surface of indwelling medical devices, such as catheters, artificial heart valves. These orgnisms have been identified as the causative agents for a wide range of nosocomial infections. These infections include indwelling-device-associated infections caused by CoNS. Once established, these infections are almost impossible to be eradicated, the patients are subjected to long-term antimicrobial therapy, and sometimes the foreign body has to be replaced. Another classic case of biofilm infection is Legionnaire's disease, an acute respiratory infection caused by aspiration of clumps of *Legionella* biofilms floating in the air (Fields *et al*., 2002). Biofilms have been associated with a list of chronic infections including cystic fibrosis, native valve endocarditis, and chronic bacterial prostatitis, even though these have not been verified by Koch's postulates (Hall-Stoodley *et al*., 2004).

1.3.2 Antimicrobial resistance of biofilm

Biofilm bacteria generally display increased antibiotic resistance. Factors attributed to biofilm resistance are summarized in Table 1.1.

Table 1.1. Factors accounting for biofilm resistance

Factors	Mechanisms	References
Limited penetration	The inability of antibiotics to reach all areas within biofilms	(Davies, 2003)
Decreased growth rate	The lowered metabolic activity in biofilms	(Shah *et al*., 2006)
Cell density	Higher cell density in biofilm compared with their planktonic counterpart	(Mikkelsen *et al.*, 2007)
Unique cell physiology	The altered transcription profiling of the biofilm bacteria	(Stanley *et al*., 2003)
Persister cells	Persisters are possibly a new resistant phenotype or just a group of very resistant cells within biofilms	(Lewis, 2005)
Altered chemical microenvironment	The extreme microenvironment within a biofilm compromises the activity of certain antimicrobials, such as low or high pH.	(Dunne, 2002)

1.4 Coagulase-negative staphylococci (CoNS) in human infections

1.4.1 Coagulase-negative staphylococci as pathogenic agents

Staphylococci are gram-positive, AT-rich cocci, which are often arranged in grape-like clusters. Historically, coagulase-negative staphylococci were treated as a group, designated *Staphylococcus albus* or *S. epidermidis*, distinguished from *S. aureus* by their inability of clotting blood plasma. This group of CoNS normally maintain a benign relationship with their host and were considered non-pathogenic. Currently, at least 38 species of CoNS have been identified, and 13 of them have been isolated from humans (Takahashi *et al.*, 1999). *S. epidermidis* represents the most commonly found and studied coagulase-negative staphylococcal species in humans (Weinstein *et al.*, 1998). Often, staphylococcal species have been each found occupying specific niches, for example, *S. capitis* on the head, *S. auricularis* in the external auditory canal, *S. saprophyticus* in the inguinal area and the perineum.

During the past few decades, increasing cases of nosocomial infections implicating to CoNS, such as bacteraemia, native and prosthetic valve endocarditis, established CoNS as human pathogens. The surveys from Nosocomial Infections Surveillance System reveal that coagulase-negative staphylococci represent the leading isolated nosocomial pathogens from intensive care unit patients. Two main reasons may account for the infections: the increasing spreading of antibiotic resistance among clinical CoNS and biofilm formation on indwelling medical devices (Venkatesh *et al.*, 2006b). Coagulase-negative staphylococci as opposed to the *S. aureus* species, are not equipped with such widespread spectrum of virulence factors, infections incited by CoNS are not generally acute (except for native valvular endocarditis) but appear predominantly in chronic forms (Otto, 2004).

1.4.2 Coagulase-negative staphylococci infections in neonatal intensive central unit (NICU)

Coagulase-negative staphylococci are identified as the most common pathogens causing late-onset sepsis (>72 hours of age) in infants born weighing less than 1500g at birth (VLBW infants). Most of these infections are catheter-related, since central venous catheters (CVCs) are needed for delivering nutrients and drugs for critically ill infants. The using of catheters in neonates increase the occurrence of bloodstream infections (BSIs), primarily caused by CoNS. This is responsible for significant mortality and morbidity in very-low-weight infants (VLBW; < 1500g) in neonate intensive central unit (Cheung and Otto, 2010).

The capability of CoNS to adhere to catheters and form biofilms plays an important role in the pathogenesis of CoNS-induced infections. The catheter hub and skin insertion site

are recognized as the most possible pathogen sources on catheters. The microorganisms colonized in the contaminated hub may transfer along the catheter and enter into the bloodstream, causing acute late-onset sepsis infections. Moreover, CVCs-related infections in neonates tend to relapse after treatment, most likely due to the biofilm formation on the catheters. The detachment of cell clusters from the mature biofilm forms the basis for continuous transmission of bacteria into the bloodstream (Raad, 1998). A recent study by Hira *et al.* (2010), using restriction fragment length polymorphism (RFLP) showed that personnel play an important role of cross-contamination with these CoNS in NICU, which carry more resistant biofilm-forming CoNS than community strains. Furthermore, almost all blood isolates were shown to be from the hands of personnel.

1.5 Staphylococcal biofilm adhesion

Staphylococcus species are commensal bacteria that reside on human skin and mucous membranes, and are found worldwide. Staphylococci has been recognized as the most frequent pathogens associated with medical device infections; it is likely due to their presence on the skin in the vicinity of medical device (Table 1.2).

Table 1.2. Biofilm associated infections of staphylococci in the presence of foreign bodies

Biofilm Infections	Indwelling Foreign Body	Reference
Bacteraemia	Almost all cases of bacteraemia due to CoNS are associated with an indwelling foreign body.	(von Eiff *et al.*, 2005)
Infections of joint prostheses	Hip, knee, elbow	(von Eiff *et al.*, 2005)
Endophthalmitis	Lens prostheses	(von Eiff *et al.*, 2005)
Peritonitis	Implanted perioneoventricular shunts and chronic outpatient's peritoneal dialysis systems	(von Eiff *et al.*, 2005)
Ventriculitis	Implanted internal or external shunts	(von Eiff *et al.*, 2005)
Urinary infections	Urinary catheters	(von Eiff *et al.*, 2005)

1.5.1 *Staphylococcus epidermidis* biofilm as a virulence factor

Staphylococcus epidermidis is recognized as the leading CoNS mediating medical devices infections (for example, catheters and prostheses). Eighty per cent of the cells within the biofilm are identified as *S. epidermidis* in medical device related infections. In contrast with biofilms formed in the natural environment, the microbial community consists of multiple species. Biofilm formation in *S. epidermidis* is extensively studied. Cells of *S. epidermidis* are present and embedded in polysaccharide in multiple layered biofilms on polymer surface as revealed by scanning electron micrographs (Uçkay *et al*., 2009).

1.5.1.1 Biofilm formation of *S. epidermidis*

Before biofilm formation, the surfaces of medical device are coated with human serum proteins forming a conditioning film. This film plays an important role in bacterial adhesion (McCann *et al*., 2008). A range of surface proteins, known as 'microbial surface

components recognizing adhesive matrix molecules' (MSCRAMMs), have been identified for binding serum proteins in staphylococci (Sillanpää *et al*., 2009).

Biofilm attachment

Initial bacterial attachment is the first critical step for the development of implant-associated infection. Two mechanisms are believed to be involved in the initial colonisation. One is that planktonic microorganisms non-specifically bind to native surfaces of medical devices. These reactions are mediated by a number of physiochemical variables such as electrostatic forces, surface tension, and temperature (Dunne, 2002). In *S. epidermidis*, several surface proteins, such as SSP-1 (280kDa) and SSP-2 (250kDa) with specific adherence functions have been identified to be involved in this type of attachment (von Eiff *et al.*, 2002).

The second mechanism is that bacteria interact with host proteins which appear in the conditioning film formed following implantation on medical devices (Wang *et al.*, 1993). Several bacterial cell surface proteins contribute significantly to the initial attachment. Heilmann *et al*. (1997) showed that the surface associated autolysin (AtlE) mediates the initial attachment by adhesion to vitronectin and fibrinogen-binding Fbe. Cell-surface-associated proteins, SdrG, SdrF and SdrH specifically bind host proteins (McCrea *et al*., 2000). Moreover, charged cell wall teichoic acids play an important role in the initial steps of biofilm formation (Vergara-Irigaray *et al*., 2008).

Biofilm accumulation

Polysaccharide intercellular adhesion was identified as an essential functional component involved in accumulation of multilayered biofilm in *S. epidermidis* (Mack *et al*., 1996). It is

a linear ß-1,6-linked glucosaminoglycan, synthesised by enzymes encoded by *ica* operon which comprise four genes, *icaA*, *icaD*, *icaB* and *icaC* in this order. There is a negative regulator (*icaR*) gene located upstream of *icaA* gene, transcribed in an opposite direction (Mack *et al*., 1996).

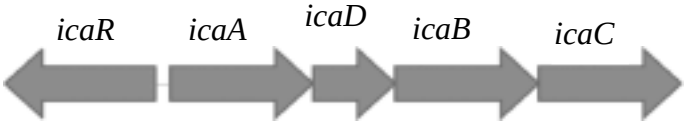

Figure 1.2. Structure of the *ica* operon in *S. epidermidis* (adapted from Mack *et al*., 1996).

Functional analysis of IcaADBC proteins revealed that proteins IcaA, IcaD and IcaC, are present the on cell membrane; IcaB is secreted in the culture supernatant. During PIA synthesis, IcaA displays N-acetylglucosaminyltransferase activity; co-expression of *icaA* and *icaD* gene increases the transferase activity. The combination of IcaA and IcaD can produce *N*-acetylglucosamine oligomers in maximal length of 20 residues. IcaB, a deacetylase, has shown sequence similarity to the *Rhizobium* NodB protein. It is likely a signal protein. It was found that only when *icaAD* co-expressed with the *icaC* gene, were full-length of oligomers have synthesised, which could be detected by anti-PIA antisera. IcaC, a transmembrane protein, may facilitate the translocation of the growing polysaccharide to cell surface (Gerke *et al.,* 1998).

Transcription studies of the *ica* operon have shown it is regulated by a variety of environmental stress stimuli, such as in the presence of salt, ethanol, temperature, nutrition, oxygen, and several antibiotics (Vuong *et al.*, 2005).

Previous work has shown that biofilm formation in *S. epidermidis* can be inactivated by insertion element *IS256* inserted in the *icaA* or *icaC* gene loci, with the former more frequently. Cells revert to a biofilm-positive phenotype by excision of *IS256* from the target region, displayed as a phase variable process (Ziebuhr *et al.*, 1999). Kiem *et al.* (2004) observed a similar phenomenon in *S. aureus*. The reversal of biofilm formation can also be mediated by an alternative strategy, promoted by proteinaceous factors (Hennig *et al*., 2007). The phase variation in biofilm formation is believed to play a role in long-term persistence and relapse of bacteria.

In addition to exopolysaccharide, surface proteins are identified to be crucial for the second phase of biofilm development. Accumulation associated protein (Aap), which is a 220 kDa LPXTG protein in *S. epidermidis,* was found more prevalent in isolates colonised on catheter surfaces than on skin, and was essential for biofilm accumulation (Vandecasteele *et al.*, 2003). Biofilm-associated protein, Bhp in *S. epidermidis*, homologous to Bap of S*. aureus*, was identified mediating the multilayered biofilm accumulation without PIA (Rohde *et al*., 2007). Giant extracellular matrix-binding protein (Embp) has recently been shown to be multifunctional, playing a role in several processes. It contributes significantly to biofilm architecture development in *S. epidermidis* (Otto, 2012).

Biofilm maturation and detachment

A mature biofilm is constituted of multilayered structures, including the main biofilm substances, host conditioning film and the substratum to which the biofilm is attached. Groups of microcolonies were found embedded in the mature biofilm structure, separated by micro-channels filled with fluid. These channels are used by the cells in the biofilm for

exchanging substances with the outside world to ensure basic living (Galiana *et al*., 2008).

Gene expression profiles of cells in a mature biofilms of both *S. epidermidis* and *S. aureus* are distinct from those grown planktonically, as revealed by microarray studies (Yao *et al*., 2005, Secor *et al*., 2011). Four metabolic types of cells are growing in *S. epidermidis* biofilms defined by (Rani *et al*., 2007) These contribute to the antibiotic tolerance within a biofilm. It is, therefore, hypothesised that the antibiotic efficacy against biofilm infections might be improved if drugs are designed to target a particular biofilm region (e.g., aerobic grown cells).

Individual cells or cell clumps in a biofilm can detach and attach to new niches, and these are believed to be crucial for transmission of biofilm associated infections (Kong *et al*., 2006b). The underlying mechanisms are largely unknown. The accessory gene regulator (*agr*) QS system was suggested play a role in this process. *S. epidermidis agr* mutant was shown to form a thicker biofilm in a rabbit model compared with its wild-type strain (Vuong *et al.*, 2004). It is likely due to the loss of phenol-soluble modulins upregulated by *agr* system in the *agr* mutant which act as surfactants and inhibit non-covalent interactions of biofilm bacteria on surfaces (Otto, 2009).

1.5.1.2 Review of the *S. epidermidis* virulence factors

Virulence properties of *S. epidermidis* are fewer compared with those of *S. aureus*, and biofilm formation has been identified as a virulence factor related to a range of acute and chronic diseases, as demonstrated by a series of animal models demonstrating *in vivo* conditions of biofilm formation (Rupp *et al*., 1999a). In addition, a list of other factors have

been recently recognized in *S. epidermidis* responsible for defeating innate immune system activities (Kocianova *et al*., 2005), for example, phenol-soluble modulins and poly-γ-DL-glutamic acid. Table 1.3 shows a review of virulence factors in *S. epidermidis* species. These include factors involved in biofilm formation, exo-enzymes and other factors.

Table 1.3. Virulence Factors of *S. epidermidis*

Factors	Functions	References
Biofilm		
Attachment to hydrophobic surfaces		
AtlE	Autolysin/adhesin: attachment to polystyrene, vitronectin binding	(Heilmann *et al.*, 1997)
SSP1, SSP2	Attachment to polystyrene	(Veenstra *et al*., 1996)
Delta-toxin	Inhibits binding to polystyrene	(McKevitt *et al*., 1990)
Attachment to host matrix proteins		
Fbe/SdrG	Fibrinogen binding, inhibition of phagocytosis	(Vernachio *et al.*, 2006)
Embp	Fibronectin binding	(Williams *et al*., 2002)
GehD	Collagen binding	(Bowden *et al*., 2002)
Accumulation		
PIA	Exopolysaccharide: cell-cell adhesion, haemagglutination	(Gerke *et al*., 1998)
AAP	Accumulation	(Hussain *et al*., 1997)
Exoenzymes		
Lipases	Persistence in fatty secretions	(Rosenstein and Götz, 2000)
Cysteine protease	Possibly tissue damage	(Dubin *et al*., 2001)
Metalloprotease Sep-P1	Lipase maturation, possibly tissue damage	(Teufel and Götz, 1993)
Serine protease GluSE	Possibly biofilm formation, degradation of fibrinogen and complement factor C5	(Otto, 2009)
Fatty acid-modifying enzyme (FAME)	Detoxification of host-produced bactericidal fatty acids	(Otto, 2009)
Virulence regulators		
agr	Affects lipase and protease production	(Vuong *et al*., 2000)
sar	Regulation of virulence factors production	(Tormo *et al*., 2005)
sigB	Affects biofilm formation	(Knobloch *et al*., 2001a)
Others		
Phenol-soluble modulin (PSM)	Several inflammatory effects	(Cogen *et al.*, 2010)
Staphyloferrin A and B	Siderophores: iron uptake	(Konetschny-Rapp *et al*., 1990)
SitABC	Possibly involved in iron uptake	(Massonet *et al*., 2006)
Lantibiotics (epidermin, Pep5)	Possibly bacterial interference	(Marsh *et al*., 2010)

1.5.2 Biofilm formation in *Staphylococcus aureus*

Biofilm formation in *S. aureus* experiences a similar process to that of *S. epidermidis*; it begins with the initial reversible bacterial adherence to a surface by some non-specific adhesion, followed by an irreversible bacterial specific attachment mediated mainly by an array of MSCRAMMS (Foster and Höök, 1998). Then a mature biofilm is developed characterized by multilayered bacterial cells stuck together and producing extracellular polymeric substances (EPS). In circumstances such as nutrient deprivation, or under heavy shear forces, detachment of clumps of the biofilm bacteria occurs. The released bacterial clumps start to attach to new niches, and initiate a new cycle of biofilm formation (Stoodley *et al.*, 2002).

1.5.2.1 Polysaccharide intercellular adhesin (PIA) mediated biofilm formation in *S. aureus*

Polysaccharide intercellular adhesin was initially purified from *S. epidermidis*. It was identified in *S. aureus* later and shown to have a similar function. Since the structure of the *N*-acetylglucosamine residues in *S. aureus* is shown totally succinylated, it was designated as poly-*N*-succinyl β-1, 6-glucosamine (PNSG) (McKenney *et al.*, 1999).

Polysaccharide intercellular adhesin has been defined as an important virulence factor for *S. epidermidis* pathogenicity in various foreign-body animal infection models (Rupp *et al.*, 2001, Rupp *et al.*, 1999a, Rupp *et al*., 1999b). However, the results showed inconsistency for *S. aureus*: It seems that biofilm formation in methicillin-resistant *S. aureus* (MRSA) is predominantly mediated by surface proteins, which are regulated by *agr* expression, while the *icaADBC*-encoded PIA mediated cell to cell adhesion was suggested to be the major mechanism of biofilm formation in methicillin-susceptible *S. aureus* (MSSA) (Izano *et al.*, 2008). Moreover, PIA production in *S. aureus* did not lead to

an increased persistence of infection in a tissue cage model of infection with this species (Kristian *et al.*, 2004).

1.5.2.2 Surface protein associated biofilm formation in *S. aureus*

Clarke and Foster (2006) demonstrated that most *S. aureus* surface proteins belong to the MSCRAMM protein family and are covalently linked to the cell wall peptidoglycan. A number of surface proteins were found to be involved in the biofilm formation in *S. aureus.* The first protein characterized mediates PIA-independent biofilm formation in *S. aureus* was biofilm associated protein (Bap). It was suggested to be essential for both initial adherence and maturation during biofilm development by the *S. aureus* bovine mastitis isolate V329 (Cucarella *et al.*, 2001). A group of over 100 surface proteins from diverse bacterial species have been found so far which have conserved functional structure with that of Bap protein, and play a similar role in biofilm formation (Lasa and Penadés, 2006).

Other proteins, such as surface protein SasG have shown global similarities to Aap from *S. epidermidis*. Multiple successive repeats were recognized as being responsible for its intercellular adhesin (Gruszka *et al.*, 2012). The N-terminal domain of surface protein C (SasC) was reported to mediate the initial attachment and accumulation of biofilm development (Schroeder *et al*., 2009). A role of protein A in biofilm development was detected and this protein is down-regulated by the accessory gene regulator *agr* (Merino *et al.*, 2009).

Furthermore, *S. aureus* surface protein-mediated biofilm infections were evaluated by different animal model systems. Protein Spa was suggested to be the major factor

responsible for biofilm formation in a murine model of subcutaneous catheter infection (Vergara-Irigaray *et al*., 2009). FnBPA and FnBPB were also found mediate PIA-independent biofilm formation in MRSA strains, and were responsible for biofilm formation in a catheter-associated murine infection model (O'Neill *et al*., 2008).
S. aureus biofilm infections represent a reservoir of *S. aureus* dissemination in the body. Due to the difficulties in treatment and a greater array of virulence factors, *S. aureus* biofilm infections need more intensive care than those of *S. epidermidis*.

1.5.3 Biofilm formation of other coagulase-negative staphylococci

In comparison with *S. epidermidis* and *S. aureus*, biofilm-associated infections with other staphylococci are far less frequent. The underlying molecular basis foreign body-associated infections are largely unknown.

A recent study showed that the biofilm structures are fundamentally different between *S. haemolyticus* and *S. epidermidis*. In *S. haemolyticus*, biofilms were mainly composed of eDNA and protein. An *ica* operon has been identified in *S. haemolyticus*, while its biofilm formation function is not elucidated (Fredheim *et al*., 2009). Similarly in *S. lugdunensis*, (Frank and Patel, 2007) reported PIA was not the major component of the extracellular slime although the homologous *ica* operon has been identified in isolates. Only about 25% of clinical isolates are capable of producing *icaADBC* encoded PIA in *in vitro* studies (von Eiff *et al*., 2002).

In addition, cell surface proteins have been suggested to play a significant role in cell attachment in other CoNS species. *S. saprophyticus* is more capable to adhere specifically to uroepithelial cells than other staphylococcal species. Several surface

proteins have been identified to mediate this binding. One is a 160KDa surface-exposed protein, designated Aas. Its amino acid sequence is homologous to the Atl and AtlE from *S. aureus* and *S. epidermidis*, respectively. Protein Ssp is identified in nearly all clinical isolates, and proved to have adhesive properties. Protein Sdrl is highly homologous in sequence and structure to the Sdr proteins from *S. aureus* and *S. epidermidis* and was confirmed to possess adhesive features. Furthermore, a previous study revealed that *S. schleiferi* expresses cell-wall-anchored fibronectin-binding protein which mediates adhesion in this species (Peacock *et al.*, 1999). A series of virulence factors of CoNS were summarized in Table 1.4.

In general, the molecular basis of biofilm formation is largely unknown in other coagulase-negative *staphylococcus* species other than *S. epidermidis*, they probably follow the similar basic principles to that of *S. epidermidis* and *S. aureus*, while different for some specific molecular determinants.

Table 1.4. Virulence factors present in coagulase-negative staphylococci

Species	Virulence Factors	Functions	References
S. saprophyticus	autolysin Aas	Mediates adherence to fibronectin and promotes haemagglutination.	(Hell *et al.*, 1998)
	Ssp (*S. saprophyticus* surface-associated protein)	Produces of surface-associated material, clumping, and binding to uroepithelial cells.	(Gatermann *et al*., 1992)
	Urease	Damaging bladder tissues. Has of lipase, elastase, and FAME activity.	(Gatermann and Marre, 1989)
S. haemolyticus	Gonococcal Growth Inhibitor (GGI)	Cause cytoplasmic leakage of gonococcal cells.	(Frenette *et al.*, 1984)
S. lugdunensis	Slush (*S. lugdunensis* synergistic haemolysin)	Similar to PSM-β of *S. epidermidis*, and to GGI of *S. haemolyticus*	(Donvito *et al*., 1997)
S. warneri	Lipase	Similar to other staphylococcal lipases, shows broad substrate specificity.	(Talòn *et al.*, 1995)
S. simulans	Lipase, FAME, and urease	Damaging bladder tissues, similar to other staphylococcus, cause a variety of animal as well as human infections.	(Gatermann and Marre, 1989
S. capitis	Lipase and FAME	Similar to other staphylococcus lipases	(Gatermann and Marre, 1989
S. hominis	Esterase, lipase, FAME, and urease	Similar to other staphylococcus lipases	(Gatermann and Marre, 1989
S. cohnii	Lipase and FAME;	Similar to other staphylococcus lipases	(Gatermann and Marre, 1989
	Lantibiotic	Similar to epidermin	(Furmanek *et al.*, 1999)
S. saccharolyticus		Cause anaerobic endocarditis and bacteremia	(Krishnan *et al*., 1996)

1.6 Genetic regulation of polysaccharide and protein biofilms of staphylococci

A number of environmental signals have been identified that guide biofilm formation in bacteria. Some of which have been extensively studied in *Staphylococcus* spp.

1.6.1 Signals inducing biofilm formation in staphylococci

1.6.1.1 Glucose and related sugars

Glucose and related sugars are essential nutrients for the metabolism of many organisms, where they function in numerous processes. Some bacteria use sugar as a source of energy, others use them to build and repair cells. These substances are also proved to have various effects on bacterial biofilm formation depending on species. They are biofilm inducers in some bacteria such as *Streptococcus mutans*, *Staphylococcus aureus*, and *Staphylococcus epidermidis* (Lim *et al.*, 2006, Shemesh *et al.*, 2007). Mack *et al*. (1992) observed that glucose induced adherence to plastic surfaces in a time-dependent manner, using stationary-phase cultures of *S. epidermidis* in a medium lacking glucose. Glucose and other sugars serve as biofilm inhibitors in some bacteria, for example, *P. aeruginosa* and *P. aureofaciens* (Dusane *et al*., 2008).

1.6.1.2 Iron acquisition

Iron is an important nutrient for bacteria, yet it is toxic to bacteria at higher concentrations. As with almost all bacteria, *Staphylococcus* spp. is dependent on iron acquisition for growth. Bacteria colonizing or infecting humans have invented two principle mechanisms to deal with the low availability of iron in human body fluids. The first involves high affinity iron binding molecules called siderophores and specific import systems, to which siderophore/iron complexes bind (Miethke and Marahiel, 2007). The second mechanism

depends on direct binding of transferrin to a membrane bound bacterial receptor (Otto, 2004).

Bacterial biofilm formation has been shown to be influenced by iron in some bacteria. Banin *et al.* (2005) has shown that a certain level of intracellular iron was critical for iron-signalling pathway, and hence for biofilm development in *Pseudomonas aeruginosa.* Fur protein has been identified in many bacteria. This protein functions as a global regulator for iron responsive genes. In *Pseudomonas* spp. the *fur* gene was shown to be essential for biofilm formation, and was also found to be involved in the regulation of biofilm formation at low iron conditions in *S. aureus* (Johnson *et al*., 2008).

1.6.1.3 Stress-inducing stimuli (anaerobiosis, osmolarity, ethanol, temperature and antimicrobials)

Several studies demonstrated the effects of oxygen on the biofilm formation in *Staphylococcus* spp. Cramton *et al.* (2001) observed increased biofilm production in both *S. epidermidis* and *S. aurues* under anaerobic conditions *in vitro*. They further demonstrated that the increased activity of σ^B under the anaerobic conditions, repressed the transcription of the negative regulation *icaR*, and augmented *icaADBC* expression, leading to a more biofilm production. However, this regulation was more stringent in *S. epidermidis*. It was suggested that the staphylococcal respiratory response regulator (SrrA) in *S. aureus* can directly promote *ica* transcription under anaerobic conditions, without modulating the *icaR* expression, therefore σ^B appeared less important under anaerobic conditions in this species. Moreover, Cotter and his colleagues made a similar observation of the influence of oxygen on biofilm development via activated σ^B, by using a rotating-disk reactor, a more precise system which controls the concentration of dissolved

oxygen. It seems that the activity of σ^B is greater under low-oxygen conditions in *S. epidermidis* (Cotter *et al.*, 2009).

It was shown that environmental osmolarity played a significant role in biofilm formation in *S. epidermidis*. PIA synthesis and biofilm formation were up-regulated under high osmolarity (Knobloch *et al.,* 2001), likely mediated through the σ^B, where *rsbU*, the first gene of σ^B was induced by NaCl or/and glucose. It has been shown in *S. epidermidis* that the *rsbU* mutants M 15 and 8400 M15 were completely deprived of the capability of biofilm formation. However, another biofilm inducer, ethanol appeared to promote biofilm formation through an *rsbU* independent pathway, by modulating the negative regulator IcaR. In addition, Møretrø *et al.* (2003) revealed that quantitative biofilm production in *S. capitis* is linearly induced by sodium chloride.

Several antimicrobial agents are biofilm inducers in *S. epidermidis in vitro.* Sub-inhibitory concentrations of tetracycline, erythromycin, clindamycin, semisynthetic streptogramin, quinupristin-dalfopristin were all found to significantly enhance *ica* expression in *S. epidermidis* (Rachid *et al*., 2000, Wang *et al*., 2010)

1.6.2 Global regulators of biofilm formation in staphylococci

1.6.2.1 Sigma factor (σ^B)

The alternative sigma factor, σ^B, is the best studied global regulator for stress response. It is activated by a serial of relayed signals stimulated by stress, and this confers the protection of the cells against adverse conditions (Francez-Charlot *et al.*, 2009).

Once a stress is sensed, the σ^B will interact with core RNA polymerase and initiate the transcriptions of σ^B regulons. σ^B regulons then produce protective protein for the cells. Here is an overview of this process (van Schaik and Abee, 2005) (Figure 1.3):

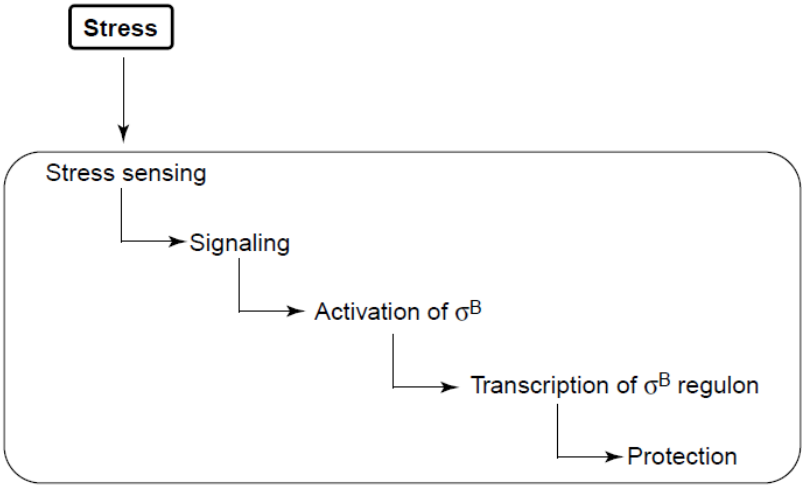

Figure 1.3. The pathway leading to the activation of σ^B. Adapted from (van Schaik and Abee, 2005).

The σ^B operons of *S. epidermidis* and *S. aureus* are homologous to the four genes of *B. subtilis*, *rsbU*, *rsbV*, *rsbW* and *sigB* (Figure 1.4). RsbU and RsbV are positive σ^B factors and RsbW is a negative factor in both *Staphylococcus* species (Knobloch *et al*., 2004), similar to that of *B. subtilis*.

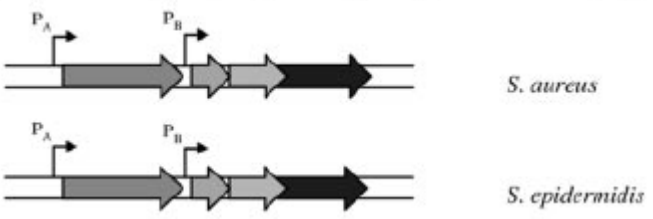

Figure 1.4. σ^B operon structures in *S. aureus* and *S. epidermidis*. Adapted from (Kazmierczak *et al.*, 2005).

Based on the knowledge of *B. sutilis*, RsbV is normally inactivated by RsbW phosphorylation, in the form of RsbV-P, and leaving the latter complex with σ^B**,** thus σ^B is unable to bind to RNA polymerase core enzyme to initiate transcription. Whenever stress is signalled, the positive σ^B factor, RsbU, becomes activated and specifically dephosphorylates RsbV-P, and complexes with RsbW, therefore releasing σ^B, then leaving the latter free to interact with RNA polymerase.

Conflicting results were obtained on the role of σ^B in biofilm formation in *S. aureus*. Data from three *S. aureus* strains using full-genome microarray revealed that a number of cell adhesion genes have been recognized being up-regulated by σ^B, and increasing biofilm formation in these strains (Rachid *et al.*, 2000). However, Valle *et al.* (2003) observed no differences in PNAG production and biofilm formation between a σ^B mutant and its isogenic wild-type strain.

In *S. aureus*, although the mechanism of σ^B operon activation remains unclear, RsbU is essential in these serial reactions, however, the mechanism is different from that of the homologous RsbU in *B. subtilis*. Studies on *S. aureus* mutants of *rsbU* and *rsbV* revealed

that an unidentified factor may exist regulating RsbV expression, and this is independent of RsbU (Senn *et al.*, 2005).

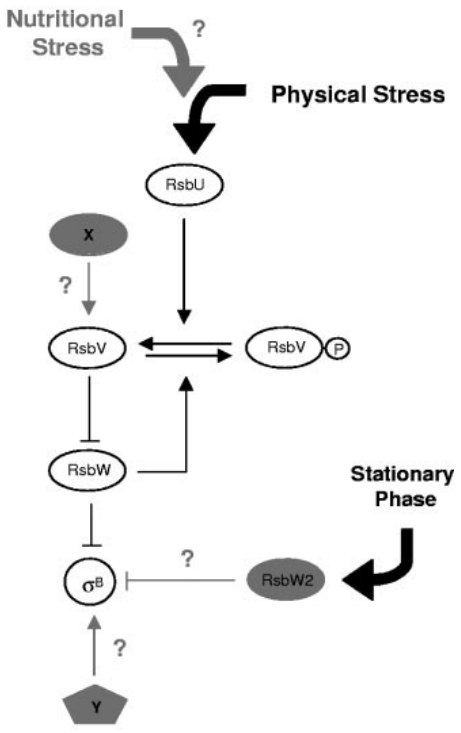

Figure 1.5. A model for the regulation of σ^B in *S. aureus*. Adapted from (Senn *et al.*, 2005).

Studies in *S. epidermidis* suggested that σ^B primarily functions through its influence on biofilm formation in this species. They suggest that the effect of σ^B on *ica* expression could be indirect, as the *ica* promoter does not appear to contain a consensus σ^B binding site. Conlon *et al.* (2002) demonstrated that stress induction of σ^B in *S. epidermidis* increased biofilm formation and synthesis of PIA by alleviation of IcaR-repression, and therefore increased *icaADBC* operon expression by stimuli such as ethanol but not in response to others (e.g. NaCl). These findings may suggest that σ^B plays a more important role in biofilm regulation in *S. epidermidis* than in *S. aureus.*

1.6.2.2 Structure and biofilm regulation of *sarA* locus in *Staphylococcus* species.

Bayer *et al*. (1996) described a global regulator, SarA, which controls numerous expressions of other virulence determinants in *S. aureus*, such as a-hemlysin, protein A, and fibronectin-binding proteins. The functional *sar* locus in *S. aureus* was shown to be a 1.2 Kb fragment, containing three overlapping transcripts designated sarA (0.58 kb), sarC (0.84 kb), and sarB (1.15 kb). These transcripts originated from three distinct promoters (P_2, P_3 and P_1), have common 3' ends, and all encode the major 372-bp *sarA* open reading frame (Figure 1.6). SarA up- or down- regulates its target genes by binding its consensus SarA recognition motif to the target promoter regions.

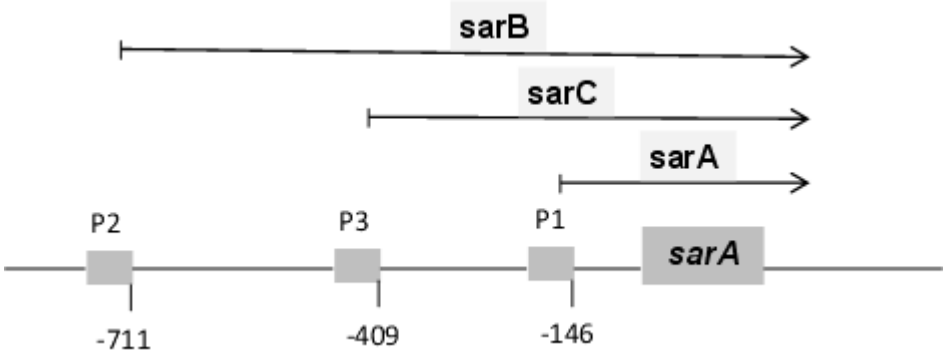

Figure 1.6. The map of the *sar* region in *S. aureus*. P1, P2, and P3 represent promoters. The arrows represent the *sar* transcripts. The distances between the 5' ends of the transcripts and the start codon of *sarA* are expressed by negative position numbers (Cheung *et al*., 2008)

SarA has been shown to be crucial for biofilm formation in *Staphylococcus* spp. As shown by Beenken *et al.* (2004), in *S. aureus*, the SarA protein binds specifically to the *bap* promoter region and regulates the expression of the *bap* gene, which encodes Bap, involved in biofilm formation. *sarA* mutants diminished the capability of Bap-dependent biofilm formation. In *S. epidermidis*, SarA has been shown by electrophoretic mobility shift assays to directly up-regulate the transcription of the *ica* locus by specifically binding to the *icaA* promoter region (Tormo *et al*., 2005).

A recent study by Weiss *et al.* (2009) showed a *sarA* mutation led to a significant increase in antibiotic susceptibility in *S. aureus* in the specific context of biofilm formation. This suggests inhibitors of *sarA* could have the capacity to enhance the efficacy of antimicrobial therapy of a *S. aueus* biofilm-associated infection. This finding demonstrated the importance of SarA-regulated biofilm formation in staphylococci in another way.

1.6.2.3 Quorum signals

Among bacterial global regulatory systems, cell-cell communication or quorum-sensing (QS) systems have gained broad attention in the scientific community.

agr *QS system*

Staphylococci have one well-characterized QS system called *agr* for accessory gene regulator (Figure 1.7) which controls the expression of virulence and other accessory genes by a classical two-component signalling module. Like QS modalities in other Gram-positive bacteria, *agr* encodes an autoactivating peptide (AIP), the inducing ligand for AgrC, and the *agr* signal receptor. Unlike other such systems, *agr* variants have shown strong cross-inhibition in heterologous combinations with important evolutionary implications. Also, unlike other systems, the effector of global gene regulation in the *agr* system is a major regulatory RNA, RNAIII.

i. Structure of *agr* system

As in other gram-positive bacteria, the *agr* system structure contains two divergently transcribed units, RNAII and RNAIII, the transcription of which is driven by the P_2 and P_3 promoters, respectively (Bischoff *et al*., 2001). The RNAII contains four genes, *agrB*,

agrD, *agrC*, and *agrA*. AgrA and C constitute a classic two-component signalling module (TCS), and the AgrB and D combine to generate the activating ligand AIP. The AIP is an autoinducing peptide of ~8 amino acids in length, which is encoded within the *agrD* gene. The staphylococcal AIP binds to a transmembrane protein, AgrC, which acts as the sensor kinase of the bacterial two-component regulatory system. Upon binding to the AIP, AgrC activates the response regulator, AgrA, which in turn induces the transcription of RNAII and RNAIII. AgrA is a DNA-binding protein that recognizes a pair of direct repeats with a consensus sequence 5 ‘ -ACAGT-TAAG-3 ‘ separated by a 12-bp spacer region. It is generally believed that RNAIII is the effector molecule of the accessory gene regulation.

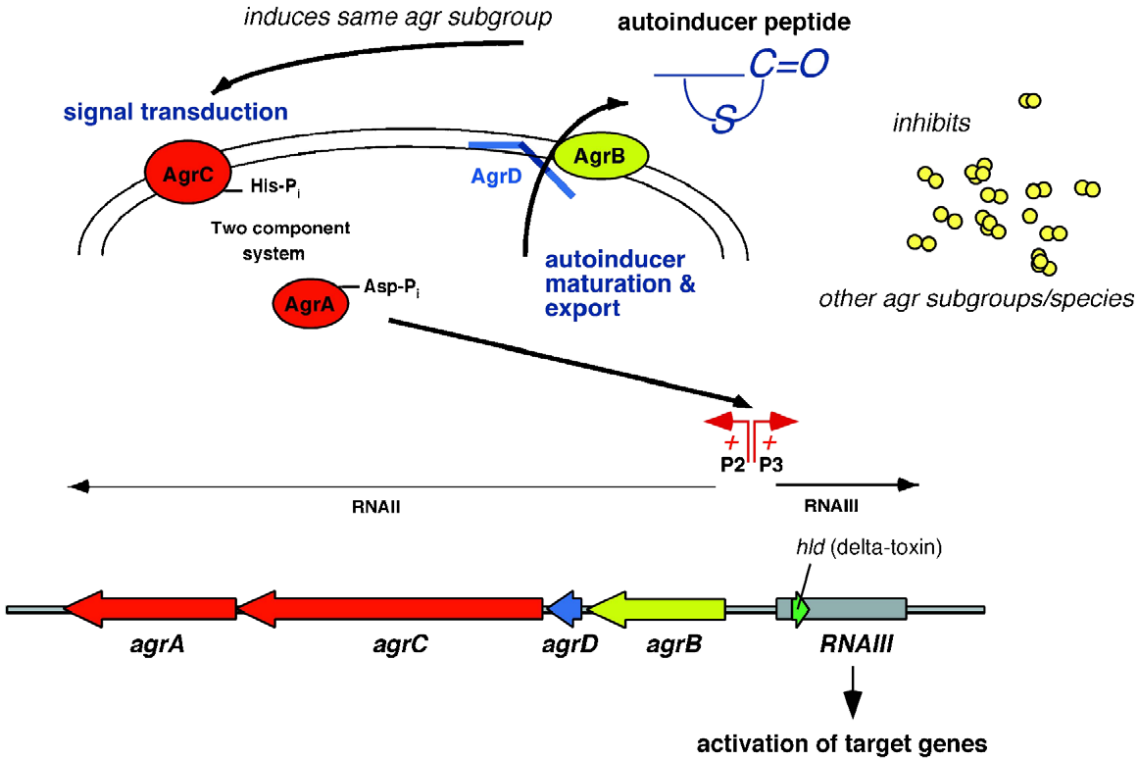

Figure 1.7. the staphylococcal *agr* quorum-sensing system. The extracellular signal of the *agr* quorum-sensing system is a posttranslationally modified peptide autoinducer, which contains a thiolactone or, in one case, a lactone ring structure. The membranelocated enzyme AgrB is responsible for the maturation and export of the autoinducing peptide. AgrA and AgrC form a twocomponent signal transduction system, which in an auto-regulatory fashion, after binding of the autoinducer to AgrC, is responsible for a rapid increase of *agr* activity at the onset of stationary growth phase. Target genes are controlled by a regulatory RNA molecule, RNAIII, in a yet unknown way. The RNAIII region contains a gene (*hld*) coding for the peptide delta-toxin (PSMg), the expression of which does not affect the quorum-sensing mechanism. Adapted from (Kong *et al.*, 2006a).

ii. The role of *agr* system in staphylococcal biofilm formation

The QS system plays an important role in staphylococcal biofilm formation (Novick and Geisinger, 2008), and mediates biofilm formation at different stages. The *agr* system facilitates the initial attachment of staphylococci to a polystyrene surface, due to the up-regulation of attachment and down-regulation of detachment molecules. The surface-attached AtlE protein, a member of the staphylococcal autolysin family, is overexpressed in an *agr* mutant of *S. epidermidis*. In contrast, the homologous Atl protein in *S. aureus* is not under *agr* control, showing that the *agr* regulons of the two species comprise different genes. However, the production of PIA is not regulated by the *agr* system in either species (Vuong *et al.*, 2000)

luxS *QS system in staphylococcal biofilm formation*

Apart from *agr* system, the *luxS* QS system has been identified in a variety of Gram-negative and Gram-positive bacteria. In *S. epidermidis, luxS* appears to function in a way similar to *agr* system in biofilm formation. The *luxS* mutant strain formed a thicker and more compact biofilm than its isogenic wild-type strain and was a more successful colonizer in an animal model of central venous catheter infection. However, different from the effects of *agr*, *luxS* affects biofilm formation by down-regulation of the *ica* gene locus and thus, by reducing production of PIA (Xu *et al*., 2006a).

In sum, QS systems have manifested numerous impacts on staphylococcal virulence, by regulating the expression of a number of toxin and other virulence factors in pathogenic staphylococci. Also, QS has shown to enhance biofilm detachment in staphylococci. In *S. epidermidis*, both the *luxS* and *agr* QS systems have shown a similar mode of regulation of biofilm formation. *luxS* represses biofilm by down-regulating PIA synthesis (Xu *et al*.,

2006a), and *agr* by up-regulation of a detergent-like substances. It was shown that QS systems control different regulons in *S. epidermidis* and *S. aureus*. It is crucial to analyse the entire regulons of QS systems and other regulation systems, and their interaction in a genome-wide manner. This will facilitate the finding of new therapeutic strategies for staphylococcal infections.

1.6.2.4 Other regulatory loci that regulate biofilm formation in staphylococci

Apart from the regulation systems mentioned above, several other regulatory loci have been summarized in Table 1.5.

Table 1.5. Other regulatory loci in staphylococci

Regulator	Mechanism	Reference
icaR	*icaR* encodes a transcriptional repressor, down-regulates *ica* operon expression related to environmental factors in *S. epidermidis.*	(Conlon *et al*., 2002)
tcaR	TcaR bound to the *ica* promoter region, appeared to be a weak negative regulator of transcription of the *ica* locus.	(Chang *et al.*, 2010)
codY	CodY represses *icaA* expression in exponential phase, the regulation is independent IcaR.	(Majerczyk *et al*., 2008)
spx	Spx is a repressor of polysaccharide intercellular adhesion in *S. aureus* by modulating the expression of *icaR* gene.	(Pamp *et al.*, 2006)
rbf	Rbf belongs to the AraC/Xyls family regulators. It is not known which gene involved in biofilm formation are regulated by Rbf.	(Luong *et al*., 2009)
mgrA	Mgr represses biofilm formation by partially regulating *agr* system RNAIII.	(Trotonda *et al*., 2008)
LytSR regulatory system	LytSR two-component system down-regulates the formation of matrix-associated eDNA in the biofilm in *S. aureus*.	(Sharma-Kuinkel *et al*., 2009)
clp proteases	Biofilm formation was reduced in the absence of ClpX or ClpC whereas it was enhanced in the absence of ClpP with unknown mechanisms in *S.aureus*.	(Frees *et al*., 2004)

1.7 Anti-biofilm strategies

Biofilm formation on medical devices contributes significantly to the difficulties encountered in treatment. Once established, device-related infections are almost impossible to eradicate. Numerous strategies have been developed to decrease the incidence of medical device related infection.

1.7.1 Development of new devices

Due to the complex mechanisms underlying specific adhesion, most approaches developed recently are focused on surface modifications of medical devices, where it is hoped to reduce the incidence of microbial adherence. The main targets are physical-

chemical modification of device surfaces and anti-infective agents coating the surface of biomaterial. However, the success is modest due to the diverse ways of bacterial colonization. It was found that the reduction of bacterial adherence by chemical and physical modification is species specific. The effect of coating with anti-infective agents is limited only to the initial batch of incoming bacteria; the bactericidal efficacy tends to be weak once dead cell layers form (Costa *et al.*, 2011).

Recently, biosurfactants turned out to be a promising approach preventing microbial adherence on medical devices because of both their surface modification properties and antimicrobial activity. The use of biosurfactants has been evaluated by numerous researchers. Biosurfactants produced by lactic acid bacteria have been shown to exert anti-adhesive ability against 76.8% of *S. aureus* and 72.9% of *S. epidermidis* (Gudiña *et al.*, 2010). However, insufficient data on toxicity to humans and the cost of large scale production are the constraints for using biosurfactants.

1.7.2 Targeting staphylococcal biofilm factors

Studies have also been involved in targeting the biosynthesis of factors related to staphylococcal biofilm formation. Burton *et al*. (2006) found that the GlmU inhibitors possessed a universal property of prevention of biofilm formation on medical devices in a range of pathogens. Additionally, dispersin B is an enzyme with anti-adhesive property, was initially found in *Actinobacillus actinomycetemcomitans* was evaluated by (Kaplan, 2010). Lysostaphin has been used for detachment of mature biofilm structures and killing of the released bacteria (Wu *et al.*, 2003). Moreover, biofilm components of *S. epidermidis* including PIA, cell wall proteins and adhesins have been used as the targets

for vaccine development against biofilm infections. However, the results obtained so far are controversial due to the versatility of this organism.

In sum, there is no guaranteed solution to increase the anti-biofilm properties of medical device, although the use of biosurfactants seems to be a promising method. The structure-function relationships as well as binding ability to the device surfaces are still challenges for the future research.

1.7.3 Vaccination

Whether immunoprophylaxis is a promising strategy for the prevention of staphylococcal device-related infections is controversial. Surface-expressed components of *S. epidermidis*, including PIA, techoic acids, proteinaceous adhesins and CWA proteins, have been identified as promising targets for vaccine development and immunomodulation (Götz, 2004). As multiple determinants are involved in the establishment of *S. epidermidis* biofilm formation, given the extraordinary versatility exhibited by this microorganism, further investigations, both pre-clinical and clinical, are warranted before an optimal approach is achieved.

1.8 Conclusions

A large amount of recent research has illustrated the key structural and regulatory factors mediating *Staphylococcus* spp. biofilms. PIA is the best characterized and most crucial determinant of staphylococcal biofilm infection by far; although a range of other factors have been identified. Additionally, animal models mimic the reality of *in vivo* environment and provide a better understanding of the detailed roles of particular components in a biofilm infection. Finally, genome wide approaches facilitate our understanding of biofilm

physiology in greater details and constitute the molecular basis for the development of anti-staphylococcal drugs and vaccines.

1.9 Objectives of the current project

Staphylococcus capitis has received increasing concern due to its heteroresistance to vancomycin (Van Der Zwet *et al*., 2002), has been implicated in infections associated with biofilm such as catheter-related bacteraemia, endocarditis, necrotizing enterocolitis in neonates and others (Nalmas *et al.*, 2008). This species can be further divided into two subspecies subsp. *urealyticus* and subsp. *capitis*. The two subspecies are distinct primarily by five properties: the urease activities, abilities to produce acid from maltose in anaerobic conditions, fatty acid profiles, colony sizes, and their DNA sequences differentiation (BANNERMAN and KLOOS, 1991). *S. capitis* can bind to a variety of human matrix proteins, including laminin, collagen and fibrinogen. The first collagen-binding Sdr protein was identified in *S. capitis*. SdrX, a member of the Sdr family of MSCRAMM proteins, has the typical features of other staphylococcal surface-associated proteins, i.e. the serine-aspartate repeat regions and the LPXTG amino acids motif (Liu *et al*., 2004)

In contrast to *S. epidermidis*, the molecular basis of the virulence of *S. capitis* in general and in the context of foreign material-associated infections is largely unknown. The presence of an *ica* operon in *S. capitis* has been reported, but to date its contribution to biofilm formation is unclear. *S. capitis* displays biofilm-forming capacity under experimental conditions only in media with high osmolarity. Quantitative biofilm production is linearly induced by sodium chloride (Møretrø *et al*., 2003). This suggests biofilm formation in *S. capits* is subject to the regulation by certain environmental factors.

Biofilm formation is considered the most important virulence factor in CoNS foreign material-associated infections. The study of biofilm characterization in clinical *S. capitis* isolates of both subspecies, its relation to the antibiotic resistance and also the regulation of biofilm formation under realistic clinical conditions may facilitate improvement in the therapy efficacy and a better control of hospital infections of this species. The topics examined to achieve the aims of this thesis were:

(i) examine the molecular epidemiology, antibiotic resistance and biofilm capacity of clinical isolates of *S. capitis* in a neonatal intensive care unit,

(ii) determine the prevalence of the *ica* operon in these clinical isolates by PCR,

(iii) compare the *ica* operons of biofilm-positive and biofilm-negative isolates by PCR-RLFP and sequencing,

(iv) use bioinformatics tools to analyse the function of the Ica proteins of *S. capitis*,

(v) examine the role of the *ica* operon in biofilm production by *S. capitis* by gene knock-out,

(vi) examine the effect of sub-inhibitory concentrations of erythromycin of expression of the *ica* gene.

CHAPTER 2

General Materials and Methods

2.1 Clinical *Staphylococcus capitis* isolates

A total of 60 clinical isolates consisting of 52 of subspecies *urealyticus* and eight of *capitis* were used in this thesis. These isolates were labelled as where they were collected from the Neonate Intensive Care Unit (NICU), Royal Children Hospital (RCH), Melbourne, Australia. All isolates had been previously assured as clinically significant, causes of bloodstream infection in babies.

The isolates were cultured on Tryptone Soya Agar or Nutrient Agar plates (Oxoid, Australia) for 24-48 hours at 37 °C. For long term storage, bacterial cultures were mixed with 15% glycerol in a cryotube and frozen at -80 °C.

2.2 General Materials

Table 2.1 General kits

Reagents and kits	Supplier
QIAEX® II Gel Extraction Kit	QIAGEN Pty Ltd - Australia
QIAquick® Gel Extraction Kit	QIAGEN Pty Ltd - Australia
QIAprep® Spin Miniprep Kit	QIAGEN Pty Ltd - Australia
RNeasy® Mini Kit	QIAGEN Pty Ltd - Australia
RNeasy® Protect Bacteria Mini Kit	QIAGEN Pty Ltd - Australia
Taq DNA Polymerase	QIAGEN Pty Ltd - Australia
TURBO DNA-*free*™	Applied Biosystems, Australia
Wizard® PCR Preps DNA Purification System	Promega, Australia

Table 2.2 General chemicals, media and solutions

Chemicals, media and solutions	Supplier
Acetic Acid Glacial	Merck Pty Limited, Australia
Agar Bacteriological (NO.1)	Oxoid, Australia
Agarose (Electrophoresis)	Bioline (Aust) Pty Ltd
Ampicillin	Sigma-Aldrich, Australia
Ammonium Oxalate	Sigma-Aldrich, Australia
Bigdye Premix (V3.1) for DNA Sequencing	Monash University, Australia
Brain Heart Infusion Broth	Oxoid, Australia
Cetyl Trimethyl Amnomium Bromide (CTAB)	Sigma-Aldrich, Australia
Crystal Violet	Sigma-Aldrich, Australia
Deoxynucleotide Triphosphate Mix (dNTP),	Bioline (Aust) Pty Ltd
Diethyl pyrocarbonate (DEPC)	Sigma-Aldrich, Australia
Electroporation Cuvette	Molecular Bioproducts, U.S.
Ethanol Absolute GR for Analysis	Sigma-Aldrich, Australia
Ethidium Bromide	Sigma-Aldrich, Australia
Ethylenediaminetetra acetic acid (EDTA)	Sigma-Aldrich, Australia
Formaldehyde 37% (12.3 M)	Sigma-Aldrich, Australia
Formamide	Sigma-Aldrich, Australia
Glycerol	Sigma-Aldrich, Australia
Isopropyl Alcohol	Sigma-Aldrich, Australia
Kanamycin	Sigma-Aldrich, Australia
Lambda DNA	Promega Corporation, Sydney, Australia
Lysostaphin from *Staphylococcus staphyloliticus*	Sigma-Aldrich, Australia
MassRuler™ Low Range DNA Ladder, 1Kb	Thermo Fisher Scientific, Australia
6 x MassRuler™ DNA Loading Dye	Thermo Fisher Scientific, Australia
β-mercaptoethanol	Sigma-Aldrich, Australia
3-[N-morpholino]propanesulfonic acid (MOPS)	Sigma-Aldrich, Australia
Nuclease Free Water	QIAGEN Pty Ltd - Australia
Phenol-Chloroform for DNA Isolation	Sigma-Aldrich, Australia
Phosphate Buffered Saline (PBS)	Sigma-Aldrich, Australia
Proteinase K	Sigma-Aldrich, Australia
Restriction Enzymes	New England Biolabs and Promega, Australia
RNAse A, DNAse Free	Promega Corporation, Sydney, Australia
Sodium acetate	Sigma-Aldrich, Australia
Sodium Chloride	Astral Scientific, Australia

Sodium Dodecyl Sulfate (SDS)	Sigma-Aldrich, Australia
Sodium Hydroxide Pellets	Merck Pty Limited, Australia
Sucrose	Sigma-Aldrich, Australia
T4 DNA ligase (400,000 cohesive end units/ml)	New England Biolabs
T4 ligase buffer	New England Biolabs
Trizma Base	Sigma-Aldrich, Australia
Tryptone	Oxoid, Australia
Tryptone Soy Broth	Oxoid, Australia
Uvette	Crown Scientific, Australia
Yeast Extract	Oxoid, Australia

2.3 Oligonucleotides

All the oligonucleotides used for PCR, sequencing and cloning were designed in-house with the software, Clone Manager 7, Version 7.11 and obtained from Sigma-Aldrich, Australia. The lyophilized powder was reconstituted at 100 µM in nuclease free water, and then diluted to 10 µM at working concentration, stored in -20 °C.

2.4 General methods

2.4.1 DNA based methods

2.4.1.1 Chromosomal DNA isolation from clinical *Staphylococcus capitis* isolates

The *S. capitis* DNA extraction was carried out according to the CTAB method of (Wilson, 1997) with modifications. Growth from a lawn culture with a bacterial strain of interest was taken off with a wire loop into a sterile eppendorf tube. The bacterial cells were washed with PBS solution once, centrifuged at 13,200 rpm for 2 mins, the supernatant was removed, and the cells were resuspended in 555 µL TE buffer (10 mM Tris-HCl, 1mM EDTA, pH 8.0) thoroughly. Lysostaphin and lysozyme were added at final concentrations 300 µg/mL, and the suspension was incubated at 37 °C for 30 mins to lyse the cell wall.

After incubation, 30 µL of 10% SDS and 3 µL of 20 mg/mL proteinase K were added to give 100 µg/mL proteinase K in 0.5% SDS in the final mixture. After thoroughly mixing, the mixture was incubated 1 hour at 37 °C for cell protein removal. Then 100µL of 5 M NaCl was added, mixed thoroughly for subsequent CTAB-nucleic acid precipitation. Eighty microliters of CTAB/NaCl solution which contains 0.7 M NaCl, 10% CTAB were added. To prepare, 0.7 M NaCl was preheated to 55-65 °C; CTAB was slowly added to dissolve, then the solution was autoclaved, and incubated 10 mins at 65 °C. An equal volume of phenol : chloroform : isoamyl alcohol (25 : 24 : 1) was added to 600 µL of the mixture, mixed thoroughly, and centrifuged at 13, 200 rpm for 5 mins. Five hundred microliters of the top (aqueous) layer was collected and 0.6 volume isopropanol was added. The mixture was inverted a few times and then incubated at room temperature for 10 mins to precipitate the nucleic acids. The precipitated DNA was collected by centrifuging the mixture at 13, 200 rpm for 5 mins. The DNA pellet was washed with 70% ethanol twice and left to air dry for 30 mins. The dried DNA pellet was suspended in an appropriate volume of nuclease free water and stored at -80 °C.

2.4.1.2 Plasmid isolation from *E. coli* recombinant strains

The difference in topology of plasmid DNA and chromosome DNA is the basic mechanism used for selective precipitation of plasmid DNA from chromosomal DNA and proteins. Minipreps were used to extract plasmid from transformed *E. coli* strains according to the method in QIAprep® Miniprep Kit. The procedure is based on alkaline lysis of bacterial cells followed by adsorption of DNA onto silica in the presence of high salt concentrations. Three basic steps are involved: a). Preparation of bacterial lysates, b). Adsorption of DNA on the membrane, then c). Elution of plasmid DNA. Cell lysis is a critical step. Cells were partially lysed using the alkaline solution in the kit; this allows

small MW plasmid DNA escape from the broken cell wall, while large MW genomic DNA remains within the cells, therefore, this step was carried out within just enough time in case the cell wall was completely lysed resulting in genomic DNA contamination. In addition, the operation should be gentle throughout the procedure, otherwise sheared genomic DNA may be released.

Generally, a single colony was first picked from a fresh plate and inoculated in 5-10 mL Luria-Bertani (LB) or nutrient broth containing an appropriate selective antibiotic in a 50-mL falcon tube, and incubated 16 hours at 37 °C, shaking at 170 rpm. The cells were harvested by centrifuging 15 mins at 4700 rpm, 4 °C. The cells were resuspended with 250 µL of cell suspension buffer from the kit, and mixed thoroughly to ensure no cell clumps were visible. The 250 µL of cell lysis buffer was added and mixed by inverting the mixture six times and the suspension was incubated at room temperature for no more than 5 mins. The cell lysis was stopped by adding 350 µL of neutralization buffer and mixed by inverting the tube six times. The cell lysate was then centrifuged at 13, 200 rpm for 10 mins at room temperature. The supernatant was applied on a QIAprep spin column, and then centrifuged at full speed for 1 min. The plasmid DNA was absorbed on the membrane. After washing with alcohol buffer, the DNA was eluted and stored in -20 °C.

2.4.1.3 Measurement of DNA concentration

The concentration of the extracted genomic DNA and plasmid DNA was determined spectrophotometricly using BioPhotometer (Eppendorf AG, Hamburg, Germany). This was carried out by quantifying diluted samples at OD 260 nm. An absorbance of 1.0 corresponds to 50 µg/mL of double stranded DNA. The concentration of DNA can be

determined by the following formula: Concentration of DNA = OD 260 X 50 µg/mL X Dilution factor. The ratio A_{260}/A_{280} provides the purity of DNA; pure preparations of DNA samples have ratios 1.80-2.0. The ratio A_{260}/ A_{230} provides the salt concentration in the sample; low salt samples have ratios between 2.2 and 2.5.

2.4.1.4 General PCR amplifications

Polymerase chain reaction (PCR) amplification of DNA templates was performed according to their relevant applications in the chapters of this thesis.

PCRs were performed using *Taq* DNA polymerase from QIAGEN. Generally, PCR master mixes were prepared containing 1x PCR buffer, 200-250 µM dNTPs, 0.2-0.4 µM of each forward and reverse primer, 2.5 U *Taq* DNA polymerase and 10-100 ng DNA. PCR reactions were performed on a PCR Express thermal cycler at one cycle at 94-95 °C for 5 mins, followed by 25-35 cycles of 94-95 °C, 30 sec; 45-62 °C, 30 sec; 72 °C for 30 sec-3 mins, final elongation 7 mins at 72 °C for 1 cycle and hold at 4 °C.

2.4.1.5 Restriction digestion

Restriction enzymes have their unique DNA reorganization sequences, cleave DNA at specific sites. The restriction digestion was performed by incubation of DNA with the enzymes in a buffer which is appropriate for its optimal performance. To set up a restriction digest with two enzymes, one common buffer was used. The amount of enzyme required and procedure varies depending on DNA samples subjected to digestion. An analytical restriction digestion was usually performed in a volume of 20 µL with 0.2-1.5 µg of substrate DNA and two- to ten-fold excess of enzyme. In a sterile tube the components were assembled as follows: nuclease free water 16.3 µL, restriction

enzyme 10X buffer 2.0 µL, Bovine serum albumin (BSA) 10 µg/mL 0.2 µL and DNA 1 µg/µL1.0 µL, then added restriction enzyme 10 U/µL 0.5 µL, mixed gently by pipetting, centrifuged for a few seconds, incubated at the enzyme's optimal temperature for 2-4 hours.

2.4.1.6 Electrophoresis

All PCR and restriction digestion products were detected on 1-2% agarose according to Sambrook *et al*. (1989) where the products were electrophoresed at constant voltage in 1X TAE running buffer (0.4 M Tris-acetate, 0.01 M EDTA; adjusted pH 8.0 with glacial acetic acid). The gel was stained with 0.5 µg/mL of ethidium bromide for 5-10 mins and photographed using Gel Doc of Quantity One (Bio-rad Laboratories Pty. Ltd., Australia) under UV light.

2.4.1.7 Extraction and purification of DNA from agarose gel

The QIAQuick Gel Extraction Kit was used for purification of the DNA fragments obtained from the agarose gel. QIAquick Kit contains a silica membrane assembly for binding of DNA in high-salt buffer and elution with low-salt buffer or water. The purification procedure removes primers, nucleotides, enzymes, mineral oil, salts, agarose, and other impurities from the DNA samples.

After restriction analysis or after running the PCR product in the agarose gel, the band of expected size was excised from the agarose gel with a clean scalpel and then the protocol given by manufacturers was followed. After purification, approximate concentration of DNA was checked on a 1% agarose gel.

2.4.1.8 Cloning techniques

2.4.1.8.1 Setting up Luria-Bertani (LB) medium and plates

LB medium (pH 7.0) contains 10 g tryptone, 5 g yeast extract and 10 g NaCl per litre of deionized water. After preparation of the medium it was autoclaved at 121 °C, 21 mins. The solution was allowed to cool to 55°C and antibiotic was added if needed. LB agar plates were prepared by adding 15 g/L agar into the above medium before autoclaving. After autoclaving, the medium was cooled to ~55°C, antibiotic was added, and the medium was poured into a plate, let to harden then stored at 4 °C in dark.

2.4.1.8.2 Competent Escherichia coli strains

One Shot® TOP10 Electrocomp™ *E. coli* and DH5α from Invitrogen Australia Pty Limited were applied for plasmid transformation in this study. There follows a brief description about these cells and their genotypes.

One Shot® TOP10 Electrocomp™ *E. coli* cells, genotype is: F^- *mcr*A Δ(*mrr-hsd*RMS-*mcr*BC) φ80*lac*ZΔM15 Δ*lac*X74 *rec*A1 *ara*D139 Δ(*ara-leu*) 7697 *gal*U *gal*K *rps*L (Str^R) *end*A1 *nup*G λ-

These cells do not require IPTG to induce expression from the lac promoter. The genotype of these cells is:

E. coli DH5α, genotype is: F^- endA1 glnV44 thi-1 recA1 relA1 gyrA96 deoR nupG Φ80d*lacZ*ΔM15 Δ(*lacZYA-argF*)U169, hsdR17(r_K^- m_K^+), λ-

This is a suitable strain for plasmid maintenance and growth, and was used to make competent cells for plasmid transformation in this study.

2.4.1.8.3 Preparation of electroporation competent cell with E. coli DH5α

The preparation of *E. coli* DH5α electro-competent cells was carried out according to Hanahan (1983). Briefly, 5-10 mL of autoclaved LB broth (1% w/v Tryptone, 0.5% w/v Yeast extract, 0.5% w/v NaCl, pH 7.0) was inoculated with 3-4 fresh host *E. coli* DH5α colonies, and incubated overnight at 37 °C on a shaker. The overnight culture was diluted 1 : 100 into 200 mL fresh LB broth. The cells were grown with shaking at 37 °C, harvested by centrifugation at 4700 rpm for 15 mins, then transferred to 4 °C when the OD_{600nm} value reached 0.3-0.4. Then the cells were chilled on ice for 30-45 mins to stop the cell growth. The cells were washed twice with 200 mL then 100 mL ice-cold sterile deionized water, respectively. A subsequent wash was performed in 4 mL of ice-cold 10% v/v glycerol. The cell pellet was resuspended in an 800 µL ice-cold 10% v/v glycerol. The cell concentration should be about 1-3 X 10^{10} cells/mL. Finally, 60 µL aliquots of cells were immediately transferred for storage to a -80 °C freezer.

2.4.1.8.4 Ligation of insert into a vector

The plasmid vector and insert DNA were pre-digested respectively with the same enzyme to produce compatible cohesive ends for efficient ligation. Generally, a 50-100 µL digestion reaction was set up. An excess of restriction enzyme and 16 hours incubation were used to cut the DNA fragments. After digestion, the cut vector and insert were run on the same crystal violet gel. To prepare the gel, the agarose gel solution was microwaved, allowed to cool to 65 °C, then 40 µL crystal violet solution (2 mg/mL) was added per 50 mL gel. After running, the DNA bands should be visible directly from the gel, there is no need to visualize the bands under UV light, this is critical to protect the ends of DNA fragments. Then the cut vector and insert were purified by QIAquick Gel Extraction Kit. After this, the same volume of the purified vector and insert were run on

one gel again to determine the ratio of vector and insert used in the subsequent ligation reaction. The amount of DNA was estimated by the brightness of the bands, compared with ladder DNA. Ratios of vector to insert from 1 : 1 to 1 : 12 have been successfully used. Usually, a 20 µL volume of ligation reaction was set up as follows:

Table 2.3. Ligation reaction

Components	Volume
Vector DNA	1 µL (~25 ng)
Insert DNA	4-12 µL (add 1 µL for positive control)
10 X Ligation Buffer	2 µL
Sterile dH_2O	X µL
T_4 DNA Ligase	1 µL

The ligation mixture was incubated at 14 °C for 16 hours, then heated at 65 °C for 10 mins to inactive the enzyme, the ligation product was purified with QIAEX II Kit according to the manufacturer's instruction, and resuspended with 16-20 µL dH_2O.

2.4.1.8.5 Electroporation

Two to five microliters of the above ligation product were used in the electroporation. The electro-competent cells were thawed on ice, and after mixing with DNA, 50-100 µL of the cells were transferred to a 2-mm gap electroporation cuvette and electrotransformed with Bio-Rad MicroPulser (Bio-Rad Laboratories, Australia), using a voltage of 2.5 kV, Ω 200 and capacitance 25 µFD. The complete electroporation procedure was performed at 4 °C, immediately after electroporation, 1 mL of fresh LB broth was added to the cuvette, and the cells were transferred to a 14-mL tube and incubated at 37 °C at 100 rpm for 1 hour for bacterial recovery and induction of antibiotic resistance. Finally, the cells were diluted 1/100 and 1/200 in LB medium, spread on LB agar with appropriate antibiotics, and incubated at 37 °C for 24-48 hours.

Calculation of transformation efficiency:

(Number of colonies on plate/ng of DNA plated)×1000 ng/µg.

2.4.1.8.6 Screening of recombinants

Ten colonies were selected for PCR screening. A 200-µL tip was gently touched on a small portion of each colony, the cells of each colony were suspended in 200-500 µL sterile dH_2O, mixed thoroughly by vertexing, then 1 µL of each of these cell suspensions was used in PCR reactions.

Each 25 µL PCR mixture contained:

Table 2.4. PCR reaction

PCR Component	Final Concentration
dH_2O	X µL
10 X PCR Buffer	1 X PCR buffer
dNTP	200-250 µM
Primer F	0.4 µM
Primer R	0.4 µM
Taq DNA Polymerase	2.5 U
DNA Template	1 µL
Total	**25 µL**

The following PCR program was used: 1 cycle for 94 °C, 10 mins. 30-35 cycles for 94 °C 30 s; 50-60 °C 30 s; 72 °C 30 s-1 min, final extension at 72 °C for 5 min. Then check the PCR products were examined on a 1.0-1.5% agarose.

Minipreps of recombinant plasmid were carried out by using QIAprep Spin Mini Kit. This was performed according to the description in section 2.5.1.2. Then the isolated plasmid

was digested with specific restriction enzymes and run on a gel to examine whether the expected sizes of vector and insert were obtained. And then DNA sequencing was performed for the final confirmation. DNA sequencing was conducted as follows:

Table 2.5. DNA sequencing reaction

Reagent	Quantity
BigDye Premix (3.1)	1 µL
Reaction Buffer (5 X)	3.5 µL
Plasmid DNA	300 ng
Primer	3-5 µmoles
Water	X µL
Total	20 µL

Cycle sequencing: 96 °C for 1 min. 30 cycles: 96 °C for 10 s; 50 °C for 5 s; 60 °C for 4 mins.

After running the program, ethanol/NaOAc precipitation was performed to clean up the sequencing products as follows: For each sequencing reaction, 2.0 µL of sterile 3 M sodium acetate (pH 5.2) and 50 µL of absolute ethanol were added, mixed thoroughly by pipetting and vortexed and left at room temperature for 10 mins to precipate the extension products. The tubes were centrifuged for 20 mins at 13, 200 rpm, then the supernatant was carefully removed and the pellet was washed twice with 250 µL of 70% ethanol. Finally the pellet was air dried for 25 mins at room temperature. The products were then sequenced by 3730 Capillary Sequencer of Micromon DNA Sequencing, Monash University, Australia.

2.4.1.8.7 Glycerol stock of transformants

For long term storage of positive transformants, bacterial cultures were mixed with 15% sterile glycerol and appropriate antibiotics in cryotubes, and frozen down at -80 °C.

2.4.2 RNA based methods

2.4.2.1 RNA isolation from clinical *Staphylococcus capitis* isolates

Total RNA from *S. capitis* isolates was extracted by using glass beads to break the cell wall, following the protocol of the RNeasy Mini Kit in combination with RNAprotect Bacteria Reagent with slightly modifications. The latter provides *in vivo* stabilization of RNA in bacteria to ensure reliable gene expression analysis. Prepared RNA was used for transcriptional analysis.

First, the bacterial cell pellet preparation was carried out using RNAprotect Bacteria Reagent. Bacteria were initially grown in Tryptone Soy Broth (TSB) medium, however, the cell pellets formed were too sticky to be resuspended thoroughly. Brain Heart Infusion (BHI) broth was then used for bacterial growth. All cell pellets were prepared from fresh cultures. The cells were harvested in mid-logarithmic growth throughout the study. Five millilitres of cell suspension was centrifuged at 5000 g, 4 °C, 10 mins, the supernatant was removed, and the cells were resuspended in 1 mL BHI broth. Two millilitres of RNAprotect Bacteria Reagent was added to a 15-mL falcon tube. The mixture was vortexed for 5 s, incubated at room temperature for 5 mins, then centrifuged for 10 mins at 5,000 g, 4 °C. The supernatant was decanted and the pellet was stored at -20 ºC. For the RNA isolation, the prepared bacterial pellets were thawed at room temperature. One millilter of RLT buffer containing β-mercaptoethanol was added to resuspend the cell pellet, and the suspension was transferred into an RNase-free, 2-mL tube containing 0.5

mL glass beads. This was followed by beating for 10 mins at 4 °C with Mini Beadbeater (DainTree Scientific PTY, Australia). The samples were placed on ice for cooling if necessary. Then they were centrifuged for 10 s at 13, 200 rpm, and the supernatant was transferred into a new tube. Then 1000 µL of 80% ethanol was added, mixed by pipetting or shaking vigorously. Subsequently the procedure described in the RNAeasy Mini Kit was followed.

2.4.2.2 Removal of DNA contamination

The TURBO DNA-*free* kit was used to remove any DNA contamination in the isolated RNA as follows: the sample was diluted to 10 µg/50µL nucleic acid. In a 50 µL reaction, 5 µL of 10 X buffer and 5 U of DNase were mixed with 42.5 µL sample, and incubated at 37 ° C for 20 mins. Next 5 µL of DNase Inactivate Reagent was added, incubated at room temperature 2 mins, centrifuged at 10, 000 g, 1.5 mins. Finally, about 42 µL of supernatant was transferred into another RNase-free tube, and stored in -80 °C.

2.4.2.3 Quantification and purity of RNA

The concentration of RNA was determined by measuring the absorbance at 260 nm (A_{260}) in a spectrophotometer. An absorbance of 1 unit at 260 nm corresponds to 44 µg of RNA per mL. The calculation of RNA quantification is shown below: Concentration of RNA sample=44 µg/mL×A_{260}×dilution factor. The ratio of the readings at 260 nm and 280 nm (A_{260}/A_{280}) provides an estimate of the purity of RNA with respect to contaminants that are absorbed in UV spectrum. Pure RNA has an A_{260}/A_{280} ratio of 1.9-2.1 in 10 mM Tris·HCl, pH 7.5.

2.4.2.4 Integrity of RNA

The integrity and size of total RNA was finally checked by denaturing agarose gel electrophoresis and ethidium bromide staining. The respective ribosomal RNAs should appear as sharp bands on the gel. If the ribosomal bands are not sharp, but appear as a smear, it is likely the sample suffered major degradation.

CHAPTER 3

Differences between two clinical *Staphylococcus capitis* subspecies revealed by biofilm, antibiotic resistance and PFGE profiling

3.1 Introduction

Coagulase-negative staphylococci (CoNS) have emerged as major causes of nosocomial infections, and of nosocomial bacteraemia in particular. These microorganisms usually infect premature neonates and immunocompromised patients, particularly those hospitalised for chemotherapy and managed with indwelling devices such as central venous catheters (Pessoa-Silva *et al.*, 2001, Chaves *et al.*, 2005).

Biofilm formation is a major mode of growth for bacteria in many natural and clinical environments, and is generally considered the most important virulence trait of clinical isolates. Research on biofilm formation in *S. epidermidis* started relatively early and has served as a model for other staphylococci, including *S. aureus* and other coagulase-negative staphylococcal species. In contrast to *S. epidermidis*, *S. capitis* displays the biofilm-forming capacity under particular experimental conditions, for example, in media with high osmolarity. Quantitative biofilm production is linearly induced by sodium chloride (Møretrø *et al.*, 2003). Polysaccharide intercellular adhesin (PIA) is the best studied factor involved in *S. epidermidis* biofilm formation. It consists of glycan of beta-1,6-linked 2-acetamido-2-deoxy-D-glucopyranosyl subunits, and its synthesis has been shown to be essential for *S. epidermidis* virulence. The *ica* operon encodes components of PIA, and comprises the *icaA, icaD, icaB* and *icaC* genes, in this order, downstream from the *icaA* promoter that controls expression of the entire operon. In addition, a regulatory gene called *icaR* is located upstream, and is transcribed in the opposite direction (Begun *et al.*, 2007).

Staphylococcus capitis has been implicated in biofilm related infections such as endocarditis (Nalmas *et al.*, 2008), urinary tract infection (Kloos and Bannerman, 1994).

Humans are likely to be the main sources or vehicles of transmission of *S. capitis* (Hira *et al.*, 2010). This species can be divided into two subspecies; subsp. *urealyticus* and subsp. *capitis*. Subsp. *urealyticus* can be distinguished from subsp. *capitis* by its urease activity, ability to produce acid from maltose in anaerobic conditions, fatty acid profile, larger colony size, and DNA sequence differentiation (Bannerman and Kloos, 1991).

Staphylococcus capitis has been endemic in the NICU of the Royal Women's Hospital in Melbourne for several years. The aim of this study was to characterize and compare the two subspecies of *Staphylococcus capitis* isolated from newborn babies with bloodstream infection. This is the first report to investigate the correlation between molecular epidemiology and phenotypic properties in clinical *S. capitis* isolates at a subspecies level.

3.2 Materials and methods

3.2.1 Bacterial isolates and growth conditions

Sixty clinical *S. capitis* isolates from babies at the NICU, Royal Women's Hospital, Melbourne were collected between 2000 and 2005. These isolates were considered to be clinically significant based on the isolation of the same organism from more than one blood culture collected within a 14-day period and/or the presence of clinical or laboratory findings suggestive of neonatal sepsis (Isaacs, 2003).They had been identified by the ID 32 Staph system (bioMérieux, Marcy l'Etoile, France). All isolates were stored in nutrient broth (Oxoid, Australia) with 15% glycerol at -80 °C and were recovered for the present study on tryptone soya agar (TSA) (Oxoid, Australia) incubated at 37 °C for 24-48 hours. Urease activity and maltose fermentation tests were performed to discriminate subsp. *urealyticus* and *capitis* (Bannerman and Kloos, 1991).

3.2.2 Antibiotic susceptibility testing and screening for *mecA* gene

Six antibiotics were chosen for this study based on use in the hospital. These were penicillin, erythromycin, clindamycin, teicoplanin, vancomycin, and oxacillin. Antibiotic susceptibility was determined by minimum inhibitory concentration (MIC) and inducible clindamycin resistance according to Clinical Laboratory Standards Institute guidelines (Wikler, 2006).

The *mecA* gene was detected by PCR, using forward primer MECAP4 and reverse primer MECAP7 (Oliveira and Lencastre, 2002), obtained from Sigma-Genosys, Sydney, Australia. PCRs were performed as described in Chapter 2. Five microliter reaction mixtures were analysed by 1% agarose (Bioline, Australia) gel electrophoresis. Nucleotide sequence determination was performed by Microcom Sequencing Facilities, Monash University, Melbourne.

3.2.3 Detection of biofilm production

Quantitative determination of biofilm production was performed using a microtitre plate assay. Each plate contained *S. epidermidis* RP62a and SP2 as positive and negative biofilm-producing controls, respectively (Christensen *et al*., 1985). In brief, bacteria were inoculated into 10 mL of tryptone soya broth (TSB) (Oxoid, Australia) and incubated overnight with shaking at 37 °C aerobically. This suspension was diluted 1:100 in TSB and TSB with 4% NaCl, respectively, and then 200 μL volumes were inoculated into 96-well polystyrene microtitre plates. The plates were incubated overnight at 37 °C in air, washed, and stained with 1% crystal violet. The optical density of the adherent biofilm was determined at 595 nm using POLARstar Omegar (BMG LABTECH Pty, Ltd., Australia). The phenotype of biofilm formation is categorised by the OD values: strong

biofilm producer, OD ≥ 0.24; weak biofilm producer 0.24 ≥ OD ≥ 0.12; biofilm-negative isolates, OD ≤ 0.12. Four wells were inoculated per isolate in a given experiment, and all isolates were tested independently on three occasions.

Qualitative detection of biofilm formation of these isolates was performed using Congo red agar (CRA), according to Freeman *et al.* (1989). Isolates were streaked onto the agar to obtain single colonies and incubated overnight at 37 °C aerobically and a further 24 hours at room temperature. The interpretation of results followed Freeman *et al.* (1989) and Arciola *et al.* (2002).

3.2.4 PFGE analysis

PFGE was performed according to (Murchan *et al*., 2003) with minor modifications. Approximately $1x10^9$ cells/mL of an overnight TSB suspension of *S. capitis* were mixed with an equal volume of 2.2% low-melting-point agarose (Progen industries Limited, Australia) and poured into the block molds (Biorad, Australia). Plugs for each isolate, 1 mm in diameter were equilibrated in *Sac*II buffer (New England Biolab) at room temperature prior to digestion, and then covered with 80 μLof *Sac*II restriction buffer containing 30 U of *Sac*II restriction enzyme. The reaction tubes were mixed gently and incubated overnight at 37 °C as recommended by the manufacture.

A 1.4% gel was prepared by using PFGE grade agarose (Amresco, Australia) in a 100 mL 0.5 × TBE and poured into a freshly cleaned gel casting frame once the agarose had cooled to 50-60 °C. Once set, the gel was positioned centrally in a contour-clamped homogenous electric field (CHEF) (Bio-Rad, Australia) tank and covered with 2000 mL of 0.5 x Tris/Borate/EDTA (TBE). The running temperature was set at 14 °C. A lamda

marker (New England Biolab) was positioned in every 3 or 4 lanes to allow later normalization of electrophoretic patterns across the gel. The total running time was 23 hours, the initial block switch time was 15 s to 60 s for 13 hours, and the second block switch time was 5 s to 15 s for 10 hours. The voltage for the run was 6 V/cm.

The gels were stained for 45 min in ethidium bromide (1 μg/mL) and destained for 1 hour and photographed using a gel document system (Bio-Rad, Australia). Digital images were stored electronically as JPG files and analysed visually with GelCompare (Applied Maths), using the Dice coefficient, represented by UPGMA with 1% optimization and 1.5% tolerance setting. Of cut-off values 75% and 80% were applied to assess similarity.

3.2.5 Statistical analysis

Antibiotic susceptibility experiments were performed at least twice. A binary logistic regression analysis was performed to assess whether the biofilm formation and antibiotic resistance was associated independently with the two subspecies, and how the biofilm formation related to the antibiotic profile. Statistical analyses were performed using GraphPad Prism 5.0 (Motulsky, 1999). This program computes *P* values using Fisher's exact test contingency table and summarizes the data by computing the odds ratio along with 95% confidence intervals.

3.3 Results

3.3.1 Molecular epidemiology of clinical *Staphylococcus capitis* isolates over 6-year period

Isolates were obtained from blood cultures from sixty episodes of sepsis at the NICU, Royal Women's Hospital, Melbourne, between 2000 and 2005 (5 from 2000, 11 from 2001, 16 from 2002, 14 from 2003, 10 from 2004 and 6 from 2005). Initially, the *Sma*I restriction enzyme was applied to 20 of the *S. capitis* isolates, but failed to differentiate adequently between these isolates (Figure 3.1). As this suggested the sequence recognized by *Sma*I is highly conserved in the *S. capitis* genome, the *Sac*II enzyme was used to analyse all 60 isolates as it provided substantial discrimination (Figure 3.2).

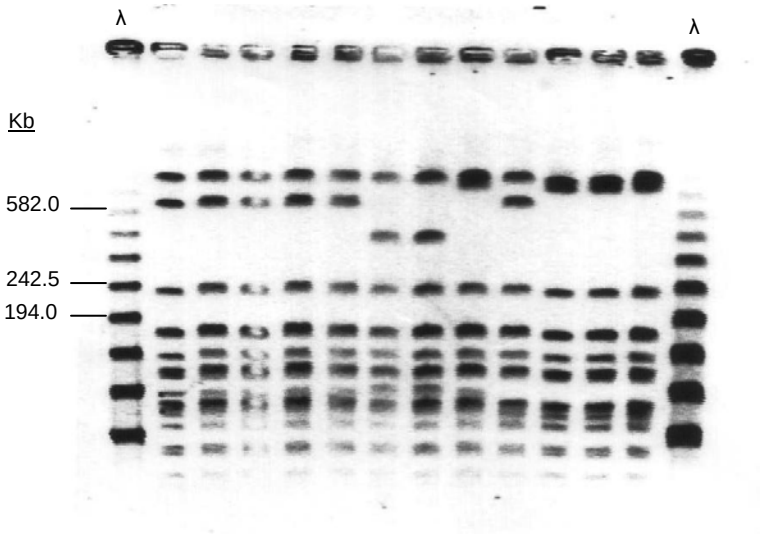

Figure 3.1. PFGE digested with *SmaI* in *S. capitis.* λ, λ PFGE marker.

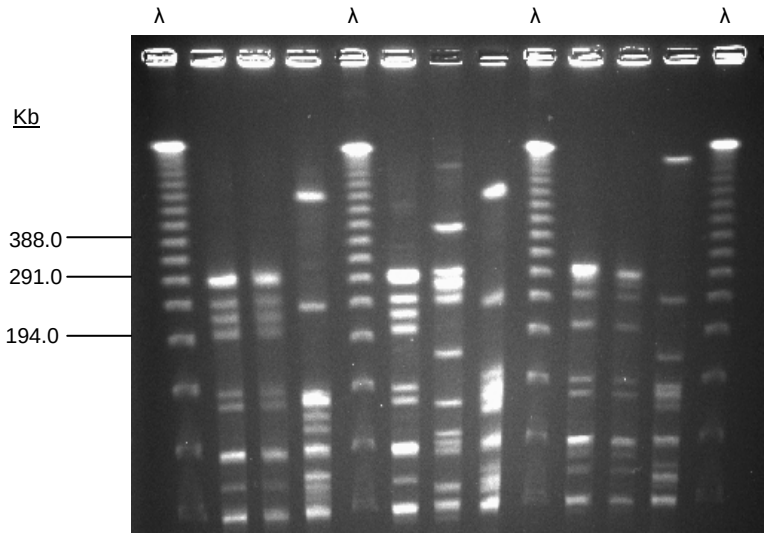

Figure 3.2. PFGE digested with *Sac*II in *S. capitis.* This is a representative of PFGE gel photos. The PFGE for all the isolates were performed under the same conditions. λ, λ PFGE marker.

The annual number of episodes of sepsis at the NICU varied over the six years of the study, peaking in 2002 and 2003 (Figure 3.3). The PFGE results clearly revealed that certain isolates of *S. capitis* became predominant in the NICU. Analysis of PFGE gels by GelCompar II yielded four major clusters of at least five isolates with ≥ 80% similarity, comprising 53 (88.3%) of all isolates. Another minor cluster comprised two isolates (52 and 61). Five isolates (39, 62, 65, 70 and 90) that were randomly distributed over the years could not be typed. There was no difference in the allocation of clusters between the 75% and 80% cut-off levels. The only exception was one isolate clustered in the PFGE type I according to the 75% cut-off and non-clustered according to the 80% cut-off level.

Cluster II, the largest cluster, comprising 34 isolates, was associated with more than half of all cases in the NICU and was apparently capable of persisting for a prolonged period. Isolates belonging to this cluster were distributed throughout the 6-year period. The

highest occurrence was in 2002 (11 isolates, 84.6% of isolates in this year). The other clusters were less prevalent, but appeared in most years throughout the period of the study (Figure 3.3).

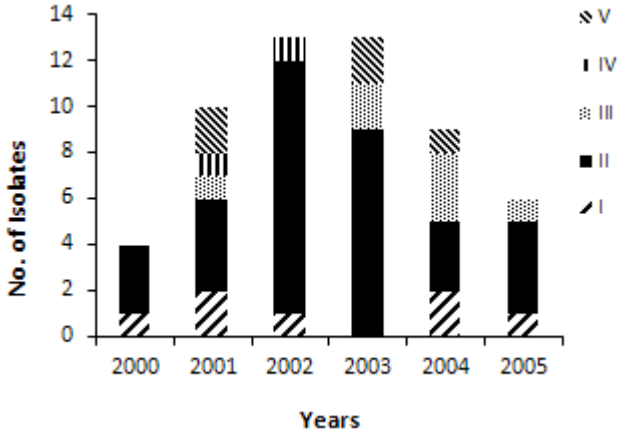

Figure 3.3. Contributions of PFGE clusters to the total infections in each year.

3.3.2 Quantitative and qualitative biofilm formation in clinical *S. capitis* isolates

The biofilm-forming ability of the sixty isolates was examined using two methods, the microtitre plate (Mtp) and appearance on Congo red agar (CRA). Fifty isolates were biofilm-positive by the microtiter plate assay, in TSB supplemented with 4% NaCl, and the remaining 10 isolates were biofilm-negative. There was a complete agreement between the results of the microtitre plate assay and production of extracellular polysaccharide indicated by colonial appearance on CRA plates. Figure 3.4 & 3.5 show the biofilm formation in Mtp and on CRA, respectively.

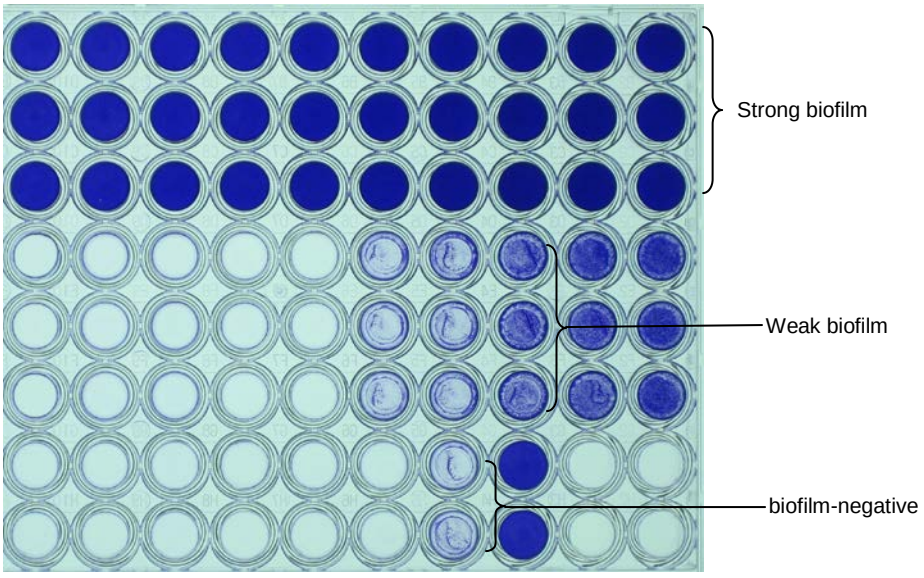

Figure 3.4. Biofilm assay with 96-well microtiter plate.

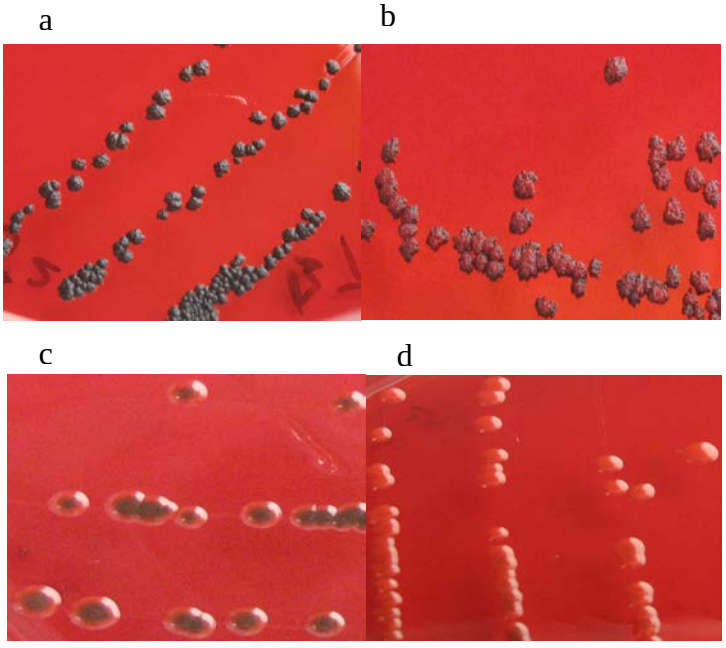

Figure 3.5. Detection of biofilm formation with congo red agar in clinical *S. capitis*. Colourimetric scale adopted for colony evaluation by Congo red agar on the clinical *S. capitis* isolates: a. black; b. borderline; c. black in the center; d. red. a, b, and c are categorized as biofilm positive, d was categorized as biofilm negative, according to Arciola *et al*. (2005).

3.3.3 Antibiotic susceptibility profile and relationship to biofilm production

Biofilm-positive isolates were, in general, more resistant than biofilm-negative isolates. The great majority of isolates were resistant to penicillin and oxacillin (87 and 85% respectively). All *S. capitis* isolated in 2005 were resistant to both antibiotics. Carriage of *mecA* gene was consistently high and was almost always associated with biofilm positivity. Forty-three isolates (72%) showed resistance to erythromycin. Limited numbers of isolates were resistant or intermediate in resistance to clindamycin (6.7%) and 10% were resistant to teicoplanin. Based on MICs, no isolates of *S. capitis* displayed reduced susceptibility to vancomycin; however, this method may not detect small populations of resistant cells, which can only be detected by population analysis profiling. Resistance to teicoplanin was observed in 10% of isolates (Table 3.1).

Table 3.1. MIC antibiotic susceptibility pattern and *mecA* gene carriage and their correlations between biofilm formation phenotype in clinical *Staphylococcus capitis*.

Antimicrobial agent	No. (%) of resistant isolates by year						No. (%) resistant isolates by biofilm phenotype		P^b value
	2000	2001	2002	2003	2004	2005	Biofilm$^+$ n^a = 50	Biofilm$^-$ n = 10	
Penicillin	5 (100)	9 (90)	14 (87.5)	10 (76.9)	9 (90)	5 (83.3)	48 (96)	4 (40)	0.0001
Erythromycin	4 (80)	8 (80)	8 (50)	9 (69.2)	8 (80)	6 (100)	41 (82)	2 (20)	0.0003
Clindamycin	0	1 (10)	2 (12.5)	0	0	1 (16.7)	4 (8)	0	1.0000
Teicoplanin	0	3 (30)	2 (12.5)	1 (7.7)	0	0	5 (10)	1 (10)	1.0000
Vancomycin	0	0	0	0	0	0	0	0	1.0000
Oxacillin	4 (80)	8 (80)	14 (87.5)	11 (84.6)	8 (80)	6 (100)	48 (96)	3 (30)	< 0.0001
mecA^{+c}	4 (80)	8 (80)	15 (93.8)	13 (100)	8 (80)	6 (100)	49 (98)	5 (50)	0.0003

[a] n is the number of isolates.
[b] *P* value is calculated. *P* value represents the comparision of the antibiotic resistance between the biofilm- positive and-negative clinical *S. capitis* isolates. A binary logistic regression analysis was performed using Fisher's test from a contingency table. $p < 0.05$ is defined as significant difference.
[c] *mecA*$^+$ is *mecA* gene carrier.

3.3.4 Genotype of subspecies and their relatedness to antibiotic resistance and biofilm production.

Fifty-two isolates identified as subsp. *urealyticus* were mainly distributed in three major PFGE clusters (I, II and III) and one minor cluster (IV). Two non-clustered isolates were also grouped into this subspecies. Members of subsp. *urealyticus* were generally resistant to oxacillin (98%) and biofilm-positive (94%). One exception was a non-clustered isolate, which were oxacillin-susceptible according to its MIC, although they carried *mec*A. Subsp. *capitis* comprised only eight isolates, which were mainly clustered in PFGE cluster V. These isolates were susceptible to all antibiotics according to MIC data, although *mecA* was identified in three of them. Only one (isolate 62) produced biofilm (Figure 3.7).

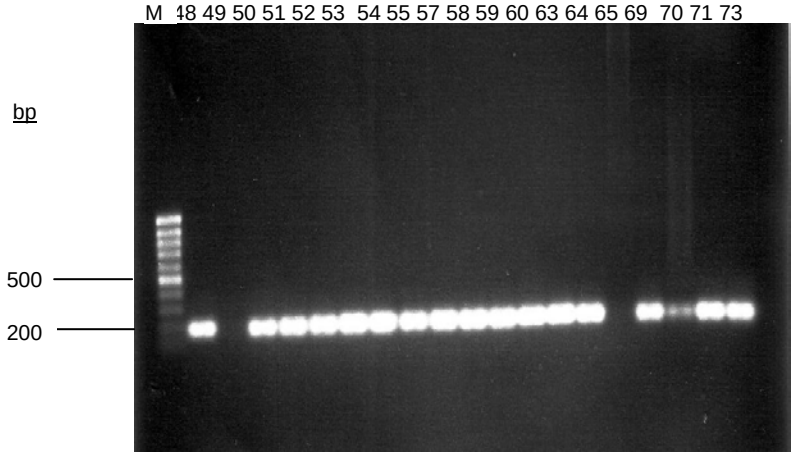

Figure 3.6. PCR detection of *mecA* gene in isolates of *S. capitis*. The isolates numbers are denoted on the top of each lane. M, low range of DNA ladder. This is a representative of *mecA* PCR photos. The PCRs of *mecA* gene for all the isolates were performed under the same conditions.

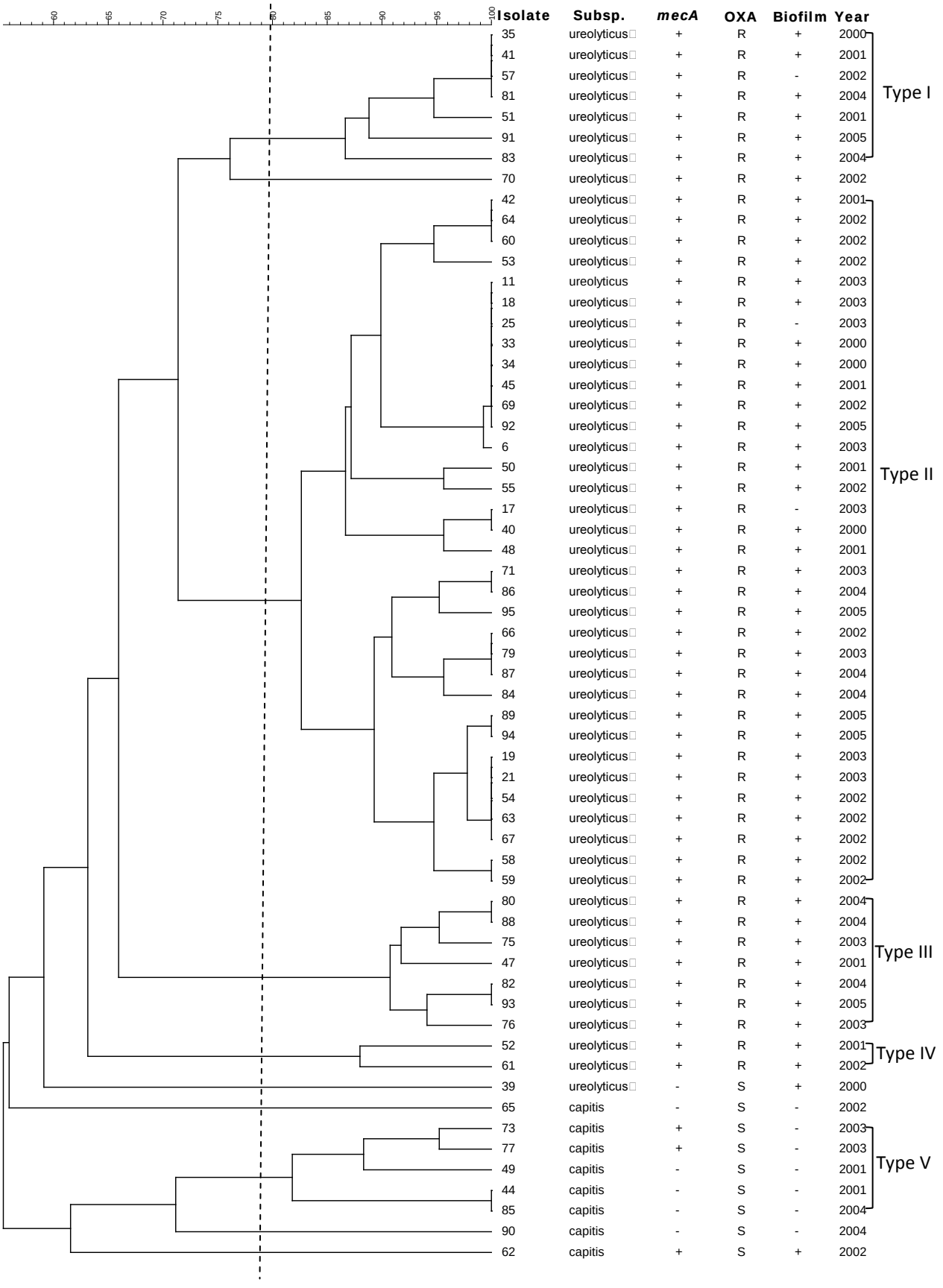
60
65
70
75
80
85
90
95
100
Isolate
Subsp.
mecA
OXA
Biofilm
Year
35 ureolyticus + R + 2000
41 ureolyticus + R + 2001
57 ureolyticus + R - 2002
81 ureolyticus + R + 2004
51 ureolyticus + R + 2001
91 ureolyticus + R + 2005
83 ureolyticus + R + 2004
70 ureolyticus + R + 2002
42 ureolyticus + R + 2001
64 ureolyticus + R + 2002
60 ureolyticus + R + 2002
53 ureolyticus + R + 2002
11 ureolyticus + R + 2003
18 ureolyticus + R + 2003
25 ureolyticus + R - 2003
33 ureolyticus + R + 2000
34 ureolyticus + R + 2000
45 ureolyticus + R + 2001
69 ureolyticus + R + 2002
92 ureolyticus + R + 2005
6 ureolyticus + R + 2003
50 ureolyticus + R + 2001
55 ureolyticus + R + 2002
17 ureolyticus + R - 2003
40 ureolyticus + R + 2000
48 ureolyticus + R + 2001
71 ureolyticus + R + 2003
86 ureolyticus + R + 2004
95 ureolyticus + R + 2005
66 ureolyticus + R + 2002
79 ureolyticus + R + 2003
87 ureolyticus + R + 2004
84 ureolyticus + R + 2004
89 ureolyticus + R + 2005
94 ureolyticus + R + 2005
19 ureolyticus + R + 2003
21 ureolyticus + R + 2003
54 ureolyticus + R + 2002
63 ureolyticus + R + 2002
67 ureolyticus + R + 2002
58 ureolyticus + R + 2002
59 ureolyticus + R + 2002
80 ureolyticus + R + 2004
88 ureolyticus + R + 2004
75 ureolyticus + R + 2003
47 ureolyticus + R + 2001
82 ureolyticus + R + 2004
93 ureolyticus + R + 2005
76 ureolyticus + R + 2003
52 ureolyticus + R + 2001
61 ureolyticus + R + 2002
39 ureolyticus - S + 2000
65 capitis - S - 2002
73 capitis + S - 2003
77 capitis + S - 2003
49 capitis - S - 2001
44 capitis - S - 2001
85 capitis - S - 2004
90 capitis - S - 2004
62 capitis + S + 2002
Type I
Type II
Type III
Type IV
Type V

Figure 3.7. Pulsed-field gel electrophoresis dendogram of the clinical *Staphylococcus capitis* isolates. The scale bar at the top of the dendogram indicates similarity. The dot line indicates the cut-off value 80% that was applied for separating the clusters.

3.4 Discussion

3.4.1 Significance of antibiotic resistance profile

Consistent with previous studies on CoNS from NICUs (Akinkunmi and Lamikanra, 2010), there were a high level of oxacillin resistance (85%) among the isolates in this study. Oxacillin resistance and *mecA* carriage reached 100% among isolates belonging to the three major PFGE clusters (I, II, and III), and a minor cluster IV (Table 3.2). All such isolates were *S. capitis* subsp. *urealyticus*. Although there was generally good agreement between the prevalence of *mecA* and expression of oxacillin resistance, there were some exceptions. Three isolates that carried *mecA* failed to express oxacillin resistance (Table 3.2). This could be explained by low levels of expression of *mecA*, resulting in small subpopulations levels that were not detected by phenotypic methods. Alternatively, the *mecA* gene may be defective in these isolates (Al-Talib *et al*., 2010). We did not detect isolates expressing non-*mecA* mediated resistance to oxacillin. High levels of resistance to erythromycin and clindamycin in *S. epidermidis* were reported by many studies (Gristina *et al*., 1989, Hamilton-Miller and Shah, 2000). In this study, about 71.7% of the isolates were resistant to erythromycin and only a few (6.7%) were resistant or showed intermediate resistance to clindamycin.

Table 3.2. Correlations of antibiotic susceptibility profiles and *mecA* gene carriage with pulsed-field gel electrophoresis (PFGE) clusters in *Staphylococcus capitis* clinical isolates.

Antimicrobial agent	No. (%) of resistant isolates in PFGE clusters					No. (%) of non-clustered resistant isolates
	I	II	III	IV	V	
Penicillin	6 (85.7)	34 (100)	7 (100)	2 (100)	0	2 (40)
Erythromycin	7 (100)	28 (82.4)	6 (85.7)	2 (100)	0	0
Clindamycin	0	1 (2.9)	0	2 (100)	0	1 (20)
Teicoplanin	2 (28.6)	3 (8.8)	1 (14.3)	0	0	0
vancomycin	0	0	0	0	0	0
Oxacillin	7 (100)	34 (100)	7 (100)	2 (100)	0	1 (20)
mecA^{+a}	7 (100)	34 (100)	7 (100)	2 (100)	2 (40)	2 (40)

[a] *mecA*$^{+}$ is *mecA* gene carrier

3.4.2 Biofilm formation of clinical *S. capitis* isolates and their prevalence in the NICU

The predominant *S. capitis* clones in the NICU setting were biofilm producing subsp. *urealyticus*. Three isolates failed to produce biofilm yet were classified into the major PFGE clusters and presented similar antibiotic resistance profiles to the other members in the major clusters. The other isolates displaying a biofilm-negative phenotype belonged to subsp. *capitis* and were susceptible to antibiotics and members of cluster V. These isolates were few in number and appeared only sporadically over the study period (Figure 3.7).

Consistent with previous studies Ziebuhr *et al*. (2006), biofilm formation of the *S. capitis* isolates showed a strong correlation with the antibiotic resistance profile. It is likely that antibiotic use led to the selection of PFGE types that contained resistant strains capable of expressing biofilm. As a consequence, the ability to express biofilm under specific conditions encountered in the NICU could be the factor giving subsp. *urealyticus* a selective advantage. Biofilms form a barrier around bacteria, protecting them from antibiotics and phagocytes and thus making treatment of infections very difficult (Boynukara *et al.*, 2007, Begun *et al.*, 2007). However, given the likely value of biofilm formation in providing a positive selective advantage, the question remains why biofilm-negative antibiotic-susceptible subsp. *capitis* isolates remained in the NICU. One possibility is that the conditions under which the *ica* operon of subsp*. capitis* expresses PIA are not the same as for subsp. *urealyticus.*

3.4.3 Relatedness of biofilm production and antibiotic resistance to two subspecies

One striking observation in this study is that biofilm formation and the presence of the *mecA* gene in these clinical *S. capitis* isolates were mainly displayed only in subsp. *urealyticus* (Figure 3.7). A global comparison of the genomes of diverse clinical strains of these two subspecies with known endemic potential would contribute our understanding *S. capitis* survival and infections in hospitals.

In conclusion, the findings presented in this chapter suggest that the endemic S. *capitis* clones confirmed to be *S. capitis* subsp. *urealyticus* are more important causes of bloodstream infections in very-low-birth-weight infants than subsp. *capitis*. It would therefore be beneficial to subspeciate *S. capitis* isolates, especially those isolated from newborn babies. The results also emphasize the importance of examining the composition and expression of the *ica* operon in relation to the pathogenic potential of *S. capitis*.

CHAPTER 4

Sequence analysis of *ica* operon in *Staphylococcus capitis*

4.1 Introduction

Cramton *et al*. (1999) showed that the *ica* operon is responsible for the extracellular biofilm matrix of *S. epidermidis*. The matrix is composed of polysaccharide intercellular adhesion (PIA), which consist mainly of β-1,6-linked N-acetylglucosamine. The entire DNA sequence of *ica* operon in *S. epidermidis*, *S. aureus* and *S. caprae* has been reported (NCBI accession numbers: SEU43366, AF086783 and AF246926). IcaA is a N-acetylglucosaminyltransferase, but no transferase activity was observed with the other proteins encoded by the *ica* operon (Gerke *et al.*, 1998).

The complete DNA sequence of *ica* operon of *S. capitis* was determined in this study. It was present in the same length in all sixty isolates of *S. capitis* subspecies *capitis* and *urealyticus* that were examined; however, these isolates exhibited different biofilm phenotypes. Most were biofilm positive, 10 isolates were biofilm-negative (Chapter 3). Whether their phenotype and the genotype correspond for biofilm formation and the function of *ica* operon in *S. capitis* have not been investigated.

Recently, the online bioinformatics tools have become available to facilitate making biological discoveries *in silico* in a highly time- and cost-efficient manner. By utilizing various bioinformatics prediction and analysis tools, hypotheses and theoretical models can be quickly generated, which could then guide the design of experiments for further validation.

The aim of this study is to determine if the *ica* operon is essential for biofilm formation in *S. capitis.* I addressed this aim in three ways: 1. to determine the status of the *ica* operon in both biofilm-positive and -negative isolates of *S. capitis*. 2. To deduce the function of

Ica proteins of *S. capitis* and propose their putative mechanisms in the polysaccharide biosynthesis pathway by comparing with the protein sequences of known functions. 3. To speculate the origin of *ica* operon in *S. capitis*, how they were selected in hospital setting.

4.2 Materials and methods

4.2.1 Bacterial isolates and growth conditions

For details of the sixty *S. capitis* isolates used for verifying the presence of the *ica* operon, One Shot® TOP10 Electrocomp™ *E. coli* for cloning and growth conditions refer to Chapter 2.

4.2.2 PCR amplification, cloning, southern blot, DNA sequence assembling and analyses

The total chromosomal DNA isolation was performed as described in Chapter 2. The entire DNA sequence of *S. capitis ica* operon was obtained by PCR. All the primers used for PCR and sequencing were listed in Table 4.1. The PCR conditions and gel electrophoresis, and purification were described in Chapter 2. PCR products were analysed by gel electrophoresis on a 1.2% agarose gel (Bioline, Australia), purified with QIAquick gel extraction kit (Qiagen). DNA sequencing was performed by Microcom Sequencing Facilities, Monash University, Melbourne. Each PCR fragment was sequenced at least twice to three times. The sequence information was obtained by blast search with data in NCBI.

The flanking region of the *icaR* was obtained by semi-random PCR, using the forward primer (Af_2) designed from *ica* chromosomal region of *S. capitis* in the NCBI database. The reverse primer ($SeipL_4$) was designed based on *S. epidermidis* RP62A DNA

sequence upstream of the *icaR* gene. The resulting PCR product was cloned into pCR-XL-TOPO vector according to the manufacture's instruction, and confirmed by southern blot with a 300 bp PCR product generated from primers Af_2 and Ar_2 as probe, and labelled with digoxigenin using the DIG labelling kit (Roche, Australia), according to the manufacture's instruction. The flanking sequence of the *icaC* gene was obtained with primers Cf and gehCb.

All the sequence information was identified by basic local alignment search tool (BLAST) analysis at the National Center for Biotechnology Information (NCBI) website. The PCR fragments were assembled with the CAP3 program, using the default parameters (Huang and Madan, 1999).

Table 4.1. Primers used for PCR experiments.

Primer	Sequence (5'-3')	Gene	Accession No.	Position	Origin (Source)
$SepiL_4$	TGGAGGGCTACTCAAGTC				This study
Rf	CAACAACGATTCTAACTACT	*icaR*	AY146584	4051	This study
Rr	TGGATAATTGGACGTATAACC	*icaR*	AY146584	4154	This study
Ar_1	CGCCTTCGTTTAAAGCGTTAGC	*icaA*		3325	This study
Af_1	GGCCTGTTACAACGAGAG	*icaA*		3530	This study
Ar_2	AACGGCGGCATTGATAATCC	*icaA*		2540	This study
Af_2	CAGCAAACTTCTTAGATTACAC	*icaA*	AY146582	2739	This study
Dr	CTCCACGTTAAGAGCGATAC	*icaD*		2295	This study
Df	ATGGTCAAGCCCAGACAG	*icaD*		2486	This study
Br	TTAGTAGCAGACACATTAGAC	*icaB*	AY146583	1571	This study
Bf	CAACTGGCTTCGTGATTAC	*icaB*	AY146583	1763	This study
Cr	TAGAACAAGAGAACTCCCTG	*icaC*	AY945929	1203	This study
Cf	TGTCAGGGAGTTCTCTTG	*icaC*	AY945929	1225	This study
gehCb	CAAGACAGTTCAGATACAGTACGC	*gehC*			(Allignet *et al*., 2001)

4.2.3 Detection of *ica* operon using expand long PCR

The *ica* operon was amplified according to the expand long template PCR system protocol (Roche Applied Science). The primers used were: forward SepiL$_4$ 5' TGGAGGGCTACTCAAGTC 3' (this study), reverse gehCb 5' CAAGACAGTTCAGATACAGTACGC 3' (3). Briefly, A 50 μL PCR mixture consisted of 5 μL of 10 x PCR buffer 1 with 1.25 mM $MgCl_2$, 350 μM of each deoxyribonucleotide (Bioline, Australia), 300 μM of each primer and 3.75 U of expand long enzyme, 50 ng of DNA. The first PCR cycling conditions used were 10 cycles of 10 s at 94 °C, annealing at 50 °C for 30 s and 4 mins for elongation at 68 °C, the second cycling conditions were 25 cycles at 94 °C for 15 s, annealing at 50 °C for 30 s and 4 mins for elongation at 68 °C. Reaction mixtures 5 μL were analysed by 1% agarose (Bioline, Australia) gel electrophoresis.

4.2.4 PCR-Restriction Fragment Length Polymorphism (RFLP)

The entire *ica* operon were amplified with forward primer SepiL$_4$ and reverse primer gehCb in Table 1. By using Elongase enzyme (Roche) under the reaction conditions described by the manufacturer, with annealing temperature at 52 °C and extension time at 7 mins, respectively. The PCR product was subjected to digestion with *Hind*III and *Taq*I restriction enzymes (Promega, Australia), which were used according to the manufacture's instruction, refer to Chapter 2.

4.2.5 Bioinformatics tools

Database searches

The PSI-BLAST ALIGNMENT (Altschul *et al*., 1997) program was used for the protein sequence database search, with default parameters. The family-based resources pfam version 26.0 was used for searching significant matched proteins. A list of related known protein data bank (PDB) structures was recognized as potential templates for protein modelling. Conserved domain search in NCBI was used for searching homologous proteins.

DNA and protein primary sequence alignment

Clone manager version 7.11 (Scientific and Education software, USA) was used to compare the primary DNA and protein sequences.

Multiple sequence alignment

Related sequences with a comparably high degree of similarity (15% identity) were aligned using Clustal Omega, with defalt parameters, which is a new multiple sequence alignment program that uses seeded guide trees and HMM profile-profile techniques to generate alignments (Sievers *et al.*, 2011).

Secondary structures

Protein secondary structures were derived the PDB coordinates of the representative proteins. Hydrophobicity analysis was carried out using web-predictor TopPred II (von Heijne, 1992). All the possible topologies that include the certain transmembrane segments and either include or exclude each of the candidate segments were automatically generated SignalP 3.0 was used to predict the presence and location of

signal peptide cleavage sites in amino acid sequences (Dyrløv Bendtsen *et al*., 2004) PSORTb v3.0 (Yu *et al.*, 2010) was used for protein localization prediction.

4.2.6 Nucleotide submission

The sequenced complete *ica* operon of clinical biofilm-positive *S. capitis* isolate 6 has been deposited in GenBank under accession number JF930147.

4.3 Results

4.3.1 Sequence of the *ica* operon in *S. capitis*

The type of genes and their organisation from 5' to 3' end are similar to those of *S. aureus*, *S. epidermidis* and *S. caprae.* The *ica* operon contains four structural genes *icaA*, *icaD*, *icaB* and *icaD* and one regulatory gene *icaR*. The structural genes are co-transcribed from the mapped *icaA* promoter, and *icaR* gene located upstream of *icaA* gene, is transcribed in opposite direction. However, in *S. capitis*, the presence of a putative surface protein gene (*Sp6*) upstream of *icaR* gene and in the same orientation as in the surrounding sequence showed no similarity to the corresponding area in the other species. The *ica* operon was present in all the sixty clinical isolates. Most subsp. *urealyticus* isolates produced biofilm, except three isolates (17, 25 and 55), and all the subsp. *capitis* isolates were biofilm-negative. All isolates carried an *ica* operon of the same length and in the same chromosomal position, suggesting the absence of biofilm formation was not related to the insertion of a mobile element. Figure 4.1 shows the map of the *ica* operon in *S. capitis* isolate 6, which is a biofilm producer.

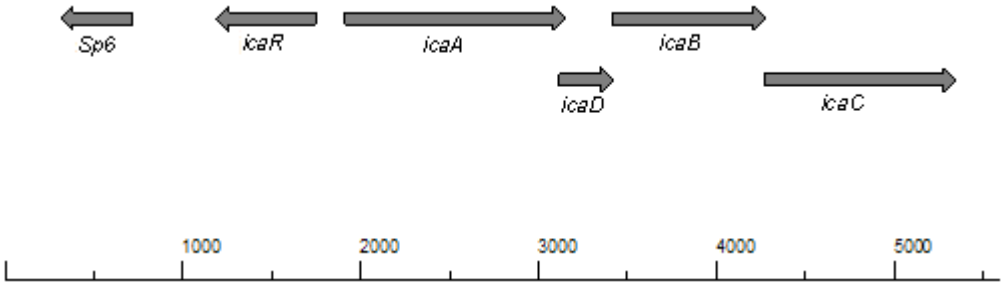

Figure 4.1. Map of the *ica* locus and surrounding chromosomal region in *S. capitis* strain 6 (accession number JF930147).

4.3.2 Sequence comparison with *S. epidermids, S. aureus* and *S. caparae*

A comparison of sequence identities between *S. capitis* isolate 6 and *S. epidermidis, S. aureus*, and *S. caprae* is shown in Table 4.2. In general, the entire *ica* operons in these species are about from 4000 bp to 5000 bp in length. They share identities ≥ 65% in DNA sequences and ≥ 66% at the protein levels.

Table 4.2. Sequence comparison of the *ica* locus between other species

Locus	Accession No.	DNA identity	Length (nt)	Protein identity	Length (aa)
icaR					
S. capitis	JF930147		561		186
S. epidermidis	SEU43366	76	558	77	185
S. aureus	AF086783	70	561	69	186
S. caprae	AF246926	89	573	89	190
icaA					
S. capitis	JF930147		1239		412
S. epidermidis	SEU43366	79	1239	83	412
S. aureus	AF086783	77	1239	81	412
S. caprae	AF246926	85	1236	91	411
icaD					
S. capitis	JF930147		306		101
S. epidermidis	SEU43366	77	306	79	101
S. aureus	AF086783	69	306	66	101
S. caprae	AF246926	86	306	91	101
icaB					
S. capitis	JF930147		864		287
S. epidermidis	SEU43366	73	870	71	289
S. aureus	AF086783	65	873	66	290
S. caprae	AF246926	85	870	88	289
icaC					
S. capitis	JF930147		1074		357
S. epidermidis	SEU43366	81	1068	82	355
S. aureus	AF086783	75	1053	75	350
S. caprae	AF246926	93	1074	94	356

4.3.3 Sequence comparison between biofilm-positive and -negative isolates

The entire *ica* operon was present in all sixty isolates in the same length (Figure 4.2). Sequence analysis was performed on the *ica* operon in five isolates: two biofilm-positive subsp. *urealyticus* (isolates 6 and 70) and one biofilm-negative subsp. *urealyticus* (isolate 17), and two biofilm-negative subsp. *capitis* (44 and 65). These isolates were selected by identifying different restriction patterns of the *ica* operon in accordance with PCR-RFLP

digested with *Taq*I and *Hind*III, respectively. *Taq*I patterns were consistent with those cut with *Hind*III (Figure 4.3).

The detailed mutations in the *ica* operon are summarized in Table 4.3, the *ica* operon of isolate 6 was used as the master sequence for comparison. Sequence analysis revealed, the *ica* operon of isolate 70 is identical to that of isolate 6; three in-frame deletions occurred in the *ica* operon of isolate 17. Various point mutations happened in the *icaC* gene of isolate 44, but none of them leads to the change of amino acid of IcaC while the mutations in *icaR* to *icaA*, *D* and *B* genes resulted in changes in amino acid sequences. In isolate 65, a stop codon was found in *icaB* gene, which led to nonsense protein missing 69 C-terminal amino acids.

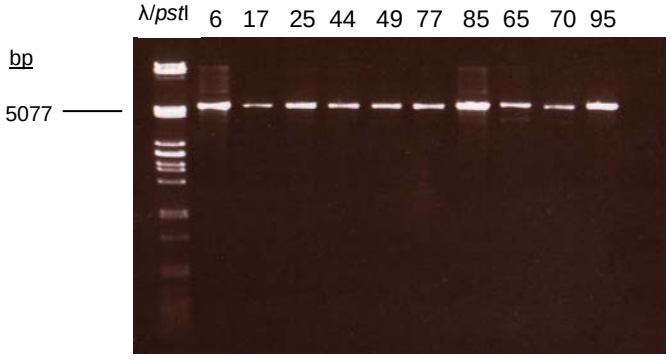

Figure 4.2. PCR of the *ica* operon in *S. capitis*. The isolates numbers are shown on the top of the gel. Isolates 6, 70, and 95 are biofilm-positive, subsp. *urealyticus*; isolates 17 and 25 are biofilm-negative subsp. *urealyticus*; isolates 44, 49, 77, 65 and 85 are biofilm-negative subsp. *capitis*. λ/*Pst*I was used as DNA ladder. This photo is used as a representive of PCR results of *ica* operons. The PCRs of the *ica* operon gene for all the isolates were performed under the same conditions.

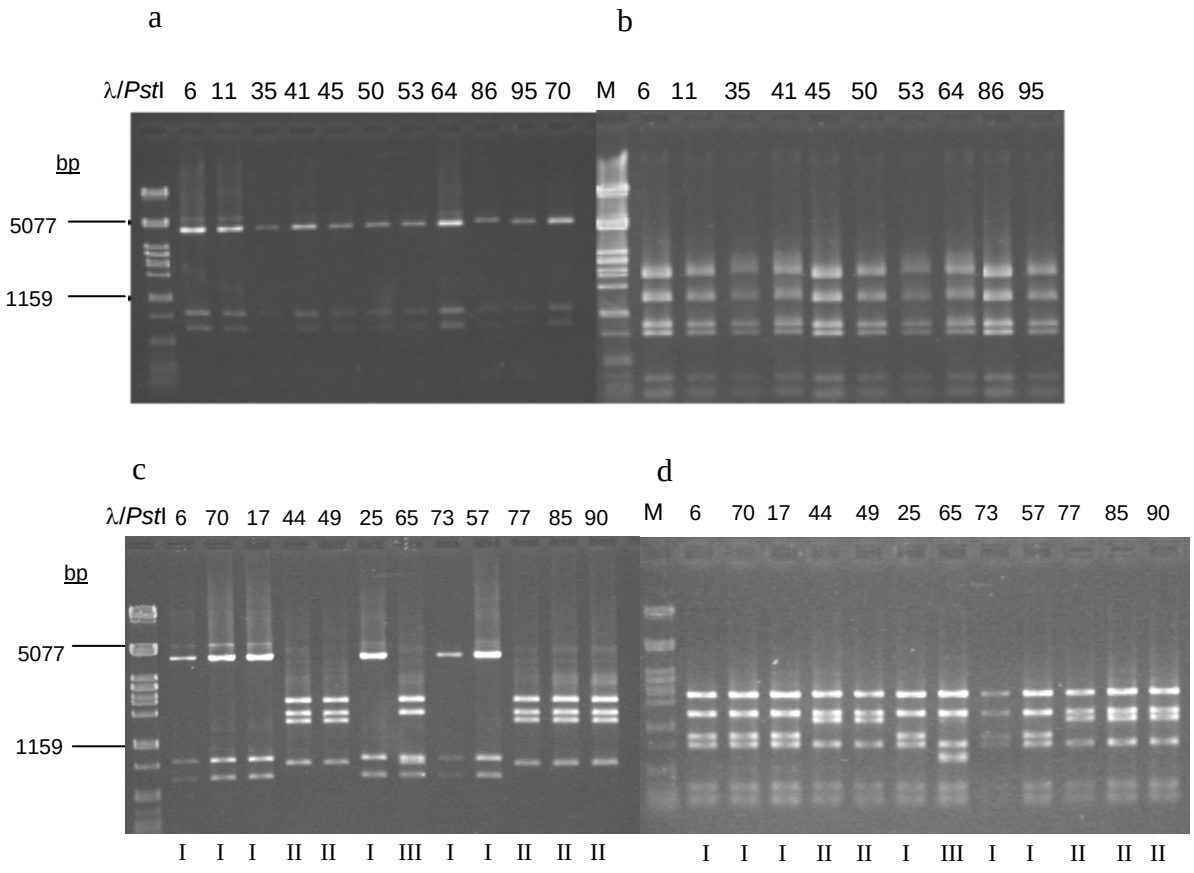

Figure 4.3. PCR-RFLP profiles of the *ica* operon in *S. capitis* isolates. a.& b. *Hind*III and *Taq*I digestion of the *ica* operon PCR product of biofilm-positive subsp. *urealyticus* isolates, respectively. The isolates numbers are labelled on the top of the lanes. c & d**.** *Hind*III and *Taq*I digestion of *ica* operon PCR product biofilm-negative subsp. *capitis* isolates, respectively. The isolates numbers are labelled on the top of the lanes, and the RFLP types are indicated under the lanes of each isolates. Isolates 6 and 70 are biofilm-positive, supsp. *urealyticus*, used as controls; isolates 17, 25, and 57 are biofilm-negative subsp. *capitis*; isolates 44, 49, 65, 73, 85 and 90 are biofilm-negative subsp. *capitis*. λ/*Pst*I was used as DNA ladder, and the Ms on b & d are correspondent to the λ/*Pst*I marker.

Table 4.3. Summary of the mutations in the *ica* operon of *S. capitis* clinical isolates

Isolate	Mutation position	Substitution, deletion or insertion	Gene loci	Translation to amino acid
6[a]				
17[b]	1587 to 1595	Deletion of AATCACTTG	*icaA*	Deletion amino acids of Q, S, I and change A to P
70[c]				100% identity
44[c]	319	A to G	*icaR*	Y to H
44	362	G to A	*icaR*	No change in amino acid
44	503	T to A	*icaR*	L to F
44	556	G to T	*icaR*	Q to K
44	971	Deletion of T	*intergenic region*	
44	984	G to A	*intergenic region*	
44☆	1331	A to G	*icaA*	N to D
44	1342	A toT	*icaA*	No change in amino acid
44	1400	G to A	*icaA*	V to I
44	1485	G to A	*icaA*	G to D
44☆	1561	T to C	*icaA*	No change in amino acid
44☆	1603	T to C	*icaA*	No change in amino acid
44	1781	G to A	*icaA*	V to I
44	1870	A to G	*icaA*	No change in amino acid
44	1908	G to T	*icaA*	V to F
44	2427	C to T	*icaD*	No change in amino acid
44	2477	T to A	*icaD*	F to Y
44	2500	A to G	*icaD*	K to E
44	2585	T to C	*icaB*	No change in amino acid
44	2636	A to G	*icaB*	No change in amino acid
44☆	2948	T to C	*icaB*	No change in amino acid
44☆	2964	A to G	*icaB*	I to V
44☆	3158	G to A	*icaB*	No change in amino acid
44	3447	A to G	*icaC*	No change in amino acid
44	3519	A to T	*icaC*	No change in amino acid
44	3624	C to T	*icaC*	No change in amino acid
44	3736	C to T	*icaC*	No change in amino acid
44	3780	C to T	*icaC*	No change in amino acid
44	3888	C to T	*icaC*	No change in amino acid
44	4098	A to C	*icaC*	No change in amino acid
44☆	4389	T to C	*icaC*	No change in amino acid
44☆	4405	T to C	*icaC*	No change in amino acid

Table 4.3. Continued.

65[e]	457	G to A	*icaR*	P to S
65	1105	A to T	*icaA*	L to F
65	1120	A to G	*icaA*	No change in amino acid
65	1331	A to G	*icaA*	No change in amino acid
65	1429	A to T	*icaA*	No change in amino acid
65	1513	C to T	*icaA*	No change in amino acid
65	1561	T to C	*icaA*	No change in amino acid
65	1603	T to C	*icaA*	No change in amino acid
65	1666	C to T	*icaA*	No change in amino acid
65	1780	A to G	*icaA*	No change in amino acid
65	2585	T to C	*icaB*	There is a stop codon on *icaB* gene of isolate 65. Nonsense protein missing 69 C-terminal amino acids.
65	2636	A to G	*icaB*	
65	2724	G to T	*icaB*	
65	2948	T to C	*icaB*	
65	2964	A to G	*icaB*	
65	3127	C to T	*icaB*	
65	3158	G to A	*icaB*	
65	3951	C to T	*icaC*	No change in amino acid
65	4389	T to C	*icaC*	No change in amino acid
65	4405	T to C	*icaC*	No change in amino acid

[a] 6, biofilm-positive, subsp. *urealyticus*, used as the master sequence for the comparison;
[b] 17, biofilm-negative, subsp. *urealyticus*; [c] 70, biofilm-positive, subsp. *urealyticus*;
[d] 44, biofilm-negative, subsp. *capitis*; [e] 65, biofilm-negative, subsp. *capitis*.
☆ Stars indicate the same mutations occurred in DNA sequences between isolates 44 and 65.

The number of matching mutations between isolates 44 and 65 indicates a common anscester with the same eight mutations. According to the small proportion of matching of mutations indicates the divergence of the two sequences occurred a long time ago, therefore, pre-date the development of modern hospital.

4.3.4 Sequence-structure relationships of Ica proteins in *S. capitis*

From the deduced primary protein sequences, the IcaA protein sequence significantly matched the functional superfamily glycosyltransferase (GTs; EC 2.4.x.y), which constitutes a large family of enzymes involved in the biosynthesis of oligosaccharides, polysaccharides, and glycoconjugates (Breton *et al*., 2006), and is present in both

prokaryotes and eukaryotes. The secondary structure elements of IcaA were derived from comparison to a chondroitin polymerase from *E. coli* (2Z86, Protein Data Bank code), which presents the highest identity to IcaA (19% identity) from multiple alignment. The similar residues, DXD motif, which has been identified among glycosyltransferases and was thought to play a role in metal ion binding and catalysis (Li *et al.*, 2001) (Figure 4.4) was also recognized in IcaA.

The deduced IcaB sequence showed similarity to those of polysaccharide deacetylases, the most similar being a carbohydrate esterase from *Bacillus anthracis* (19% overall identity) (2J13, Protein Data Bank code). This identity suggests that IcaB has deacetylase activity. The functional residues responsible for binding and catalysis were identified by alignment with related known Protein Data Bank (PDB) structures (Figure 4.5).

IcaC exhibits similarity to acyltransferase, from conserved domain search. The highest identity was to a membrane-bound acyltransferase from *Bacillus subtilis* (26% identity). Alignment of the sequence with related acyltransferases is shown in Figure 4.6.

Analysis from the deduced IcaD sequence revealed that it is a cytoplasmic membrane protein. No significant protein structures can be matched. Hydrophobicity plots suggested two transmembrane domains are present in the IcaD (Figure 4.7).

A conserved domain search revealed that IcaR belongs to the tetracycline repressor (TetR) family of proteins. The IcaR crystal structure of *S. epidermidis* has been reported. Figure 4.8 shows the interaction of the IcaR with the *ica* operator in *S. epidermidis*. The palindromic sequence of *S. capitis* was therefore deduced as shown in Figure 4.9.The

key residues and their locations are identical to those of *S. epidermidis*. The location of the palindromatic sequence in *S. capitis* was drawn in Figure 4.10. The alignment of the helix-turn-helix sequence is shown in IcaR proteins from four *Staphylococcus* species: *S. epidermidis*, *S. aureus*, *S. caprae* and *S. capitis* in Figure 4.11.

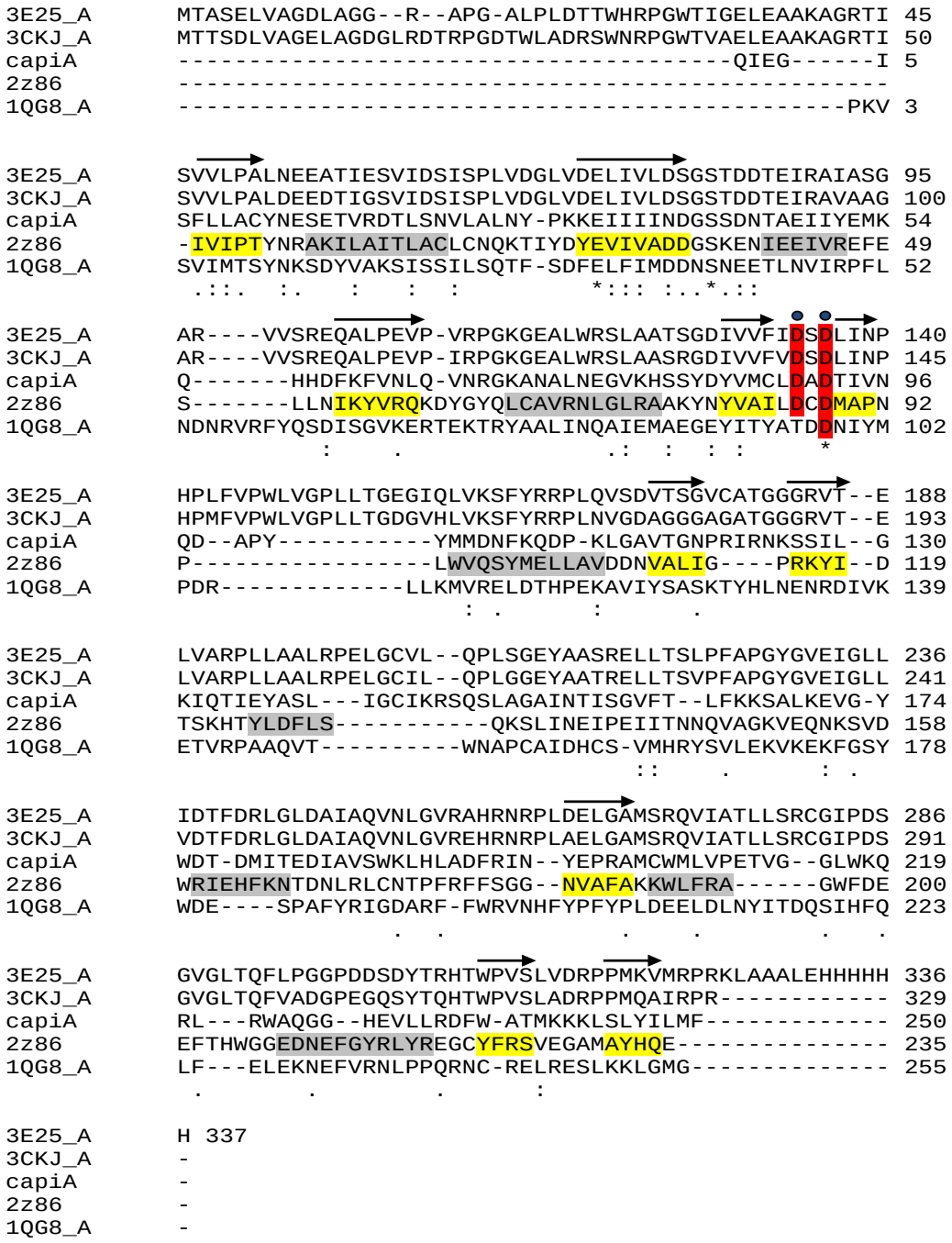

Figure 4.4. Alignment of IcaA with its homologues. Partial IcaA sequence, identified as capiA in the alignment, which were deleted 44 amino acids in N-termino and 116 amino acids in C-terminois from the wildtype IcaA sequence, to have a better alignment. The Putative conserved domains have been detected in NCBI, showed it is case-like glycosyltransferase. Aligned with a glycosyltransferase from *a Mycobacterium* species (Protein Data Bank code 3E25 *and* 3CKJ)*, a* chondroitin polymerase from *E. coli* (Protein Data Bank code 2Z86)*,* and a nucleotide-diphospho-sugar transferase from *B. subtilis* (Protein Data Bank code 1QG8). Yellow colour with a black arrow over the alignment represents β-sheet, light grey colour represents α-helics. DXD are denoted by red and indicated with blue dot over the sequence.

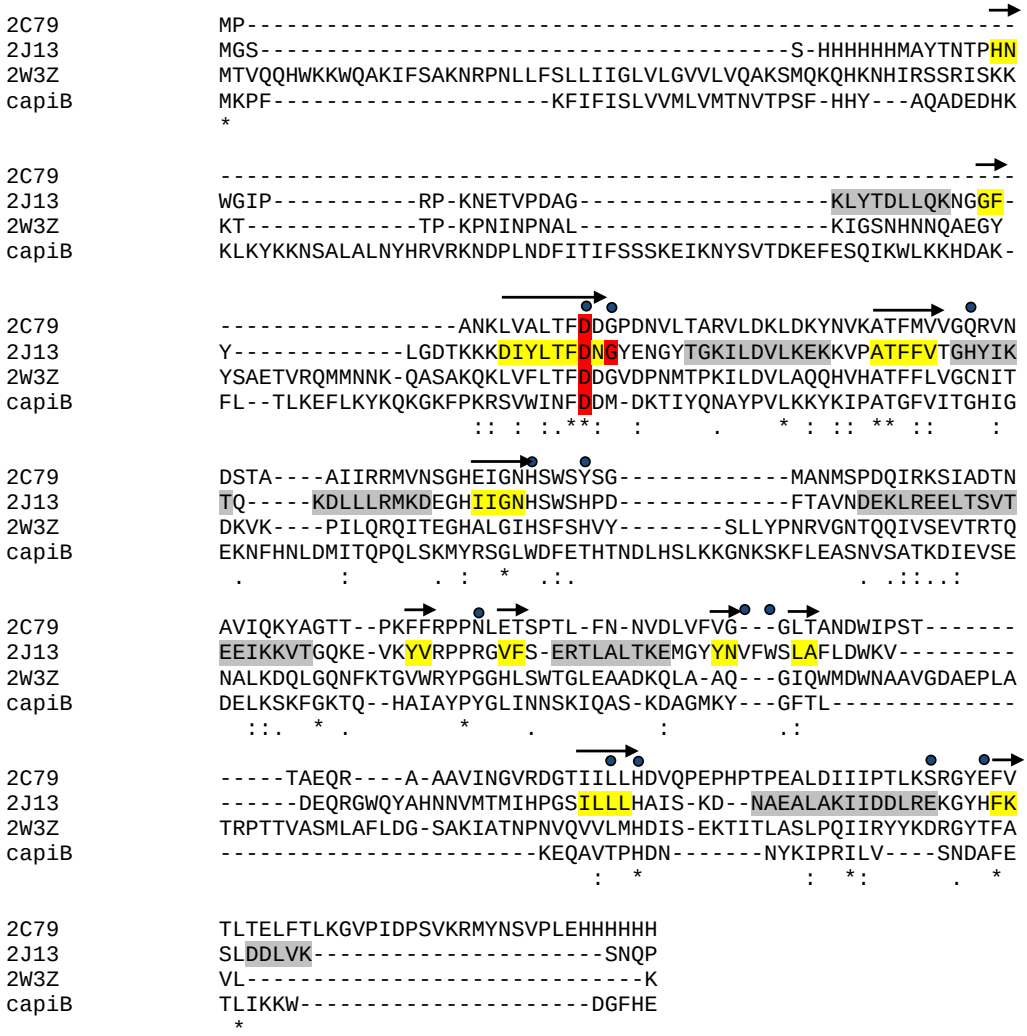

Figure 4.5. Alignment of IcaB with its homologues. IcaB sequence, identified as capiB in the alignment, is aligned with a peptidoglycan deacetylases from *Clostridium thermocellum* (Protein Data Bank code 2C79), a carbohydrate esterase from *Bacillus anthracis* (Protein Data Bank code 2J13), polysaccharide deacetylase from *Streptococcus mutans* (Protein Data Bank code 2W3Z). Secondary structure elements deriving from 2J13 Protein Data Bank coordinates which presents the highest identity to capiB (19% identity) are drawn over the alignment, yellow colour with a black arrow over the alignment represents β-sheet, light grey colour represents α-helics. Conserved residues are denoted by red and other binding sites are indicated with blue dot over the sequence.

```
capiC           ---MNKNRLELVYLRTFICIIIIVTHLLTQITLEHEHLSGSSLVLQYYIRNIVIFGTPSF 57
YFIQ_BACSU      -----MQIKEIFMIRCISCLSVVLLHIISMVLMLQAEALADISHTVDSFRTLLMFSTPAF 55
MDMB_STRMY      MPPRVVRLPSLTGLRWFAALAVFACHIAQQQFFADQQVG----TALLHITTLGSIAVSVF 56
OAC_BPSFV       ----MHKSNCFDTARLVAAMMVLVSHHYALSGQPEPYLFG--------FESAGGIAVIIF 48
                      .   :   * . .: :.  *         .             : .   :..  *

capiC           IVLSQLLTTLNYKS--VSVQYLISRFKYIFIPYLLVG-----LFYSYSESLLTASSFKKQ 110
YFIQ_BACSU      IFISEFLLARSYPDG-VPDGFLKKRGKVIFVPFLFIAAIDALLMTSAMGGEVTFLAFVQK 114
MDMB_STRMY      FLLSGFVLAWSARDKDSVTTFWRRRFAKIYPLHLVTFLIAGVIIFSLAEPTLPGGSVWDG 116
OAC_BPSFV       FSISGYLISKSAIRSDSFIDFMAKRARRIFP-ALVPCSILTYFLFGWILNDFSAEYFSHD 107
                : :*  : : .         :   *   *:   *.       :: .     ..   . .

capiC           FFENVILGQWYG------------YFIIIIMQFFILSYLIYKINYKLFNSKILLVLAFV 157
YFIQ_BACSU      YLANVFLGNFIG------------YFILVIFQFYMLHMMFHEY-LKKASPKWVLSISFV 160
MDMB_STRMY      LVPDLLLVQSWLPEPTIIAGFNTPSWSLSCEFAFYLTFPLWYRLVRKIPVRRLWWCAAGI 176
OAC_BPSFV       IVRKTISSIFMS------------QAPDADITSHLIHAGINGSLWTLPLEFLCYIITGV 154
                 . . :                        :  .:          .         : :

capiC           VQQTFLYYFNHSDAFHTFVKHYYPLSENTMILGWIFYFFLGGFIGYNYQRVLSFLEKYLV 217
YFIQ_BACSU      VTAAYLGYFSAASPAPASEEGGAFPFFWVPFAGWLFYFCLAYYCGKEYKRFLALLNQYRW 220
MDMB_STRMY      AAAVICVPFVTSQFPASAETAPGMPLNELWFACWLPPVRMLEFV---LGIVMALILRTGV 233
OAC_BPSFV       AVAHLKNGKAFIVILLVFVS-LSLIGSVSENRDVMFSIPLWLYP----LRGLAFFFGATM 209
                .                               :  . :  :        ::::

capiC           IMIMLALGSYVLFIALSGD-DYWNVTSFTYSLTLYNSIMFFVLIG---ICAHFKTMLLNT 273
YFIQ_BACSU      VVYGAAIASGALVVTVSYVGEIGMISSKRPDIMLYSTSMIFLCFH---LFSKMKHVPK-I 276
MDMB_STRMY      WRGPGVVSSALLLAAAYGVTQVVPPMFTIAACSIVPAALLITALANADVQGLRTGLRSAV 293
OAC_BPSFV       AMYEKSWNVSNVKITVVSLLAMYAYASYGKGIDYTMTCYILVSFS---TIAICTSVGDPL 266
                          :  :                    :  ::  :      .  . :

capiC           VQMISAFSFFIYLLHPIILDSLFAYTN-------IFEDNTVVFLAVSLLMIIGICIGVGM 326
YFIQ_BACSU      MMFISNYSFSIYLLHAYFMIIGYVLLL-------NMPEIPAVPAVLLLFAVCTAGPIMTS 329
MDMB_STRMY      LVRLGEWSFAFYLVHFMVIRYGHRLMGGELGYARQWSTASAGALALAMLAVAIVAGGLLH 353
OAC_BPSFV       VKGRFDYSYGVYIYAFPVQQVVINTLH--------------MGFYPSMLLSAVTVLFLSH 312
                :     :*: .*:    .                            ::        :

capiC           MLREFYIFRFVIGKQPYKLQFNNYQPSWKSH--- 357
YFIQ_BACSU      WALNKFKYGYLFVGKIYQPKQKKVTVEVRDHAG- 362
MDMB_STRMY      TVVENPCMRLLGRRRPVATAPDPATDEAPKLTRA 387
OAC_BPSFV       LSWNLVEKRFLTRSSPKLSLD------------ 333
                   :     :
```

Figure 4.6. Alignment of amino acid sequence of IcaC with several acyltransferases. Highly conserved amino acid residues are indicated by stars under the alignment. YFIQ_BACSU, acyltransferase mdmB from *Streptomyces mycarofaciens*. capiC, IcaC from *S. capitis*. MDMB_STRMY, membrane-bound acyltransferase yfiQ from *Bacillus subtilis*. OAC_BPSFV, O-acetyl transferase from *Enterobacteria phage*. Highly conserved amino acid residues are indicated with stars under the alignment. Conserved residues are denoted by red.

```
capiD           MVKPRQRKYPTVKSSLNIVRESLFIAISCAFWIYCVVVMIVYIGTLINSQVESVITIRIA 60
epiD            MVKPRQRQYPTVTSYLNIVRESLFITISGVFWMYCIVVMIVYIGTLINSQMESVITIRIA 60
                *******:****.* **********:** .**:**:**************:*********

capiD           LNVENIEIYKIFELMGLFSIIIFLFFTFSLIFQKIKKGREV 101
epiD            LNVENTEIYKLFGWMSLFVLIIFIFFTFSLAFQKYKKGRDI 101
                ***** ****:*  *.** :***:****** *** ****::
```

Figure 4.7. Alignment of *S. capitis* IcaD with its counterparts of *S. epidermidis*. capiD, IcaD of *S. capitis*. epiD, IcaD of *S. epidermidis*. Conserved residues are indicated with stars under the alignment.

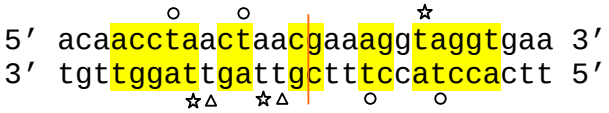

Figure 4.8. Interaction of IcaR and the *ica* operator in *S. epidermidis*. The partial palindromic sequence is highlighted with yellow. Approximate locations of the interface with different IcaR monomers are shown as colour bars. Triangles, circles and stars indicate the locations of the key residues Leu23, Lys33 and Ala35, respectively (Jeng *et al*., 2008). The palindromic sequence is located from 730 to 757 bp in the published sequence (accession number, SEU43366).

```
capiR       ACAGCCTAACTAACGAAAGGTAGGTAGA
epiR        ACAACCTAACTAACGAAAGGTAGGTGAA
            *** ********************  *
```

Figure 4.9. Comparison of the Deduced IcaR palindromic sequence of *S. capitis* with that of *S. epidermidis*. The partial palindromic sequence of *S. epidermidis* is highlighted with yellow. Approximate locations of the interface with different IcaR monomers are shown as colour bars. The identical sequences were indicated with stars under the alignment.

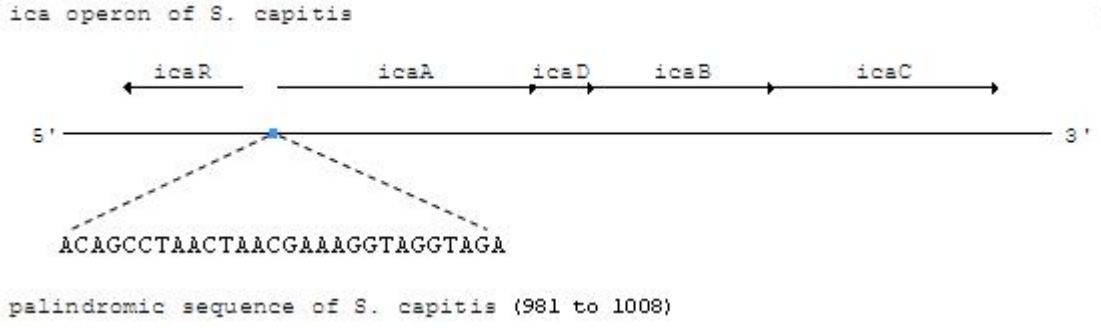

Figure 4.10. The position of the deduced palindromic sequence of *S. capitis* in the *ica* operon of isolate 6. The deduced palindromic sequence is a 28-bp fragment, highlighted with blue, locating from position 981 to 1008 bp from 5' to 3' end, the sequence is indicated.

```
capiR           LKNKIIDNAITLFSEKGYYGTTLDDIAKSVNIKKASLYYHYDNKEEIYRKSVENCFNYFK 60
Caprae          LKNKIIDNAITLFSEKGYYGTTLDDIAKSVNIKKASLYYHYSNKEEIYRKSVENCFNYFK 60
epiR            MKDKIIDNAITLFSEKGYDGTTLDDISKSVNIKKASLYYHYDNKEEIYRKSVENCFNYFI 60
AurR            LKDKIIDNAITLFSEKGYDGTTLDDIAKSVNIKKASLYYHFDSKKSIYEQSVKCCFDYLN 60
                :*:*************** *******:************:..*:.**.:**: **:*:

capiR           TFILESNNDSNYSIDGLYQFLFEFIFDIDERYIRLYVQLSSAPEELSSEIHNHLLGVNEV 120
Caprae          TFILENNSDSNYSIDGLYQFLFEFIFDIDERYIRLYVQLSSAPDELTPEIHNHLKEVNEV 120
epiR            DFLLR-NHDDNYSIDGLYQFLFKFIFDVDERYIKLYVQLSSAPEALNSEIKHHLQEINTT 119
AurR            NIIMMNQNKSNYSIDALYQFLFEFIFDIEERYIRMYVQLSNTPEEFSGNIYGQIQDLNQS 120
                 :::  : ..*****.******:****::****::*****.:*: :. :*  ::  :*

capiR           LDSEIIKYYDPSNISMGKEDFQNLILLFLESWYLRASFSQRFGVTEENKNCYKDQVYSLL 180
Caprae          LDSEIIRYYDPSEMSMGKEDFQNLILLFLESWYLRASFSQKFGVIEENKNCYKDQVYSLL 180
epiR            LHDELIKYYDPTHIALDKEDFINLILLFLETWYFRASFSQKFGIIEDSKNRFKDQVYSLL 179
AurR            LSKEIAKFYDESKIKMTKEDFQNLILLFLESWYLKASFSQKFGAVEESKSQFKDEVYSLL 180
                * .*: ::** :.: : **** ********:**::*****:**  *:.*. :**:*****

capiR           NVFIKK---- 186
Caprae          NVFVKNNFGN 190
epiR            NVFLKK---- 185
AurR            NIFLKK---- 186
                *:*:*:
```

Figure 4.11. Alignment of the helix-turn-helix of *S. epidermidis* with other *staphylococcus icaR* genes. capiR, *icaR* of *S. capitis*. Caprae, *icaR* of *S. caprae*. epiR, *icaR* of *S. epidermidis*. AurR, *icaR* of *S. aureus*. The H-T-H sequence is highlighted with yellow colour.

4.3.5 Putative mechanisms of Ica proteins in the polysaccharide synthesis pathway

IcaA is a protein of 412 amino acids length, which shares 83% identity to that of in *S.*

epidermidis and functions as a glycosyltransferase by secondary structure prediction.

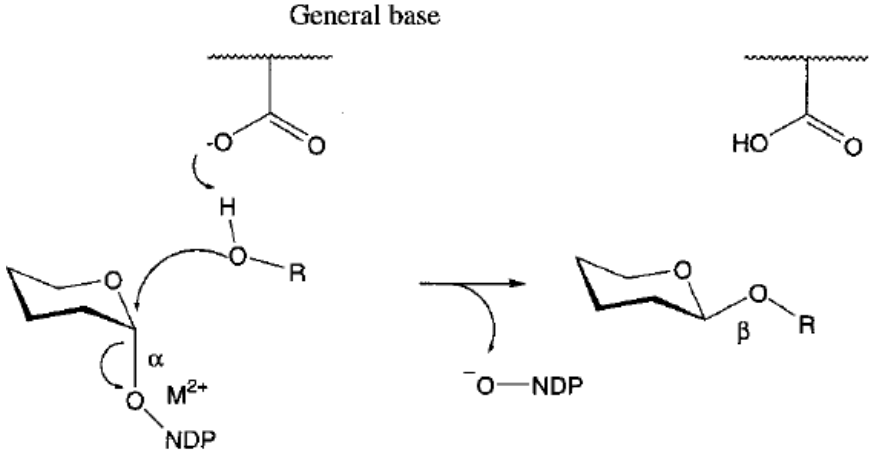

Figure 4.12. The putative catalytic mechanism for an inverting nucleotide-sugar glycosyltransferase (Charnock and Davies, 1999). Likely catalytic mechanism for an inverting NDP-sugar transferase. An α-linked nucleotide-diphospho-sugar donor yields a product with β-configuration. The sugar acceptor is activated for nucleophilic attack by a general base. It is widely believed that a divalent metal ion (Mn^{2+}) assists leaving group departure.

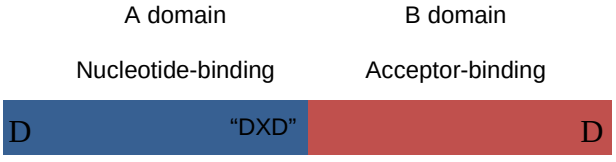

Figure 4.13. Schematic representation of a nucleotide-diphosho-sugar transferase from *Bacillus subtili,* SpsA (protein data bank code), which has similarity to IcaA of *S. capitis* (18% identity). This figure is indicating the position of important catalytic and UDP-binding residues.

Similar to SpsA (Figure 4.13), In IcaA of *S. capitis*, the N-terminal region is a classical nucleotide-binding domain, the "signature motifs" DXD of family GT-2 are contained in this N-terminal UDP binding domain. The C-terminal domain is the site for binding of the acceptor species.

Similar to that of *S. epidermidis*, the topology of IcaA in *S. capitis* shows that it is membrane-bound (Figure 4.14), which is a correlate with its essential transferase activity.

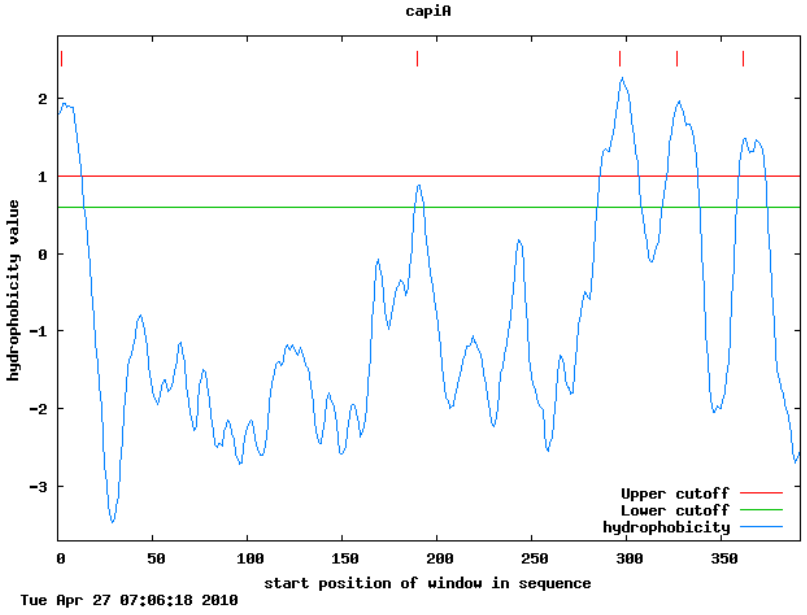

Figure 4.14. Hydrophobicity plots of IcaA of *S. capitis* 6. Five transmembrane helices in IcaA are present, with one is located at the N terminus and four at the C terminus.

IcaD is predicted to be a 101 amino acid cytoplasmic membrane protein. No concrete function has been proposed for IcaD in the pathway of polysaccharide synthesis. It has been reported that, in *S. epidermidis*, IcaA alone exhibited a weak glycosyltransferase activity. Analysis by thin layer chromatography revealed that the IcaAD mature protein synthesized extended oligomers of a maximal length of 20 residues, but did not form polymers comprising full-length polysaccharide intercellular adhesion (PIA), which are at least 130 residues in length (Gerke *et al*., 1998). It has been proposed that IcaD might be necessary to activate the conformation of IcaA protein. Two transmembrane domains are presented in IcaD (Figure 4.15), it might act as a chaperone to direct the membrane insertion of IcaA according to Gerke *et al*. (1998).

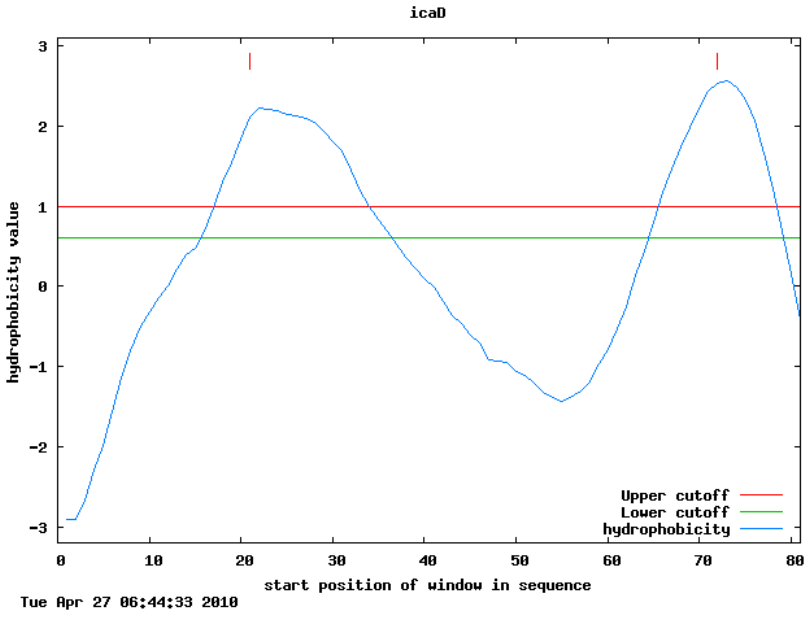

Figure 4.15. Hydrophobicity plot of IcaD of *S. capitis* 6. Two transmembrane helices in IcaA are present.

IcaB is predicted to have a length of 287-amino-acids, with an N-terminal 30-amino-acid signal sequence (Figure 4.16), resulting in 257 amino acids in length for the final mature protein. Figure 4.17 shows the hodrophobicity of the matured IcaB protein, without the signal peptide. Secondary structure analysis revealed that IcaB contains a putative polysaccharide *N*-deacetylase and belongs to the carbohydrate esterase family 4 (CE4), (Wang *et al.*, 2004) suggesting that IcaB may modify polysaccharides during synthesis.

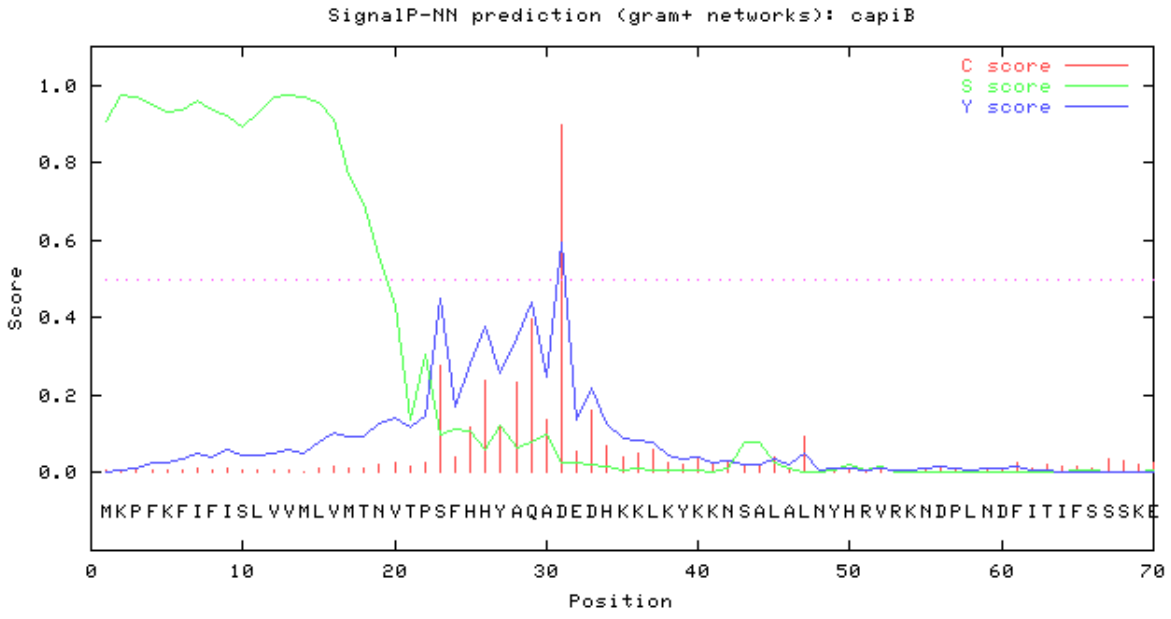

Figure 4.16. Signal protein prediction of IcaB. The presence and location of signal peptide cleavage site in amino acid sequences is indicated. Most likely cleavage site is between position 30 and 31: AQA-DE.

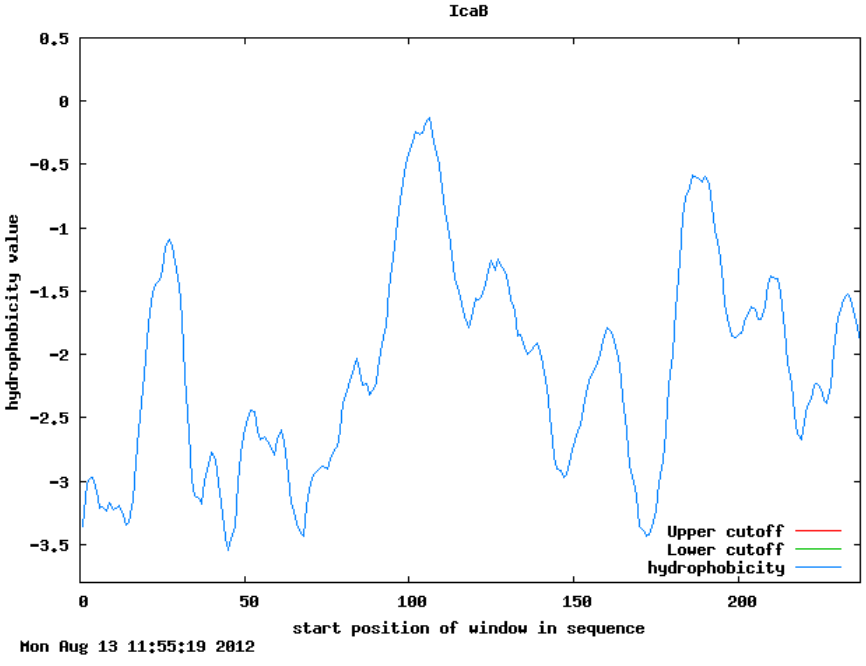

Figure 4.17. Hydrophobicity plot of IcaB of *S. capitis* 6 with removal of the 30 amino acid signal peptide.

The IcaC protein of *S. capitis* is predicted to be a transmembrane protein has a length of 357 amino acids with 10 transmembrane domains (Figure 4.18). The conserved functional domain search revealed that IcaC is homologous to an acetyltransferase from *Bacillus subtilis* (26% identity). The activity of IcaC may be required for modifying the growing polysaccharide chain according to the reaction:

Acetyl-CoA + polysaccharide ⟶ Acetyl-polysacchride + CoA.

The enzyme requires acetyl-CoA for its activity. It might transfers the acetyl-group from the acetyl-CoA to polysaccharide located outside of membrane, and CoA returns to the cell. The conserved histidine residue highlighted in the alignment is likely to be responsible for the deprotonation of the substrates. The other conserved residues may have functions in the catalysis. This protein confers an opposite modification of polysaccharide correspond to that of IcaB. The combination of IcaBC might be necessary for the bacteria to avoid the host immune system. Similarly, the oatA acetyltransferase of *S. aureus* aids resistance to the host immune defence. OatA is distantly related to IcaC. (Bera *et al.*, 2006).

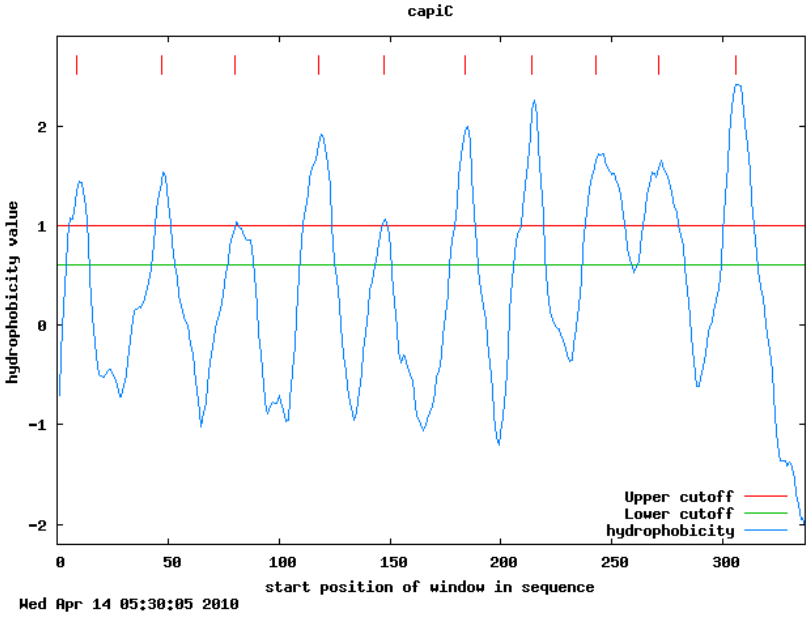

Figure 4.18. Hydrophobicity plot of IcaC of *S. capitis* isolate 6.

4.4 Discussion

4.4.1 The status of *ica* operon in *S. capitis*

The DNA sequence of *ica* operon in *S. capitis* were identified in this study. It contains four structural genes closely related to *S. caprae*, *S. epidermidis* and *S. aureus icaA*, *icaD*, *icaB* and *icaC* gene (≥65% identity). The regulatory *icaR* gene (≥ 70% iden*t*ity), is located upstream of *icaA*, transcribed in an opposite direction. The amino acid sequences deduced from the genes exhibited 66% to 94% identity to those of *S. caprae*, *S. epidermidis* and *S. aureus*. This operon was present in all the sixty clinical isolates in the same length, suggesting the biofilm-negative phenotype is not related to the insertion of a mobile element such as an insertion sequence or a transposon. The *ica* operon has been

verified is required for the biosynthesis of polysaccharide intercellular adhesion (PIA) in *S. epidermidis* and *S. aureus*. The degree of identity to other *staphylococcus* species at DNA and protein level suggests a similar function of *ica* operon in *S. capitis*.

Sequence comparison between the *ica* operon of the two bofilm positive isolates revealed even belonging to two PFGE types, the *ica* operon are of 100% identity. However, the three biofilm-negative isolates showed sequence variations. Isolate 44 had a deletion mutation in the -10 promoter element compared with that of biofilm-positive isolates (Chapter 6). This mutation might prevent the transcription of the *ica* genes, resulting in the inability to express PIA. In isolate 65, a stop codon occurred in the *icaB* gene; this nonsense mutation resulted in a predicted truncated protein, missing 69 C-terminal amino acids. An in-frame three amino acid deletion in the *icaA* gene of isolate 17 was identified (in IcaA, Gln^{192}, Ser^{193}, and Ile^{194}) and Ala^{195} was substituted with Pro. Figure 4.19 shows the topology of *icaA* in 17. The changes of its membrane-protein topology (four transmembrane locations) compared with that of 6 (five transmembrane locations) (Figure 4.14), might lead to the inability to produce biofilm in this isolate.

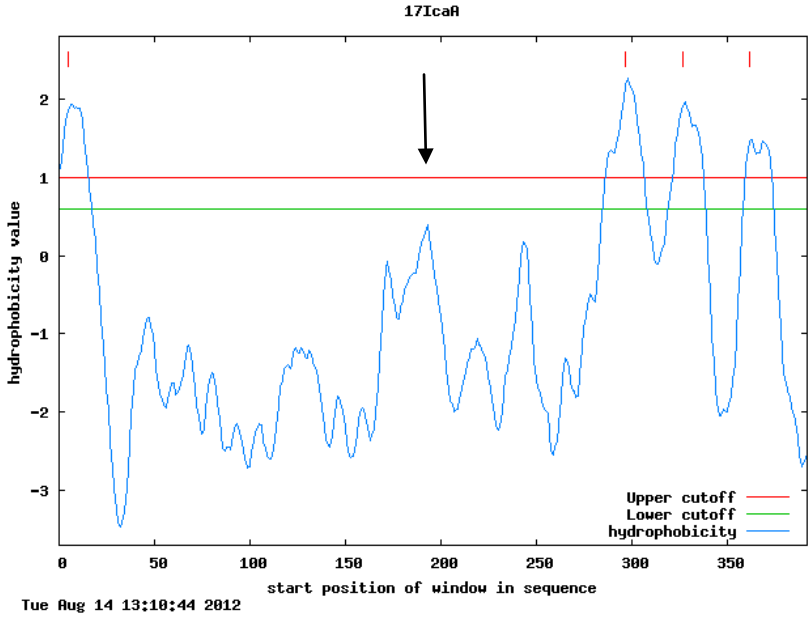

Figure 4.19. Hydrophobicity plot of IcaA of isolate 17. The arrow shows the position of change of hydrophobicity in isolate 17 compared with the wildtype profile (Figure 4.14).

4.4.2 The putative function of Ica proteins in *S. capitis*

The structures of Ica proteins have been proposed by performing multiple alignments with known protein structures. IcaA protein was shown similarity to a superfamily glycosyltransferase, at the highest identity of 19%. IcaB was shown homologous to polysaccharide deacetylase with 19% the highest identity. IcaC contains a conserved domain which is homologous to acyltransferase with 26% the highest identity. The IcaB and IcaC proteins in *S. capitis* seem to exhibit opposite functions. This might assist the bacteria escaping from the host immune system by modifying the polysaachrides. No functional structure has been identified homologous to IcaD, it shows 79% identity to that to *S. epidermidis*, might confer the similar function, that the gene is co-expressed with IcaA, produces a longer *N*-Acetylglucosamine oligomers and increases the enzyme

activities (Gerke *et al.*, 1998). The sequence analyses presented here suggest that IcaA and IcaD, are involved in the biosynthesis of the sugar backbone of PIA. IcaAD may constitute *N*-acetylglucosaminyltransferase activity in which IcaA represents the structual transferase that requires IcaD for full activity. IcaC may facilitate transfer of synthesised sugar to the outside of the membrane, and IcaB, might be responsible for modification of the polysaachride polymer.

4.4.3 Origin of the *ica* operon in *S. capitis*

The Ica proteins show remote homology to the well-defined functional protein families. This suggests the *ica* operon has existed for millions of years, long time before the hospitals were established. The accumulation of many mutations in the *ica* operon of biofilm-negative isolates, suggests the ancient origin of this phenotype. It is possible that the *ica* operon in biofilm-negative isolates has existed longer time due to the mutations on the genes. The genetic origin of *ica* genes in staphylococci is unknown. It is also uncertain how biofilm-forming isolates establish and disseminate within the hospital setting. The operon might be initially transmitted into hospital by transduction mediated via bacterial phage. It was suggested that horizontal gene transfer between staphylococci and other low-GC gram-positive bacteria is common and contributes to resistance and virulence development (Al-Talib *et al.*, 2010). Occurrence of the *ica* operon in *S. capitis* strains of different genetic backgrounds would suggest mobility and horizontal transfer of the operon of biofilm-mediating genes among these strains. The close contact of bacteria within a biofilm may facilitate horizontal exchange of genetic information.

In summary, the entire *ica* operon was identified and analysed. It showed similarities to that of other *staphylococcus* species. And it showed identical DNA sequences between

two biofilm-positive isolates, which belong to subsp. *urealyticus*. Several point mutations occurred in the *ica* operon in biofilm-negative isolates confirmed to be subsp*. capitis*. Whether these mutations were critical factors causing the biofilm-negative phenotype in these isolates remains a question to be answered, as biofilm formation is regulated by numerous factors. Many of the variations in the *ica* operons of bioflim-negative subsp. *capitis* might simply be natural variation in this group of *S. capitis* isolates. The putative function of Ica proteins in *S. capitis* was also proposed based on online bioinformatics tools. However, the computer-based prediction remains to be examined by actual experiments such as gene knock-out.

CHAPTER 5

Effects of sub-inhibitory concentrations of erythromycin on the expression of biofilm-related genes and biofilm formation in clinical *Staphylococcus capitis* isolates

5.1 Introduction

Recent studies indicated the emergence of *S. capitis* as a significant pathogen causing late-onset sepsis in very-low-birth-weight (VLBW) infants (1,500g) (Ng *et al.*, 2006, Van Der Zwet *et al*., 2002). The pathogenic potential of *S. capitis* has been attributed to the ability to form biofilms on polymer surface (Nalmas *et al*., 2008).

Biofilm formation proceeds in two processes (Heilmann *et al.*, 1996). Primary attachment of bacterial cells to a polymer surface is followed by accumulation of bacteria in a multilayered biofilm. The synthesis of polysaccharide intercellular adhesion (PIA), which mediates cell-to-cell adhesion, has been recognized to be essential for cell accumulation in *S. epidermidis*. The *icaADBC* operon is responsible for its synthesis (Cramton *et al*., 1999). The *icaADBC* locus has been detected in *S. aureus* and a range of other coagulase negative staphylococci (CoNS) and was confirmed to be prevalent in all sixty clinical isolates that examined (Chapter 4).

Phenotypically, biofilm formation is affected by various environmental conditions (Dobinsky *et al.*, 2003, Knobloch *et al.*, 2001a, Cotter *et al.*, 2009). Although there is limited knowledge on the regulation of the *ica* operon, recent data suggest the involvement of positive sigma factor *rsbU*, *icaR*, and *sarA* (Weiss *et al*., 2009, Knobloch *et al*., 2004).

It has been shown that sub-inhibitory antibiotic concentrations can influence the expression of important bacterial virulence factors of bacteria, such as adhesins and toxins (Bernardo *et al.*, 2004b, Cummins *et al*., 2009). In addition, several reports showed sub-inhibitory concentrations of tetracycline and erythromycin enhanced biofilm formation

in *S. epidermidis* (Rachid *et al*., 2000, Wang *et al*., 2010). However, there is no information on *S. capitis.*

The aim of this study was: 1. to examine the effects of sub-inhibitory concentrations of erythromycin on biofilm formation in the two subspecies of *S. capitis*. 2. To assess transcriptional activities of biofilm-related genes in the two subspecies in the presence of erythromycin to gain an insight into the regulatory mechanisms.

5.2 Materials and methods

5.2.1 Bacterial strains and growth conditions

Clinical isolates 6, 17, 44, 65 and 70 which have had the *ica* operons sequenced (Chapter 4) were used for testing the effects of sub-inhibitory concentrations of erythromycin on biofilm formation. Two isolates, 6 and 44, were selected as representatives for the gene expression study. Isolate 6 belongs to subspecies *urealyticus*, is a biofilm producer in TSB supplemented with 4% NaCl. Isolate 44 belongs to subspecies *capitis*, exhibits a biofilm-negative phenotype when grown in TSB supplemented with NaCl. Both isolates carry the *ica* operon in the same length, however, some mutations occurred in the *ica* operon of isolate 44, based on sequence analysis.

Because the bacterial cell pellets in TSB were too sticky for RNA isolation, therefore, Brain Heart Infusion (BHI) (Oxiod, Australia) was used in gene expression experiment as a substitution. The two isolates 6 and 44 selected for gene expression assay were grown in BHI broth containing 0.85% NaCl (not supplemented) in the presence of erythromycin concentrations at 1/32 and 1/2 of the MICs of 6 and 44, respectively. Cultures were incubated at 37 °C aerobically with gentle shaking. The MIC of erythromycin for isolate 6

is 512 µg/mL; it was grown in 16 µg/mL of erythromycin, which is the serum achievable concentration (Baltch *et al.*, 1998). The MIC of erythromycin for isolate 44 is 0.5 µg/mL, a sub-inhibitory concentration 0.25 µg/mL, was used to grow this bacterium. After measurement of the optical density of the cultures, the bacteria were harvested for RNA extractions as described subsequently.

5.2.2 Phenotypic characterization of biofilm formation by microtitre plate assay (MtP)

The test was performed following the method described by Christensen *et al*. (1985), with minor modifications. Briefly, overnight cultures were diluted 1:100 with Trypticase Soy Broth (TSB) (Oxiod, Australia) containing 0.85% NaCl with various concentrations of erythromycin, dependent on the MICs of each isolate, and 200 µL per well were seeded in 96-well microtiter plates (Corning, Australia). The plates were incubated at 37°C for 20 hours. After four washes in phosphate buffered saline solution (pH 7.2), wells were dried for 1 hour at 55°C, and the adherent biofilms were stained with Hücker crystal violet. Finally, the plates were rinsed under running tap water, air-dried, and OD_{595nm} was read by a POLARstar Omega (BMG, Labtech pty. Ltd., Australia). In accordance with the original method, isolates with OD_{595nm} 0.12 were considered as negative (NP), those with OD values 0.12 and 0.24 were regarded as weak biofilm-producers (WP). An OD 0.24 was indicative of biofilm-producing bacteria strains (P). For each isolate the MtP test was repeated in duplicate, and consistent results were obtained.

The dose-dependent responses of biofilm formation in isolate 6 were examined. The concentraions used were from 1/2 × MIC (256 µg/mL) to 1/128 × MIC (4 µg/mL) according to MIC test for erythromycin.

5.2.3 Growth curve construction for isolates 6 and 44

Isolates 6 and 44 were grown in 10 mL of BHI broth in 37 °C for 16 hours with shaking at 170 rpm. Five hundred microliters of each overnight culture was inoculated into 50 mL of pre-warmed BHI containing 0.85% NaCl with 16 or 0.25 µg/mL of erythromycin (for isolates 6 and 44, respectively). Cultures were incubated at 37°C, with gentle shaking. The amount of growth of bacterial cultures was measured by spectrophotometry at OD_{600nm} and viable counts were performed by standard plate count every two hours for the first 8 hours, then at longer intervals for 24 hours for isolate 6 or 48 hours for isolate 44. Each growth curve was repeated in a separate experiment and plate count was duplicated for each growth.

5.2.4 RNA isolation

For RNA isolation from culture, bacteria were grown in BHI containing 0.85% NaCl with and without erythromycin to the desired growth phase. A pellet of approximately 5×10^9 bacteria was then resuspended in 1 ml RLT buffer (QIAGEN), and the mixture was disrupted with 0.5 ml of 0.1mm glass beads in a high-speed Mini BeadBeater-8 (BioSpec Products, USA). Total RNA was isolated as directed in the instructions provided by the manufacturer of QIAGEN. RNA was isolated and purified as described previously (Chapter 2 section 2.5.2).

Contaminating DNA was degraded by digesting RNA samples with *TURBO DNA-free* Kit as described previously (Chapter 2 section 2.5.2.2).

5.2.5 Quantification of specific transcripts with real-time RT-PCR

Oligonucleotide primers used in the gene regulation study are listed in Table 5.1. Forward primers were used for reverse transcription. The cDNA synthesis was performed using the RNeasy® Mini Kit (QIAGEN, Australia) according to manufacture's instruction with modification. For each gene, a dilution series of newly synthesized cDNA was included in quantitative PCR to examine the efficiency of PCR and subsequent relative quantitative calculations.

RNA for reverse transcription was isolated from two separate cultures of isolates of 6 and 44. Briefly, one microgram of RNA and 0.4 µM of primer in a total volume of 14 µL were heated at 65 °C for 10 mins and immediately chilled on ice for at least 3 mins. The reverse transcription reaction master mix was prepared in a total volume of 5 µL, which consisted of 2 µL of 1×RT buffer, 2 µL of 5mM dNTP, and 2 U of RNAase inhibitor. The mixture was gently mixed, added to the RNA-primer mixture followed by addition of 1 µL of reverse transcriptase (200 U/µL). Reverse transcriptase was substituted by RNase-free water for the negative control. The reaction mixture was gently mixed, incubated at 37 °C for 1 hour. After cDNA synthesis, 230 µL of molecular-grade water was added to the samples.

Quantitative PCR was performed with the MiniOpticon (Bio-Rad) using iQ SYBR Green Supermix (Bio-Rad) according to the manufacturer's instructions. The PCR reaction was performed in a total volume of 25 µL consisting of 12.5 µL of iQ SYBR Green Supermix, 1 µL of 10 µM forward and reverse primers respectively, 2.5 µL of the diluted cDNA solution, and 8 µL of molecular-grade water. Primers icaAf/r, icaRf/r, sarAf/r and rsbUf/r were used for amplifying the cDNA-specific fragments for the *icaA*, *icaR*, *sarA* and *rsbU*

gene, respectively. Each PCR was performed in triplicate. PCR conditions were as follows: cycle1 (1×): 95 °C for 5 min; cycle 2 (40×): 95 °C for 30 s, 55 °C for 30 s, 72 °C for 30 s; cycle 3 (100×): 95 °C for 10 s (decrease setpoint temperature after cycle 2 by 0.5 °C, and enable melt curve data collection and analysis). Each specific amplicon was verified by the presence of a single melting temperature peak and by the presence of a single band of expected size on a 2.5% agarose gel after electrophoresis. Cycle threshold values were determined by the CFX softeware (Bio-Rad).

The relative changes in gene transcription between the included and calibrated samples were calculated using the method described by QIGEN. Briefly, mid-log phase RNA was extracted and reverse transcribed to cDNA, 10 fold dilutions were used to generate a standard curve for every gene by using the Cycle Threshold (Ct) versus the logarithm of each dilution factor. Total RNA was extracted from two independent bacterial cultures. All reactions for each target gene were performed in triplicate and in the same PCR run.

Standard curves were constructed for both target and reference gene by plotting Ct values (Y-axis) against the log of template amount of dilution (X-axis). The amount of target and reference cDNA was calculated in samples of interest using the Ct value and corresponding standard curve. The amount of target cDNA was divided by the amount of reference cDNA to calculate the normalized amount of target. The normalized target amount of untreated sample (calibrator) was set as 1; the relative expression level of target gene in samples of interest calculated by dividing the normalized target amounts by the value of the calibrator.

Table 5.1. Primers used for gene regulations in this study.

Gene	Forward primer (5' to 3')	Reverse primer (5' to 3')	Accession No.	Origin (source)
icaA	GGGCTATGGAAACAACG	TGTCGGATACCAACTCAC	AY146582	This study
icaR	CAACAACGATTCTAACTACTC	TGGATAATTGGACGTATAACC	AY146584	This study
sarA	ACGAACACGATGAAAGAACAG	TTCGCTTCAGTGATACGTTTG	NZ_ACFR01000002	This study
rsbU	CTCTATTTCGTGCCTCAG	GTGTGCTTGGAGTAAGTC	AFTX01000024	This study

5.2.6 Validation of housekeeping genes for quantitative PCR

Candidate reference genes were selected from those most commonly used in the literature (Vandecasteele *et al.*, 2001, Theis *et al*., 2007). All the primers for these housekeeping genes are listed in Table 5.2. The genes: *gyrB*, encoding the B subunit of the DNA gyrase; *recA*, encoding protein RecA, which contributes to homologous recombination, DNA repair, and the SOS response; *tuf*, encoding elongation factor Tu; *rpoB*, encoding the β subunit of bacterial RNA polymerase; and *sodA*, encoding the manganese-dependent superoxide dismutase selected and validated. PCR primers used in this study are listed in Table 5.2. All the primers were designed using Clone manager 7 (Scientific and Educational Software, USA). The reverse transcriptase quantitative PCR reactions and standard curves were set up as described above.

Table 5.2. Primers of the housekeeping genes used in this study.

Gene	Forward primer (5' to 3')	Reverse primer (5' to 3')	Accession No.	Origin (source)
gyrB	CCTCCAGCATGTAATACC	GAGGCTTGCACCATTTAG	CP000029	Conlon *et al*., 2002
recA	TAAAGTAGCACCTCCATTCAG	CCAAGCACCAGATTTATCAAC	FN554702	This study
rpoB	AGTTGTAACCGTCCCAAGTC	AATGGCACTGAACACGAAGG	NZ_ACFR01000002	This study
tuf	CTGAAGCTGGTGACAACATC	ACGTCCACCTTCGTCTTTAG	AF298798	This study
sodA	TCAGCAGTTGAAGGAACAG	TGACCGCCACCATTATTAC	AJ343941	This study

5.2.7 Statistical analysis

Data were presented as means ± standard errors of the mean (SEM). A statistical test was applied to look for significant differences between experimental conditions for each candidate housekeeping gene. A one-way analysis of variance (ANOVA) was conducted, followed by Dunnett's post-hoc analysis to compare each time set against the control group mean. A p value < 0.05 was considered statistically different. Calculations were performed using the SPSS software (SPSS Inc).

5.2.8 Sequence alignment

Intergenic regions between *icaA* and *icaR* gene in the *ica* operon of isolates 6 and 44 were aligned by using ClustalW2 (http://www.ebi.ac.uk/Tools/msa/clustalw2/) with default parameter in this study.

5.3 Results

5.3.1 Biofilm formation of *S. capitis* in response to erythromycin

The five isolates (6, 17, 44, 65 and 70) for which the *ica* operons had been sequenced were tested their biofilm formation in the presence of erythromycin. They represented the two subspecies. The concentrations of erythromycin used in biofilm assay were determined by their MIC values, respectively. Sub-inhibitory concentrations were employed.

The results showed that erythromycin induced biofilm formation in isolate 6, a strong biofilm producer under standard biofilm assay conditions (TSB with 4% NaCl), in a dose dependent manner (Figure 5.1); the OD_{595nm} in the presence of 1/32 × MIC (16 µg/mL)

the amount of biofilm produced was only half of that produced at 1/2 × MIC (256 µg/mL). However, the other biofilm-positive isolate 70, only marginally enhanced its biofilm production in the presence of ½ (0.25 µg/mL) × MIC. This is probably due to its low MIC value (0.5 µg/mL), the sub-inhibitory concentrations were not high enough to increase its biofilm production. Among the three biofilm-negative isolates, 17 (MIC, 2 µg/mL) formed weak biofilm in the presence of 1 µg/mL of erythromycin, its OD_{595nm} increased from 0.06 ± 0.004 to 0.24 ± 0.008. The other two biofilm-negative isolates, 44 (MIC, 0.5 µg/mL) and 65 (MIC, 0.25 µg/mL), remained biofilm-negative in the presence of erythromycin (Figure 5.2).

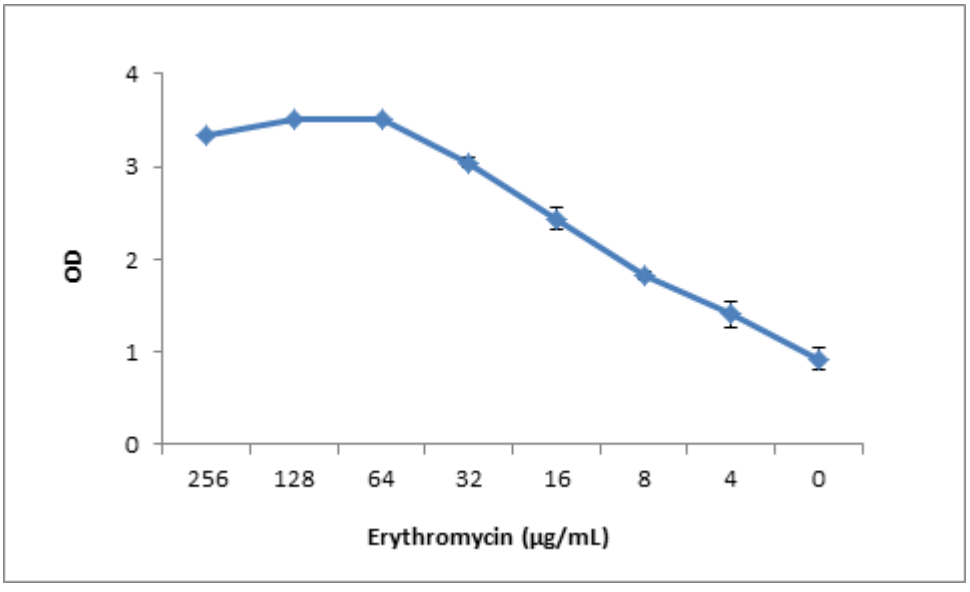

Figure 5.1. Biofilm formation of isolate 6 in the presence of sub-inhibitory concentrations of erythromycin. Error bars indicate standard error means, and the assay was tested in triplicate experiments.

Biofilm formation decreased at 256 µg/mL of erythromycin, it is probably due to the inhibition of erythromycin at this high concentration, resulted in lower cell number for biofilm production. The actual values of biofilm formation at 128 and 64 µg/mL were

probably higher than shown in the figure; it was believed go beyond the range of the measure of the machine.

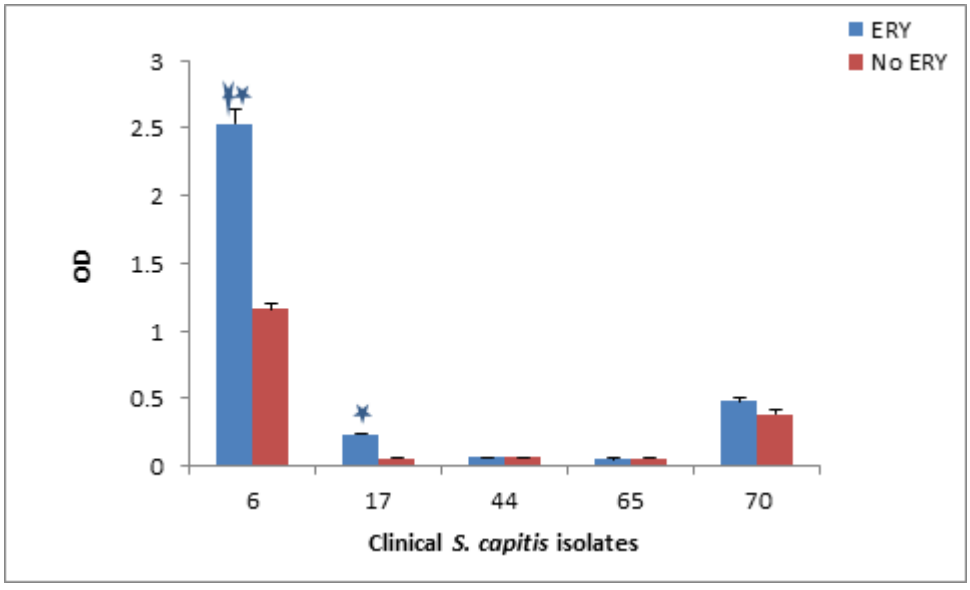

Figure 5.2. Biofilm formation of isolates in the presence and absence of erythromycin (ERY). The concentration of ERY used for isolate 6 is 16 µg/mL, 1/32 × MIC. The concentrations for all the other isolates were 1/2 × MICs, respectively. (Isolate 17, 1 µg/mL; isolate 44, 0.25 µg/mL; isolate 65, 0.125 µg/mL; isolate 70, 0.25 µg/mL). Error bars indicate standard error means, and the assay was tested in duplicate experiments. * $p < 0.05$; ** $p < 0.01$.

5.3.2 Growth curves

To determine the desired growth phase to be employed for the gene regulation study, the growth of isolates 6 and 44 were examined in the presence and absence of erythromycin (Figures 5.3 and 5.4).

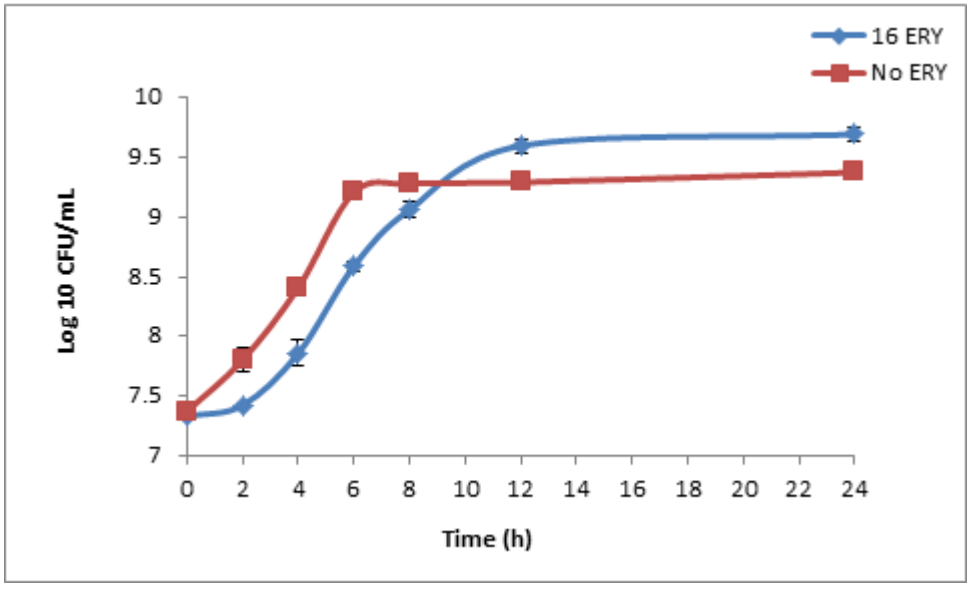

Figure 5.3. Growth of isolate 6 in the presence of 16 µg/mL (1/32 × MIC) of erythromycin compared with no erythromycin. Error bars indicate standard error means. The growth curves were tested in duplicate experiments.

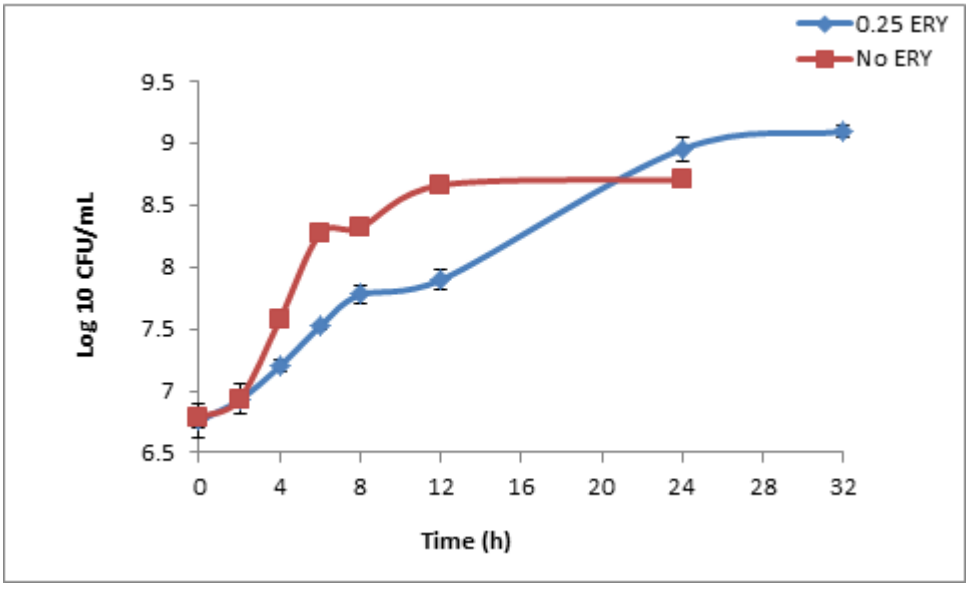

Figure 5.4. Growth of isolate 44 in the presence of 0.25 µg/mL (1/2 × MIC) of erythromycin compared with no erythromycin. Error bars indicate standard error means. The growth curves were tested in duplicate experiments.

From the growth curves shown above, it can be seen that isolate 6, of which MIC is 512 µg/mL, delayed the time to reach mid log phase in the presence of erythromycin. It reached mid-log phased approximately 2 hours latter when it was grown in the presence of 16 µg/mL of erythromycin, compare with growth in BHI without erythromycin. The level of 16 µg/mL of erythromycin is a serum achievable concentration (Baltch *et al*., 1998). Isolate 44 displayed a different growth manner in the presence of its 1/2 × MIC (0.25 µg/mL), probably because the resistant bacterial population grew out the inhibition of the antibiotic. The cell population was still increasing after 12 hours incubation and continued to increase until 24 hours of incubation. However, erythromycin did not change its time to reach mid log phase. This isolate reached mid-log phase at about 4 hours' growth in both the absence and presence of erythromycin.

5.3.3 Validation of housekeeping genes for reverse transcriptase real-time PCR

The gene expression of candidate housekeeping genes *tuf*, *recA*, *gyrB*, *rpoB* and *sodA*, was examined for isolate 6. The bacterial pellets were collected at mid-log phase in the presence and absence of erythromycin, and were shown in Figure 5.5.

a

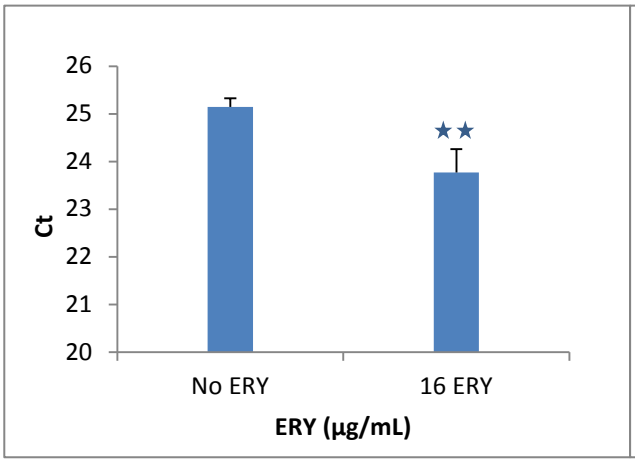
26
25
24
23
22
21
20
Ct
★★
No ERY
16 ERY
ERY (µg/mL)

b

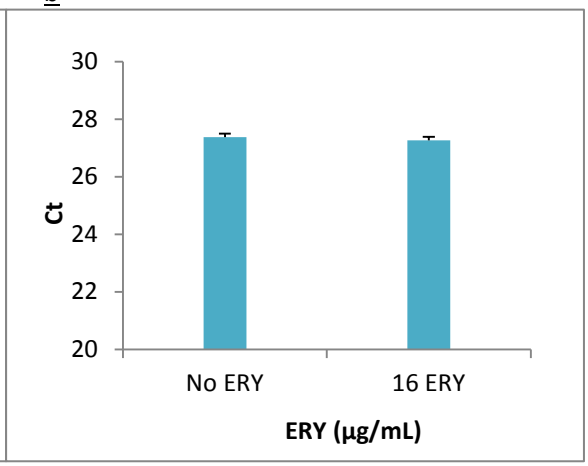
30
28
26
24
22
20
Ct
No ERY
16 ERY
ERY (µg/mL)

c

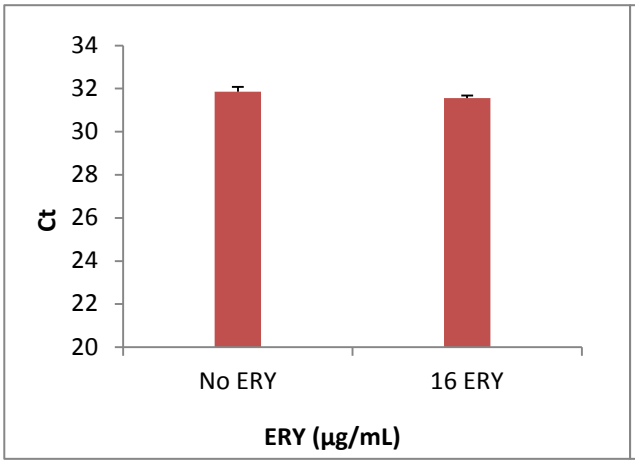
34
32
30
28
26
24
22
20
Ct
No ERY
16 ERY
ERY (µg/mL)

d

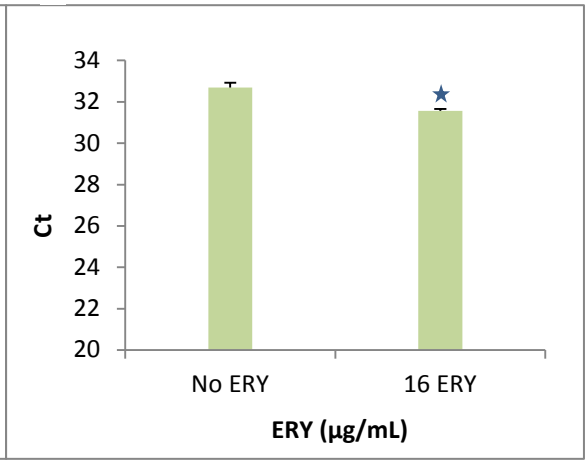
34
32
30
28
26
24
22
20
Ct
★
No ERY
16 ERY
ERY (µg/mL)

e

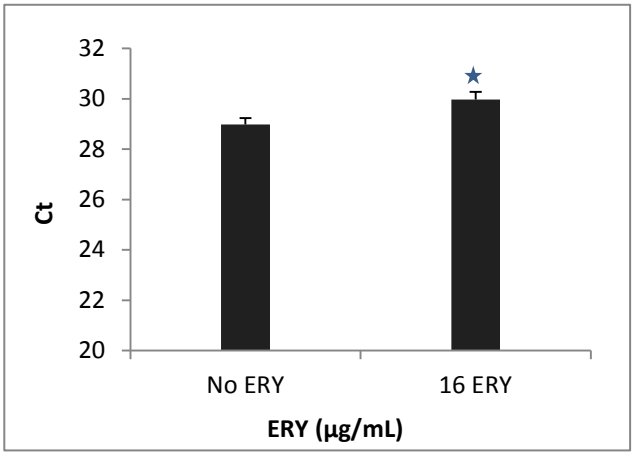
32
30
28
26
24
22
20
Ct
★
No ERY
16 ERY
ERY (µg/mL)

Figure 5.5. Effects of erythromycin (16 µg/mL) on the expression of housekeeping genes: a, *tuf*; b, *gyrB*; c, *recA*; d, *rpoB*; e, *sodA*. Changes in gene expression were analysed by One-way ANOVA (see methods for details). Error bars indicate standard error means. Each gene was assessed in triplicate experiment. ★ $p < 0.05$, ★★ $p < 0.01$ vs. no erythromycin controls. ERY, erythromycin.

As shown in the graphs, the expression of three housekeeping genes *tuf*, *sodA* and *rpoB* differed significantly under the two conditions. The expression of *tuf* and *rpoB* decreased, whereas the expression of *sodA* increased in the presence of erythromycin. The *gyrB* and *recA* genes were stable under this stress factor.

5.3.4 Primary sequence analysis of intergenic region located between the *icaR* and *icaA* in *S. capitis*

The primary sequence of the intergenic region from *icaA* to *icaR* gene in the *ica* operon of isolate 6 is shown in Figure 5.6, with deduced promoter elements for *icaA* and *icaR* gene and the SarA binding site. Figure 5.7 shows the comparison of the intergenic regions of *ica* operon of isolates 6 and 44. A single nucleiotide T was deleted in the -10 elecment of isolate 44.

```
                RBS                                    -10
  1  ttctaaaatc tccccttat ttaatttaaa ttcgttatat tacaggaaaa
     aagattttag aggggaata aattaaattt aagcaatata atgtcctttt
       SarA binding site                                -35
 51  ttaagttaaa attacaaata ttactgttca agtataacaa cattctattg
     aattcaattt taatgtttat aatgacaagt tcatattgtt gtaagataac
                    -35          -10                  RBS
101  caaattgaaa cactttcgat tagtatatgc gatacagcct aactaacgaa
     gtttaacttt gtgaaagcta atcatatacg ctatgtcgga ttgattgctt

151  aggtaggtag ataag
     tccatccatc tattc
```

Figure 5.6. The primary intergenic region of isolate 6.The putative promoter region of *icaA* gene -10 and -35 boxes and its ribosome binding site (RBS) deduced from Vadeboncoeur *et al.* (2000) are highlighted with grey. The *icaR* promoter regions and ribosome binding site are highlighted with yellow. The SarA binding site deduced from (Chien *et al*., 1999) is highlighted with red.

```
6       TTCTAAAATCTCCCCCTTATTTAATTTAAATTCGTTATATTACAGGAAAATTAAGTTAAA 60
44      TTCTAAAATCTCCCCCTTATTTAATTTAAATTCGTTATATTACAGGAAAATTAAGTTAAA 60
        ************************************************************
                                                  -35
6       ATTACAAATATTACTGTTCAAGTATAACAACATTCTATTGCAAATTGAAACACTTTCGAT 120
44      ATTACAAATATTACTGTTCAAGTATAACAACATTCTATTGCAAATTGAAACACTTTCGAT 120
        ************************************************************
         -10                            RBS
6       TAGTATATGCGATACAGCCTAACTAACGAAAGGTAGGTAGATAAG 165
44      TAG-ATATGCGATACAACCTAACTAACGAAAGGTAGGTAGATAAG 164
        *** ************ ****************************
```

Figure 5.7. Alignment of intergenic region of *ica* operon in isolate 6 and 44. The putative promoter region of *icaA* -35 and -10 boxes and the ribosome binding site are indicated by underlining the selected sequence in the sequence of 6.

5.3.5 Example of calculation to demonstrate calculation of relative gene expression

Expression of the four genes: *icaA*, *icaR*, *sarA*, and *rsbU* was assessed in response to erythromycin in clinical isolates 6 and 44 using mid-log planktonic cells.

Standard curves of the four target genes and the housekeeping gene *gyrB* were constructed based on the cycle threshold values versus the log cDNA of isolate 6. These curves were used as consensus standards for both isolates in subsequent relative expression calculations (Figure 5.8).

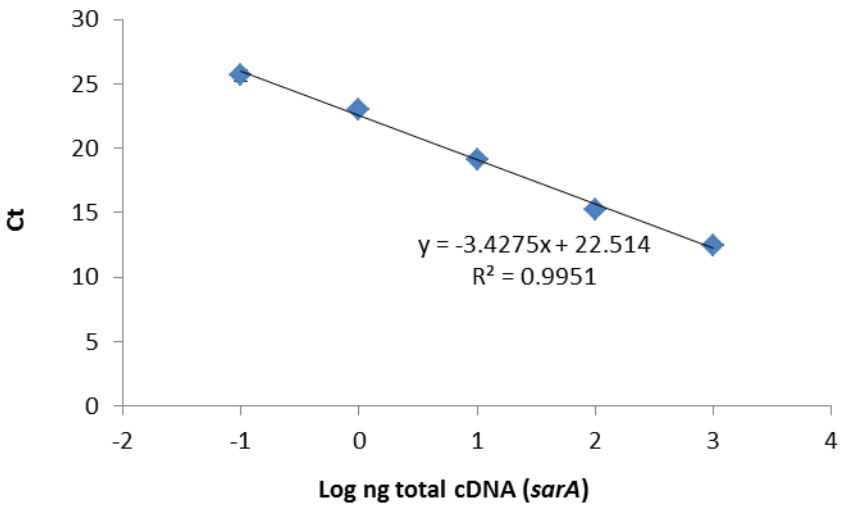
Ct
y = -3.4275x + 22.514
R² = 0.9951
Log ng total cDNA (sarA)

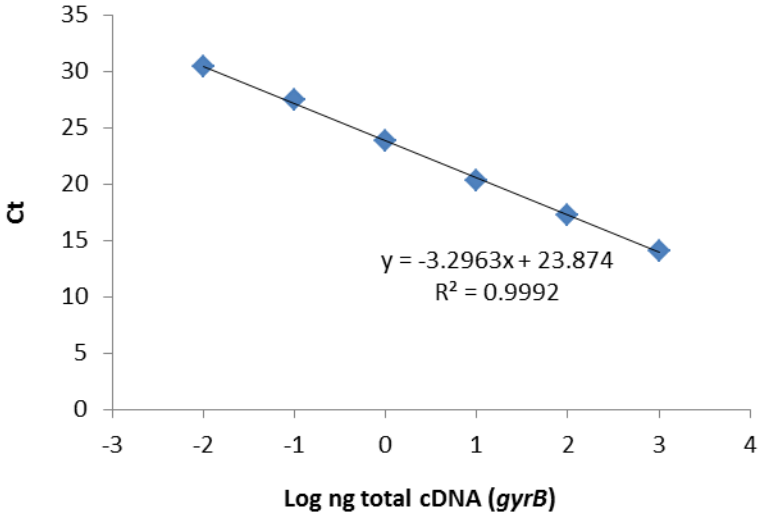
Ct
y = -3.2963x + 23.874
R² = 0.9992
Log ng total cDNA (gyrB)

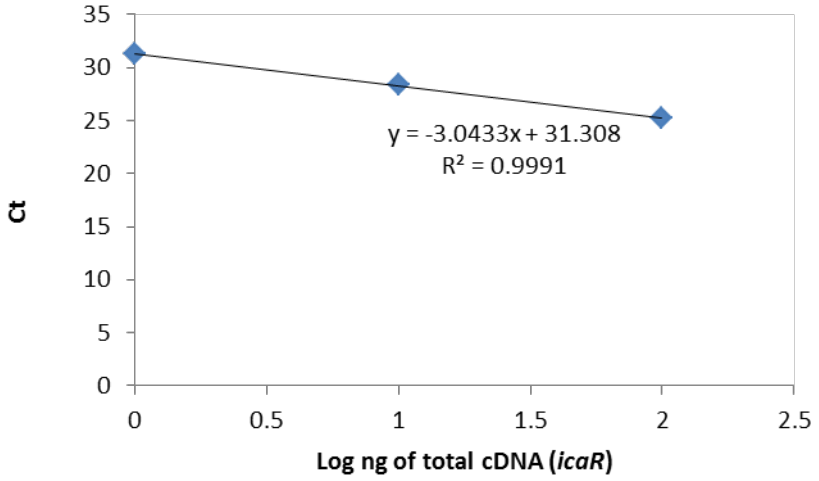
Ct
y = -3.0433x + 31.308
R² = 0.9991
Log ng of total cDNA (icaR)

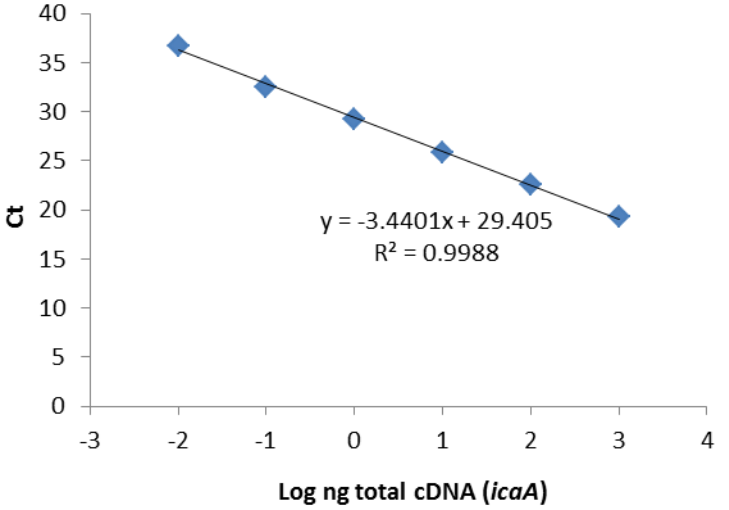
Ct
y = -3.4401x + 29.405
R² = 0.9988
Log ng total cDNA (icaA)

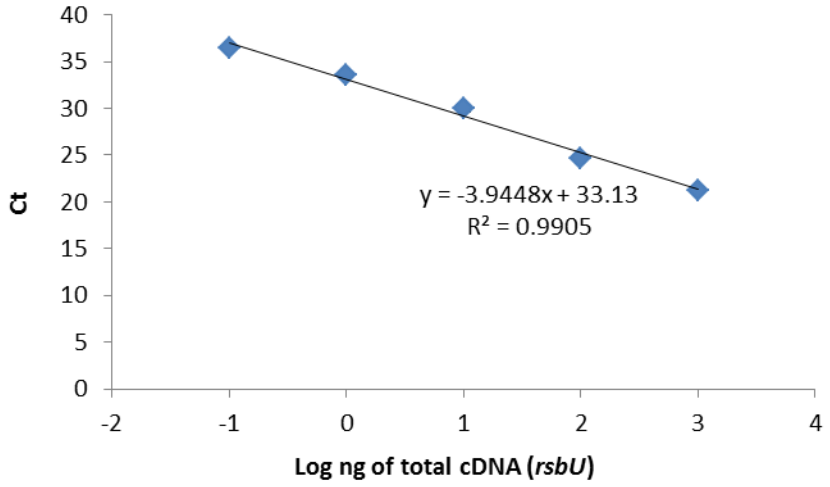

Figure 5.8. Relative quantification with different PCR efficiencies. Standard curves were generated for *icaA*, *icaR*, *sarA, rsbU* and the housekeeping gene *gyrB* using cDNA. Real-time RT-PCR was performed using gene-specific primers indicated previously. Error bars indicate standard error means, each gene was run duplicated, if an unexpected value occurred, another run was performed.

The relative amounts of target and reference cDNA were determined using the appropriate standard curve. Relative gene expression of the four target genes in the presence of erythromycin is summarized in Table 5.5.

Generally, the results revealed the two isolates 6 and 44 responded differently to erythromycin at mid-log phase. In isolate 6, *icaA* and *sarA* gene showed elevated expression, whereas *rsbU* and *icaR* were down-regulated compared with untreated cells. A reverse manner of reaction to erythromycin was observed in isolate 44. In mid-log phase, *icaR*, the repressor of *ica* operon, showed a strong up-regulation. However, the *icaA* and *sarA* genes were down-regulated. The *rsbU* gene was weakly up-regulated in this growth stage.

The relative expression of the *icaA* gene of isolate 6 in the presence of erythromycin was used as an example to demonstrate relative quantification. Table 5.3 shows the data used to generate standard curves.

Table 5.3. Data used to generate standard curve of *icaA* gene.

Template amount (ng)	Log ng total cDNA (*gyrB*)	Ct (Mean)	
		gyrB	*icaA*
1000	3	14.12	19.25833
100	2	17.24833	22.49833
10	1	20.36167	25.88
1	0	23.79667	29.29167
0.1	-1	27.43	32.56
0.01	-2	30.39833	36.62
Slope		-3.2963	-3.4401
PCR efficiency		93.30%	91.35%

Table 5.4. Quantification and normalization of *icaA* and *gyrB* expression levels.

Sample	*icaA* Ct	*gyrB* Ct	*icaA* cDNA amount	*gyrB* cDNA amount	Normalized amount	Ratio
ERY 0	31.16833	27.62833	-0.51258	-1.13895	0.45	1
ERY 16	33.30167	27.27167	-1.13272	-1.03075	1.09893	2.4421

Bacterial cells were untreated or treated with 16 µg/mL of erythromycin. Total RNA was purified and, after real-time RT-PCR, the relative amounts of target and reference cDNA were determined using the appropriate standard curve (see Figure 5.7). The calculation of normalized amount of both treated and untreated was described in methods.

Table 5.5. Relative gene expression of biofilm-related genes in *S. capitis* in the presence of erythromycin at mid-log phase.

	Relative gene expression	
Gene	Isolate 6 (subsp. *urealyticus* biofilm-positive)	Isolate 44 (subsp. *capitis* biofilm-negative)
icaA	2.4421	0.257462
icaR	0.6641	8.0586
SarA	1.522337	0.76512
rsbU	0.665441	1.1241

5.4 Discussion

5.4.1 Validation of housekeeping genes

Accurate normalization of gene-expression levels is an absolute prerequisite for reliable results for expression of genes of interest. Ideally, the internal control genes for expression studies should not be influenced by the conditions of the experiments. Five housekeeping genes *tuf*, *gyrB*, *recA*, *rpoB* and *sodA* have been demonstrated to be the least affected in the presence of a range of conditions (Theis *et al*., 2007). They were chosen and evaluated by real-time reverse transcriptase PCR in this study. The genes *gyrB* and *recA* were shown to be stably expressed, whereas all the others were influenced by the current experimental conditions. The *gyrB* gene was selected for the subsequent regulation study due to its reliable cycle threshold value (about 27 ± 0.13) in the presence and absence of erythromycin. Therefore, the internal control used for the gene expression study as the normaliser has been validated.

5.4.2 Transcriptional analysis of biofilm-related genes in response to erythromycin

It has been reported that numerous environmental factors such as high osmolarity (NaCl), ethanol, oxygen, antibiotics can affect biofilm formation in staphylococci (Cotter *et al*., 2009, Dobinsky *et al*., 2003, Rachid *et al*., 2000). In this study, the phenotypic expression of biofilm formation of clinical *S. capitis* was shown to be influenced by erythromycin. Four genes, *icaA*, *icaR*, *sarA* (which encodes a global factor) and *rsbU* (a positive regulator for the activity of σ^B) have been identified to be involved in biofilm formation in *S. epidermidis* and *S. aureus* (Trotonda *et al*., 2005, Tormo *et al*., 2005). To assess whether the expression of these genes in *S. capitis* is affected by erythromycin and to what extent, real-time reverse transcriptase PCR was performed with RNA prepared from mid-log phase planktonic cells of clinical isolates 6 and 44, which represent the two subspecies of *S. capitis*.

The results revealed different responses of these two isolates to erythromycin. In isolate 6, which is a biofilm producer and belonging to subsp. *urealyticus*, the expression of *icaA* and *sarA* gene were up-regulated, and *icaR* was down-expressed. This result is consistent with the results of the phenotypic assay and the findings of other studies which demonstrated that SarA is an essential positive regulator of biofilm formation in *S. epidermidis* (Tormo *et al.*, 2005); however, it represses *icaR* expression in *S. aureus* (Cerca *et al*., 2008). Handke *et al*. (2007) suggested that SarA has a direct effect on the *ica* transcription. In this study, the conserved SarA binding site was identified, located upstream of the *icaA* promoter and overlapping with the *icaR* promoter at the -35 region in the primary sequence of the intergenic region of *S. capitis* (Figure 5.5). Combined with the results of the expression study, these results suggested that SarA confers a similar role in biofilm formation in *S. capitis* to that of *S. epidermidis*. RsbU regulates biofilm

formation via activation of sigma factor repressing the *icaR* expression in *S. epidermidis*. In contrast to this study, *rsbU* was shown down-regulated in mid log phase compared with untreated cells in *S. capitis*. The down-regulation did not lead to the decrease of *icaA* expression and up-regulation of *icaR* in this isolate. A probable explanation for this finding is the presence an alternative sigma factor which activates sigma B, thereby, modulating biofilm development in *S. capitis*. Alternatively, the regulation by RsbU may start at a different time point, such as stationary phase. This possibly needs testing by further experiments.

Surprisingly, in isolate 44, the same four genes displayed a reverse expression manner, compared with expression in isolate 6. Both *icaA* and *sarA* were down-regulated and *icaR* was up-expressed in the presence of erythromycin. This result indirectly demonstrated the *icaA* promoter in isolate 44 is functional, even though a single nucleotide deletion was revealed by sequence comparison, as shown in Figure 5.6. *rsbU* expression was marginally increased, however, the expected effects on *icaA* and *icaR* were not observed. It can't be concluded that the biofilm-negative phenotype of this isolate is due to its gene regulation system at this stage. Further experiments are needed to assess the gene expression at different time points. Also, several clinical isolates with similar background (PFGE type) should be used to investigate the gene expression to address the roles of these regulators in biofilm formation in this subspecies.

In addition, isolate 17, which exhibits a biofilm-negative phenotype in 4% NaCl, and belongs to subsp. *urealyticus*, produced weak biofilm in the presence of its half MIC of erythromycin. This suggests an alternative biofilm formation pathway was adopted in the presence of erythromycin in this isolate.

In summary, despite the observations presented above, the mechanisms underlying the biofilm formation induced by erythromycin in *S. capitis* is far from being elucidated. However, these preliminary studies provide a fundamental knowledge guiding future experiments.

In addition to *sarA* and *rsbU*, several other global regulators have recently been identified impacting biofilm formation in staphylococci. *In Bacillus subtilis*, Spx was characterized as a novel type of global regulator whose activity is regulated by the redox status of the cells (Rochat *et al.*, 2012). In *S. aureus*, Spx affects biofilm formation via modulating the expression of *icaR* (Pamp *et al.*, 2006). LuxS, the two-component of quorum sensing system, negatively regulates biofilm formation in *S. epidermidis* (Xu *et al*., 2006a). The erythromycin-induced biofilm formation shown in this study might be representative of the macrolide class of antibiotics, and may have clinical implications, particular for medical device-related bacterial biofilm infections, since the levels of erythromycin at which *S. capitis* biofilm formation were enhanced are readily achievable in the clinical setting. Further studies of erythromycin-induced biofilm growth in *S. capitis* are warranted.

CHAPTER 6

ica operon disruption for the analysis of its function in clinical *Staphylococcus capitis* isolate

6.1 Introduction

Clinical isolates of coagulase-negative staphylococci (CoNS) often elaborate a biofilm involved in adherence and accumulation on medical devices and resistance to host defences. The staphylococci elaborate a polysaccharide adhesion (PIA), which mediates cell adherence to biomaterials, termed polysaccharide intercellular adhesin (PIA), which is thought to mediate bacterial accumulation into cellular aggregates. PIA is a polymer of β-1, 6-linked *N*-acetyl glucosamine, encoded by the *ica* locus and is well studied in *S. epidermidis* and *S. aureus* (Heilmann *et al.*, 1996, Gerke *et al.*, 1998).

Biofilm formation in *S. capitis* has been rarely studied, and whether the biofilm is biosynthesized by products of *ica* locus is unknown. The *ica* locus was present in all sixty clinical isolates examined in this study (Chapter 4). Most of the isolates produced biofilm only under certain conditions. Sequencing results showed some single nucleotide variations between the biofilm positive and negative isolates.

Gene targeting is a powerful molecular genetic technique that has been widely used to understand specific gene function *in vivo* (Lenaerts *et al*., 2003, Matsuda *et al.*, 2004). To elucidate the function of the *ica* locus in *S. capitis*, attempts were made to generate a gene knock-out mutant of a biofilm positive isolate. Although the attempts were unsuccessful, the process of troubleshooting and the problems encountered provides valuable lessons for future research.

Construction of stable knockouts requires the exchange by homologous recombination of a chromosomal wild-type gene with a mutated or inactivated allele. The established method for allele replacement requires the use of an antibiotic resistance cassette to

mark the mutated allele or gene deletion. A tetracycline resistant gene from *S. aureus* was used as the selective marker for allele exchange in this study. The method involves the construction of a plasmid that is temperature sensitive for replication and is a shuttle vector that can replicate in both *Escherichia coli* and *Staphylococcus* spp. Initially, the shuttle vector was constructed in *E. coli* and then transformed into a clinical *S. capitis* isolate of interest.

6.2 Materials and Methods

6.2.1 Antibiotic susceptibility tests

Antibiotic susceptibility tests were used to select an appropriate antibiotic sensitive strain as the cloning host. Eleven biofilm positive isolates, that displayed a susceptible phenotype, were initially selected according to the antibiotic resistant profile determined in previous tests. Minimum inhibition concentrations (MICs) of chloramphenicol and tetracycline were determined according to the CLSI guidelines (Wikler, 2006). Chloramphenicol and tetracycline were used as antibiotic selection markers in the subsequent allele exchange.

6.2.2 Bacterial strains and growth conditions

The bacterial strains and plasmids used in this study are listed in Table 6.1. For genetic manipulation, clinical isolate 60 was chosen. This isolate and its derivatives were grown in trypticase soy broth (TSB) at 30, 37 and 42 °C. When necessary, tetracycline at 2 or 3 µg/mL, chloramphenicol at 8 or 10 µg/mL were added to the medium. *Escherichia coli* DH5α was grown in nutrient broth (NB) containing, when necessary, ampicillin at 100 µg/ mL. Solid medium was prepared by addition of 1.3% agar.

Table 6.1. Strains and plasmids used in this study.

Strain or plasmid	Genotype or relevant characteristics	Origin or references
S. capitis 60	Wild-type clinical isolate, biofilm positive	(Royal Children Hospital, Melbourne)
E. coli DH5α	F^- endA1 glnV44 thi-1 recA1 relA1 gyrA96 deoR nupG Φ80d*lacZ*ΔM15 Δ(*lacZYA-argF*)U169, hsdR17(r_K^- m_K^+), λ-	(Laboratory stock)
pBT2	Low-copy-number shuttle vector with Amp^r in *E. coli* and temperature-sensitive replication with Cm^r in *S. aureus*	(Brükner, 1997)
pSK7749	Donator of *tet* gene (Tet^r). A *Hind*III fragment carrying the *tetA*(K) gene	(Simpson *et al*., 2000)
pBTΔtetA(K)	Mutant vector for homologous recombination of the *ica* gene cluster in *S. capitis*. *tetA*(K) was used to insert into *ica* locus as resistance selection marker	(This study)

Abbreviations: Amp^r, Tet^r, Cm^r, resistance to ampicillin, tetracycline and chloramphenicol, respectively.

6.2.3 Construction of the tetracycline resistance cassette plasmids

The *ica* operon was replaced with the tetracycline resistant gene *tetA*(*K*)from plasmid pSK7749 (Simpson *et al*., 2000) by homologous recombination. The *E. coli-Staphylococcus* shuttle vector pBT2 was used for cloning the mutagenesis construct. Plasmid constructions were carried out in *E. coli* DH5α.

First, a 700 bp DNA fragment upstream and containing part of *icaR* gene of clinical isolate 6 was amplified by phusion DNA polymerase (NEB, Australia) with primers *EcoR*I-RF2 (5'-CTCCGAATTCAAGAGCACCCACAATGAC-3') and *Sac*I-RR (5'-CGCCGAGCTCCTATAGATGGGCTTTACCAG-3'). PCRs were performed according to manufacture's instruction, as follows: PCR master mixes were prepared containing 1x Phusion HF Buffer, 250 µM dNTPs, 0.4 µM of each forward and reverse primer, 0.5 U *Taq* DNA polymerase and 50 ng DNA. PCR reactions were performed on a PCR Express thermal cycler at one cycle at 98 °C for 30 s, followed by 25 cycles of 98 °C, 10 s; 52 °C, 30 s; 72 °C for 23 mins, final elongation 7 mins at 72 °C for 1 cycle and hold at 4 °C. The

PCR product was digested with *EcoR*I and *Sac*I enzymes (Section 2.4.1.5) (NEB, Australia), and then cloned into the plasmid pBT2 via *EcoR*I and *Sac*I sites, resulted in plasmid pBT2-A. This construct was transformed into competent *E. coli* DH5α by electroporation (Section 2.4.1.8). Positive clones were selected on NA plates containing 100 µg/mL of ampicillin. Secondly, a 720 bp DNA fragment downstream and containing partial *icaC* gene was amplified with primers *Xma*I-CR (5'-TGCGCCCGGGTACGGTTCAAATGGTAAGC-3') and *BamH*I-lipF (5'-CTGCGGATCCTTCCCATTCACGGTAACTG-3'). The PCRs were performed the same as the previous insert, except for annealing at 58 °C. This PCR product was digested with *Xma*I and *BamH*I (Section 2.4.1.5) (NEB, Australia), and cloned into pBT2-A via *Xma*I and *BamH*I sites (Section 2.4.1.8), resulted in plasmid pBT2-B. Finally, the pBT2-B plasmid was linearized with *Sma*I (Section 2.4.1.5). A 1700 bp *Hind*III (NEB, Australia) fragment from pSK7749, encompassing the *tetA*(K) gene and its promoter was digested with *Hind*III and filled in with klenow (NEB, Australia) according to manufacture's instructions. Briefly, master mix containing 10 U of Klenow, 1× NEBuffer 2, and 1 µL of 2.5 mM dNTPs (Bioline, Australia) were incubated at 37 °C for 30 mins. The Klenow was then heat inactivated at 75 °C for 20 mins. The linearized vector was dephosphorylated with Antarctic Phosphatase (NEB, Australia) according to the manufacture's instructions. Briefly, 1× Antarctic Phosphatase Reaction Buffer was added to 4 µg of DNA cut with *Sma*I. Five units of Antarctic Phosphatase was added and mixed gently. The reaction mixture was incubated for 15 mins at 37°C. Heat inactivated for 5 mins at 65°C. Both the filled-in fragment and the dephosphorylated vector were purified with QIAEX® II Gel Extraction Kit according to manufacture's instruction. Then proceeded blunt end ligation as follows: the ligation mixture contained 1 × T_4 Buffer, 2 µg of the linearized vector, 2 µg of insert, 10 U of T_4 DNA ligase, and Polyethylene glycol (PEG) (13 %) (Sigma) in a 20-

μL of reaction, the mixture was incubated at 22 °C for 4 hours, resulted in the final mutagenesis construct pBT2Δ*tetA*(K). These plasmids were confirmed by sequencing using the ABI sequencing mix V3.1 according to the manufacturer's instructions. Figure 6.1 shows the flow chart for the series of cloning.

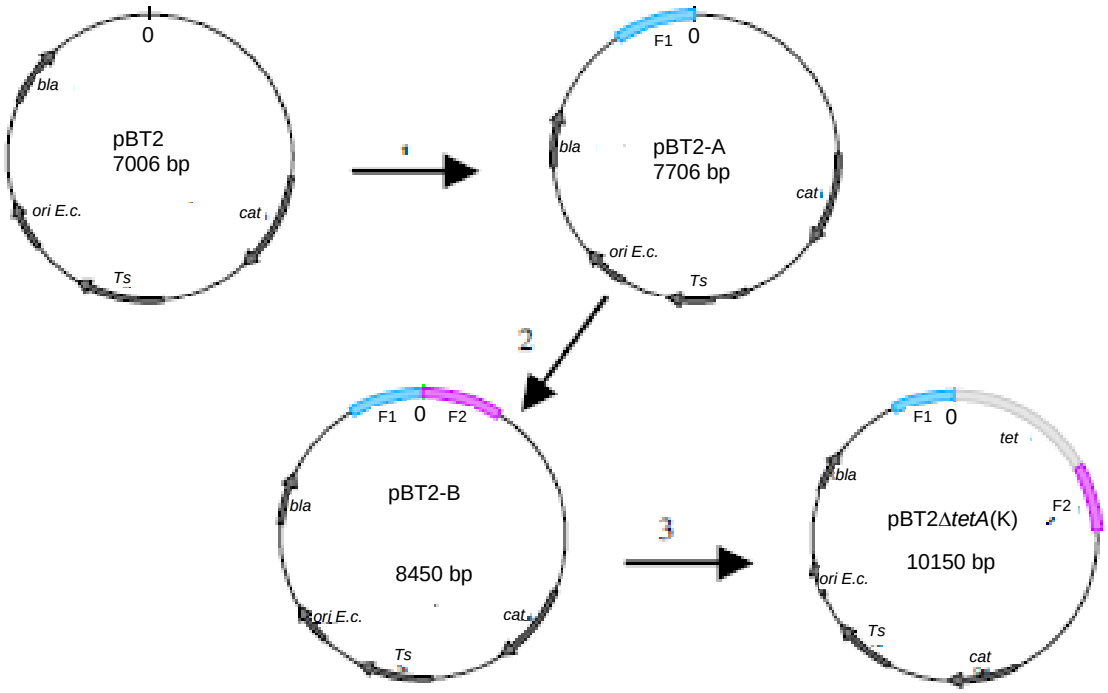

Figure 6.1. Construction of the mutant vector pBT2Δ*tetA*(K). The blue and pink fragments represent the inserted flanking fragments, upstream of *icaR* gene and downstream of *icaC* gene respectively.

6.2.4 Plasmid isolation

Plasmid DNA prepared from *E. coli* was purified with QIAprep® spin Miniprep Kit (Qiagen, Australia) according to the manufacturer's instructions. After purification, the DNA was concentrated by ethanol precipitation. Briefly, 1/10 volume of 3 M Na-acetate pH 5.2, and 2 to 2.5 volumes of ice-cold 100% ethanol were added to the DNA sample , mixed, and stored at -20°C for at least 1 hour to precipitate the DNA. The precipitated DNA was recovered by centrifugation at full speed in a microcentrifuge for 15-20 mins at 4 °C. The ethanol was poured off and the pellet was washed twice with room-temperature 70% ethanol. The DNA pellets were air-dried. The DNA was resuspended in a suitable volume of molecular grade water to a final concentration of at least 4 µg/µL.

6.2.5 Introduction of recombinant plasmid DNA into *S. capitis* isolate

6.2.5.1 Preparation of electro-competent cells of clinical *S. capitis* isolate 60

Staphylococcus capitis strain 60 was used as bacterial host in the allele exchange experiments. The bacterial cells were grown in TSB medium.

First, to determine the effects of growth phase and optimal cell number for making electroporation-competent cells, a growth curve was generated by growing the bacteria in TSB at 37°C for 5 hours, sampling at 1-hour intervals. The OD_{600nm} was measured; colonies were counted on NA plates.

6.2.5.2 Making competent cells according to the optimized protocol:

A 5 mL volume of an overnight culture of a fresh colony of *S. capitis* isolate 60 was inoculated into 500 mL of TSB. The culture was incubated with shaking at 200 rpm at 37 °C until the OD_{600nm} was 0.5. The cells were divided into 4 sterile bottles, and placed on

ice for 30 min to stop the cell growth. The cells were harvested by centrifugation at 12,000 g for 15 mins at 4 °C, then washed three times with 500 mL, 250 mL then 80 mL of sterile ice-cold MilliQ water, harvesting by centrifugation at 12,000 g for 15 mins at 4 °C between each washing. The cells were resuspended in 10 mL ice-cold 10% glycerol, then washed once with 5 mL ice-cold 10% glycerol. Finally, the cells were resuspended with 1 mL ice-cold 10% glycerol at a cell density of about 4.5×10^{10} cells/mL. Aliquots of 100 µL of cells were immediately distributed in ice-chilled eppendorf tubes and stored in -80 °C for no more than three months.

6.2.5.3 Heat inactivation of the host restriction system of *S. capitis* isolate 60

In order to determine the optimal temperature and exposure time intervals for inactivation of the host restriction system, a viability test was performed at 46, 49, 52 and 55 °C. Three vials of electrocompetent cells for each temperature were incubated at different temperatures and the samples were removed from the heat block every minute for 5 mins. Immediately after removal from the heat block, the samples were diluted in TSB. Five dilutions were chosen for subsequent viable counts: 10^{-3}, 10^{-4}, 10^{-5}, 10^{-6} and 10^{-7}. Duplicate aliquots were spread on NA plates without antibiotics, and incubated at 37 °C for 24 hours. The optimal temperature and time combination for transformation of electrocompetent cells was determined as the highest temperature which did not affect cell viability during a given exposure time.

6.2.5.4 Electroporation procedures

The optimized electroporation protocol was as follows: competent cells were placed on ice for 5 mins or until thawed and incubated at room temperature for 20 mins. The host restriction system was heat inactivated by exposure to 55 °C for 1 min. Immediately after

removal from the heat block, competent cells were placed on ice and 500 µL electroporation buffer at room temperature consisting of 0.5 M sucrose and 10% glycerol was added to the cells, then the cells were pelleted by centrifugation at 5000 g for 15 mins at 4 °C and resuspended in 60-70 µL of the electroporation buffer. The cells were incubated at room temperature for 30 mins. The plasmid from *E. coli* was thawed; about 4-5 µg was added to the cells and the mixture was incubated at room temperature for 10 mins prior to electroporation. Parameters for electroporation were set as: 100 Ω, field strength 2.1 kV/cm, at room temperature, and with 1 mm gap electroporation cuvettes. Immediately after electroporation, 1 mL of fresh TSB medium was added and the cells were transferred into a 10 mL tube, and incubated at 37 °C for 2 hours. The cells were diluted 1/10 in TSB medium, plated on Heart Infusion Agar (HIA) (Oxiod, Australia) containing 5 µg/mL of chloramphenicol, and incubated at 30 °C for 4-5 days.

6.2.5.4 Analysing and interpreting results: calculating transformation efficiency

The average colonies grown on the chloramphenicol plates were determined and the amount of DNA that was spread on each plate was calculated. The example below was used to calculate the transformation efficiency.

The amount of DNA plated on each plate: 1 µL of 4 µg/µL of freshly made stock plasmid DNA was added to 100 µL of competent cells. After transformation, 900 µL of TSB was added prior to expression. 10 µL (equivalent to 40 ng of DNA) was then diluted in 990 µL of TSB broth and 100 µL (equivalent to 4 ng) is plated on a single plate.

If 100 colonies are counted on the plate, the transformation efficiency is:

100 transformants/4 ng X 1000ng/µg=2.5 x10^4 transformants/µg of DNA

6.2.6 Confirmation of the transformants

Confirmation of transformants was performed as follows: first, colonies on the chloramphenicol plates were gram stained to make sure they are not contaminated, then the colonies were streaked on fresh chloramphenicol plates to obtain a pure culture, then incubated at 30 °C for 72 hours. Finally, plasmid isolations were performed using QIAGEN kit with modifications: four to five fresh colonies were inoculated into 4 x10 mL of 5 µg/mL chloramphenicol TSB broth, incubated at 30 °C with shaking at 170 rpm for 16 hours, until the OD_{600nm} reached 1.3, (~1×10^8 cell/mL). This number is critical to determine the amount of enzymes used subsequently. The overnight bacterial culture was centrifuged at 4700 rpm, 15 mins at 4 °C, then the cells were resuspended with 2 mL of P1 buffer (0.5 mL for each tube) and 300 µg/mL of lysostaphin and 300 µg/mL of lysozyme were added. The cells were incubated at 37 °C, with shaking at 100 rpm, for 15 mins to partially break cell wall. After this, 200 µg/mL of proteinase K was added to remove native cell proteins, such as DNase, and incubated at 37 °C, for 30 mins, with shaking at 100 rpm. Then the instructions of the QIAGEN kit were followed. The plasmid concentrations were 10 to 20 µg/mL for recombinant strain 60. About 500 ng of the purified plasmid was run on a DNA gel to confirm that transformation had been successful. Also, the constructed mutant vector was further confirmed by digested with *EcoR*I and *Pst*I restriction enzymes.

6.2.7 Induction of tetracycline resistance in *S. capitis*

A single colony of the transfermant under test was inoculated in 10 mL of NB containing 0.25, 0.5, 0.75, 1, and 1.9 µg/mL of tetracycline, respectively, and incubated at 30 °C for

14-16 hours with shaking. When the culture reached to stationary phase, the OD_{600nm} 1.0, the cell density was ~ 10^8 cell/mL, 100 µL aliquot of each culture were inoculated onto NA plates containing 0.5, 1, 2, 3, 5, 8, and 10 µg/mL of tetracycline, and incubated at 30 °C for 4-5 days. Uninduced culture and the host strain were used as controls.

6.2.8 Glycerol stock

The colonies obtained after induction with tetracycline were streaked on NA containing 3 µg/mL of tetracycline and incubated at 30 °C to obtain a pure culture. A single colony was grown in NB containing 2 µg/mL of tetracycline at 30 °C until the OD_{600nm} measured 0.5, 0.85 mL of this bacterial culture was added 0.15 mL of sterile glycerol, mixed, then stored in -80 °C.

6.2.9 Optimized procedure for gene replacement in *S. capitis*

6.2.9.1 Plasmid curing

Ethidium bromide (EB) was used as chemical curing agent to eliminate plasmid(s) of the recombinant strain. Prior to curing, inhibition tests were performed on this strain to determine a sub-lethal concentration of EB. Concentrations of 10, 20, 30, 40, 50, 60, 70, 80, 90, 100 120, 150 and 200 µg/mL of EB were tested. The EB was inoculated with the recombinant strain (10^7 cells/mL) in 96-well microtitre plates, and incubated at 37 and 42 °C for 24 hours, in the dark. All EB concentrations were set up in triplicate. The sub-lethal concentration was defined as the highest concentration which did not affect bacterial growth.

6.2.9.2 Growth curves of the recombinant strain in EB combined at different temperatures

A single colony of the recombinant strain being tested was inoculated into a 10-mL of TSB containing 2 µg/mL of tetracycline, incubated at 30 °C with shaking at 100 rpm overnight. This overnight culture was diluted 1:100 in a 50-mL TSB containing EB, and incubated at 42, 44 and 46 °C, with shaking at 100 rpm for 8 hours. The OD_{600nm} was measured, and 100 µL of the cell cultures were plated on NA every 2 hours to generate growth curves. This test was performed in triplicate. A control without EB was performed at the same time at each temperature. Regression analysis was performed to examine whether the addition of EB affected cell growth for each temperature. In addition, the growth of recombinant bacteria at 37 and 40 °C without EB was examined in the same way.

6.2.9.3 Isolation of colonies of *S. capitis* that had undergone allele exchange

The recombinant strain was grown in TSB containing 2 µg Tet/mL at 30 °C to late stationary phase. Subsequently, the culture was diluted 1:100 in 500 mL fresh TSB containing EB, and the temperature was shifted to 37 and 42 °C, with shaking at 150 rpm for 24 hours. Then a 1/100 dilution of each culture is made into fresh TSB plus EB. These serial passages were continued for twelve passages. Cell plating was performed starting from the fourth passage. Appropriate dilutions were spread on NA and incubated at 37 °C for 24 hours. The colonies from these plates were patched onto chloramphenicol plates (5 µg/mL) and NA plates. Colonies that failed to grow on the antibiotic plates were subcultured from the matched nutrient agar plates onto a second set of chloramphenicol plates to confirm curing of the plasmid. The desired tetracycline-resistant, chloramphenicol-sensitive colonies were further evaluated by PCR to confirm inactivation of *ica* gene cluster. Figure 6.2 shows the allelic exchange diagram.

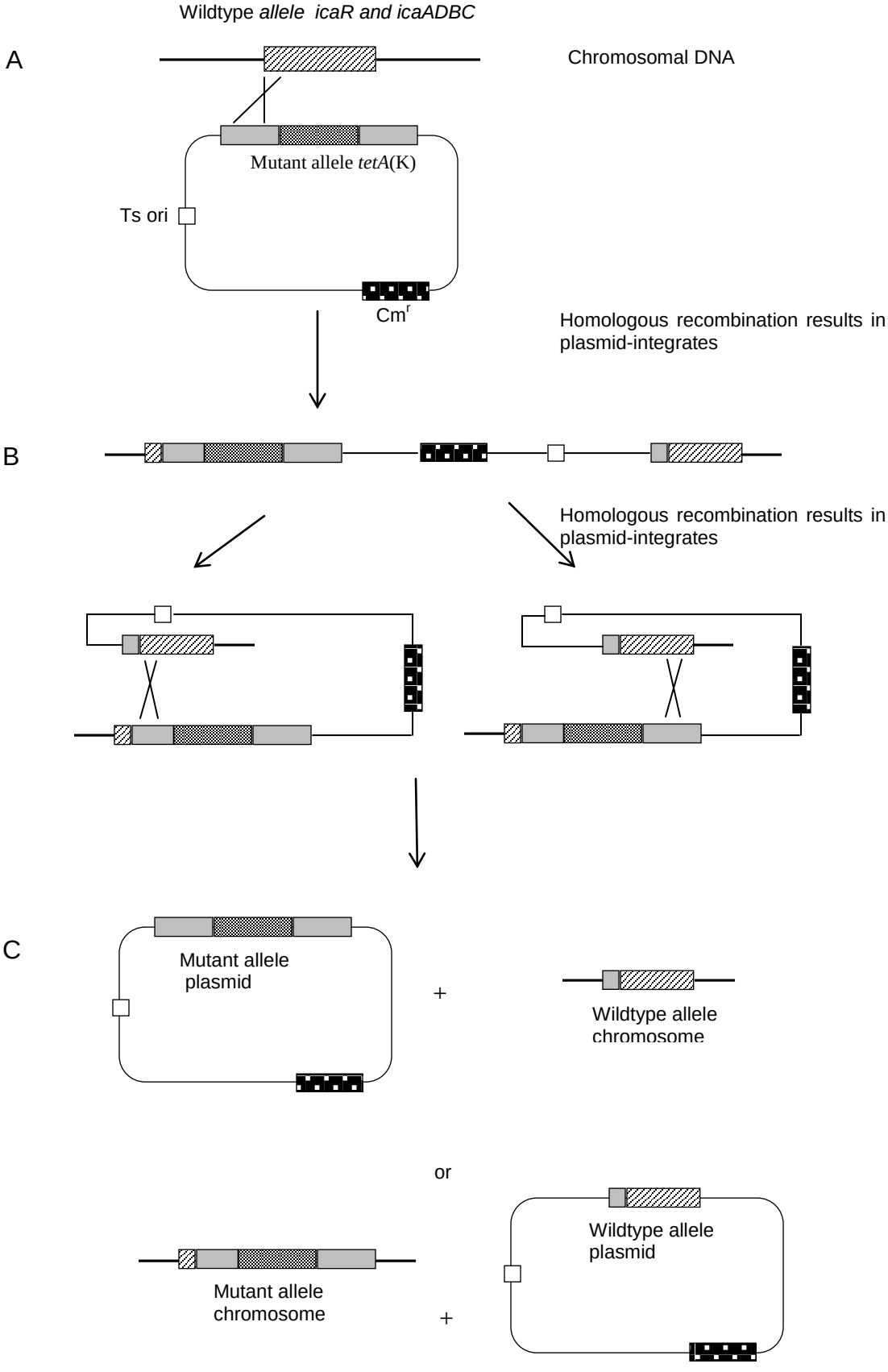
Wildtype *allele icaR and icaADBC*
A
Chromosomal DNA
Mutant allele *tetA*(K)
Ts ori
Cm^r
Homologous recombination results in plasmid-integrates
B
Homologous recombination results in plasmid-integrates
C
Mutant allele plasmid
+
Wildtype allele chromosome
or
Mutant allele chromosome
+
Wildtype allele plasmid

Figure 6.2. Allelic exchange mutagenesis. Chromosome DNA is depicted as thick lines. Plasmid DNA is depicted as thin lines. Genetic features are depicted as rectangles or boxes that are differentiated by shading or a pattern. Arrows point to the results of recombination events. A. A chromosomally encoded wildtype copy of a target gene contains DNA that is homologous to a cloned mutant allele that is disrupted using a unique selectable marker. The mutant allele of the target gene is carried on a plasmid with a temperature-sensitive origin of replication and a second selectable marker. B. Bacteria mediated homologous recombination, the location denoted with a large cross, allows for the chromosomal integration of the plasmid containing the mutant allele. C. A second recombination event excises a plasmid. The resulting products are either the original DNA elements or a strain which now has the mutant allele of the target gene within the chromosome the wild-type allele on the plasmid. The products are determined by the location of the recombination events. If the second crossover occurs on the opposite side of the target gene-disrupting marker, the chromosome of the resulting bacterial will contain the mutant allele of the target gene.

6.3 Results

6.3.1 Confirmation of the constructed tetracycline resistance cassette in *E. coli*

The mutant constructions were verified by restriction digestion, PCR and sequencing as shown in the Figure 6.3 and Figure 6.4.

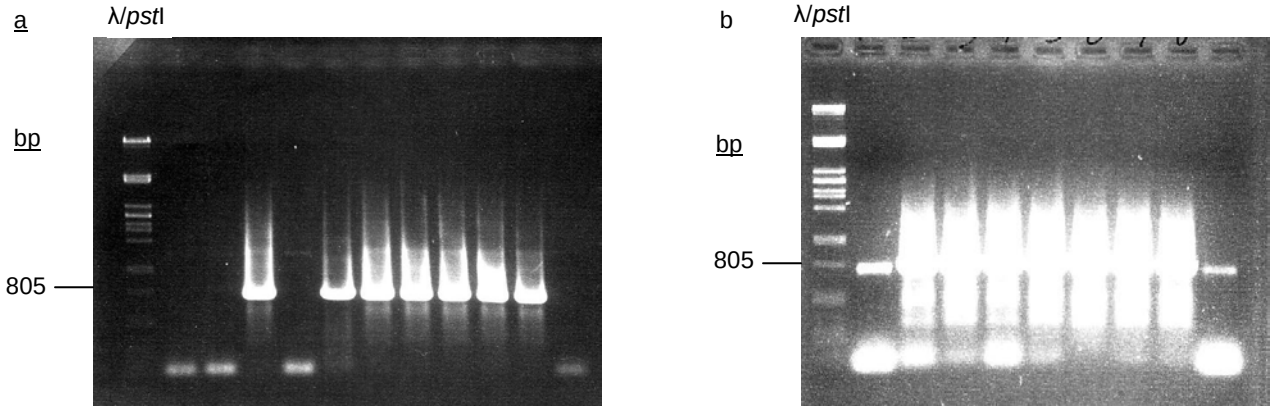

Figure 6.3. PCR confirmations for the flanking regions which inserted into pBT2-A and pBT2-B. a. The fragments flanking *icaR* gene, with primers *EcoR*I-RF2 and *Sac*I-RR. b. The fragment flanking *icaC* gene, with primers *Xma*I-CR and *BamH*I-lipF. The fragmens for both a & b are of expected sizes. λ/*Pst*I, DNA Ladder.

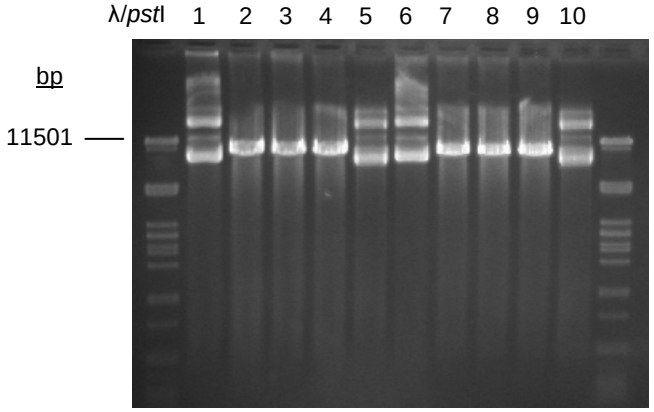

Fgure 6.4. Verification of the mutant construction with restriction digestion. Lane1 and Lane 5, uncut vector from the same colony 1. Lane 2 to Lane 4, the vector was cut with *EcoR*I, *BamH*I and *Hind*III, respectively. Lane 6 and Lane 10, uncut vector from another colony 2. Lane 7 to Lane 9, the vector was cut with *EcoR*I, *BamH*I and *Hind*III, respectively.

6.3.2 Selection of a clinical isolate as a host strain for allele exchange

Genetic and physiological properties of a strain can critically influence the results of genetic manipulation. Most clinical isolates harbour plasmids which frequently confer antibiotic resistance to potential host strains. This intrinsic resistance can severely limit the scope of genetic manipulation. The first step in genetic engineering with clinical isolates is to select an appropriate strain which is plasmid-free and sensitive to the antibiotics to be used for selection. In this study, eleven biofilm positive isolates were initially chosen according to their antibiotic resistant profiles: they were susceptible to antibiotics used in the hospital. The MICs of chloramphenicol and tetracycline were further determined for these isolates, since the constructed mutagenesis plasmid carried the antibiotic resistant genes to those two antibiotics as selection for subsequent cloning and allele exchange.

Isolates 35, 60 and 91 were shown to be sensitive to both of the antibiotics (MICs of chloramphenicol were 4 µg/mL, and tetracycline were 1 µg/mL). Typing by pulsed-field electrophoresis (PFGE) had shown previously (Chapter 3) that these isolates belong to two PFGE types (35 and 91 belong to type I, 60 belongs to type II). Finally, isolate 60 was chosen as the host strain for genetic manipulation.

6.3.3 Optimization of electroporation transformation

Several parameters for transformation of plasmid into *S. capitis* were investigated as described below.

6.3.3.1 Preparation of electrocompetent cells.

Growth condition is important for preparing electro-competent cells. According to the literature (Schenk and Laddaga, 1992), B2 medium consisting of 1.0% casein hydrolysate, 2.5% yeast extract, 0.5% glucose, 2.5% NaCl and 0.1% K_2HPO_4 (pH 7.5) was initially chosen for growing bacteria. However, the high salt composition of this medium induced biofilm in strain 60, and this was considered to potentially reduce the competency of the cells. TSB medium was therefore used as a replacement.

To determine the effects of growth phase on transformation, *S. capitis* isolate 60 was grown in TSB at 37 °C for five hours, until late log phase or early stationary phase was reached. Cells were harvested at three different OD_{600nm} readings 0.2, 0.5, and 1.2 which represented early, mid and late exponential (log) phase stages (Figure 6.5). The results demonstrated that the OD_{600nm} 0.45-0.55 gave approximately 4- to 10-fold increase in transformation efficiency compared with the other time points (Figure 6.6).

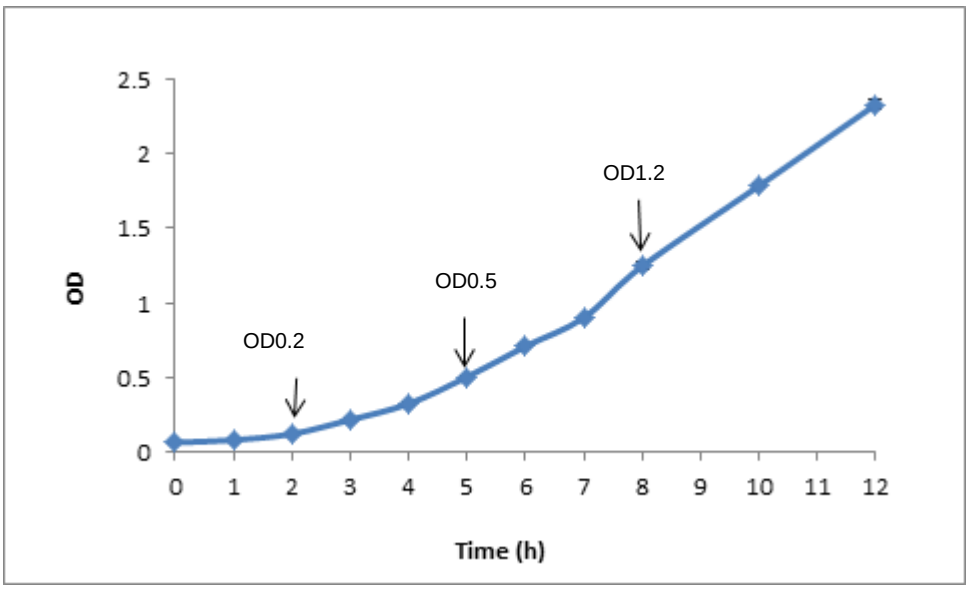

Figure 6.5. Growth curve of the recombinant strain 60 in TSB. The means and SE values from triplicates are presented.

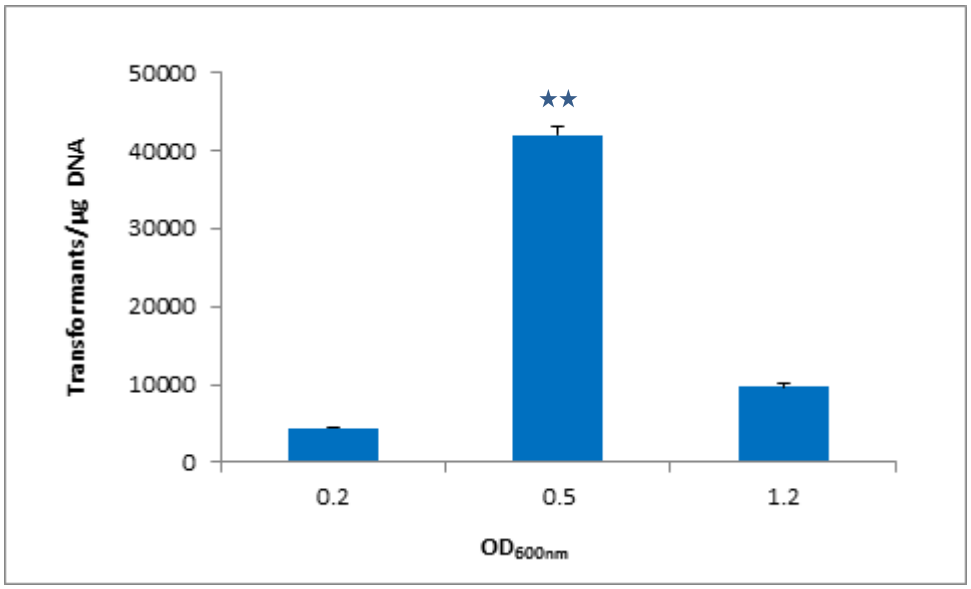

Figure 6.6. Effects of growth phase on transformation efficiency. The means and SE values from triplicates are presented. ★★$p < 0.01$.

6.3.3.2 Inactivation of *S. capitis* restriction system by heat treatment.

Host restriction systems hinder the introduction of foreign DNA, such as plasmids, into bacterial strains and limit the construction of mutants and other analyses. Previous authors have overcome this problem by temporary inactivation of host restriction systems by heat treatment before electroporation (Kienesberger *et al*., 2007), and obtained an approximately 1000-fold increase in transformation efficiency for interspecies DNA transfer between *E. coli* and *Salmonella Typhimurium/enteritidis*.

This study used a shuttle vector and DNA prepared from *E. coli*. To examine the effect of heat treatment on host restriction systems, a series of optimization experiments was performed. The viability of the recipient host at different temperatures and times was first determined by viable counts.

At 55 °C, the majority of *S. capitis* cells were killed within the first five minutes. At 49 and 52 °C, the viability decreased much more slowly. In contrast, heating to 46 °C for 5 mins had no effect on the viability within the first five minutes (Figure 6.7).

The optimal conditions for heat treatment were also determined. After thawing the electrocompetent cells on ice, cells were incubated on a heat block at 55 °C for 1 min. A washing step after the heat treatment was introduced, and proved to be necessary in order to reduce conductivity and prevent arcing in the electroporation step.

The transformation efficiency was investigated under both heat-treated and untreated conditions. The result showed that the short heat treatment before electroporation improved the transformation efficiency dramatically (Figure 6.8).

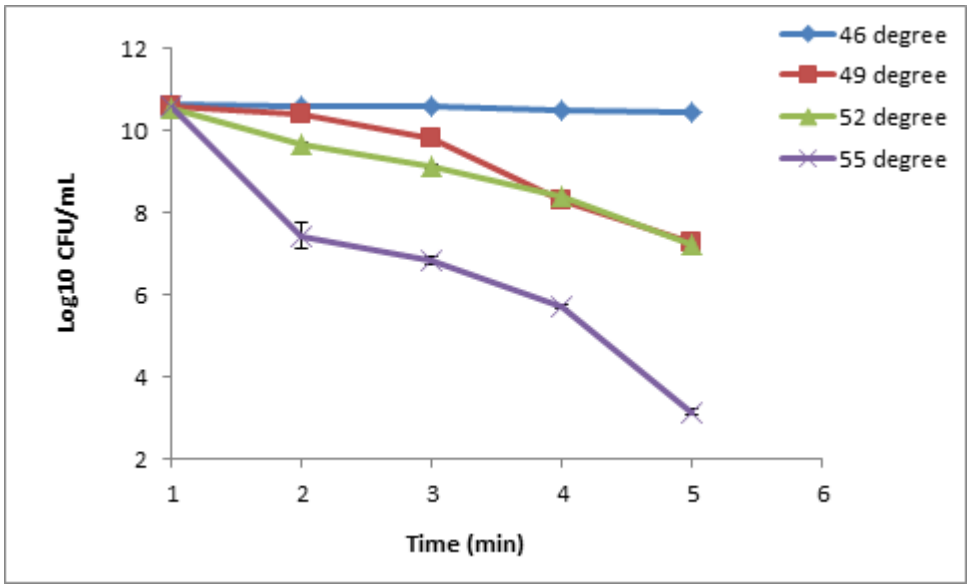

Figure 6.7. Cell viability after heat treatment within 5 mins. Data was shown in triplicated for each temperature and time duration. Each data point represents the mean and SE of three experiments.

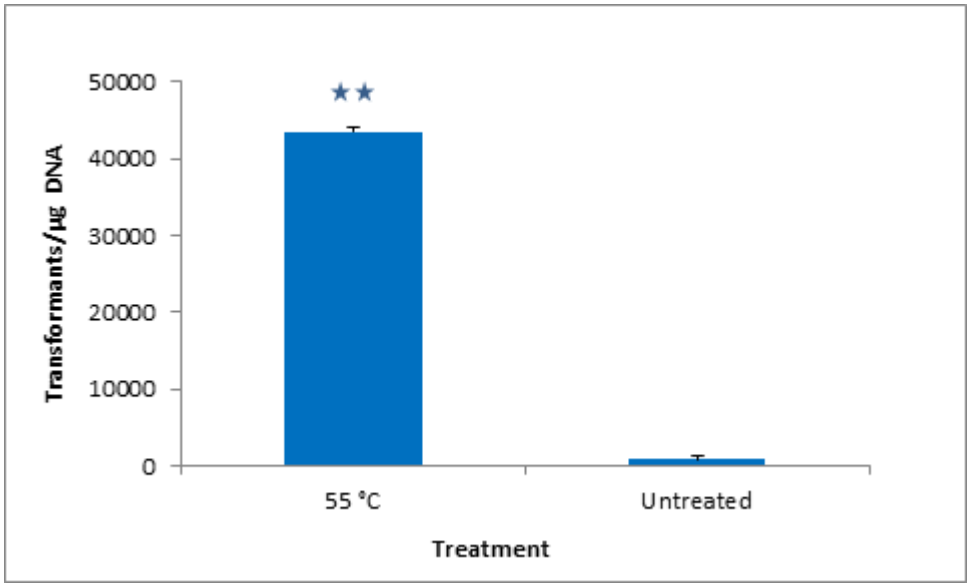

Figure 6.8. Effects of heat-treatment on transformation efficiency. The results were shown the transformation efficiency by pre-treated the competent cells at 55 °C for 1 min comparing with the untreated cells. $^{**}p < 0.01$.

6.3.3.3 The electroporation step

Several parameters were evaluated to study their effects on transformation frequency.

i. Different amounts of plasmid DNA from 0.1 to 6 µg were added to the electroporation mixture containing about 1×10^{10} cells/mL. Figure 6.9 shows that the maximum number of transformants was obtained at 4 µg of plasmid DNA. The transformation efficiency reduced with increasing the plasmid DNA amount.

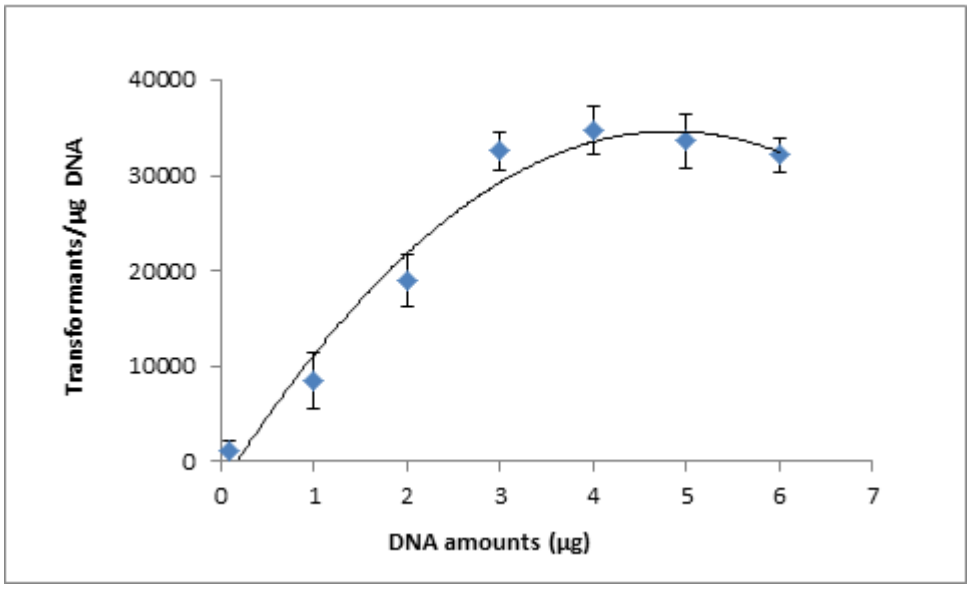

Figure 6.9. Effects of plasmid DNA amounts in the electroporation mixture on the transformation frequency. The results are present as transformation efficiency. Each data point represents the mean and SE of three experiments.

ii. Pre-incubation of cells with DNA

According to a previous study, pre-incubation of cells with plasmid DNA increased the transformation efficiency; it was suggested that binding the DNA to the cell surface is necessary for efficient transformation.

In this study, however, no improvement in transformation efficiency was observed by introducing a pre-electroporation step. Four microgram of plasmid DNA was incubated with electroporation mixture for 1 min, 5 mins, 10 mins and 30 mins prior to electroporation, but no changes in the transformation efficiency were observed. At 30 mins pre-incubation, the transformation efficiency decreased significantly at 30 mins incubation (Figure 6.10), possibly due to cell lysis.

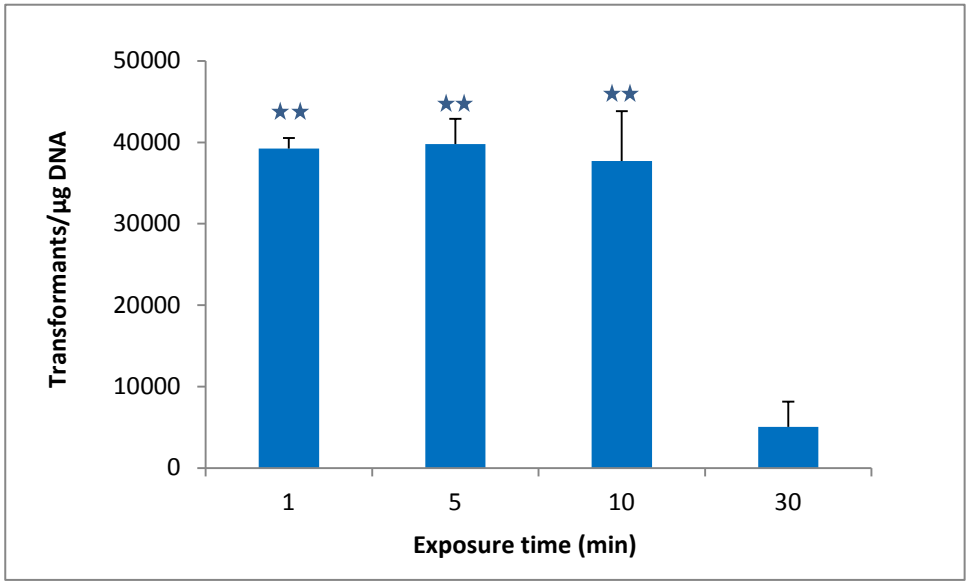

Figure 6.10. Effects of pre-incubation of DNA with cells on transformation efficiency. Each data point represents the mean and SE of three experiments. ★★ $p < 0.01$.

iii. Effect of temperature during electroporation on transformation efficiency

Temperature during the electroporation process is considered to be an important factor affecting the efficiency of transformation (Schenk and Laddaga, 1992). In the current study, to examine the effect of temperature on the transformation efficiency, the complete electroporation procedure was performed both on ice and at room temperature.

Following procedure was performed: thawing the electrocompetent cells on ice, following incubation at room temperature for 30 mins, then subsequently performing the electroporation at room temperature resulted in at least eightfold increase in the transformation efficiency compared with cells kept on ice and electroporated with pre-cooled cuvettes. These results were consistent with previous studies (Figure 6.11).

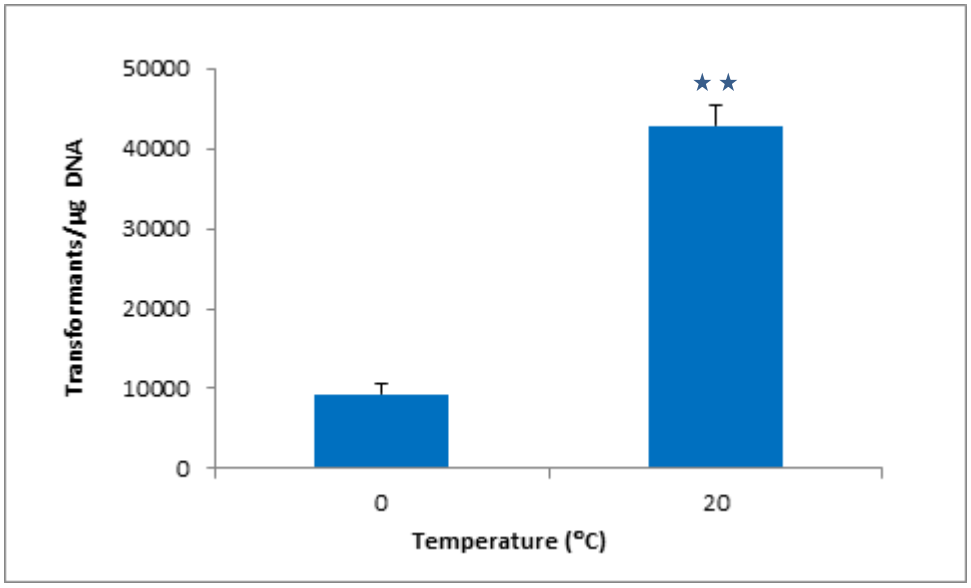

Figure 6.11. Effect of different temperatures during electroporation on the transformation efficiency. Each data point represents the mean and SE of three experiments. ★★ $p < 0.01$.

iv. Electroporation buffer

Augustin and Götz (1990) reported that the optimal electroporation buffer for *S. epidermidis* was 10% glycerol in distilled water, and that the concentrated *S. epidermidis* cells can be stored in this buffer at -70 °C for four months without losing transformation capacity.

In this study, 0.5 M sucrose was added to the original 10% glycerol buffer, as an additional cryoprotector. There was no difference between the novel electroporation buffer compared with the original 10% glycerol buffer on transformation efficiency. However, the addition of sucrose reduced the risks of arching during electroporation (Figure 6.12).

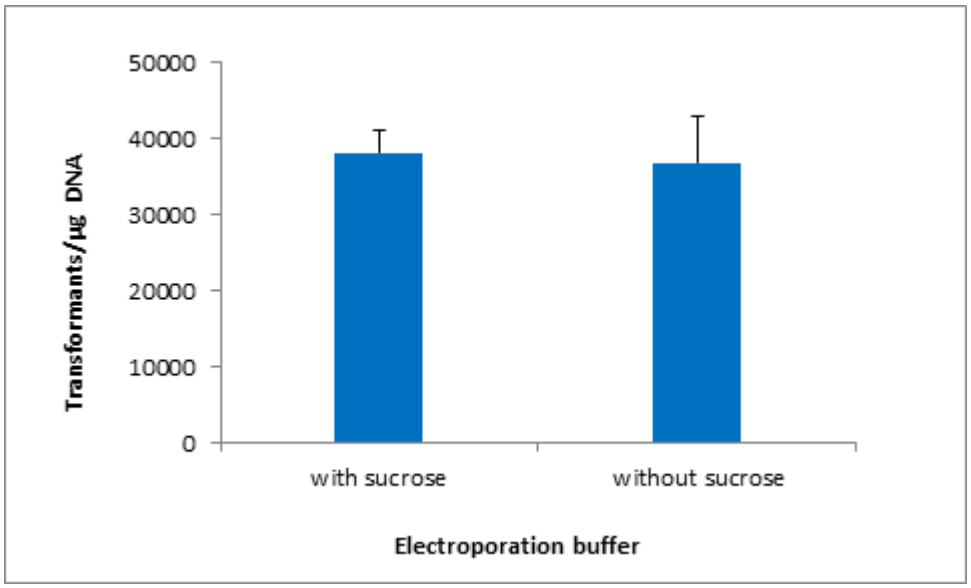

Figure 6.12. Effects of electroporation buffer on transformation efficiency. Each data point represents the mean and SE of three experiments.

v. Electroporation procedure

Field strength setting up was also considered a critical factor which can affect the transformation efficiency. In this study, field strengths 2.1, 2.3 and 2.5 kV/cm were tested. The results presented in Figure 6.13 show that the optimal field strength was 2.1 kV/cm when using a 0.1 cm gap electroporation cuvette for 75 µL of transformation mixture electroporated at room temperature. The transformation efficiency decreased with increased field strength, possibly due to cell damages

because of the higher field strength. Also, higher field strength increased the risk of arching.

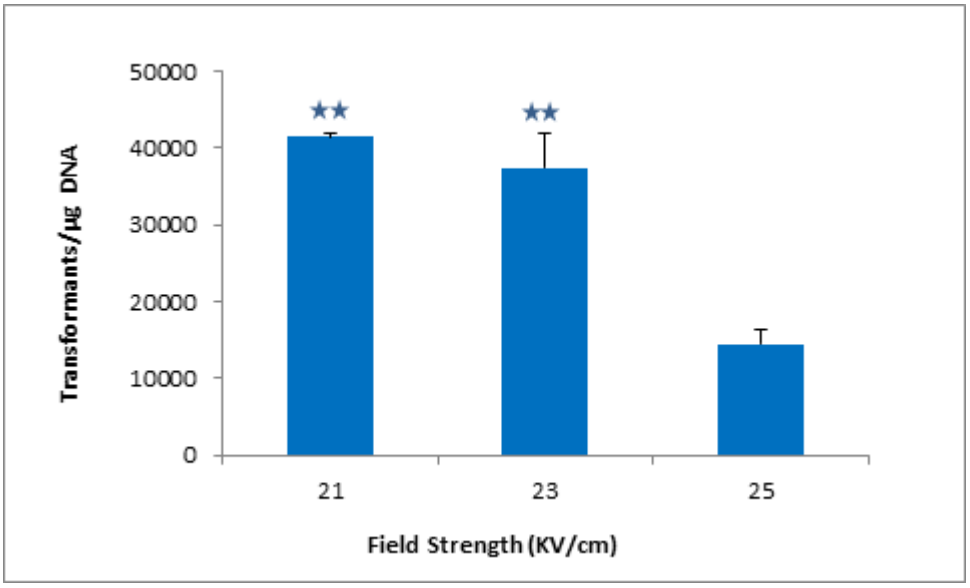

Figure 6.13. Effects of field strength on the transformation efficiency. Each data point represents the mean and SE of three experiments. ★★p < 0.01.

The novel heat-treatment protocol combined with the optimized protocols for the preparation of electrocompetent cells and the electroporation procedure yielded a transformation efficiency of approximately 10^4 transformants per transformation when *S. capitis* cells were electrotransformed with plasmid DNA pBT2*ΔtetA*(K) from *E. coli.*

6.3.3.4 Confirmation of the transformants

The transformed plasmids were isolated from *S. capitis*, verified by restriction digestion with *EcoR*I and *Pst*I shown in Figure 6.14. The plasmids isolated from *E. coli* and from the transformed *S. capitis* were generated fragments of the same size when cut with the two restriction enzymes.

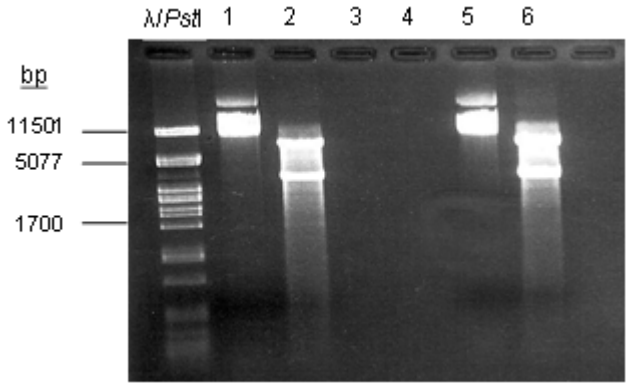

Figure 6.14. Verification of the transformation from plasmid isolations of the mutant vector from *S. capitis*. Lane 1 & 2, vector from *E. coli*; Lane 5 & 6, vector from *S. capitis*. Lane 1, uncut vector, Lane 2, vector was digested with *Eco*RI and *Pst*I. Lane 5, uncut vector, Lane 6, vector was digested with *Eco*RI and *Pst*I.

6.3.4 Induction of tetracycline resistance in *S. capitis*

Initially, MIC tests with tetracycline were performed in broth according to the CLSI guidelines, to determine the susceptibility of the recombinant strain carrying the *tetA*(K) gene on the transformed recombinant plasmid. The host strain was tested in parallel as a control. Cultures were incubated at 30, 37 and 42 °C. In the absence of induction, no difference in susceptibility was observed between the recombinant and host strains, which both had an MIC of 1 µg/mL of tetracycline.

Next, bacteria were pre-incubated in a range of sub-inhibitory concentrations of tetracycline (0.25 to 1.9 µg/mL) at 30 °C till the cell density reached to 10^8 cells/mL, then 100 µL of cell suspensions were plated onto NA containing tetracycline plates (3 µg/mL). The untreated culture and host strain were used as controls. When comparing the two treatments (no pre-incubation and tetracycline pre-incubation), both the host strain and untreated culture only grew on 0.5 µg/mL tetracycline plates. In contrast, the tetracycline

pre-incubation led to 6-fold increase in resistance in the recombinant strain, from 0.5 to 3 µg/mL of tetracycline, and the cells failed to grow in higher concentrations of tetracycline. Cell pre-grown with 0.75 µg/mL of tetracycline showed a significantly higher capability of induction of tetracycline resistance compared with other concentrations (Figure 6.15).

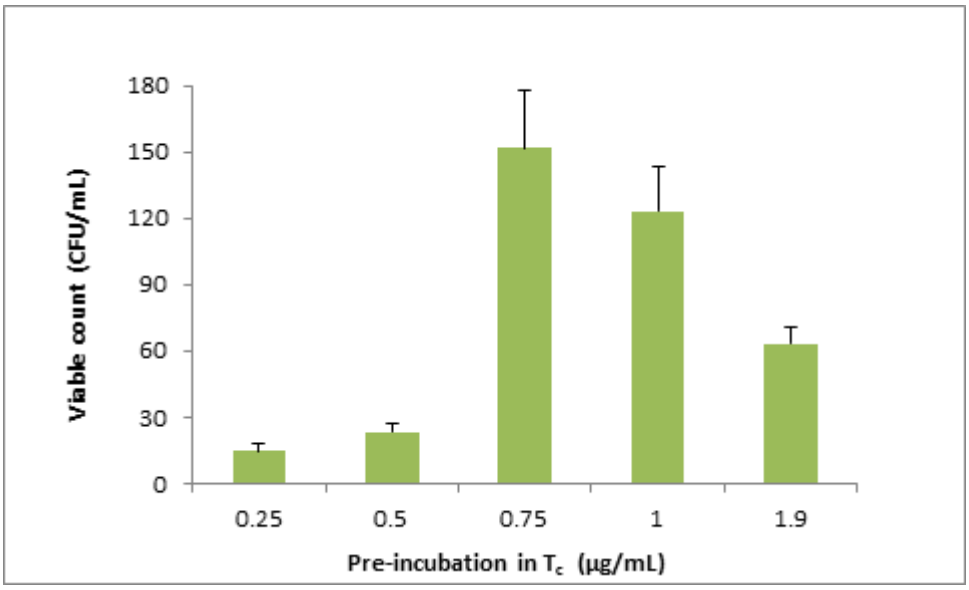

Figure 6.15. Viable counts for inducible tetracycline resistance in the recombinant *S. capitis* strain. Each data point represents the mean and SE of three experiments. Pre-incubation of cells with different concentrations of tetracycline, grown in 30 °C, till cell density to 10^8 cells/mL, 100 µL of the cell suspension was plated on NA containing 3 µg/mL of tetracycline plates, incubated at 30 °C, for 4 to 5 days. T_c, Tetracycline. ** P<0.01, represent significant differences.

6.3.5 Allele exchange

6.3.5.1 Effects of EB combined with high temperature on plasmid curing of the recombinant strain

Initially, recombinant cells were grown at 43 °C in TSB for 7 passages (24 hours for every passage). No cured colony was obtained from about 10000 colonies selected. It seems the plasmid curing from the cells was very slow. Therefore, the curing agent (EB) combined with high temperature was employed to cure the plasmid subsequently.

Prior to the plasmid curing experiment, the sub-inhibitory concentration of EB for the strain was determined by inhibition tests at 37 °C and 42 °C. The cell concentration selected was approximately the starting cell concentration in every passage. The sub-inhibitory concentration was defined as the highest concentration which did not affect bacterial growth. Fifty microgram per mL of EB was determined to be the sub-inhibitory concentration for treating this strain at both temperatures.

Growth of the recombinant strain with and without EB (50 µg/mL) at various temperatures was examined to investigate whether the EB addition affected cell growth (Figure 6.16-18).

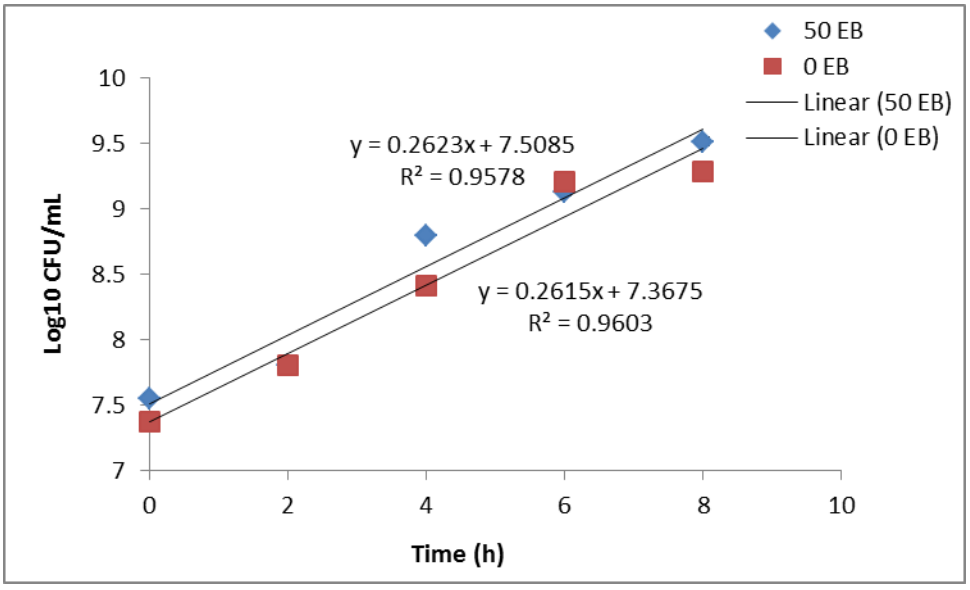

Figure 6.16. Recombinant strain grown at 42°C with and without EB in TSB. Each data point represents the mean and SE of three experiments.

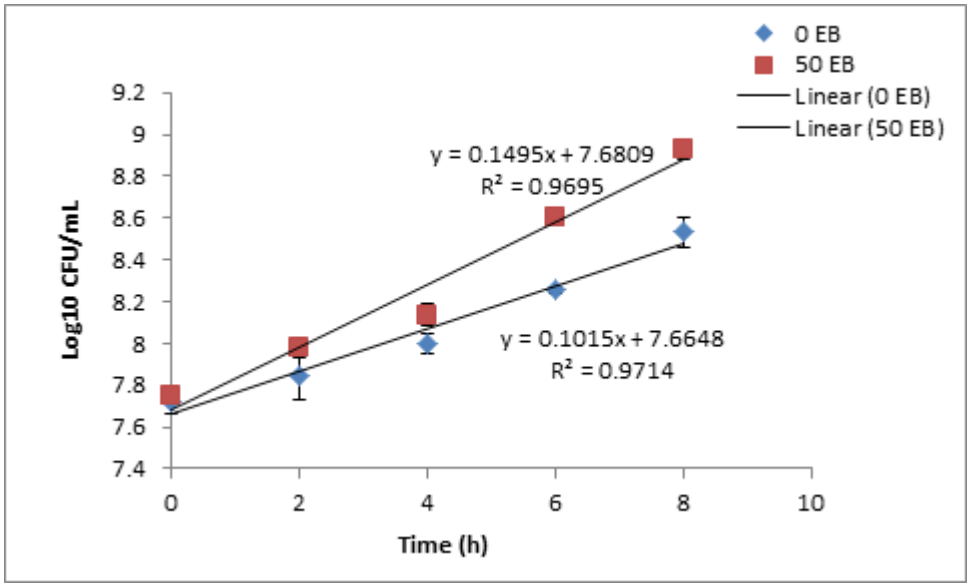

Figure 6.17. Recombinant strain grown at 44°C with and without EB in TSB. Each data point represents the mean and SE of three experiments.

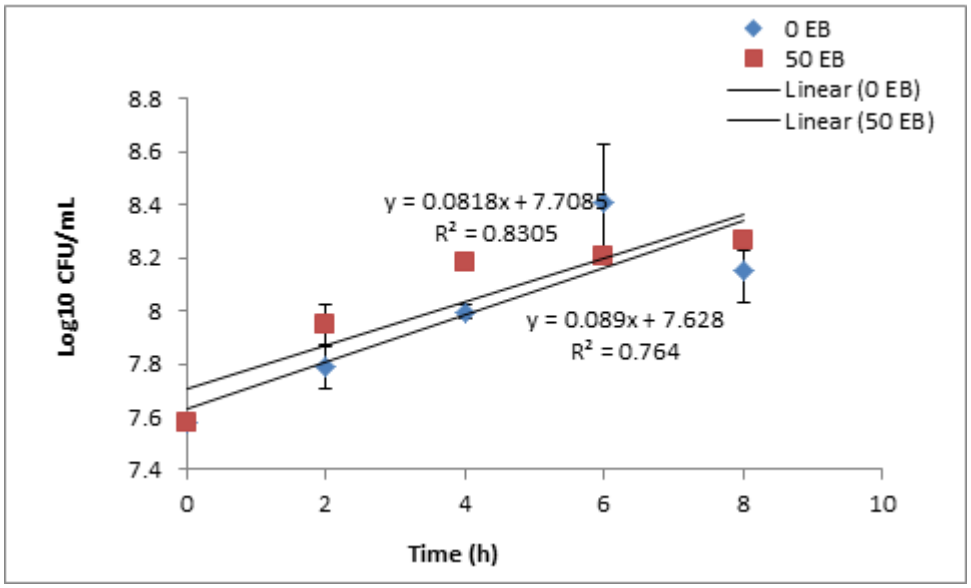

Figure 6.18. Recombinant strain grown at 46 °C with and without EB in TSB. Each data point represents the mean and SE of three experiments.

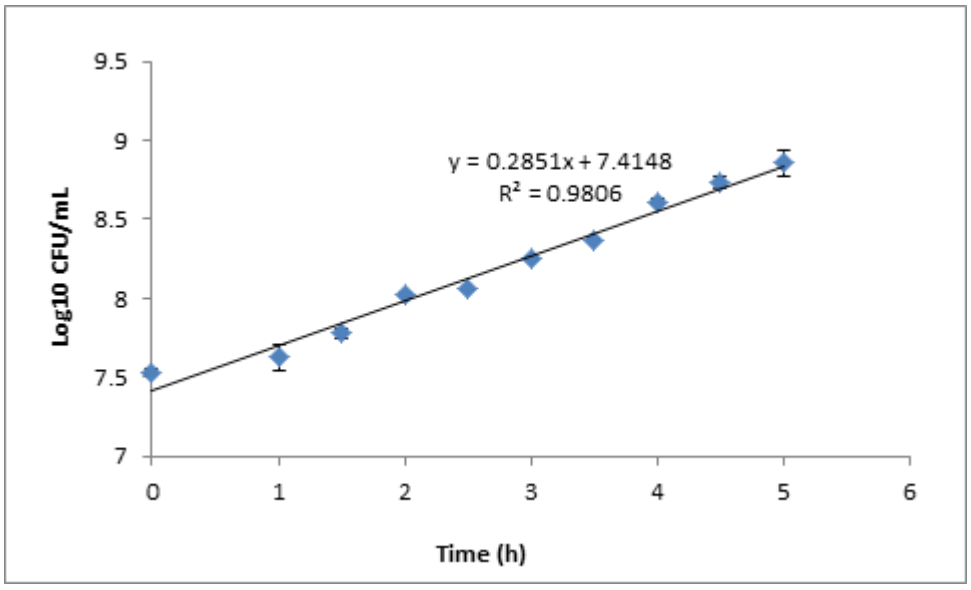

Figure 6.19. Recombinant strain grown at 37°C without EB in TSB. Each data point represents the mean and SE of three experiments.

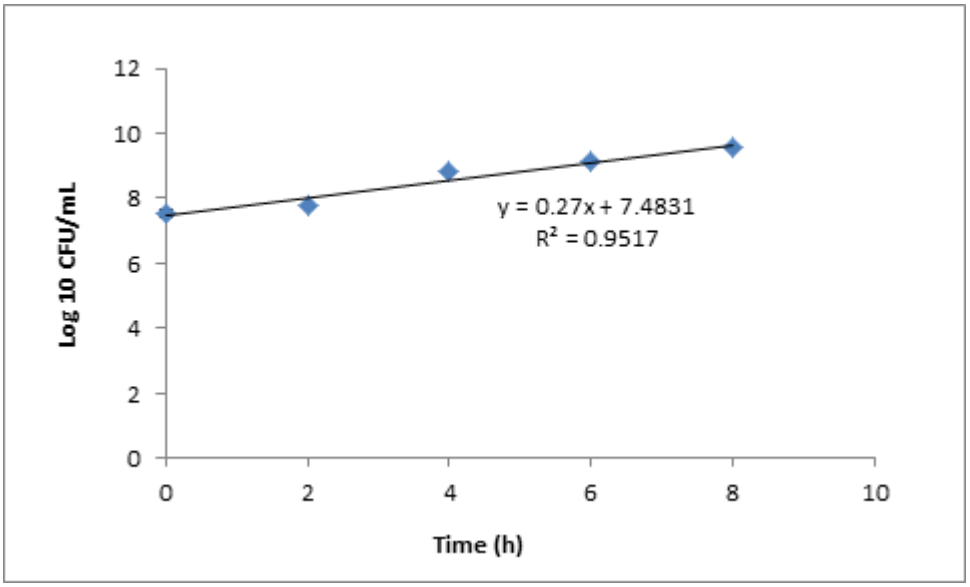

Figure 6.20. Recombinant strain grown at 40°C without EB in TSB. Each data point represents the mean and SE of three experiments.

According to the results shown in the Figures 11 to 15, bacterial growth were not affected by 50 µg/mL of EB at each temperature tested. However, growth rates were reduced dramatically above 42 °C with and without EB.

6.3.5.2 Rate of elimination of the mutant plasmid

In a separate curing experiment, the rate of loss of the plasmid was determined by growing the bacteria in TSB containing 50 µg/mL of EB at 37 and 42 °C. Elimination of the plasmid was determined by determining the percentage of colonies with reduced resistance to chloramphenicol. Reduced chloramphenicol resistance was determined by streaking the colonies on NA containing 5 µg/mL of chloramphenicol and comparing with non-cured recombinant strain as positive control (grows at 10 µg/mL). The first observed elimination of plasmid was in the 4^{th} passage (24 hours for every passage) at 42 °C. Between the 4^{th} and 12^{th} passage, totally about 4000 colonies were examined for plasmid curing. The plasmid curing rate ranged from 0.14% (4th passage) to 3% (12^{th} passage).

In contrast, bacteria grown in EB at 37 °C revealed that no cured colony was present even up to the 12^{th} passage.

Table 6.2. Plasmid curing during passage at 42 °C

Passage	No. of colonies Tested	No. of Cured colonies	[a]Tet^R (%) (2 µg/mL)	[b]$Chlora^s$ (%) (5 µg/mL)
4^{th}	700	1	100	0.14
6^{th}	800	0	100	0
8^{th}	700	3	100	0.43
10^{th}	800	11	100	1.4
12^{th}	1000	30	100	3

a, Tet^R: Tetracycline resistance.
b, $Chlora^s$: Chloramphenicol sensitive.

6.3.6 Allele replacement in *S. capitis*

Eight of the colonies displaying tetracycline-resistance and reduced resistance to chloramphenicol were selected for genotyping by PCR to determine whether the *ica* loci was replaced by the tetracycline resistant gene. It was shown that the crossover did not occur on both sides of the *ica* gene cluster by amplifying crossover regions.

6.4 Discussion

6.4.1 Optimization of the procedures for transformation

Gram-positive bacteria are in general more resistant to plasmid DNA transformation than gram-negative bacteria. This is mainly attributed to its thicker cell wall, which consists of a single membrane and a very large exterior peptidoglycan layer, acting as a physical barrier for the DNA, and making efficient transformation of Gram-positive bacteria far more challenging (Lacks *et al*., 1974).

In this study, the electroporation parameters were optimized for the Gram-positive bacterium *S. capitis*, yielded an approximate transformation efficiency of 4×10^4 transformants per μg of DNA. A number of parameters were thoroughly investigated, including: (i) the preparation of electrocompetent cells; (ii) the heat treatment of cells before electroporation; and (iii) the electroporation step itself.

6.4.1.1 Improvement of transformation efficiency via cell growth phase

The exponential phase is the most critical cell growth phase and cells in this phase are recommended for use in transformation experiments to facilitate maximum exogenous DNA uptake. The observations of this study were consistent with the study for *S.*

epidermidis (Schenk and Laddaga, 1992). This study found optimal transformation efficiency was obtained when cells were harvested at mid log phase. In contrast, (Wu *et al.*, 2010) found that the highest cell transformation occurred at early log phase. This is surprising since early log phase stage is generally coupled with lower cell density, which leads to lower transformation efficiency. The effect of cell number on transformation efficiency was not examined in the current study. Studies conducted in other species such as *S. aureus* revealed a continuous increase in cell transformation in response to a continuous increase in electroporation cell number (Schenk and Laddaga, 1992). In addition, the differences in cell wall composition during different growth phases might be a major contributor to the variations in transformation efficiency.

6.4.1.2 Improvement of transformation efficiency by heat treatment of competent cells prior to electroporation

One of the most important bacterial defences against uptake of foreign DNA is restriction-modification (R-M) system. These systems, comprising restriction endonucleases and methyl-transferases, recognize and modify specific DNA sequences, protecting self DNA from restriction while eliminating potentially harmful foreign DNA which lacks appropriate modifications (Murray, 2000).

To solve the problem of interspecies DNA transfer, a previous study used a short heat treatment of the competent cell in order to temporarily inactivate the host restriction system (Kienesberger *et al*., 2007). This method was optimized and successfully employed to enable crossing of the species restriction barrier and improve the frequency of transformation of *S. capitis* with DNA prepared from *E. coli*. The results suggested that

the restriction system doesindeed hinder DNA transfer between species, as heat treatment dramatically increased transformation efficiency.

6.4.1.3 Effects of DNA amount on transformation efficiency

The transformation efficiency increased linearly with the enhanced amount of DNA. The maximum efficiency was achieved when 4 µg of DNA was used for electroporation in 4 × 10^{10} cell/mL, and slightly dropped thereafter. Similar results were obtained by Schenk and Laddaga (1992).

There is no clear explanation for these results. Transformation efficiency is defined as the number of cells transformed out of one microgram DNA. It is likely that a limited interaction between DNA molecules and bacterial cells could be responsible for the lower transformation efficiency with lower amounts of DNA. In some other species such as *Corynebacterium pseudotuberculosis*, there was an inverse proportion relationship between the quantity of transforming plasmid DNA and transformation efficiency (Dorella *et al*., 2006). A possible explanation may be competition or interaction of plasmid DNA with the cells. In addition, the salt concentration in foreign DNA might contribute to the reduced transformation efficiency. Peng *et al* (2009) showed that DNA desalting could significantly improve the transformation efficiency of *Bacillus thuringiensis*.

6.4.1.4 Effects of temperature during electroporation on transformation efficiency.

In this study, electroporation temperature influenced the transformation efficiency dramatically. This is consistent with results from Augustin and Götz, (1990), who demonstrated higher transformation frequencies for *S. epidermidis* at 20 °C than at 4 °C. Similar observations have also been made for *S. aureus* by Schenk and Laddaga (1992).

The observed increases in cell transformation efficiency with incubation temperature could be due to higher temperature inducing the interaction of DNA molecules and the bacterial cell membrane.

6.4.1.5 Electroporation parameters

Field strength is an important factor in transformation. It was found that 20 KV cm^{-1} achieved the highest transformation efficiency. The transformation efficiency reduced significantly with increasing field strength. It is suggested that cells were damaged at high field strength which resulted in lower efficiency.

6.4.1.6 Electroporation buffer was also evaluated as a factor in electroporation

In order to optimize electroporation, sucrose (0.5 M) was added to the original 10% glycerol buffer. In this buffer, sucrose possibly provided good osmolarity protection after heat treatment and in high electric fields. Sucrose did not improve electroporation efficiency, but did reduce the risk of arching during electroporation.

In summary, this study supports previous findings, using other staphylococcal species, that temporary inactivation of host restriction system by short heat treatment, DNA amount, cell growth phase, electroporation temperature and electroporation parameters are essential variables that can efficiently be manipulated independently to enhance cell electro-transformation efficiency in *S. capitis*.

6.4.2 Inducible resistance to tetracycline in the recombinant strain 60

Resistance to tetracycline in S*taphylococcus* spp. is often plasmid-mediated, and usually inducible (Trzcinski *et al*., 2000). The feature of insertion of a protein or proteins in the

membrane envelope may be similar in all the cases. This view is supported by the data of (Levy *et al*., 1974) and (Boldur and Sompolinsky, 1974).

In contrast to the observations of ASHESHOV (1975) that inducible tetracycline resistance occurred only in tetracycline resistant strains, and not in sensitive strains, the results presented here indicate a low-level elevation of tetracycline resistance after induction with tetracycline in the recombinant strain carrying a *tetA(K)* gene on plasmid. The basal resistance level of the strain was low (0.5 µg/mL of tetracycline). Similar findings with the gram-negative bacterium *E. coli* were reported by FRANKLIN (1967). There are two explanations for these findings. One is the bacterial population constitutively produces a small amount of the protein responsible for resistance, but this amount increases upon induction with tetracycline. A more likely explanation is selection from a heterogeneous bacterial population causing the development of tetracycline resistance. It might be that the population of the recombinant strain was heterogeneous, being composed of cells of both the sensitive and the resistant phenotype, and that only the resistant cells developed colonies on tetracycline plates. The experimental results reported here supported the second possibility. When 100 µL of the overnight induced culture (10^8 cells/ mL) was plated on tetracycline plates without dilution, no more than twenty colonies grew.

In addition, if tetracycline was an inducer and the induction was concentration dependent, it would be expected that the highest concentration of the drug with no significant inhibitory effect would be the most rapidly effective in induction. The results in Figure 6.11 show the highest induction was occurred at 0.75 µg/mL, while higher concentrations of

tetracycline did not increase the number of resistant colonies; this might be due to the inhibitory effects of the drug at higher concentrations.

6.4.3 Allelic exchange

Allele exchange is a classical method of using a suicide plasmid that is unable to replicate in the studied strain under certain conditions to deliver an inactivated allele of the gene in the chromosome. Although it is easy to perform with many bacteria, it remains very difficult with others.

In this study, a shuttle plasmid pBT2 was used to deliver the mutant allele. Although this method has been used to efficiently manipulate inactivation of a gene locus in other *Staphylococcus* species (Brückner, 1997), this is the first study applying it in *S. capitis,* in which the genetic and physiological properties are far less studied. Several problems were encountered, which made the gene knockout ultimately impractical.

First, the expression of the tetracycline resistance gene in *S. capitis* was poor. The *tetA*(K) gene, which was used as a marker for selection to inactive the *ica* gene cluster, is carried on a *Hind*III fragment from a copy of a pT181-like region on the chromosome of a *S. aureus* clinical isolate (Simpson *et al.*, 2000). After transformtion into *S. capitis*, the transformants induced in the presence of 0.75 µg/mL of tetracycline grew at on NA containing 3 µg/mL of tetracycline. This is only a marginal increase in resistance compared with the original host strain, which grows in 0.5 µg/mL of tetracycline. The poor gene expression is probably due to a weak promoter (Simpson *et al.,* 2000), or different gene regulation in *S. capitis* from that in *S. aureus*. This weak gene expression made it extremely difficult to screen out a tetracycline resistant colony when *tetA*(K) is present as

only a single copy in the chromosome of a integrant, rather than multiple copies carried by a cell harbouring the mutant construct pBT2Δ*tetA*(K).

Second, the slow cell growth of the *S. capitis* strain made it difficult to cure plasmid from the cells. Initially, passaged the bacteria at 43 °C for seven days, failed to reveal a true mutant or cured plasmid in ten thousand colonies. This suggested the plasmids are lost slowly in this species or particular strain. Further examination of the growth of this strain at different temperatures, revealed only 2 log growths per day at ≤ 42 °C, and growth was even slower at higher temperatures. The replication defect of vector pBT2 is not stringent at 43 °C (Úbeda *et al.*, 2007). Considering that the rate of plasmid curing depends on the relative rates of bacterial growth compared to that of plasmid replication in the bacteria, curing treatment by temperature only may not be enough to eliminate the plasmid in this situation if the curing frequency was extremely low. Therefore, a curing agent, EB was used in combination with incubation at 42 °C. Using this strategy, colonies cured of plasmids were obtained after four passages.

Most of the plasmid cured colonies displayed the desired phenotype which is $tet^{r}CM^{s}$ by streaking on tetracycline plates (2 µg/mL) and chloramphenicol plates (10 µg/mL). However, their genotypes confirmed by PCR on crossover regions revealed that gene replacement had not occurred at the desired loci in the chromosome.

Third, reassessment of the sequences of the insertion revealed a 263-bp region located in the F3 fragment which was homologous to the whole genome shotgun sequence of *S. capitis* with 98% identity (Figure 6.17). A blast search showed the sequence was part of staphylococcal insertion element IS*257.* The *tetA*(K) gene came from a copy of a pT181-

like plasmid co-integrated into the chromosome of SK1660 (a *S. aureus* clinical isolate) as a consequence of IS*257* insertion (Simpson *et al*., 2000). This *Hind*III fragment carrying the *tetA*(K) gene was obtained from another laboratory, and was not thoroughly sequenced before insertion into the constructed vector.

Generally, longer homologous regions yield higher frequencies of recombination, while the frequency variations were observed at different genetic loci. Gene replacement can be achieved with 0.3 kb of homology using this system as indicated by the model paper (Brückener, 1997). This 263 bp homologous region might interfere with the homologous recombination between the flanking fragments (F1 and F2) and chromosome DNA, consequently reducing the occurrence of double crossover (Figure 6. 21).

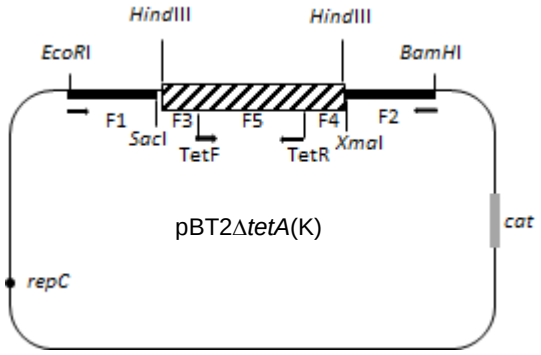

Figure 6.21. Mutant construct of pBT2Δ*tetA(K).* Two flanking fragments F1, 704- bp and F2, 734-bp were used as homologous regions for double crossover with the chromosome. Insertion sequence is a 1700- bp *HindIII* fragment carrying the *tetA(K)* gene, and is located in between the two flanking regions. F3, partial staphylococcal insertion element of IS*257*. F4 plus F5, the *tetA*(*K*) gene.

In addition, it was assumed that the relative sizes of the deletion and insertion segments may have a significant effect on the frequency of mutants generated by allelic exchange (about 3400 bp deletion versus 1700 bp insertion in this study). No experiments were performed to confirm this assumption. The model paper (Brückener, 1997) did not provide this information, while the sizes of inserts were longer or similar to that of

deletions in this paper. This might be an explanation for the differences in allelic exchange efficiency observed between the model paper and the present study.

In summary, although not a true mutant was obtained from about 16000 colonies, significant outcomes were achieved in the transformation step. By optimizing parameters, the vector from *E. coli* was successfully delivered to a clinical *S. capitis* isolate of study without using the intermediate host RN4220. This saved the time needed for making competent cells and plasmid isolation from RN4220, and made the transformation step easier to perform. This method provides a platform for this kind of study and may be practical in a range of gram-positive bacteria.

Since the double crossover and plasmid curing can be very rare events because the frequencies may be low and because illegitimate recombination may occur (McFadden, 1996), allelic exchange mutants may represent only a small fraction of the transformants. Therefore extensive screening is required to isolate a desired mutant. Double crossover may be impractical in some species or a particular strain. A novel allelic replacement strategy with counter selectable marker has been applied in several bacterial genetic manipulations and proved to be particularly advantageous (Reyrat *et al.*, 1998, Bae and Schneewind, 2006). The difficulties in allelic exchange encountered in this study are valuable lessons for future studies.

CHAPTER 7

General discussion

7.1 Correlation of phenotypic biofilm formation, antibiotic resistant profiling and epidemiology of clinical *S. capitis* isolates

Coagulase-negative staphylococci (CoNS) are the most frequent cause of late-onset sepsis among newborns in neonatal intensive care units (NICU). The high incidence of these infections is partially due to their ability to form biofilms (Venkatesh *et al*., 2006a). Biofilm formation is considered to be the most important virulence factors among this genus of bacteria, and has been found mediated by numerous factor, such as surface proteins and polysaccharide intercellular adhesion (PIA). PIA is encoded by the *ica* operon, and has been recognized to be required for biofilm formation in *S. epidermidis* (Williams *et al*., 2002, Gerke *et al*., 1998).

Staphylococcus capitis, which is further divided into two subspecies, subsp. *capitis* and *urealyticus*, according to their distinct characteristics (urease activities and maltose fermentation), is part of the normal flora of the skin of the human scalp, face, neck, and ears and has been associated with prosthetic valve endocarditis (Nalmas *et al.*, 2008). *Staphylococcus capitis* has recently been endemic in the Royal Women's Hospital NICU, causing blood-stream infections in newborn infants. In current study, antibiotic resistance and biofilm formation in clinically significant *S. capitis* isolates were examined, to gain an insight into their establishment and transmission in the clinical setting.

Most of the biofilm producing *S. capitis* isolated from newborns belonged to subsp. *urealyticus*, and were clustered into three major PFGE types (I, II and III). These isolates represent the predominant clones prevalent in the NICU setting. The other isolates

exhibited a biofilm-negative phenotype, mainly belonged to subsp. *capitis*, were grouped into a single PFGE type V, and only sporadically occurred over the years of the study. Antibiotic profiling showed increased antibiotic resistance was associated with enhanced biofilm formation in the isolates. These results are consistent with other studies (Ziebuhr *et al.*, 2006). This association between biofilm formation and antibiotic resistance could be explained if the antibiotics utilized in the hospital drove the selection of certain PFGE types which containing bacterial communities expressing biofilm under conditions encountered on the skin of newborns and and on inserted catheters. One significant observation in this study was shown a strong association between the biofilm formation and the carriage of the *mecA* gene, which codes for methicillin (oxacillin) resistance. This finding is in agreement with that of (Hira *et al.*, 2007), in which, *S. epidermidis* isolates causing sepsis collected in a NICU were examined for the incidence of *mecA* and *icaA* genes. *MecA* was present 87% of the biofilm producing *icaA* carriers.

Although most subsp. *urealyticus* isolates belonging to the major PFGE types, exhibited the biofilm-positive phenotype, several other isolates classified in these PFGE types were biofilm-negative, yet displayed similar antibiotic profiles to their biofilm-positive conterparts. These biofilm-negative isolates carried the *ica* genes, although with various substitutions or deletions (Table 4.3). It is likely that these isolates are capable of biofilm formation but are regulated by an alternative pathway or mechanism. Isolate 17, for example, has an in-frame deletion in *icaA* gene, resulting in missing one transmembrane location compared with its biofilm-positive counterparts (Chapter 4, Figure 4.19). This isolates was biofilm-negative in TSB containing 4% NaCl, but displayed biofilm-forming capacity when grown in a sub-inhibitory concentration of erythromycin. The PIA-independent mechanisms of biofilm formation have been discussed in numerous studies

recently. Sublethal doses of vancomycin induce biofilm formation through an autolysis-dependent mechanism in vancomycin-non-susceptible *S. aureus* (Hsu *et al.*, 2011). Moreover, deletion of *saeRS* in *S. epidermidis* resulted in an increase in biofilm-forming ability, which was associated with increased eDNA release and up-regulated Aap expression. The increased eDNA release from SE1457ΔsaeRS was associated with increased bacterial autolysis and decreased bacterial cell viability in the planktonic/biofilm states (Lou *et al*., 2011).

The subsp. *capitis* isolates examined in this study, although exhibiting an antibiotic-susceptible phenotype, were mostly non-biofilm producers under the experimental conditions used and represented a smaller number compared with the other subspecies. However, this subspecies was circulating in the NICU for several years and causing infections in newborns. The *ica* operon of subsp. *capitis* was generally of the same length as the *ica* operon of biofilm-positive isolates of both subspecies, but single nucleotide deletions were common in subsp. *capitis* (Table 4.3). In terms of biofilm formation, these isolates might adopt a different regulatory pathway as discussed above; it is also likely that other virulence-associated factors or properties facilitate bacterial fitness in the clinical setting.

7.2 The role of *ica* operon in the biofilm formation in *S. capitis* and its origin

The biofilm matrix of *S. epidermidis* and *S. aureus* consists predominantly of PIA, which is composed of linear β-1, 6-linked glucosaminylglycans and encoded by products of the intercellular adhesion (*ica*) locus (Gerke *et al*., 1998, Cramton *et al*., 1999).

The *ica* operon was identified in *S. capitis* in this study. Sequence comparisons showed similarity to that of *S. epidermidis* and *S. aureus*. The structures of Ica proteins in *S. capitis* suggested their responsibilities in the biosynthesis of polysaccharide. IcaA protein showed similarity to a superfamily of glycosyltransferase with the highest identity of 19%. IcaB was shown to be a signal protein, homologous to polysaccharide deacetylase, it is likely to be responsible for modifying the synthesed polysaccharides. IcaC is a transmembrane protein, which probably facilitates transporting the sugar outside the cell membrane, contains a conserved domain which is homologous to acyltransferases. No functional structure has been identified homologous to IcaD, but it shows 79% identity to the IcaD of *S. epidermidis*, and might confer the similar function, that the gene is co-expressed with *icaA*, producing a longer *N*-Acetylglucosamine oligomers and increasing the enzyme activities (Gerke *et al*., 1998). In general, the data of sequence analysis suggest the role of the *ica* operon in the biofilm formation in *S. capitis*.

Sequence analysis also revealed that the *ica* operon was identical in the two biofilm-positive, subsp. *urealyticus* isolates that was examined, whereas several mutations occurred in the biofilm-negative *ica* operons. Moreover, PCR-RFLP showed that all 10 biofilm-positive isolates that were examined displayed the same profiles, whereas there were variations between the profiles of 10 biofilm-negative isolates. It is not possible to draw the conclusion that the biofilm-negative phenotype resulted from these mutations, because mutations in DNA/protein sequences do not necessarily lead to the loss of protein functions. Also, the expression of *ica* genes is known to be regulated by numerous environmental factors (Lim *et al*., 2004, Knobloch *et al*., 2001b, Cotter *et al*., 2008, Bernardo *et al*., 2004a). Once exposed to the appropriate environment, all the *S. capitis* isolates might have the capacity to express biofilm.

Knowledge of the origin/reservoir of the *ica* operon is important to understand the evolution of biofilm-positive *S. capitis* isolates in the hospital environment. Here, the single clone hypothesis of the evolutionary origin of methicillin-resistant *S. aureus* (MRSA) is used as a reference example for comparison. This hypothesis is based on early analyses of the restriction fragment length polymorphisms (RFLP) obtained for MRSA isolates collected worldwide by using probes for *mecA*, suggesting that *mecA* entered the *S. aureus* population on one occasion and resulted in the formation of a single MRSA clone that has since spread around the world (Kreiswirth *et al*., 1993). The PCR-RFLP showing a single pattern for biofilm-positive isolates and three patterns for biofilm-negative isolates, combined with the sequencing data of the *ica* operon might suggest the biofilm-positive *ica* operon was acquired only once by the bacteria, and resulting in a single clone which since spread in the hospital, whereas the biofilm-negative *ica* operon was on acquired at least three occasions. However, this results need to be further verified with a broader selection of isolates from different sites. In addition, the BLAST search of the Ica proteins revealed that they showed low similarities or remote relatedness to their closest homologs with the exception of the Ica proteins in other *Staphylococcus* species. This suggests the *ica* operon has existed among staphylococci associated with humans, long before hospitals were established. The *ica* operon might initially have been transmitted into commensal staphylococci from other species by transduction via bacterial phage or other mobile elements. Staphylococci capable of expressing biofilm and antibiotic resistance would have a selective advantage in modern NICU where insertable plastic devices are used extensively.

To further understand the mechanisms underlying the biofilm formation of *S. capitis*, biofilm assays and the expression of the biofilm-related including the structural gene *icaA*,

its negative regulator *icaR*, and two global regulators *sarA* and *rsbU*, were assessed under sub-inhibitory conconcentrations of antibiotics which are easily achievable in NICU. Two isolates (a biofilm-positive, subsp. *urealyticus*; a biofilm-negative, subsp. *capitis*) were grown in broth containing serum achievable concentrations of erythromycin, but without the usual supplementation with 4% NaCl. The biofilm-positive isolate responded by up-regulation of *sarA* and *rsbU*, and down-regulation of the negative regulator *icaR*. A reverse expression of these genes in the biofilm-negative isolate was observed. This suggests that gene regulation of *ica* operon plays a role on biofilm formation in *S. capitis*. However, the mechanism of regulation remains to be characterized. In order to confirm the role of the *ica* operon in biofilm formation in *S*. *capitis* and directly address the function of the *ica* operon in biofilm formation in *S. capitis*. Several attempts were made to knock out the *ica* gene of a biofilm-positive isolate by reciprocal recombination. Although colonies containing the mutant plasmid were obtained, double crossover was not achieved.

In summary, the data on phenotypic biofilm assays, antibiotic resistant profiling combined with the molecular epidemiology shown by PFGE, sequence analysis of the *ica* operon and the gene regulations presented in this study demonstrated the role of *ica* operon in biofilm formation in *S. capitis*. Also, it suggests that biofilm formation may be a useful characteristic distinguishing the two subspecies.

7.3 Clinical implication of biofilm formation of *S. capitis* in blood-stream infections in newborn infants

It is now well established that biofilm formation plays a significant role in catheter-related bloodstream infections with *S. epidermidis* (von Eiff *et al*., 2002). *S. capitis* is associated with biofilm-related infections such as endocarditis (Nalmas *et al*., 2008). Although, no studies have demonstrated biofilm formation by *S. capitis in vivo*, this species produces biofilm *in vitro* under specific conditions that may exist in the hospital environment, such as the presence of sub-inhibitory concentrations of antibiotics. Biofilm production may be initiated by particular conditions, which are presently unknown.

The precise source of *S. capitis* infecting newborns in NICUs is unknown, but evidence suggests that human-to human transmission is the most likely mode. To date, no environmental isolates of *S. capitis* have been recovered (Kassem *et al*., 2011). This was demonstrated by swabbing 15 clinical surfaces in an isolation room occupied by a patient before and after routine cleaning. (Klánová and Lajèíková, 2006) (Klánová and Lajèíková, 2006 detected *S. capitis* subsp. *ure* Klánová and Lajèíková (2006)ectious patient's room in the hospital. The indoor air was not considered an environmental reservoir for the organism, because the bacterial concentrations were low. However, this provides evidence that the organism can be frequently shed from humans to the environment. A recent study by Hira *et al*. (2010) demonstrated that NICU personnel carried more multiresistant and *mecA*- and *icaA*-positive CoNS than community isolates. Personnel also carried fewer antibiotic-resistant CoNS after a period of absence. Furthermore, almost all blood isolates from the sample period were related to isolates from the hands of personnel. These findings suggested that virulent CoNS are acquired

in the NICU, and personnel are likely to be an important cause for cross-contamination with these CoNS.

The specific factors that promote biofilm formation in *S. capitis* in NICU are not known, but they may be different from those of *S. epidermidis*, although the pathways and sequence of events is probably similar. Critically ill infants require the delivery of nutrients and drugs over long periods of time typically delivered by central venous catheters (CVCs). The skin insertion site and the catheter hub are the most important sources of catheter colonization. At the contaminated hub, the organisms may form biofilm and embed themselves in it. As the biofilm matures, small clusters of cells may detach from the mature biofilm, forming the basis for continual seeding of bacteria into the bloodstream (Liñares, 2007).

7.4 The prevalence of biofilm-negative, subsp. *capitis* isolates in neonatal intensive care unit (NICU)

Subsp. *urealyticus* isolates in the current study displayed a significant association between the biofilm formation, antibiotic resistance and the prevalence of the isolates. The isolates of subsp. *capitis* were biofilm-negative under the experimental conditions used; exhibited a more sensitive antibiotic resistant phenotype, and were less prevalent than the isolates of subsp. *urealyticus*. Why they have been circulating in the NICU over years is a matter for speculation. One likely explanation for the endemic clones' persistence in the NICU may be their slower growth under various conditions compared with the other subspecies as revealed in this study (Chapter 5). With a slow generation time, the host's immune system may not readily recognize the bacteria or may not be triggered sufficiently to eliminate them. The slow growth might impart advantageous

properties and enhance their pathogenic potential by facilitating their survival in the clinical setting.

7.5 Improvement of the hospital practices for controlling the spread of *S. capitis*

According to the data of this study, effective control of bloodstream infections by *S. capitis* requires real-time epidemiological surveillance of each unit. In addition, it has been demonstrated that virulent *S. capitis* isolates are acquired on the NICU, and personnel are likely to be the carriers of these isolates. Therefore, the importance of good hand hygiene is stressed for reducing the transmission of S*. capitis.*

In conclusion, the epidemiology of two subspecies of *S. capitis* combined with their biofilm performance and antibiotic resistance profiling suggest that under certain conditions, biofilm formation is an important trait to assist the differentiation of the two subspecies. It would be beneficial to sub-speciate the bacteria to understand their exact role in NICU infections. Sequence analysis of the *ica* operon indicated its role in biofilm formation in *S. capitis*, and also, suggested a possible origin for the biofilm-positive and -negative *S. capitis* isolates. In addition, this preliminary study of biofilm-related gene expression in the presence of sub-inhibitory concentrations of antibiotics suggests the two subspecies might adopt different regulatory pathways for biofilm formation. However, this needs further verification.

References

ABEE, T., KOVACS, A. T., KUIPERS, O. P. & VAN DER VEEN, S. 2011. Biofilm formation and dispersal in Gram-positive bacteria. *Current opinion in biotechnology,* 22**,** 172-9.

AL-TALIB, H., YEAN, C., AL-KHATEEB, A., SINGH, K.-K., HASAN, H., AL-JASHAMY, K. & RAVICHANDRAN, M. 2010. Comparative Evaluation of Five Culture Media with Triplex PCR Assay for Detection of Methicillin-Resistant *Staphylococcus aureus*. *Current Microbiology,* 61**,** 1-6.

ALLIGNET, J., AUBERT, S., DYKE, K. G. H. & EL SOLH, N. 2001. *Staphylococcus caprae* Strains Carry Determinants Known To Be Involved in Pathogenicity: a Gene Encoding an Autolysin-Binding Fibronectin and the ica Operon Involved in Biofilm Formation. *INFECTION AND IMMUNITY,* 69**,** 712-718.

ALTSCHUL, S. F., MADDEN, T. L., SCHÄFFER, A. A., ZHANG, J., ZHANG, Z., MILLER, W. & LIPMAN, D. J. 1997. Gapped BLAST and PSI-BLAST: a new generation of protein database search programs. *Nucleic Acids Research,* 25**,** 3389-3402.

ARCIOLA, C. R., CAMPOCCIA, D., GAMBERINI, S., CERVELLATI, M., DONATI, E. & MONTANARO, L. 2002. Detection of slime production by means of an optimised Congo red agar plate test based on a colourimetric scale in *Staphylococcus epidermidis* clinical isolates genotyped for ica locus. *Biomaterials,* 23**,** 4233-4239.

ASHESHOV, E. H. 1975. The Genetics of Tetracycline Resistance in *Staphylococcus aureus*. *Microbiology,* 88**,** 132-140.

BAE, T. & SCHNEEWIND, O. 2006. Allelic replacement in *Staphylococcus aureus* with inducible counter-selection. *Plasmid,* 55**,** 58-63.

BALTCH, A. L., SMITH, R. P., FRANKE, M. A. & MICHELSEN, P. B. 1998. Antibacterial Effects of Levofloxacin, Erythromycin, and Rifampin in a Human Monocyte System againstLegionella pneumophila. *ANTIMICROBIAL AGENTS AND CHEMOTHERAPY,* 42**,** 3153-3156.

BANIN, E., VASIL, M. L. & GREENBERG, E. P. 2005. Iron and *Pseudomonas aeruginosa* biofilm formation. *Proceedings of the National Academy of Sciences of the United States of America,* 102**,** 11076-11081.

BANNERMAN, T. L. & KLOOS, W. E. 1991. *Staphylococcus capitis* subsp. *ureolyticus* subsp. nov. from Human Skin. *International Journal of Systematic Bacteriology,* 41**,** 144-147.

BAYER, M. G., HEINRICHS, J. H. & CHEUNG, A. L. 1996. The molecular architecture of the sar locus in *Staphylococcus aureus*. *Journal of Bacteriology,* 178**,** 4563-70.

BEENKEN, K. E., DUNMAN, P. M., MCALEESE, F., MACAPAGAL, D., MURPHY, E., PROJAN, S. J., BLEVINS, J. S. & SMELTZER, M. S. 2004. Global Gene Expression in *Staphylococcus aureus* Biofilms. *Journal of Bacteriology,* 186**,** 4665-4684.

BEGUN, J., GAIANI, J. M., ROHDE, H., MACK, D., CALDERWOOD, S. B., AUSUBEL, F. M. & SIFRI, C. D. 2007. Staphylococcal Biofilm

Exopolysaccharide Protects against Caenorhabditis elegans Immune Defenses. *PLoS Pathog,* 3**,** e57.

BERA, A., BISWAS, R., HERBERT, S. & GÖTZ, F. 2006. The Presence of Peptidoglycan O-Acetyltransferase in Various Staphylococcal Species Correlates with Lysozyme Resistance and Pathogenicity. *INFECTION AND IMMUNITY,* 74**,** 4598-4604.

BERNARDO, K., PAKULAT, N., FLEER, S., SCHNAITH, A., UTERMOHLEN, O., KRUT, O., MULLER, S. & KRONKE, M. 2004a. Subinhibitory Concentrations of Linezolid Reduce *Staphylococcus aureus* Virulence Factor Expression. *Antimicrobial agents and chemotherapy,* 48**,** 546-555.

BERNARDO, K., PAKULAT, N., FLEER, S., SCHNAITH, A., UTERMÖHLEN, O., KRUT, O., MÜLLER, S. & KRÖNKE, M. 2004b. Subinhibitory Concentrations of Linezolid Reduce *Staphylococcus aureus* Virulence Factor Expression. *ANTIMICROBIAL AGENTS AND CHEMOTHERAPY,* 48**,** 546-555.

BISCHOFF, M., ENTENZA, J. M. & GIACHINO, P. 2001. Influence of a Functional sigB Operon on the Global Regulators sar and agr in*Staphylococcus aureus*. *Journal of Bacteriology,* 183**,** 5171-5179.

BOLDUR, I. & SOMPOLINSKY, D. 1974. Antigen Specific for Bacteria Resistant to Tetracycline. *ANTIMICROBIAL AGENTS AND CHEMOTHERAPY,* 6**,** 117-120.

BOLES, B. R. & HORSWILL, A. R. 2008. *agr*-Mediated Dispersal of *Staphylococcus aureus* Biofilms. *PLoS Pathog,* 4**,** e1000052.

BOLES, B. R., THOENDEL, M. & SINGH, P. K. 2005. Rhamnolipids mediate detachment of Pseudomonas aeruginosa from biofilms. *Molecular Microbiology,* 57**,** 1210-1223.

BOWDEN, M. G., VISAI, L., LONGSHAW, C. M., HOLLAND, K. T., SPEZIALE, P. & HÖÖK, M. 2002. Is the GehD Lipase from *Staphylococcus epidermidis* a Collagen Binding Adhesin? *Journal of Biological Chemistry,* 277**,** 43017-43023.

BOYNUKARA, B., GULHAN, T., GURTURK, K., ALISARLI, M. & OGUN, E. 2007. Evolution of slime production by coagulase-negative staphylococci and enterotoxigenic characteristics of *Staphylococcus aureus* strains isolated from various human clinical specimens. *Journal of Medical Microbiology,* 56**,** 1296-1300.

BRANDA, S. S., GONZÁLEZ-PASTOR, J. E., BEN-YEHUDA, S., LOSICK, R. & KOLTER, R. 2001. Fruiting body formation by Bacillus subtilis. *Proceedings of the National Academy of Sciences,* 98**,** 11621-11626.

BRETON, C., ŠNAJDROVÁ, L., JEANNEAU, C., KOČA, J. & IMBERTY, A. 2006. Structures and mechanisms of glycosyltransferases. *Glycobiology,* 16**,** 29R-37R.

BRÜCKNER, R. 1997. Gene replacement in *Staphylococcus carnosus* and *Staphylococcus xylosus*. *FEMS Microbiology Letters,* 151**,** 1-8.

BURTON, E., GAWANDE, P. V., YAKANDAWALA, N., LOVETRI, K., ZHANEL, G. G., ROMEO, T., FRIESEN, A. D. & MADHYASTHA, S. 2006. Antibiofilm Activity of GlmU Enzyme Inhibitors against Catheter-Associated Uropathogens. *Antimicrobial Agents and Chemotherapy,* 50**,** 1835-1840.

CAIAZZA, N. C. & O'TOOLE, G. A. 2003. Alpha-Toxin Is Required for Biofilm Formation by *Staphylococcus aureus*. *Journal of bacteriology,* 185**,** 3214-3217.

CERCA, N., BROOKS, J. L. & JEFFERSON, K. K. 2008. Regulation of the Intercellular Adhesin Locus Regulator (icaR) by SarA, σB, and IcaR in *Staphylococcus aureus*. *Journal of Bacteriology,* 190**,** 6530-6533.

CHANG, Y.-M., JENG, W.-Y., KO, T.-P., YEH, Y.-J., CHEN, C. K.-M. & WANG, A. H.-J. 2010. Structural study of TcaR and its complexes with multiple antibiotics from *Staphylococcus epidermidis*. *Proceedings of the National Academy of Sciences*.

CHARNOCK, S. J. & DAVIES, G. J. 1999. Structure of the Nucleotide-Diphospho-Sugar Transferase, SpsA from Bacillus subtilis, in Native and Nucleotide-Complexed Forms. *Biochemistry,* 38**,** 6380-6385.

CHAVES, F., GARCÍA-ÁLVAREZ, M., SANZ, F., ALBA, C. & OTERO, J. R. 2005. Nosocomial Spread of a *Staphylococcus hominis* subsp. *novobiosepticus* Strain Causing Sepsis in a Neonatal Intensive Care Unit. *Journal of Clinical Microbiology,* 43**,** 4877-4879.

CHEUNG, A. L., NISHINA, K. & MANNA, A. C. 2008. SarA of *Staphylococcus aureus* binds to the sarA promoter to regulate gene expression. *Journal of Bacteriology,* 190**,** 2239-2243.

CHEUNG, G. Y. C. & OTTO, M. 2010. Understanding the significance of *Staphylococcus epidermidis* bacteremia in babies and children. *Current Opinion in Infectious Diseases,* 23**,** 208-216.

CHIEN, Y.-T., MANNA, A. C., PROJAN, S. J. & CHEUNG, A. L. 1999. SarA, a Global Regulator of Virulence Determinants in*Staphylococcus aureus*, Binds to a Conserved Motif Essential for sar-dependent Gene Regulation. *Journal of Biological Chemistry,* 274**,** 37169-37176.

CHRISTENSEN, G. D., SIMPSON, W. A., YOUNGER, J. J., BADDOUR, L. M., BARRETT, F. F., MELTON, D. M. & BEACHEY, E. H. 1985. Adherence of coagulase-negative staphylococci to plastic tissue culture plates: a quantitative model for the adherence of staphylococci to medical devices. *Journal of Clinical Microbiology,* 22**,** 996-1006.

CLARKE, S. R. & FOSTER, S. J. 2006. Surface Adhesins of *Staphylococcus aureus*. *In:* ROBERT, K. P. (ed.) *Advances in Microbial Physiology.* Academic Press.

COGEN, A. L., YAMASAKI, K., MUTO, J., SANCHEZ, K. M., CROTTY ALEXANDER, L., TANIOS, J., LAI, Y., KIM, J. E., NIZET, V. & GALLO, R. L. 2010. *Staphylococcus epidermidis* Antimicrobial δ-Toxin (Phenol-Soluble Modulin-γ) Cooperates with Host Antimicrobial Peptides to Kill Group A Streptococcus. *PLoS ONE,* 5**,** e8557.

CONLON, K. M., HUMPHREYS, H. & O'GARA, J. P. 2002. icaR Encodes a Transcriptional Repressor Involved in Environmental Regulation of ica Operon Expression and Biofilm Formation in *Staphylococcus epidermidis*. *Journal of Bacteriology,* 184**,** 4400-4408.

COSTA, F., CARVALHO, I. F., MONTELARO, R. C., GOMES, P. & MARTINS, M. C. L. 2011. Covalent immobilization of antimicrobial peptides (AMPs) onto biomaterial surfaces. *Acta Biomaterialia,* 7**,** 1431-1440.

COSTERTON, J. W., STEWART, P. S. & GREENBERG, E. P. 1999. Bacterial Biofilms: A Common Cause of Persistent Infections. *Science,* 284**,** 1318-1322.

COTTER, J. J., O'GARA, J. P., MACK, D. & CASEY, E. 2008. Oxygen-Mediated Regulation of Biofilm Development Is Controlled by the Alternative Sigma Factor B in *Staphylococcus epidermidis*. *Applied and Environmental Microbiology,* 75**,** 261-264.

COTTER, J. J., O'GARA, J. P., MACK, D. & CASEY, E. 2009. Oxygen-Mediated Regulation of Biofilm Development Is Controlled by the Alternative Sigma Factor σB in *Staphylococcus epidermidis*. *Applied and Environmental Microbiology,* 75**,** 261-264.

CRAMTON, S. E., GERKE, C., SCHNELL, N. F., NICHOLS, W. W. & GÖTZ, F. 1999. The Intercellular Adhesion (ica) Locus Is Present in *Staphylococcus aureus* and Is Required for Biofilm Formation. *INFECTION AND IMMUNITY,* 67**,** 5427-5433.

CRAMTON, S. E., ULRICH, M., GÖTZ, F. & DÖRING, G. 2001. Anaerobic Conditions Induce Expression of Polysaccharide Intercellular Adhesin in *Staphylococcus aureus* and *Staphylococcus epidermidis*. *INFECTION AND IMMUNITY,* 69**,** 4079-4085.

CUCARELLA, C., SOLANO, C., VALLE, J., AMORENA, B., LASA, Í. & PENADÉS, J. R. 2001. Bap, a *Staphylococcus aureus* Surface Protein Involved in Biofilm Formation. *Journal of bacteriology,* 183**,** 2888-2896.

CUMMINS, J., REEN, F. J., BAYSSE, C., MOOIJ, M. J. & O'GARA, F. 2009. Subinhibitory concentrations of the cationic antimicrobial peptide colistin induce the pseudomonas quinolone signal in *Pseudomonas aeruginosa*. *Microbiology (Reading, England),* 155**,** 2826-2837.

DAVIES, D. 2003. Understanding biofilm resistance to antibacterial agents. *Nat Rev Drug Discov,* 2**,** 114-122.

DAVIES, D. G., PARSEK, M. R., PEARSON, J. P., IGLEWSKI, B. H., COSTERTON, J. W. & GREENBERG, E. P. 1998. The Involvement of Cell-to-Cell Signals in the Development of a Bacterial Biofilm. *Science,* 280**,** 295-298.

DOBINSKY, S., KIEL, K., ROHDE, H., BARTSCHT, K., KNOBLOCH, J. K.-M., HORSTKOTTE, M. A. & MACK, D. 2003. Glucose-Related Dissociation between icaADBC Transcription and Biofilm Expression by *Staphylococcus epidermidis*: Evidence for an Additional Factor Required for Polysaccharide Intercellular Adhesin Synthesis. *Journal of Bacteriology,* 185**,** 2879-2886.

DONVITO, B., ETIENNE, J., DENOROY, L., GREENLAND, T., BENITO, Y. & VANDENESCH, F. 1997. Synergistic hemolytic activity of *Staphylococcus lugdunensis* is mediated by three peptides encoded by a non-agr genetic locus. *INFECTION AND IMMUNITY,* 65**,** 95-100.

DORELLA, F. A., ESTEVAM, E. M., CARDOSO, P. G., SAVASSI, B. M., OLIVEIRA, S. C., AZEVEDO, V. & MIYOSHI, A. 2006. An improved protocol for electrotransformation of Corynebacterium pseudotuberculosis. *Veterinary Microbiology,* 114**,** 298-303.

DUBIN, G., CHMIEL, D., MAK, P., RAKWALSKA, M., RZYCHON, M. & DUBIN, A. 2001. Molecular Cloning and Biochemical Characterisation of Proteases from *Staphylococcus epidermidis*. *Biological Chemistry.*

DUNNE, W. M. 2002. Bacterial Adhesion: Seen Any Good Biofilms Lately? *Clinical Microbiology Reviews,* 15**,** 155-166.

DUSANE, D. H., RAJPUT, J. K., KUMAR, A. R., NANCHARAIAH, Y. V., VENUGOPALAN, V. P. & ZINJARDE, S. S. 2008. Disruption of fungal and bacterial biofilms by lauroyl glucose. *Letters in Applied Microbiology,* 47**,** 374-379.

DYRLØV BENDTSEN, J., NIELSEN, H., VON HEIJNE, G. & BRUNAK, S. 2004. Improved Prediction of Signal Peptides: SignalP 3.0. *Journal of Molecular Biology,* 340**,** 783-795.

FIELDS, B. S., BENSON, R. F. & BESSER, R. E. 2002. Legionella and Legionnaires' Disease: 25 Years of Investigation. *Clinical Microbiology Reviews,* 15**,** 506-526.

FITZPATRICK, F., HUMPHREYS, H. & O'GARA, J. P. 2005. The genetics of staphylococcal biofilm formation—will a greater understanding of pathogenesis lead to better management of device-related infection? *Clinical Microbiology and Infection,* 11**,** 967-973.

FOSTER, T. J. & HÖÖK, M. 1998. Surface protein adhesins of *Staphylococcus aureus. Trends in Microbiology,* 6**,** 484-488.

FRANCEZ-CHARLOT, A., FRUNZKE, J., REICHEN, C., EBNETER, J. Z., GOURION, B. & VORHOLT, J. A. 2009. Sigma factor mimicry involved in regulation of general stress response. *Proceedings of the National Academy of Sciences*.

FRANK, K. L. & PATEL, R. 2007. Poly-N-Acetylglucosamine Is Not a Major Component of the Extracellular Matrix in Biofilms Formed by icaADBC-Positive *Staphylococcus lugdunensis* Isolates. *INFECTION AND IMMUNITY,* 75**,** 4728-4742.

FRANKLIN, T. J. 1967. Resistance of Escherichia coli to Tetracyclines. *Biochem. J.,* 105**,** 371-378.

FREDHEIM, E. G. A., KLINGENBERG, C., ROHDE, H., FRANKENBERGER, S., GAUSTAD, P., FLÆGSTAD, T. & SOLLID, J. E. 2009. Biofilm Formation by *Staphylococcus haemolyticus*. *Journal of Clinical Microbiology,* 47**,** 1172-1180.

FREEMAN, D. J., FALKINER, F. R. & KEANE, C. T. 1989. New method for detecting slime production by coagulase negative staphylococci. *Journal of Clinical Pathology,* 42**,** 872-874.

FREES, D., CHASTANET, A., QAZI, S., SØRENSEN, K., HILL, P., MSADEK, T. & INGMER, H. 2004. Clp ATPases are required for stress tolerance, intracellular replication and biofilm formation in *Staphylococcus aureus*. *Molecular Microbiology,* 54**,** 1445-1462.

FRENETTE, M., BEAUDET, R. & BISAILLON, J. G. 1984. Chemical and biological characterization of a gonococcal growth inhibitor produced by *Staphylococcus haemolyticus* isolated from urogenital flora. *INFECTION AND IMMUNITY,* 46**,** 340-345.

FRIEDMAN, L. & KOLTER, R. 2004. Genes involved in matrix formation in *Pseudomonas aeruginosa* PA14 biofilms. *Molecular Microbiology,* 51**,** 675-690.

FROELIGER, E. H. & FIVES-TAYLOR, P. 2001. *Streptococcus parasanguis*Fimbria-Associated Adhesin Fap1 Is Required for Biofilm Formation. *Infection and Immunity,* 69**,** 2512-2519.

FURMANEK, B., KACZOROWSKI, T., BUGALSKI, R., BIELAWSKI, K., BOGDANOWICZ, J. & PODHAJSKA, A. A. J. 1999. Identification,

characterization and purification of the lantibiotic staphylococcin T, a natural gallidermin variant. *Journal of Applied Microbiology,* 87**,** 856-866.
GALIANA, E., FOURR, S. & ENGLER, G. 2008. Phytophthora parasiticabiofilm formation: installation and organization of microcolonies on the surface of a host plant. *Environmental Microbiology,* 10**,** 2164-2171.
GATERMANN, S. & MARRE, R. 1989. Cloning and expression of *Staphylococcus saprophyticus* urease gene sequences in *Staphylococcus carnosus* and contribution of the enzyme to virulence. *INFECTION AND IMMUNITY,* 57**,** 2998-3002.
GATERMANN, S., MEYER, H. G. & WANNER, G. 1992. *Staphylococcus saprophyticus* hemagglutinin is a 160-kilodalton surface polypeptide. *INFECTION AND IMMUNITY,* 60**,** 4127-4132.
GAVÍN, R., RABAAN, A. A., MERINO, S., TOMÁS, J. M., GRYLLOS, I. & SHAW, J. G. 2002. Lateral flagella of Aeromonas species are essential for epithelial cell adherence and biofilm formation. *Molecular Microbiology,* 43**,** 383-397.
GERKE, C., KRAFT, A., SÜßMUTH, R., SCHWEITZER, O. & GÖTZ, F. 1998. Characterization of theN-Acetylglucosaminyltransferase Activity Involved in the Biosynthesis of the *Staphylococcus epidermidis*Polysaccharide Intercellular Adhesin. *Journal of Biological Chemistry,* 273**,** 18586-18593.
GÖTZ, F. 2004. Staphylococci in colonization and disease: prospective targets for drugs and vaccines. *Current Opinion in Microbiology,* 7**,** 477-487.
GRISTINA, A. G., JENNINGS, R. A., NAYLOR, P. T., MYRVIK, Q. N. & WEBB, L. X. 1989. Comparative in vitro antibiotic resistance of surface-colonizing coagulase-negative staphylococci. *ANTIMICROBIAL AGENTS AND CHEMOTHERAPY,* 33**,** 813-816.
GRUSZKA, D. T., WOJDYLA, J. A., BINGHAM, R. J., TURKENBURG, J. P., MANFIELD, I. W., STEWARD, A., LEECH, A. P., GEOGHEGAN, J. A., FOSTER, T. J., CLARKE, J. & POTTS, J. R. 2012. Staphylococcal biofilm-forming protein has a contiguous rod-like structure. *Proceedings of the National Academy of Sciences,* 109**,** E1011–E1018.
GUDIÑA, E. J., ROCHA, V., TEIXEIRA, J. A. & RODRIGUES, L. R. 2010. Antimicrobial and antiadhesive properties of a biosurfactant isolated from Lactobacillus paracasei ssp. paracasei A20. *Letters in Applied Microbiology,* 50**,** 419-424.
HABIMANA, O., MEYRAND, M., MEYLHEUC, T., KULAKAUSKAS, S. & BRIANDET, R. 2009. Genetic Features of Resident Biofilms Determine Attachment of Listeria monocytogenes. *Applied and Environmental Microbiology,* 75**,** 7814-7821.
HALL-STOODLEY, L., COSTERTON, J. W. & STOODLEY, P. 2004. Bacterial biofilms: from the natural environment to infectious diseases. *Nature reviews. Microbiology,* 2**,** 95-108.
HALL-STOODLEY, L. & STOODLEY, P. 2002. Developmental regulation of microbial biofilms. *Current opinion in biotechnology,* 13**,** 228-233.
HALL-STOODLEY, L. & STOODLEY, P. 2005. Biofilm formation and dispersal and the transmission of human pathogens. *Trends in Microbiology,* 13**,** 7-10.

HAMILTON-MILLER, J. M. T. & SHAH, S. 2000. Patterns of phenotypic resistance to the macrolide-lincosamide-ketolide-streptogramin group of antibiotics in staphylococci. *Journal of Antimicrobial Chemotherapy,* 46**,** 941-949.

HAMON, M. A. & LAZAZZERA, B. A. 2001. The sporulation transcription factor Spo0A is required for biofilm development in Bacillus subtilis. *Molecular Microbiology,* 42**,** 1199-1209.

HANDKE, L. D., SLATER, S. R., CONLON, K. M., O'DONNELL, S. T., OLSON, M. E., BRYANT, K. A., RUPP, M. E., O'GARA, J. P. & FEY, P. D. 2007. σB and SarA independently regulate polysaccharide intercellular adhesin production in *Staphylococcus epidermidis*. *Canadian Journal of Microbiology,* 53**,** 82-91.

HEILMANN, C., GERKE, C., PERDREAU-REMINGTON, F. & GÖTZ, F. 1996. Characterization of Tn917 insertion mutants of *Staphylococcus epidermidis* affected in biofilm formation. *INFECTION AND IMMUNITY,* 64**,** 277-82.

HEILMANN, C., HUSSAIN, M., PETERS, G. & GÖTZ, F. 1997. Evidence for autolysin-mediated primary attachment of *Staphylococcus epidermidis* to a polystyrene surface. *Molecular Microbiology,* 24**,** 1013-1024.

HELL, W., MEYER, H.-G. W. & GATERMANN, S. G. 1998. Cloning of aas, a gene encoding a *Staphylococcus saprophyticus* surface protein with adhesive and autolytic properties. *Molecular Microbiology,* 29**,** 871-881.

HENNIG, S., NYUNT WAI, S. & ZIEBUHR, W. 2007. Spontaneous switch to PIA-independent biofilm formation in an ica-positive *Staphylococcus epidermidis* isolate. *International journal of medical microbiology : IJMM,* 297**,** 117-122.

HIRA, V., SLUIJTER, M., ESTEVÃO, S., HORST-KREFT, D., OTT, A., DE GROOT, R., HERMANS, P. W. M. & KORNELISSE, R. F. 2007. Clinical and Molecular Epidemiologic Characteristics of Coagulase-Negative Staphylococcal Bloodstream Infections in Intensive Care Neonates. *The Pediatric Infectious Disease Journal,* 26**,** 607-612 10.1097/INF.0b013e318060cc03.

HIRA, V., SLUIJTER, M., GOESSENS, W. H. F., OTT, A., DE GROOT, R., HERMANS, P. W. M. & KORNELISSE, R. F. 2010. Coagulase-Negative Staphylococcal Skin Carriage among Neonatal Intensive Care Unit Personnel: from Population to Infection. *Journal of Clinical Microbiology,* 48**,** 3876-3881.

HSU, C.-Y., LIN, M.-H., CHEN, C.-C., CHIEN, S.-C., CHENG, Y.-H., SU, I. N. & SHU, J.-C. 2011. Vancomycin promotes the bacterial autolysis, release of extracellular DNA, and biofilm formation in vancomycin-non-susceptible *Staphylococcus aureus*. *FEMS Immunology & Medical Microbiology,* 63**,** 236-247.

HUANG, X. & MADAN, A. 1999. CAP3: A DNA Sequence Assembly Program. *Genome Research,* 9**,** 868-877.

HUSSAIN, M., HERRMANN, M., VON EIFF, C., PERDREAU-REMINGTON, F. & PETERS, G. 1997. A 140-kilodalton extracellular protein is essential for the accumulation of *Staphylococcus epidermidis* strains on surfaces. *INFECTION AND IMMUNITY,* 65**,** 519-24.

ISAACS, D. 2003. A ten year, multicentre study of coagulase negative staphylococcal infections in Australasian neonatal units. *Archives of Disease in Childhood - Fetal and Neonatal Edition,* 88**,** F89-F93.

IZANO, E. A., AMARANTE, M. A., KHER, W. B. & KAPLAN, J. B. 2008. Differential Roles of Poly-N-Acetylglucosamine Surface Polysaccharide and Extracellular

DNA in *Staphylococcus aureus* and *Staphylococcus epidermidis* Biofilms. *Applied and Environmental Microbiology,* 74**,** 470-476.
JACKSON, K. D., STARKEY, M., KREMER, S., PARSEK, M. R. & WOZNIAK, D. J. 2004. Identification of psl, a locus encoding a potential exopolysaccharide that is essential for *Pseudomonas aeruginosa* PAO1 biofilm formation. *Journal of bacteriology,* 186**,** 4466-75.
JOHNSON, M., COCKAYNE, A. & MORRISSEY, J. A. 2008. Iron-Regulated Biofilm Formation in *Staphylococcus aureus* Newman Requires ica and the Secreted Protein Emp. *INFECTION AND IMMUNITY,* 76**,** 1756-1765.
KAPLAN, J. B. 2010. Biofilm Dispersal: Mechanisms, Clinical Implications, and Potential Therapeutic Uses. *Journal of Dental Research,* 89**,** 205-218.
KARATAN, E. & WATNICK, P. 2009. Signals, Regulatory Networks, and Materials That Build and Break Bacterial Biofilms. *Microbiology and Molecular Biology Reviews,* 73**,** 310-347.
KASSEM, I. I., ESSEILI, M. A. & SIGLER, V. 2011. Detection and differentiation of staphylococcal contamination of clinical surfaces using denaturing gradient gel electrophoresis. *Journal of Hospital Infection,* 78**,** 187-193.
KAZMIERCZAK, M. J., WIEDMANN, M. & BOOR, K. J. 2005. Alternative Sigma Factors and Their Roles in Bacterial Virulence. *Microbiology and Molecular Biology Reviews,* 69**,** 527-543.
KIEM, S., OH, W. S., PECK, K. R., LEE, N. Y., LEE, J.-Y., SONG, J.-H., HWANG, E. S., KIM, E.-C., CHA, C. Y. & CHOE, K.-W. 2004. Phase Variation of Biofilm Formation in *Staphylococcus aureus* by IS256 Insertion and Its Impact on the Capacity Adhering to Polyurethane Surface. *J Korean Med Sci,* 19**,** 779-782.
KIENESBERGER, S., GORKIEWICZ, G., JOAINIG, M. M., SCHEICHER, S. R., LEITNER, E. & ZECHNER, E. L. 2007. Development of Experimental Genetic Tools for Campylobacter fetus. *Applied and Environmental Microbiology,* 73**,** 4619-4630.
KJELLEBERG, S. & MOLIN, S. 2002. Is there a role for quorum sensing signals in bacterial biofilms? *Current Opinion in Microbiology,* 5**,** 254-258.
KLÁNOVÁ, K. & LAJÈÍKOVÁ, A. 2006. Use of Ozone to Reduce Bacteria and Moulds in the Air and on Surfaces. *Indoor and Built Environment,* 15**,** 81-84.
KLOOS, W. E. & BANNERMAN, T. L. 1994. Update on clinical significance of coagulase-negative staphylococci. *Clinical Microbiology Reviews,* 7**,** 117-140.
KNOBLOCH, J. K.-M., BARTSCHT, K., SABOTTKE, A., ROHDE, H., FEUCHT, H.-H. & MACK, D. 2001a. Biofilm Formation by *Staphylococcus epidermidis* Depends on Functional RsbU, an Activator of thesigB Operon: Differential Activation Mechanisms Due to Ethanol and Salt Stress. *Journal of Bacteriology,* 183**,** 2624-2633.
KNOBLOCH, J. K.-M., JÄGER, S., HORSTKOTTE, M. A., ROHDE, H. & MACK, D. 2004. RsbU-Dependent Regulation of *Staphylococcus epidermidis* Biofilm Formation Is Mediated via the Alternative Sigma Factor σB by Repression of the Negative Regulator Gene icaR. *INFECTION AND IMMUNITY,* 72**,** 3838-3848.
KNOBLOCH, J. K. M., BARTSCHT, K., SABOTTKE, A., ROHDE, H., FEUCHT, H. H. & MACK, D. 2001b. Biofilm Formation by *Staphylococcus epidermidis* Depends on Functional RsbU, an Activator of the sigB Operon: Differential Activation

Mechanisms Due to Ethanol and Salt Stress. *Journal of bacteriology,* 183**,** 2624-2633.
KOCIANOVA, S., VUONG, C., YAO, Y., VOYICH, J. M., FISCHER, E. R., DELEO, F. R. & OTTO, M. 2005. Key role of poly-γ-dl-glutamic acid in immune evasion and virulence of *Staphylococcus epidermidis*. *The Journal of Clinical Investigation,* 115**,** 688-694.
KONETSCHNY-RAPP, S., JUNG, G., MEIWES, J. & ZÄHNER, H. 1990. Staphyloferrin A: a structurally new siderophore from staphylococci. *European Journal of Biochemistry,* 191**,** 65-74.
KONG, K.-F., VUONG, C. & OTTO, M. 2006a. Staphylococcus quorum sensing in biofilm formation and infection. *International Journal of Medical Microbiology,* 296**,** 133-139.
KREISWIRTH, B., KORNBLUM, J., ARBEIT, R., EISNER, W., MASLOW, J., MCGEER, A., LOW, D. & NOVICK, R. 1993. Evidence for a clonal origin of methicillin resistance in *Staphylococcus aureus*. *Science,* 259**,** 227-230.
KRISHNAN, S., HAGLUND, L., ASHFAQ, A., LEIST, P. & ROAT, T. 1996. Prosthetic Valve Endocarditis Due to *Staphylococcus saccharolyticus*. *Clinical Infectious Diseases,* 22**,** 722-723.
KRISTIAN, S. A., GOLDA, T., FERRACIN, F., CRAMTON, S. E., NEUMEISTER, B., PESCHEL, A., GÖTZ, F. & LANDMANN, R. 2004. The ability of biofilm formation does not influence virulence of *Staphylococcus aureus* and host response in a mouse tissue cage infection model. *Microbial Pathogenesis,* 36**,** 237-245.
LACKS, S., GREENBERG, B. & NEUBERGER, M. 1974. Role of a Deoxyribonuclease in the Genetic Transformation of Diplococcus pneumoniae. *Proceedings of the National Academy of Sciences,* 71**,** 2305-2309.
LASA, I. & PENADÉS, J. R. 2006. Bap: A family of surface proteins involved in biofilm formation. *Research in Microbiology,* 157**,** 99-107.
LAZAZZERA, B. A. 2005. Lessons from DNA microarray analysis: the gene expression profile of biofilms. *Current Opinion in Microbiology,* 8**,** 222-7.
LENAERTS, A. J. M., GRUPPO, V., BROOKS, J. V. & ORME, I. M. 2003. Rapid In Vivo Screening of Experimental Drugs for Tuberculosis Using Gamma Interferon Gene-Disrupted Mice. *ANTIMICROBIAL AGENTS AND CHEMOTHERAPY,* 47**,** 783-785.
LEVY, S. B., MCMURRY, L. & PALMER, E. 1974. R Factor Proteins Synthesized in *Escherichia coli* Minicells: Membrane-Associated R Factor Proteins. *Journal of Bacteriology,* 120**,** 1464-1471.
LEWIS, K. 2005 Persister cells and the Riddle of Biofilm Survival. *Biochemistry (Moscow),* 70**,** 267-74.
LI, J., RANCOUR, D. M., ALLENDE, M. L., WORTH, C. A., DARLING, D. S., GILBERT, J. B., MENON, A. K. & YOUNG JR., W. W. 2001. The DXD motif is required for GM2 synthase activity but is not critical for nucleotide binding. *Glycobiology,* 11**,** 217-229.
LIM, B., BEYHAN, S., MEIR, J. & YILDIZ, F. H. 2006. Cyclic-diGMP signal transduction systems in Vibrio cholerae: modulation of rugosity and biofilm formation. *Molecular Microbiology,* 60**,** 331-348.

LIM, Y., JANA, M., LUONG, T. T. & LEE, C. Y. 2004. Control of Glucose- and NaCl-Induced Biofilm Formation by rbf in *Staphylococcus aureus*. *Journal of bacteriology,* 186**,** 722-729.

LIÑARES, J. 2007. Diagnosis of Catheter-Related Bloodstream Infection: Conservative Techniques. *Clinical Infectious Diseases,* 44**,** 827-829.

LIU, Y., AMES, B., GOROVITS, E., PRATER, B. D., SYRIBEYS, P., VERNACHIO, J. H. & PATTI, J. M. 2004. SdrX, a Serine-Aspartate Repeat Protein Expressed by *Staphylococcus capitis* with Collagen VI Binding Activity. *INFECTION AND IMMUNITY,* 72**,** 6237-6244.

LOU, Q., ZHU, T., HU, J., BEN, H., YANG, J., YU, F., LIU, J., WU, Y., FISCHER, A., FRANCOIS, P., SCHRENZEL, J. & QU, D. 2011. Role of the SaeRS two-component regulatory system in *Staphylococcus epidermidis* autolysis and biofilm formation. *BMC Microbiology,* 11**,** 146.

LUONG, T. T., LEI, M. G. & LEE, C. Y. 2009. *Staphylococcus aureus* Rbf Activates Biofilm Formation In Vitro and Promotes Virulence in a Murine Foreign Body Infection Model. *INFECTION AND IMMUNITY,* 77**,** 335-340.

MA, L., CONOVER, M., LU, H., PARSEK, M. R., BAYLES, K. & WOZNIAK, D. J. 2009. Assembly and Development of the *Pseudomonas aeruginosa* Biofilm Matrix. *PLoS Pathog,* 5**,** e1000354.

MACK, D., HAEDER, M., SIEMSSEN, N. & LAUFS, R. 1996. Association of Biofilm Production of Coagulase-Negative Staphylococci with Expression of a Specific Polysaccharide Intercellular Adhesin. *Journal of Infectious Diseases,* 174**,** 881-883.

MACK, D., SIEMSSEN, N. & LAUFS, R. 1992. Parallel induction by glucose of adherence and a polysaccharide antigen specific for plastic-adherent *Staphylococcus epidermidis*: evidence for functional relation to intercellular adhesion. *INFECTION AND IMMUNITY,* 60**,** 2048-2057.

MAJERCZYK, C. D., SADYKOV, M. R., LUONG, T. T., LEE, C., SOMERVILLE, G. A. & SONENSHEIN, A. L. 2008. *Staphylococcus aureus* CodY Negatively Regulates Virulence Gene Expression. *Journal of Bacteriology,* 190**,** 2257-2265.

MARSH, A., O'SULLIVAN, O., ROSS, R. P., COTTER, P. & HILL, C. 2010. In silico analysis highlights the frequency and diversity of type 1 lantibiotic gene clusters in genome sequenced bacteria. *BMC Genomics,* 11**,** 679.

MASSONET, C., PINTENS, V., MERCKX, R., ANNE, J., LAMMERTYN, E. & VAN ELDERE, J. 2006. Effect of iron on the expression of sirR and sitABC in biofilm-associated *Staphylococcus epidermidis*. *BMC Microbiology,* 6**,** 103.

MATSUDA, E., SHIGEOKA, T., IIDA, R., YAMANAKA, S., KAWAICHI, M. & ISHIDA, Y. 2004. Expression profiling with arrays of randomly disrupted genes in mouse embryonic stem cells leads to in vivo functional analysis. *Proceedings of the National Academy of Sciences,* 101**,** 4170-4174.

MCCANN, M. T., GILMORE, B. F. & GORMAN, S. P. 2008. *Staphylococcus epidermidis* device-related infections: pathogenesis and clinical management. *Journal of Pharmacy and Pharmacology,* 60**,** 1551-1571.

MCCREA, K. W., HARTFORD, O., DAVIS, S., EIDHIN, D. N., LINA, G., SPEZIALE, P., FOSTER, T. J. & HÖÖK, M. 2000. The serine-aspartate repeat (Sdr) protein family in *Staphylococcus epidermidis*. *Microbiology,* 146**,** 1535-1546.

MCFADDEN, J. 1996. Recombination in mycobacteria. *Molecular Microbiology,* 21**,** 205-211.
MCKENNEY, D., POULIOT, K. L., WANG, Y., MURTHY, V., ULRICH, M., DÖRING, G., LEE, J. C., GOLDMANN, D. A. & PIER, G. B. 1999. Broadly Protective Vaccine for *Staphylococcus aureus* Based on an in Vivo-Expressed Antigen. *Science,* 284**,** 1523-1527.
MCKEVITT, A. I., BJORNSON, G. L., MAURACHER, C. A. & SCHEIFELE, D. W. 1990. Amino acid sequence of a deltalike toxin from *Staphylococcus epidermidis*. *INFECTION AND IMMUNITY,* 58**,** 1473-1475.
MERINO, N., TOLEDO-ARANA, A., VERGARA-IRIGARAY, M., VALLE, J., SOLANO, C., CALVO, E., LOPEZ, J. A., FOSTER, T. J., PENADÉS, J. R. & LASA, I. 2009. Protein A-Mediated Multicellular Behavior in *Staphylococcus aureus*. *Journal of Bacteriology,* 191**,** 832-843.
MIETHKE, M. & MARAHIEL, M. A. 2007. Siderophore-Based Iron Acquisition and Pathogen Control. *Microbiology and Molecular Biology Reviews,* 71**,** 413-451.
MIKKELSEN, H., DUCK, Z., LILLEY, K. S. & WELCH, M. 2007. Interrelationships between Colonies, Biofilms, and Planktonic Cells of Pseudomonas aeruginosa. *Journal of Bacteriology,* 189**,** 2411-2416.
MOLIN, S. & TOLKER-NIELSEN, T. 2003. Gene transfer occurs with enhanced efficiency in biofilms and induces enhanced stabilisation of the biofilm structure. *Current opinion in biotechnology,* 14**,** 255-261.
MØRETRØ, T., HERMANSEN, L., HOLCK, A. L., SIDHU, M. S., RUDI, K. & LANGSRUD, S. 2003. Biofilm Formation and the Presence of the Intercellular Adhesion Locus ica among Staphylococci from Food and Food Processing Environments. *Applied and Environmental Microbiology,* 69**,** 5648-5655.
MOTULSKY, H. 1999. *Analyzing Data with GraphPad Prism*, GraphPad Software Incorporated.
MURCHAN, S., KAUFMANN, M. E., DEPLANO, A., DE RYCK, R., STRUELENS, M., ZINN, C. E., FUSSING, V., SALMENLINNA, S., VUOPIO-VARKILA, J., EL SOLH, N., CUNY, C., WITTE, W., TASSIOS, P. T., LEGAKIS, N., VAN LEEUWEN, W., VAN BELKUM, A., VINDEL, A., LACONCHA, I., GARAIZAR, J., HAEGGMAN, S., OLSSON-LILJEQUIST, B., RANSJO, U., COOMBES, G. & COOKSON, B. 2003. Harmonization of Pulsed-Field Gel Electrophoresis Protocols for Epidemiological Typing of Strains of Methicillin-Resistant *Staphylococcus aureus*: a Single Approach Developed by Consensus in 10 European Laboratories and Its Application for Tracing the Spread of Related Strains. *Journal of Clinical Microbiology,* 41**,** 1574-1585.
MURRAY, N. E. 2000. Type I Restriction Systems: Sophisticated Molecular Machines (a Legacy of Bertani and Weigle). *Microbiology and Molecular Biology Reviews,* 64**,** 412-434.
NALMAS, S., BISHBURG, E., MEURILLIO, J., KHOOBIAR, S. & COHEN, M. 2008. *Staphylococcus capitis* prosthetic valve endocarditis: Report of two rare cases and review of literature. *Heart & Lung: The Journal of Acute and Critical Care,* 37**,** 380-384.
NG, P. C., CHOW, V. C. Y., LEE, C. H., LING, J. M. L., WONG, H. L. & CHAN, R. C. Y. 2006. Persistent *Staphylococcus Capitis* Septicemia in A Preterm Infant. *The*

Pediatric Infectious Disease Journal, 25**,** 652-654 10.1097/01.inf.0000225785.32137.d3.
NIJLAND, R., HALL, M. J. & BURGESS, J. G. 2010. Dispersal of Biofilms by Secreted, Matrix Degrading, Bacterial DNase. *PLoS ONE,* 5**,** e15668.
NOVICK, R. P. & GEISINGER, E. 2008. Quorum Sensing in Staphylococci. *Annual Review of Genetics,* 42**,** 541-564.
O'NEILL, E., POZZI, C., HOUSTON, P., HUMPHREYS, H., ROBINSON, D. A., LOUGHMAN, A., FOSTER, T. J. & O'GARA, J. P. 2008. A Novel *Staphylococcus aureus* Biofilm Phenotype Mediated by the Fibronectin-Binding Proteins, FnBPA and FnBPB. *Journal of Bacteriology,* 190**,** 3835-3850.
OLIVEIRA, D. C. & LENCASTRE, H. D. 2002. Multiplex PCR Strategy for Rapid Identification of Structural Types and Variants of the mec Element in Methicillin-Resistant *Staphylococcus aureus*. *ANTIMICROBIAL AGENTS AND CHEMOTHERAPY,* 46**,** 2155-2161.
OTTO, M. 2004. Virulence factors of the coagulase-negative staphylococci. *Frontiers in Bioscience,* 9**,** 841-863.
OTTO, M. 2009. *Staphylococcus epidermidis*--the 'accidental' pathogen. *Nature reviews. Microbiology,* 7**,** 555-67.
OTTO, M. 2012. Staphylococcal Infections: Mechanisms of Biofilm Maturation and Detachment as Critical Determinants of Pathogenicity. *Annual Review of Medicine,* 64**,** null.
PAMP , S. J., FREES, D., ENGELMANN, S., HECKER, M. & INGMER, H. 2006. Spx Is a Global Effector Impacting Stress Tolerance and Biofilm Formation in *Staphylococcus aureus*. *Journal of Bacteriology,* 188**,** 4861-4870.
PEACOCK, S. J., LINA, G., ETIENNE, J. & FOSTER, T. J. 1999. *Staphylococcus schleiferi* subsp.*schleiferi* Expresses a Fibronectin-Binding Protein. *INFECTION AND IMMUNITY,* 67**,** 4272-4275.
PENG, D., LUO, Y., GUO, S., ZENG, H., JU, S., YU, Z. & SUN, M. 2009. Elaboration of an electroporation protocol for large plasmids and wild-type strains of *Bacillus thuringiensis*. *Journal of Applied Microbiology,* 106**,** 1849-1858.
PESSOA-SILVA, C. L., MIYASAKI, C. H., DE ALMEIDA, M. F., KOPELMAN, B. I., RAGGIO, R. L. & WEY, S. B. 2001. Neonatal late-onset bloodstream infection: Attributable mortality, excess of length of stay and risk factors. *European Journal of Epidemiology,* 17**,** 715-720.
PIRIOU, P., DUKAN, S., LEVI, Y. & JAMGE, P. A. 1997. Prevention of bacterial growth in drinking water distribution systems. *Water Science and Technology,* 35**,** 283-287.
RAAD, I. 1998. Intravascular-catheter-related infections. *The Lancet,* 351**,** 893-898.
RACHID, S., OHLSEN, K., WITTE, W., HACKER, J. & ZIEBUHR, W. 2000. Effect of Subinhibitory Antibiotic Concentrations on Polysaccharide Intercellular Adhesin Expression in Biofilm-Forming *Staphylococcus epidermidis*. *ANTIMICROBIAL AGENTS AND CHEMOTHERAPY,* 44**,** 3357-3363.
RANI, S. A., PITTS, B., BEYENAL, H., VELUCHAMY, R. A., LEWANDOWSKI, Z., DAVISON, W. M., BUCKINGHAM-MEYER, K. & STEWART, P. S. 2007. Spatial Patterns of DNA Replication, Protein Synthesis, and Oxygen Concentration

within Bacterial Biofilms Reveal Diverse Physiological States. *Journal of Bacteriology,* 189**,** 4223-4233.
REYRAT, J.-M., PELICIC, V., GICQUEL, B. & RAPPUOLI, R. 1998. Counterselectable Markers: Untapped Tools for Bacterial Genetics and Pathogenesis. *INFECTION AND IMMUNITY,* 66**,** 4011-4017.
RIEU, A., BRIANDET, R., HABIMANA, O., GARMYN, D., GUZZO, J. & PIVETEAU, P. 2008. Listeria monocytogenes EGD-e Biofilms: No Mushrooms but a Network of Knitted Chains. *Applied and Environmental Microbiology,* 74**,** 4491-4497.
ROCHAT, T., NICOLAS, P., DELUMEAU, O., RABATINOVÁ, A., KORELUSOVÁ, J., LEDUC, A., BESSIÈRES, P., DERVYN, E., KRÁSNÝ, L. & NOIROT, P. 2012. Genome-wide identification of genes directly regulated by the pleiotropic transcription factor Spx in *Bacillus subtilis*. *Nucleic Acids Research*.
ROHDE, H., BURANDT, E. C., SIEMSSEN, N., FROMMELT, L., BURDELSKI, C., WURSTER, S., SCHERPE, S., DAVIES, A. P., HARRIS, L. G., HORSTKOTTE, M. A., KNOBLOCH, J. K. M., RAGUNATH, C., KAPLAN, J. B. & MACK, D. 2007. Polysaccharide intercellular adhesin or protein factors in biofilm accumulation of *Staphylococcus epidermidis* and *Staphylococcus aureus* isolated from prosthetic hip and knee joint infections. *Biomaterials,* 28**,** 1711-1720.
ROSENSTEIN, R. & GÖTZ, F. 2000. Staphylococcal lipases: Biochemical and molecular characterization. *Biochimie,* 82**,** 1005-1014.
RUPP, M. E., FEY, P. D., HEILMANN, C. & GÖTZ, F. 2001. Characterization of the Importance of *Staphylococcus epidermidis* Autolysin and Polysaccharide Intercellular Adhesin in the Pathogenesis of Intravascular Catheter-Associated Infection in a Rat Model. *Journal of Infectious Diseases,* 183**,** 1038-1042.
RUPP, M. E., ULPHANI, J. S., FEY, P. D., BARTSCHT, K. & MACK, D. 1999a. Characterization of the Importance of Polysaccharide Intercellular Adhesin/Hemagglutinin of *Staphylococcus epidermidis* in the Pathogenesis of Biomaterial-Based Infection in a Mouse Foreign Body Infection Model. *Infection and Immunity,* 67**,** 2627-2632.
RUPP, M. E., ULPHANI, J. S., FEY, P. D. & MACK, D. 1999b. Characterization of *Staphylococcus epidermidis*Polysaccharide Intercellular Adhesin/Hemagglutinin in the Pathogenesis of Intravascular Catheter-Associated Infection in a Rat Model. *Infection and Immunity,* 67**,** 2656-2659.
SARAH E. CRAMTON, C. G., NORBERT F. SCHNELL, WRIGHT W. NICHOLS, AND FRIEDRICH GÖTZ, 1999 The Intercellular Adhesion (ica) Locus Is Present in *S. aureus* and is required for biofilm formation. *Infect Immun.,* 67**,** 5427–5433.
SAUER, K., CAMPER, A. K., EHRLICH, G. D., COSTERTON, J. W. & DAVIES, D. G. 2002. *Pseudomonas aeruginosa* Displays Multiple Phenotypes during Development as a Biofilm. *Journal of Bacteriology,* 184**,** 1140-1154.
SCHENK, S. & LADDAGA, R. A. 1992. Improved method for electroporation of *Staphylococcus aureus*. *FEMS Microbiology Letters,* 94**,** 133-138.
SCHROEDER, K., JULARIC, M., HORSBURGH, S. M., HIRSCHHAUSEN, N., NEUMANN, C., BERTLING, A., SCHULTE, A., FOSTER, S., KEHREL, B. E., PETERS, G. & HEILMANN, C. 2009. Molecular Characterization of a Novel *Staphylococcus aureus* Surface Protein (SasC) Involved in Cell Aggregation and Biofilm Accumulation. *PLoS ONE,* 4**,** e7567.

SECOR, P., JAMES, G., FLECKMAN, P., OLERUD, J., MCINNERNEY, K. & STEWART, P. 2011. *Staphylococcus aureus* Biofilm and Planktonic cultures differentially impact gene expression, mapk phosphorylation, and cytokine production in human keratinocytes. *BMC Microbiology,* 11**,** 143.

SENN, M. M., GIACHINO, P., HOMEROVA, D., STEINHUBER, A., STRASSNER, J., KORMANEC, J., FLÜCKIGER, U., BERGER-BÄCHI, B. & BISCHOFF, M. 2005. Molecular Analysis and Organization of the σB Operon in *Staphylococcus aureus*. *Journal of Bacteriology,* 187**,** 8006-8019.

SHAH, D., ZHANG, Z., KHODURSKY, A., KALDALU, N., KURG, K. & LEWIS, K. 2006. Persisters: a distinct physiological state of E. coli. *BMC Microbiology,* 6**,** 53.

SHARMA-KUINKEL, B. K., MANN, E. E., AHN, J.-S., KUECHENMEISTER, L. J., DUNMAN, P. M. & BAYLES, K. W. 2009. The *Staphylococcus aureus* LytSR Two-Component Regulatory System Affects Biofilm Formation. *Journal of Bacteriology,* 191**,** 4767-4775.

SHEMESH, M., TAM, A. & STEINBERG, D. 2007. Expression of biofilm-associated genes of *Streptococcus mutans* in response to glucose and sucrose. *Journal of Medical Microbiology,* 56**,** 1528-1535.

SIEVERS, F., WILM, A., DINEEN, D., GIBSON, T. J., KARPLUS, K., LI, W., LOPEZ, R., MCWILLIAM, H., REMMERT, M., SODING, J., THOMPSON, J. D. & HIGGINS, D. G. 2011. Fast, scalable generation of high-quality protein multiple sequence alignments using Clustal Omega. *Mol Syst Biol,* 7.

SILLANPÄÄ, J., NALLAPAREDDY, S. R., HOUSTON, J., GANESH, V. K., BOURGOGNE, A., SINGH, K. V., MURRAY, B. E. & HÖÖK, M. 2009. A family of fibrinogen-binding MSCRAMMs from *Enterococcus faecalis*. *Microbiology,* 155**,** 2390-2400.

SIMPSON, A. E., SKURRAY, R. A. & FIRTH, N. 2000. An IS257-Derived Hybrid Promoter Directs Transcription of a tetA(K) Tetracycline Resistance Gene in the*Staphylococcus aureus* Chromosomal mecRegion. *Journal of Bacteriology,* 182**,** 3345-3352.

STANLEY, N. R., BRITTON, R. A., GROSSMAN, A. D. & LAZAZZERA, B. A. 2003. Identification of Catabolite Repression as a Physiological Regulator of Biofilm Formation by *Bacillus subtilis* by Use of DNA Microarrays. *Journal of Bacteriology,* 185**,** 1951-1957.

STOODLEY, P., SAUER, K., DAVIES, D. G. & COSTERTON, J. W. 2002. Biofilms as complex differentiated communities. *Annual review of microbiology,* 56**,** 187-209.

TAKAHASHI, T., SATOH, I. & KIKUCHI, N. 1999. NOTE. *International Journal of Systematic Bacteriology,* 49**,** 725-728.

TALÒN, R., DUBLET, N., MONTEL, M.-C. & CANTONNET, M. 1995. Purification and characterization of extracellular *Staphylococcus warneri* lipase. *Current Microbiology,* 30**,** 11-16.

TEUFEL, P. & GÖTZ, F. 1993. Characterization of an extracellular metalloprotease with elastase activity from *Staphylococcus epidermidis*. *Journal of Bacteriology,* 175**,** 4218-4224.

THEIS, T., SKURRAY, R. & BROWN, M. 2007. Identification of suitable internal controls to study expression of a *Staphylococcus aureus* multidrug resistance system by quantitative real-time PCR. *J Microbiol Methods,* 70**,** 355 - 362.

TORMO, M. Á., MARTÍ, M., VALLE, J., MANNA, A. C., CHEUNG, A. L., LASA, I. & PENADÉS, J. R. 2005. SarA Is an Essential Positive Regulator of *Staphylococcus epidermidis* Biofilm Development. *Journal of Bacteriology,* 187**,** 2348-2356.

TROTONDA, M. P., TAMBER, S., MEMMI, G. & CHEUNG, A. L. 2008. MgrA Represses Biofilm Formation in *Staphylococcus aureus. INFECTION AND IMMUNITY,* 76**,** 5645-5654.

TRZCINSKI, K., COOPER, B. S., HRYNIEWICZ, W. & DOWSON, C. G. 2000. Expression of resistance to tetracyclines in strains of methicillin-resistant *Staphylococcus aureus. Journal of Antimicrobial Chemotherapy,* 45**,** 763-770.

ÚBEDA, C., BARRY, P., PENADÉS, J. R. & NOVICK, R. P. 2007. A pathogenicity island replicon in *Staphylococcus aureus* replicates as an unstable plasmid. *Proceedings of the National Academy of Sciences,* 104**,** 14182-14188.

UÇKAY, I., PITTET, D., VAUDAUX, P., SAX, H., LEW, D. & WALDVOGEL, F. 2009. Foreign body infections due to *Staphylococcus epidermidis*. *Annals of Medicine,* 41**,** 109-119.

VALLE, J., TOLEDO-ARANA, A., BERASAIN, C., GHIGO, J.-M., AMORENA, B., PENADÉS, J. R. & LASA, I. 2003. SarA and not σB is essential for biofilm development by *Staphylococcus aureus*. *Molecular Microbiology,* 48**,** 1075-1087.

VAN DER VEEN, S. & ABEE, T. 2010. Dependence of Continuous-Flow Biofilm Formation by Listeria monocytogenes EGD-e on SOS Response Factor YneA. *Applied and Environmental Microbiology,* 76**,** 1992-1995.

VAN DER ZWET, W. C., DEBETS-OSSENKOPP, Y. J., REINDERS, E., KAPI, M., SAVELKOUL, P. H. M., VAN ELBURG, R. M., HIRAMATSU, K. & VANDENBROUCKE-GRAULS, C. M. J. E. 2002. Nosocomial Spread of a *Staphylococcus capitis* Strain with Heteroresistance to Vancomycin in a Neonatal Intensive Care Unit. *Journal of Clinical Microbiology,* 40**,** 2520-2525.

VAN SCHAIK, W. & ABEE, T. 2005. The role of sigmaB in the stress response of Gram-positive bacteria -- targets for food preservation and safety. *Current opinion in biotechnology,* 16**,** 218-224.

VANDECASTEELE, S. J., PEETERMANS, W. E., MERCKX, R. & VAN ELDERE, J. 2001. Quantification of Expression of *Staphylococcus epidermidis* Housekeeping Genes with Taqman Quantitative PCR during In Vitro Growth and under Different Conditions. *Journal of Bacteriology,* 183**,** 7094-7101.

VANDECASTEELE, S. J., PEETERMANS, W. E., R MERCKX, R., RIJNDERS, B. J. A. & VAN ELDERE, J. 2003. Reliability of the ica, aap and atlE genes in the discrimination between invasive, colonizing and contaminant *Staphylococcus epidermidis* isolates in the diagnosis of catheter-related infections. *Clinical Microbiology and Infection,* 9**,** 114-119.

VEENSTRA, G. J., CREMERS, F. F., VAN DIJK, H. & FLEER, A. 1996. Ultrastructural organization and regulation of a biomaterial adhesin of *Staphylococcus epidermidis*. *Journal of Bacteriology,* 178**,** 537-41.

VENKATESH, B., BABUJEE, L., LIU, H., HEDLEY, P., FUJIKAWA, T., BIRCH, P., TOTH, I. & TSUYUMU, S. 2006a. The Erwinia chrysanthemi 3937 PhoQ sensor kinase regulates several virulence determinants. *J Bacteriol,* 188**,** 3088 - 3098.

VENKATESH, M. P., PLACENCIA, F. & WEISMAN, L. E. 2006b. Coagulase-negative staphylococcal infections in the neonate and child: an update. *Seminars in pediatric infectious diseases,* 17**,** 120-7.
VENTRE, I., GOODMAN, A. L., VALLET-GELY, I., VASSEUR, P., SOSCIA, C., MOLIN, S., BLEVES, S., LAZDUNSKI, A., LORY, S. & FILLOUX, A. 2006. Multiple sensors control reciprocal expression of *Pseudomonas aeruginosa* regulatory RNA and virulence genes. *Proceedings of the National Academy of Sciences of the United States of America,* 103**,** 171-176.
VERGARA-IRIGARAY, M., MAIRA-LITRÁN, T., MERINO, N., PIER, G. B., PENADÉS, J. R. & LASA, I. 2008. Wall teichoic acids are dispensable for anchoring the PNAG exopolysaccharide to the *Staphylococcus aureus* cell surface. *Microbiology,* 154**,** 865-877.
VERGARA-IRIGARAY, M., VALLE, J., MERINO, N., LATASA, C., GARCÍA, B., RUIZ DE LOS MOZOS, I., SOLANO, C., TOLEDO-ARANA, A., PENADÉS, J. R. & LASA, I. 2009. Relevant Role of Fibronectin-Binding Proteins in *Staphylococcus aureus* Biofilm-Associated Foreign-Body Infections. *INFECTION AND IMMUNITY,* 77**,** 3978-3991.
VERNACHIO, J. H., BAYER, A. S., AMES, B., BRYANT, D., PRATER, B. D., SYRIBEYS, P. J., GOROVITS, E. L. & PATTI, J. M. 2006. Human Immunoglobulin G Recognizing Fibrinogen-Binding Surface Proteins Is Protective against both *Staphylococcus aureus* and *Staphylococcus epidermidis* Infections In Vivo. *ANTIMICROBIAL AGENTS AND CHEMOTHERAPY,* 50**,** 511-518.
VON EIFF, C., JANSEN, B., KOHNEN, W. & BECKER, K. 2005. Infections Associated with Medical Devices: Pathogenesis, Management and Prophylaxis. *Drugs,* 65**,** 179-214.
VON EIFF, C., PETERS, G. & HEILMANN, C. 2002. Pathogenesis of infections due to coagulasenegative staphylococci. *The Lancet Infectious Diseases,* 2**,** 677-685.
VON HEIJNE, G. 1992. Membrane protein structure prediction: Hydrophobicity analysis and the positive-inside rule. *Journal of Molecular Biology,* 225**,** 487-494.
VUONG, C., KIDDER, J. B., JACOBSON, E. R., OTTO, M., PROCTOR, R. A. & SOMERVILLE, G. A. 2005. *Staphylococcus epidermidis* Polysaccharide Intercellular Adhesin Production Significantly Increases during Tricarboxylic Acid Cycle Stress. *Journal of Bacteriology,* 187**,** 2967-2973.
VUONG, C., KOCIANOVA, S., YAO, Y., CARMODY, A. B. & OTTO, M. 2004. Increased Colonization of Indwelling Medical Devices by Quorum-Sensing Mutants of *Staphylococcus epidermidis* In Vivo. *Journal of Infectious Diseases,* 190**,** 1498-1505.
VUONG, C., SAENZ, H. L., GÖTZ, F. & OTTO, M. 2000. Impact of the agr Quorum-Sensing System on Adherence to Polystyrene in *Staphylococcus aureus*. *Journal of Infectious Diseases,* 182**,** 1688-1693.
WANG, I.-W., ANDERSON, J. M. & MARCHANT, R. E. 1993. *Staphylococcus epidermidis* Adhesion to Hydrophobic Biomedical Polymer Is Mediated by Platelets. *Journal of Infectious Diseases,* 167**,** 329-336.
WANG, Q., SUN, F. J., LIU, Y., XIONG, L. R., XIE, L. L. & XIA, P. Y. 2010. Enhancement of biofilm formation by subinhibitory concentrations of macrolides

in icaADBC-positive and -negative clinical isolates of *Staphylococcus epidermidis*. *ANTIMICROBIAL AGENTS AND CHEMOTHERAPY,* 54**,** 2707-11.

WANG, X., PRESTON, J. F. & ROMEO, T. 2004. The pgaABCD Locus of *Escherichia coli* Promotes the Synthesis of a Polysaccharide Adhesin Required for Biofilm Formation. *Journal of Bacteriology,* 186**,** 2724-2734.

WEINSTEIN, M. P., MIRRETT, S., VAN PELT, L., MCKINNON, M., ZIMMER, B. L., KLOOS, W. & RELLER, L. B. 1998. Clinical Importance of Identifying Coagulase-Negative Staphylococci Isolated from Blood Cultures: Evaluation of MicroScan Rapid and Dried Overnight Gram-Positive Panels versus a Conventional Reference Method. *Journal of Clinical Microbiology,* 36**,** 2089-2092.

WEISS, E. C., SPENCER, H. J., DAILY, S. J., WEISS, B. D. & SMELTZER, M. S. 2009. Impact of sarA on Antibiotic Susceptibility of *Staphylococcus aureus* in a Catheter-Associated In Vitro Model of Biofilm Formation. *ANTIMICROBIAL AGENTS AND CHEMOTHERAPY,* 53**,** 2475-2482.

WHITCHURCH, C. B., TOLKER-NIELSEN, T., RAGAS, P. C. & MATTICK, J. S. 2002. Extracellular DNA Required for Bacterial Biofilm Formation. *Science,* 295**,** 1487.

WIJMAN, J. G. E., DE LEEUW, P. P. L. A., MOEZELAAR, R., ZWIETERING, M. H. & ABEE, T. 2007. Air-Liquid Interface Biofilms of *Bacillus cereus*: Formation, Sporulation, and Dispersion. *Applied and Environmental Microbiology,* 73**,** 1481-1488.

WIKLER, M. A. 2006. *Performance standards for antimicrobial susceptibility testing: sixteenth informational supplement,* Clinical and Laboratory Standards Institute.

WILLIAMS, R. J., HENDERSON, B., SHARP, L. J. & NAIR, S. P. 2002. Identification of a Fibronectin-Binding Protein from *Staphylococcus epidermidis*. *INFECTION AND IMMUNITY,* 70**,** 6805-6810.

WILSON, I. G. 1997. Inhibition and facilitation of nucleic acid amplification. *Applied and Environmental Microbiology,* 63**,** 3741-51.

WU, J. A., KUSUMA, C., MOND, J. J. & KOKAI-KUN, J. F. 2003. Lysostaphin Disrupts *Staphylococcus aureus* and *Staphylococcus epidermidis* Biofilms on Artificial Surfaces. *ANTIMICROBIAL AGENTS AND CHEMOTHERAPY,* 47**,** 3407-3414.

WU, N., MATAND, K., KEBEDE, B., ACQUAAH, G. & WILLIAMS, S. 2010. *Enhancing DNA electrotransformation efficiency in Escherichia coli DH10B electrocompetent cells*.

XU, L., LI, H., VUONG, C., VADYVALOO, V., WANG, J., YAO, Y., OTTO, M. & GAO, Q. 2006a. Role of the luxS Quorum-Sensing System in Biofilm Formation and Virulence of *Staphylococcus epidermidis*. *INFECTION AND IMMUNITY,* 74**,** 488-496.

XU, L., LI, H., VUONG, C., VADYVALOO, V., WANG, J., YAO, Y., OTTO, M. & GAO, Q. 2006b. Role of the luxS quorum-sensing system in biofilm formation and virulence of *Staphylococcus epidermidis*. *Infection and immunity,* 74**,** 488-96.

YANG, L., NILSSON, M., GJERMANSEN, M., GIVSKOV, M. & TOLKER-NIELSEN, T. 2009. Pyoverdine and PQS mediated subpopulation interactions involved in *Pseudomonas aeruginosa* biofilm formation. *Molecular Microbiology,* 74**,** 1380-1392.

YAO, Y., STURDEVANT, D. E. & OTTO, M. 2005. Genomewide Analysis of Gene Expression in *Staphylococcus epidermidis* Biofilms: Insights into the Pathophysiology of S. epidermidis Biofilms and the Role of Phenol-Soluble Modulins in Formation of Biofilms. *Journal of Infectious Diseases,* 191**,** 289-298.

YMELE-LEKI, P. & ROSS, J. M. 2007. Erosion from *Staphylococcus aureus* Biofilms Grown under Physiologically Relevant Fluid Shear Forces Yields Bacterial Cells with Reduced Avidity to Collagen. *Applied and Environmental Microbiology,* 73**,** 1834-1841.

YU, N. Y., WAGNER, J. R., LAIRD, M. R., MELLI, G., REY, S., LO, R., DAO, P., SAHINALP, S. C., ESTER, M., FOSTER, L. J. & BRINKMAN, F. S. L. 2010. PSORTb 3.0: improved protein subcellular localization prediction with refined localization subcategories and predictive capabilities for all prokaryotes. *Bioinformatics,* 26**,** 1608-1615.

ZIEBUHR, W., HENNIG, S., ECKART, M., KRÄNZLER, H., BATZILLA, C. & KOZITSKAYA, S. 2006. Nosocomial infections by *Staphylococcus epidermidis*: how a commensal bacterium turns into a pathogen. *International Journal of Antimicrobial Agents,* 28, Supplement 1**,** 14-20.

ZIEBUHR, W., KRIMMER, V., RACHID, S., LÖßNER, I., GÖTZ, F. & HACKER, J. 1999. A novel mechanism of phase variation of virulence in *Staphylococcus epidermidis*: evidence for control of the polysaccharide intercellular adhesin synthesis by alternating insertion and excision of the insertion sequence element IS256. *Molecular Microbiology,* 32**,** 345-356.

ZOTTOLA, E. A. & SASAHARA, K. C. 1994. Microbial biofilms in the food processing industry—Should they be a concern? *International Journal of Food Microbiology,* 23**,** 125-148.

Appendices

Appendix 1 Urease and Maltose Fermentation Tests on the clinical *S. capitis* isolates

Isolate	Urease Test	Maltose Fermentation	Isolate	Urease Test	Maltose Fermentation
35	positive	positive	87	positive	positive
41	positive	positive	84	positive	positive
57	positive	positive (w)	89	positive	positive (w)
81	negative	positive	94	positive	positive
91	positive	positive	19	negative	positive
83	positive (w)[a]	positive	21	positive	positive
70	positive	positive	54	positive	positive
42	positive	positive	63	positive	positive
64	positive	positive	67	positive	positive
60	positive	positive	58	positive	positive
53	positive	positive	59	positive	positive
11	positive	positive	80	positive	positive
18	positive (w)	positive	88	positive	positive
25	positive	positive (w)	75	positive	positive
33	positive	positive	47	positive	positive
34	positive	positive (w)	82	negative	positive
45	positive	positive	93	positive	positive
69	positive	positive	76	positive	positive
92	positive	positive (w)	52	positive	positive
6	positive	positive	61	positive	positive
50	positive (w)	positive	39	positive	positive
55	positive (w)	positive	65	negative	positive
17	positive	positive (w)	73	negative	negative
40	positive	positive	77	negative	negative
48	negative	positive (w)	49	negative	negative
71	positive	positive	44	negative	positive
86	positive	positive	85	negative	negative
95	positive	positive	90	negative	negative
66	positive	positive	62	negative	negative
79	positive	positive			

[a]w:weak

Appendix 2 Minimum inhibition concentration (MIC) test on the clinical *S. capitis* isolates

Isolate	Subsp.	MICs (μg/mL)											
		PEN		ERY		CLIN		TEC		VAN		OXA	
35	*urealyticus*	4	4	1	1	1	0.25	<2	<2	1	1	2	2
41	*urealyticus*	>8	>8	512	512	0.25	0.25	<2	<2	1	1	4	4
57	*urealyticus*	2	2	1	1	0.25	0.25	16	16	2	2	2	2
81	*urealyticus*	>8	>8	1	1	0.25	0.25	<2	<2	1	1	4	4
51	*urealyticus*	8	8	512	512	0.25	0.25	32	32	2	2	8	8
91	*urealyticus*	0.12	0.12	1	1	0.25	0.25	<2	<2	0.5	0.5	2	2
83	*urealyticus*	>8	>8	1	1	0.25	0.25	<2	<2	1	1	2	2
70	*urealyticus*	4	4	0.5	0.5	0.25	0.25	<2	<2	1	1	0.5	0.5
42	*urealyticus*	>8	>8	512	512	0.25	0.25	<2	<2	1	1	4	4
64	*urealyticus*	2	2	512	512	0.125	0.125	<2	<2	1	1	4	4
60	*urealyticus*	8	8	1	1	0.125	0.125	<2	<2	<1	<1	4	4
53	*urealyticus*	8	8	512	512	0.25	0.25	<2	<2	<0.5	<0.5	4	4
11	*urealyticus*	8	8	512	512	0.125	0.125	<2	<2	1	1	4	4
18	*urealyticus*	>8	>8	256	256	0.125	0.125	<2	<2	<0.5	<0.5	2	2
25	*urealyticus*	8	8	1	1	0.125	0.125	16	16	1	1	4	4
33	*urealyticus*	8	8	512	512	0.25	0.25	<2	<2	<1	<1	8	8
34	*urealyticus*	4	4	512	512	0.25	0.25	<2	<2	1	1	8	8
45	*urealyticus*	>8	>8	512	512	0.125	0.125	<2	<2	1	1	4	4
69	*urealyticus*	>8	>8	16	16	0.125	0.125	16	16	2	2	8	8
92	*urealyticus*	>8	>8	1	1	0.25	0.25	<2	<2	<1	<1	8	8
6	*urealyticus*	8	8	512	512	0.125	0.125	32	32	<0.5	<0.5	8	8
50	*urealyticus*	2	2	512	512	0.125	0.125	<2	<2	1	1	4	4
55	*urealyticus*	8	8	1	1	0.125	0.125	<2	<2	<1	<1	8	8
17	*urealyticus*	8	8	2	2	0.125	0.125	8	8	2	2	2	2
40	*urealyticus*	>8	>8	512	512	0.125	0.125	<2	<2	<0.5	<0.5	8	8
48	*urealyticus*	8	8	256	256	0.25	0.25	16	16	1	1	8	8
71	*urealyticus*	>8	>8	1	1	0.25	0.25	<2	<2	0.5	0.5	2	2
86	*urealyticus*	>8	>8	1	1	0.25	0.25	<2	<2	1	1	8	8

95	*urealyticus*	>8	>8	1	1	0.25	0.25	<2	<2	1	1	2	2
66	*urealyticus*	8	8	1	1	0.25	0.25	<2	<2	1	1	8	8
79	*urealyticus*	>8	>8	1	1	0.25	0.25	<2	<2	1	1	4	4
87	*urealyticus*	>8	>8	1	1	0.25	0.25	<2	<2	1	1	4	4
84	*urealyticus*	>8	>8	1	1	0.125	0.125			1	1	8	8
89	*urealyticus*	>8	>8	>512	>512	0.25	0.25	<2	<2	<0.5	<0.5	4	4
94	*urealyticus*	>8	>8	1	1	0.125	0.125	<2	<2	1	1	4	4
19	*urealyticus*	>8	>8	1	1	0.25	0.25	<2	<2	<0.5	<0.5	16	16
21	*urealyticus*	8	8	1	1	0.125	0.125	<2	<2	<0.5	<0.5	2	2
54	*urealyticus*	2	2	0.5	0.5	0.125	0.125	<2	<2	1	1	2	2
63	*urealyticus*	4	4	0.5	0.5	0.25	0.25	<2	<2	1	1	2	2
67	*urealyticus*	8	8	0.5	0.5	0.125	0.125	<2	<2	1	1	2	2
58	*urealyticus*	2	2	0.5	0.5	0.125	0.125	<2	<2	1	1	2	2
59	*urealyticus*	4	4	0.5	0.5	0.125	0.125	<2	<2	1	1	2	2
80	*urealyticus*	>8	>8	1	1	0.25	0.25	<2	<2	1	1	<1	<1
88	*urealyticus*	>8	>8	2	2	0.25	0.25	<2	<2	1	1	8	8
75	*urealyticus*	>8	>8	1	1	0.25	0.25	<2	<2	1	1	4	4
47	*urealyticus*	2	2	512	512	0.06	0.06	32	32	4	4	8	8
82	*urealyticus*	>8	>8	1	1	0.25	0.25	<2	<2	1	1	4	4
93	*urealyticus*	>8	>8	1	1	0.25	0.25	<2	<2	1	1	4	4
76	*urealyticus*	>8	>8	0.5	0.5	0.25	0.25	<2	<2	1	1	2	2
52	*urealyticus*	>8	>8	>512	>512	>1024	>1024	<2	<2	1	1	8	8
61	*urealyticus*	4	4	>512	>512	>1024	>1024	4	4	1	1	2	2
39	*urealyticus*	2	2	<0.5	<0.5	0.25	0.25	<2	<2	1	1	0.25	0.25
65	*capitis*	0.03	0.03	0.25	0.25	0.125	0.125	<2	<2	0.5	0.5	0.125	0.125
73	*capitis*	0.03	0.03	0.5	0.5	0.125	0.125	<2	<2	1	1	0.25	0.25
77	*capitis*	0.03	0.03	0.5	0.5	0.25	0.25	<2	<2	1	1	0.25	0.25
49	*capitis*	0.12	0.12	0.5	0.5	0.125	0.125	<2	<2	1	1	0.125	0.125
44	*capitis*	0.06	0.06	0.5	0.5	0.125	0.125	<2	<2	1	1	0.25	0.25
85	*capitis*	0.06	0.06	0.5	0.5	0.125	0.125	<2	<2	1	1	0.25	0.25
90	*capitis*	0.5	0.5	0.5	0.5	0.125	0.125	<2	<2	1	1	0.25	0.25
62	*capitis*	0.03	0.03	0.5	0.5	1	1	<2	<2	1	1	0.25	0.25

PEN: penicillin, ERY: erythromycin, CLIN: clindamycin, TEC: tecoplainin, VAN: vancomycin, OXA: oxacillin.

Appendix 3 Biofilm assays by microtitre plate tests

A representive of the biofilm assay results:

Medium \OD\Isolate	RP62a[a]	91	92	93	94	95	90	44	57	49	85	SP2[b]
TSB+4%NaCl	1.469	2.064	3.203	3.313	1.698	3.101	0.051	0.053	0.051	0.049	0.056	0.061
TSB+4%NaCl	1.518	0.910	3.299	3.296	1.546	2.978	0.054	0.053	0.053	0.049	0.055	0.062
TSB+4%NaCl	1.386	0.855	3.256	3.303	1.958	3.032	0.050	0.051	0.053	0.049	0.054	0.068
TSB+4%NaCl	1.270	1.164	3.348	3.268	2.959	3.310	0.053	0.048	0.057	0.049	0.054	0.068
TSB+4%NaCl	2.238	1.530	3.253	3.212	2.919	3.343	0.054	0.053	0.055	0.053	0.051	0.059
TSB+4%NaCl	2.592	1.837	3.294	3.286	3.039	3.281	0.053	0.052	0.055	0.054	0.052	0.063
TSB+4%NaCl	2.580	2.223	3.281	3.309	3.035	3.316	0.053	0.051	0.054	0.052	0.053	0.064
TSB+4%NaCl	2.260	2.455	3.296	3.255	2.997	3.278	0.054	0.051	0.060	0.053	0.055	0.064
TSB+4%NaCl	2.943	2.810	3.284	3.340	3.247	3.319	0.055	0.058	0.056	0.057	0.056	0.065
TSB+4%NaCl	2.808	3.278	3.306	3.285	1.947	3.326	0.049	0.060	0.058	0.056	0.056	0.084
TSB+4%NaCl	2.632	3.230	3.288	3.356	3.350	3.312	0.050	0.064	0.057	0.057	0.054	0.060
TSB+4%NaCl	2.497	3.236	3.247	3.263	3.132	3.268	0.056	0.060	0.056	0.062	0.057	0.065

[a]RP62A was used as the positive control;
[b]SP2 was used as the negative control.

Appendix 4 Biofim assays of *S. capitis* in erythromycin

Medium\Isolate	6	17	44	65	70
BHI+0.85%NaCl With ERY	2.359	0.223	0.062	0.055	0.452
	2.359	0.223	0.062	0.055	0.452
	2.359	0.223	0.062	0.055	0.452
	2.7	0.25	0.062	0.051	0.51
	2.7	0.25	0.062	0.051	0.51
	2.7	0.25	0.062	0.051	0.51
BHI+0.85%NaCl Without ERY	1.226	0.053	0.063	0.059	0.342
	1.226	0.053	0.063	0.059	0.342
	1.226	0.053	0.063	0.059	0.342
	1.091	0.066	0.063	0.058	0.43
	1.091	0.066	0.063	0.058	0.43
	1.091	0.066	0.063	0.058	0.43

ERY: erythromycin

Appendix 6 RNA integrity and the removal of DNA contamination

Isolation of intact RNA is essential for gene expression assay, RNA integrity was tested on FA gel before gene expression analysis.

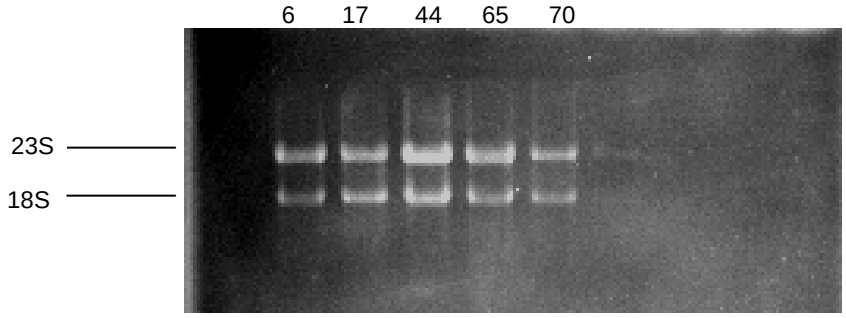

Figure 1. RNA gel photo for testing RNA integrity. The isolate numbers are indicated on the top of each lane.

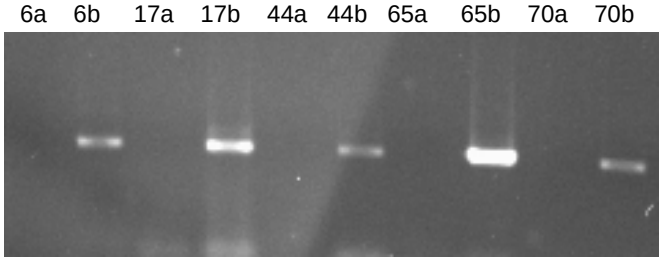

Figure 2. Testing the removal of DNA contamination by Reverse transcript-PCR with primers for *icaA* gene expression. The isolate numbers are indicated on the top of each lane. a, reverse transcriptase negative; b, reverse transcriptase positive.

Appendix 7 Validation of housekeeping genes in the presence and absence of erythromycin with isolate 6

tuf gene						
Condition	Ct1	Ct2	Ct3	Ct4	Ct5	Ct6
No ERY	25.19	25.18	25.12	25.68	24.95	24.77
16 ERY	24.48	24.76	24.35	22.9	23.09	23.03
recA gene						
Condition	Ct1	Ct2	Ct3	Ct4	Ct5	Ct6
No ERY	31.85	32.18	32.25	31.59	32.03	31.21
16 ERY	31.69	31.38	31.33	31.6	31.52	31.87
gyrB gene						
Condition	Ct1	Ct2	Ct3	Ct4	Ct5	Ct6
No ERY	27.23	27.45	27.26	27.12	27.46	27.74
16 ERY	27.12	27.29	27	27.26	27.6	27.36
rpoB gene						
Condition	Ct1	Ct2	Ct3	Ct4	Ct5	Ct6
No ERY	32.51	32.14	33.16	32.8	33.1	32.49
16 ERY	31.72	31.54	31.65	31.67	31.49	31.28
sodA gene						
Condition	Ct1	Ct2	Ct3	Ct4	Ct5	Ct6
No ERY	29.24	29.57	29.27	28.56	28.8	28.46
16 ERY	30.52	30.29	30.47	29.24	29.7	29.59

Ct, Cycle threshold. ERY, erythromycin

Appendix 8 Target gene expression data

Table 1. Cycle Threshold (Ct) values for standard curve of each gene

Log ng total cDNA *gyrB*	**Ct1**	**Ct2**	**Ct3**	**Ct4**	**Ct5**	**Ct6**
3	14.07	14.18	14.24	13.98	14.2	14.05
2	17.05	17.41	17.44	17.21	17.01	17.37
1	20.42	20.57	20.3	20.22	20.31	20.35
0	23.72	23.8	24.06	23.58	23.67	23.95
-1	27.05	27.57	27.39	27.56	27.89	27.12
-2	30.37	30.1	31	29.86	30.6	30.46
Log ng total cDNA *icaA*	**Ct1**	**Ct2**	**Ct3**	**Ct4**	**Ct5**	**Ct6**
3	19.19	19.3	19.49	19.25	19.21	19.11
2	22.34	22.74	22.63	22.5	22.68	22.1
1	25.88	25.96	25.8	25.87	26.01	25.76
0	29.35	29.17	29.44	29.22	29.3	29.27
-1	32.65	33.01	32.16	32.89	32.98	31.67
-2	36.7	37.01	36.9	35.9	37.2	36.01
Log ng total cDNA *icaR*	**Ct1**	**Ct2**	**Ct3**	**Ct4**	**Ct5**	**Ct6**
2	25.1	25.12	25.07	25.8	24.9	25.02
1	28.67	28.19	27.9	29.01	28.3	28.16
0	30.68	31.13	31.27	31.75	31.34	31.36
Log ng total cDNA *sarA*	**Ct1**	**Ct2**	**Ct3**	**Ct4**	**Ct5**	**Ct6**
3	12.43	12.41	12.23	12.45	12.63	12.36
2	15.36	15.09	15.27	15.1	15.61	14.98
1	19.06	19.1	19.06	19.1	19.2	18.99
0	22.83	23.07	23.11	23.01	22.98	23.24
-1	24.43	26.14	26.51	25.67	26.19	24.98
Log ng total cDNA *rsbU*	**Ct1**	**Ct2**	**Ct3**	**Ct4**	**Ct5**	**Ct6**
3	21.3	21.67	20.69	21.5	21.9	20.39
2	24.5	24.49	24.25	24.56	25.1	24.96
1	29.41	30.2	30.39	29.13	30.26	30.41
0	33.23	33.93	33.71	33.29	33.76	33.49
-1	36.96	36.09	36.65	36.79	36.43	36.1

Table 2. Cycle threshold (Ct) in the presence or absence of erythromycin for target genes and house keeping gene gyrBf in isolate 6.

gyrB	**Ct1**	**Ct2**	**Ct3**	**Ct4**	**Ct5**	**Ct6**
N	28.12	27.97	27.74	27.23	27.45	27.26
E	27.26	27.6	27.36	27.12	27	27.29
icaA	**Ct1**	**Ct2**	**Ct3**	**Ct4**	**Ct5**	**Ct6**
N	31.07	31.22	30.82	31.23	31.76	30.91
E	33.58	33.41	33.06	33.6	33.2	32.96
icaR	**Ct1**	**Ct2**	**Ct3**	**Ct4**	**Ct5**	**Ct6**
N	28.06	27.75	27.7	27.68	27.51	27.92
E	29.08	29.1	29.28	29.3	28.92	29.41
SarA	**Ct1**	**Ct2**	**Ct3**	**Ct4**	**Ct5**	**Ct6**
N	26.92	27.16	27.98	27.26	27.65	27.29
E	29.24	29.25	29.28	29.34	29.16	29.01
rsbU	**Ct1**	**Ct2**	**Ct3**	**Ct4**	**Ct5**	**Ct6**
N	28.42	27.82	27.94	27.9	26.69	27.49
E	29.55	30.01	29.36	30.26	30.67	29.64

N, no erythromycin, E, in the presence of erythromycin.

Table 3. Cycle threshold (Ct) in the presence or absence of erythromycin for target genes and house keeping gene gyrBf in isolate 44.

icaA	**Ct1**	**Ct2**	**Ct3**	**Ct4**	**Ct5**	**Ct6**
N	32.85	33.34	32.64	32.9	33.01	32.97
E	30.1	30.01	30.89	30.1	29.98	30.56
icaR	**Ct1**	**Ct2**	**Ct3**	**Ct4**	**Ct5**	**Ct6**
N	29.26	30.31	29.9	29.46	29.67	29.61
E	27.08	27.36	27.1	27.01	26.98	27.31
SarA	**Ct1**	**Ct2**	**Ct3**	**Ct4**	**Ct5**	**Ct6**
N	28.57	29.64	29.53	29.01	28.99	29.91
E	26.96	27.36	28.28	26.98	27.01	28.01
rsbU	**Ct1**	**Ct2**	**Ct3**	**Ct4**	**Ct5**	**Ct6**
N	30.11	29.45	29.66	30.01	29.59	30.1
E	30.31	29.4	28.2	30.31	29.56	29.77

N, no erythromycin, E, in the presence of erythromycin

Appendix 9 Data for *ica* gene Knock out

Table 1. Effect of cell growth phase on the transformation efficiency

OD	Transformans1	Transformants2	Transformants3
0.2	16 25 13	10 27 11	24 18 13
0.5	178 150 201	134 167 183	160 124 212
1.2	51 32 44	26 43 39	31 44 38

Table 2. Effect of heat-treatment on transformation efficiency

Treatment	Transformants1	Transformants2	Transformants3
55 °C, 1 min	179	185	173
Untreated	0	2	6
55 °C, 1 min	212	138	156
Untreated	1	0	2
55 °C, 1 min	191	176	154
Untreated	0	9	11

Table 3. Viable cells after heat treatment with different temperatures (CFU/mL)

Temp (°C)	Time (min)				
	1	2	3	4	5
46	39000000000	40100000000	31000000000	29000000000	23500000000
49	41000000000	27000000000	6700000000	210000000	17200000
52	35000000000	5100000000	1620000000	330000000	21000000
55	41000000000	56000000	9670000	560000	1300
Temp (°C)	Time (min)				
	1	2	3	4	5
46	42000000000	35000000000	43000000000	27000000000	25000000000
49	39000000000	20000000000	5900000000	190000000	19000000
52	31000000000	4200000000	1500000000	230000000	16000000
55	36700000000	7000000	8100000	430000	1140
Temp (°C)	Time (min)				
	1	2	3	4	5
46	45000000000	35000000000	46000000000	38000000000	37000000000
49	38500000000	27000000000	6300000000	167000000	23000000
52	36000000000	4800000000	1120000000	176000000	13000000
55	38000000000	53000000	4600000	590000	1900

Table 4. Effect of DNA amount on transformation efficiency

DNA (µg)	Transformants1	Transformants2	Transformants3
0.1	1	0	0
1	9	3	7
2	53	37	46
3	72	99	91
4	153	116	205
5	113	196	135
6	173	237	198
0.1	0	0	0
1	3	2	8
2	26	56	41
3	57	175	94
4	179	143	200
5	177	210	195
6	163	207	243
0.1	0	0	0
1	10	5	4
2	29	22	31
3	67	78	146
4	159	157	182
5	195	203	189
6	176	165	173

Table 5. Incubation of DNA with competent cells

Time (min)	Transformants1	Transformants2	Transformants3
1	127	113	203
5	139	201	130
10	143	176	151
30	32	12	26
1	163	189	144
5	201	169	175
10	231	126	136
30	11	10	16
1	98	163	213
5	146	175	216
10	211	186	173
30	9	0	18

Table 6. Transformation temperature on transformation efficiency

Temperaure °C	Transformants1	Transformants2	Transformants3
0	46	37	25
20	189	210	176
0	12	56	71
20	175	201	97
0	34	10	44
20	153	165	176

Table 7. Effects of Electroporation buffer on transformation efficiency

Buffer condition	Transformants1	Transformants2	Transformants3
with sucrose	193	201	136
without sucrose	167	157	198
with sucrose	186	133	106
without sucrose	174	131	116
with sucrose	98	186	130
without sucrose	109	193	203

Table 8. Effects of field strength on transformation efficiency

Field strength (KV)	Transformants1	Transformants2	Transformants3
2.1	191	176	139
2.3	176	201	165
2.5	75	53	89
2.1	220	116	165
2.3	107	153	100
2.5	31	70	65
2.1	167	134	185
2.3	176	168	103
2.5	25	67	46

Table 9. Inducible tetracycline resistance in *S. capitis*

Pre-incubation with Tc (µg/mL)	Colonies resistant to 3 µg/mL of Tc		
0.25	1	1	1
0.5	2	2	3
0.75	20	17	15
1	9	14	11
1.9	6	5	4
0.25	1	2	3
0.5	4	2	1
0.75	21	3	15
1	18	5	17
1.9	6	8	9
0.25	0	0	0
0.5	0	0	0
0.75	0	0	0
1	0	0	0
1.9	0	0	0